

# **Cancer Immunotherapy for Pancreatic Ductal Adenocarcinoma**

**From Bench to Bedside and Beyond**

**Sai Ping Lau**

Cancer Immunotherapy for Pancreatic Ductal Adenocarcinoma

Sai Ping Lau

Cancer Immunotherapy for Pancreatic Ductal Adenocarcinoma  
From Bench to Bedside and Beyond

Sai Ping Lau

Cover and layout design: Sai Ping Lau  
Printing: Ridderprint BV, Ridderkerk, The Netherlands  
ISBN: 978-94-6458-986-3

The research in this thesis was financially supported by TKI-LSH Health~Holland and Stichting Overleven met Alveesklierkanker.

© 2023 Sai Ping Lau, Rotterdam, The Netherlands  
All rights reserved. No part of this thesis may be reproduced, stored in a retrieval system of any nature, or transmitted in any form or by any means, without permission of the author, or when appropriate, from the publishers of the publications.

**Cancer Immunotherapy for Pancreatic Ductal Adenocarcinoma  
From Bench to Bedside and Beyond**

Tumor immunotherapie voor pancreas ductaal adenocarcinoom

Proefschrift

ter verkrijging van de graad van doctor aan de  
Erasmus Universiteit Rotterdam  
op gezag van de  
rector magnificus

Prof.dr. A.L. Bredenoord

en volgens besluit van het College voor Promoties.  
De openbare verdediging zal plaatsvinden op

woensdag 3 mei 2023 om 15.30 uur

door

Sai Ping Lau  
geboren te 's-Gravenhage.

## PROMOTIECOMMISSIE

Promotoren: Prof.dr. C.H.J. van Eijck  
Prof.dr. J.G.J.V. Aerts

Overige leden: Prof.dr. P.M. Van Hagen  
Prof.dr. J.W. Wilmink  
Dr. B.A. Bonsing

## TABLE OF CONTENTS

<b>Chapter 1</b>	Introduction and outline of this thesis	7
<b>Chapter 2</b>	Het pancreascarcinoom: toch niet immuun voor therapie? Ontwikkelingen in de immunotherapie voor ductaal adenocarcinoom van het pancreas (Dutch)	17
<b>Chapter 3</b>	Dendritic cell vaccination and CD40-agonist combination therapy licenses T cell-dependent antitumor immunity in a pancreatic carcinoma murine model	31
<b>Chapter 4</b>	Autologous dendritic cells pulsed with allogeneic tumour cell lysate induce tumour-reactive T-cell responses in patients with pancreatic cancer: A phase I study	77
<b>Chapter 5</b>	Dataset from a proteomics analysis of tumor antigens shared between an allogenic tumor cell lysate vaccine and pancreatic tumor tissue	121
<b>Chapter 6</b>	Rationally combining immunotherapies to improve efficacy of immune checkpoint blockade in solid tumors	133
<b>Chapter 7</b>	Safety and tumor-specific immunological responses of combined dendritic cell vaccination and anti-CD40 agonistic antibody treatment for patients with metastatic pancreatic cancer: protocol for a phase I, open-label, single-arm, dose-escalation study (REACTiVe-2 trial)	157
<b>Chapter 8</b>	Immunomodulatory effects of stereotactic body radiotherapy and vaccination with heat-killed mycobacterium obuense (IMM-101) in patients with locally advanced pancreatic cancer	181
<b>Chapter 9</b>	Discussion and future perspectives	205
<b>Chapter 10</b>	Summary	215
<b>Appendices</b>	List of publications	228
	List of contributing authors	232
	PhD portfolio	237
	Acknowledgements	238
	Curriculum vitae auctoris	245



# CHAPTER 1

---

Introduction and outline of this thesis





## INTRODUCTION

Immunotherapy rendered striking results and revolutionized treatment across numerous malignancies.(1-4) It has been endorsed as a new treatment modality and recently the Nobel Prize in Physiology/Medicine was awarded to two pioneers for their discovery of cancer therapy by inhibition of negative immune regulation. These so-called immune checkpoint blockers (ICB) induced clinical efficacy which led to the Food and Drug Administration (FDA) approval of ICB for various malignancies. In 2017 FDA granted accelerated approval to an anti-PD-1 ICB antibody for all solid tumors with mismatch repair deficiency or high microsatellite instability (MSI) underlining the impact of immunotherapy in medicine.

However, patients with pancreatic ductal adenocarcinoma (PDAC) are largely refractory to this kind of therapy.(1, 5, 6) This has been reasoned to be multifactorial. Contributing factors for PDAC are an immunosuppressive tumor microenvironment, sparseness of intratumoral effector T cells(7, 8), and a low tumor mutational burden.(9, 10) Nonetheless, further exploration of novel immune-based therapies in PDAC is desired as PDAC is the third-leading cause of cancer-related death in the United States and fourth in the Netherlands; and long-term survival of patients with PDAC treated with conventional treatment modalities is uncommon.(11, 12) The current mainstay of treatment for PDAC involves surgery, radio and/or chemotherapy. Surgical resection is performed with curative intent. However, only 20% of all patients diagnosed with PDAC is eligible for surgery.(13) Even after surgery, long-term survival is exceptional as the 5-year overall survival is less than 10%.(11) The majority of patients present with advanced disease. When appropriate, patients with advanced disease are treated with FOLFIRINOX, a combination chemotherapy consisting of fluorouracil, leucovorin, irinotecan and oxaliplatin. Also, the sequential use of FOLFIRINOX and stereotactic body radiotherapy (SBRT) has previously been investigated in patients with locally advanced pancreatic cancer (LAPC) in order to downstage disease for resection and promote radical resection.(14) For patients with metastatic disease, FOLFIRINOX is associated with survival advantage. A median overall survival of 11.1 months has been observed in metastatic cancer patients receiving FOLFIRINOX.(15) However, chemotherapy-related toxicity is as high as 60%, leading to early termination of treatment.(16, 17)

## PANCREATIC ADENOCARCINOMA IS A SITE OF IMMUNE PRIVILEGE

Cancer immunotherapy is a form of therapy able to augment our immune system in order to fight malignant neoplasms. The relation between our immune system and cancer cells has been illustrated by Chen and Mellman in their cancer-immunity cycle in which subsequent stepwise events leads to an anti-tumor immune response.(18) In short, the capture and processing of tumor-associated antigens by antigen presenting cells leads to the priming and activation of effector T cells. Homing of T cells and interaction of the T-cell receptor to their cognate tumor antigen presented by tumor cells on major histocompatibility complex (MHC) proteins leads to

cancer cell destruction and the release of more tumor-associated antigens. In the most optimal condition, this self-propagating immune response leads to absolute tumor control. However, in practice multiple tumor-specific defense and immune restricting mechanisms counteract these effector responses, and this tumor-immune imbalance leads to tumor growth. Although different tumors share plethora characteristics, each tumor also has its own characteristic defense mechanism leading to resistance against anti-tumor surveillance and defining its aggressiveness. A histopathological hallmark of pancreatic cancer is the presence of desmoplastic stroma. This creates a dense extracellular surrounding able to physically exclude effector T cells and contributing to an “immune-privileged” tumor microenvironment.(19) In addition, antigen presenting cells like conventional dendritic cells (cDC) are limited, and cDC-mediated T-cell priming is impaired during pancreatic carcinogenesis compared to other types of tumors.(20, 21) Immunosuppressive leukocytes in PDAC like regulatory T cells (Tregs) are able to directly restrain T-cell effector function or indirectly through inhibiting DC expansion.(22) It has also been demonstrated that tumor cell downregulation of surface MHC-I proteins through autophagy evades T cell recognition and increase the fitness of PDAC cells.(23) Furthermore, the recruitment of immunosuppressive myeloid cell populations can alter immunological and clinical outcome. The presence of immunosuppressive myeloid cells can lead to T-cell exclusion within the tumor microenvironment and high densities of CD15+ARG1+ granulocytic cells and tumor-associated M2-macrophages is associated with worse survival in patients with PDAC.(24, 25) At last, next to paucity, intratumoral CD8+ T cells display markers of exhaustion leading to diminished effector function and immune failure in pancreatic cancer.(7, 26)

## **THE ONCOIMMUNOLOGICAL EQUILIBRIUM BEARS MANY TARGETS**

The introduction of various immunotherapeutic agents acting at different levels within the cancer-immunity cycle can skew the balance in favor of anti-tumor immunity. Cancer vaccines, in the form of DC-based, peptide or whole tumor cell vaccines are able to prime circulating new or expand existing T-cell repertoires specific against tumor antigens and thereby break tolerance. Adoptive T-cell transfer in which (genetically engineered) T cells are infused into the patient can directly target cancer cells. Moreover, blocking negative immune-feedback mechanisms can “release” the brakes of our immune system. Antibodies targeting the PD-1/PD-L1 and CTLA-4/B7 axis have been tested comprehensively. Also, administration of other co-stimulatory agents such as STING, ICOS, CD40 agonists and pro-inflammatory cytokines (*e.g.* IL-12, IFN $\gamma$ ) can be supportive.(27, 28) Chemokine inhibitors like CCR2/CCR5 and CXCR2/CXCR4 antagonists hamper the entry of immunosuppressive cells into the tumor.(29, 30) Oncolytic viruses, chemo and radiotherapy can also act as immune modulators and enhance cancer immunosurveillance by for example inducing immunogenic cell death; the process of tumor cell killing, release of damage-associated molecular patterns (DAMPs) and tumor-associated antigens, and subsequent induction of innate and adaptive immune responses.(31, 32) Specific

for stroma-rich tumors, extracellular matrix modulation could promote tumor-infiltrating lymphocytes and may induce synergy with other immunotherapeutic options.

## IMMUNOLOGICAL OPPORTUNITIES IN PANCREATIC CANCER

In contrast to immune-inflamed “hot” tumors like melanoma and non-small cell lung cancer, patients with PDAC seem not to have survival benefits from current immunotherapeutic strategies. However, fundamental studies investigating the mechanical properties of PDAC hint at the potential of immunomodulation. In addition, recent seminal work with rational combination strategies in PDAC shows promising survival when immunogenicity is resurrected. A subset of PDAC patients with a high mutational burden and improved intra-tumoral lymphoid infiltration demonstrate superior survival compared to other patients with PDAC.(33-36) Patients with hypermutated microsatellite instability (MSI)-high PDAC tumors demonstrate response to checkpoint therapy.(37) However, these MSI-high tumors only comprise of <1% of all patients with PDAC. Furthermore, histopathological analysis demonstrated the upregulation of various alternative immune checkpoints (*e.g.* TIGIT, TIM-3, VISTA) in PDAC samples with high cytolytic activity, offering alternative ICB targets.(9) Also, the presence of T cells in tertiary lymphoid organs was associated with a favorable prognostic outcome in patients with PDAC.(38, 39) This observation support the potential effect of T-cell therapy in PDAC. Stomnes et al. previously engineered T cells expressing high-affinity T-cell receptor (TCR) against the tumor antigen mesothelin leading to infiltration of engineered cells in murine PDAC tumors and promoting survival.(40) Also, the vaccination of synthetic peptides, mimicking epitopes of tumor antigens, against mutant KRAS in patients with resected PDAC induced longevity T-cell reactivity.(41) Recently, durable tumor response was observed in a patient with previously progressive pancreatic cancer treated with autologous T cells transduced with TCRs targeting mutant KRAS G12D present on tumor cells.(42) Targeting the desmoplastic stroma of pancreatic cancer may also improve immunotherapy efficacy. It has been demonstrated that cancer-associated fibroblasts promote pancreatic tumor cell proliferation and invasion,(43) and targeting fibroblast activation protein (FAP) sensitized tumors to tumor vaccines and ICB.(44, 45) Furthermore, anti-CD40 combined with chemotherapy was able to induce T-cell dependent tumor regression and potentiates ICB efficacy in experimental PDAC models.(46) Anti-CD40 was able to restore dendritic cell function, increase tumor permeability and tumoricidal chemotherapy was used to induce antigen spilling.(20, 47, 48) The first results of the phase 1b PRINCE study combining anti-CD40 with chemotherapy with and without an ICB in patients with untreated metastatic PDAC demonstrated tolerability and clinical activity in 58% of the study patients.(49) These are a few examples illustrating the potency of immunotherapy in PDAC.

## AIMS AND OUTLINE OF THIS THESIS

In this thesis we aim to reveal mechanical insights and explore effective immunotherapeutic options for PDAC. In the second chapter we will elaborate on the PDAC tumor biology and most meaningful immunological treatment strategies investigated in PDAC. We will explore the use of dendritic cell-based therapy in a murine PDAC model and the potency of combination immunotherapy with a CD40 agonist in established pancreatic disease (Chapter 3). Also, extensive immunomonitoring will be performed to improve our understanding of therapeutic mechanisms of action. In Chapter 4, we translate our findings of dendritic cell-based therapy to patients with resected pancreatic cancer (REACTiVe trial), and go into detail in the technique and results behind the identification of tumor antigens found in study patients in the REACTiVe trial (Chapter 5). Next, we discuss combination strategies with immune checkpoint blockers for solid tumors (Chapter 6). In Chapter 7 we will set out the rationale and study protocol of the phase I dose-escalation REACTiVe-2 trial in which we combine dendritic cell vaccination and anti-CD40 agonistic antibody treatment for patients with metastatic pancreatic cancer. At last, the safety and immunomodulatory effects of stereotactic body radiotherapy and vaccination with the heat-inactivated *Mycobacterium obuense* (IMM-101) in patients with locally advanced pancreatic cancer will be presented (Chapter 8).

## REFERENCES

1. Brahmer JR, Tykodi SS, Chow LQ, Hwu WJ, Topalian SL, Hwu P, et al. Safety and activity of anti-PD-L1 antibody in patients with advanced cancer. *N Engl J Med*. 2012;366(26):2455-65.
2. Antonia SJ, López-Martin JA, Bendell J, Ott PA, Taylor M, Eder JP, et al. Nivolumab alone and nivolumab plus ipilimumab in recurrent small-cell lung cancer (CheckMate 032): a multicentre, open-label, phase 1/2 trial. *Lancet Oncol*. 2016;17(7):883-95.
3. Robert C, Long GV, Brady B, Dutriaux C, Maio M, Mortier L, et al. Nivolumab in previously untreated melanoma without BRAF mutation. *N Engl J Med*. 2015;372(4):320-30.
4. Borghaei H, Paz-Ares L, Horn L, Spigel DR, Steins M, Ready NE, et al. Nivolumab versus Docetaxel in Advanced Nonsquamous Non-Small-Cell Lung Cancer. *New England Journal of Medicine*. 2015;373(17):1627-39.
5. Royal RE, Levy C, Turner K, Mathur A, Hughes M, Kammula US, et al. Phase 2 trial of single agent Ipilimumab (anti-CTLA-4) for locally advanced or metastatic pancreatic adenocarcinoma. *J Immunother*. 2010;33(8):828-33.
6. O'Reilly EM, Oh D-Y, Dhani N, Renouf DJ, Lee MA, Sun W, et al. Durvalumab With or Without Tremelimumab for Patients With Metastatic Pancreatic Ductal Adenocarcinoma: A Phase 2 Randomized Clinical Trial. *JAMA Oncology*. 2019;5(10):1431-8.
7. Stromnes IM, Hulbert A, Pierce RH, Greenberg PD, Hingorani SR. T-cell Localization, Activation, and Clonal Expansion in Human Pancreatic Ductal Adenocarcinoma. *Cancer Immunol Res*. 2017;5(11):978-91.
8. Clark CE, Hingorani SR, Mick R, Combs C, Tuveson DA, Vonderheide RH. Dynamics of the immune reaction to pancreatic cancer from inception to invasion. *Cancer Res*. 2007;67(19):9518-27.
9. Balli D, Rech AJ, Stanger BZ, Vonderheide RH. Immune Cytolytic Activity Stratifies Molecular Subsets of Human Pancreatic Cancer. *Clin Cancer Res*. 2017;23(12):3129-38.
10. Alexandrov LB, Nik-Zainal S, Wedge DC, Aparicio SAJR, Behjati S, Biankin AV, et al. Signatures of mutational processes in human cancer. *Nature*. 2013;500(7463):415-21.
11. Siegel RL, Miller KD, Fuchs HE, Jemal A. Cancer statistics, 2022. *CA Cancer J Clin*. 2022;72(1):7-33.
12. Fest J, Ruiter R, van Rooij FJ, van der Geest LG, Lemmens VE, Ikram MA, et al. Underestimation of pancreatic cancer in the national cancer registry - Reconsidering the incidence and survival rates. *Eur J Cancer*. 2017;72:186-91.
13. Matsumoto I, Murakami Y, Shinzeki M, Asari S, Goto T, Tani M, et al. Proposed preoperative risk factors for early recurrence in patients with resectable pancreatic ductal adenocarcinoma after surgical resection: A multi-center retrospective study. *Pancreatology*. 2015;15(6):674-80.
14. Suker M, Nuyttens JJ, Eskens F, Haberkorn BCM, Coene PLO, van der Harst E, et al. Efficacy and feasibility of stereotactic radiotherapy after folfirinnox in patients with locally advanced pancreatic cancer (LAPC-1 trial). *EClinicalMedicine*. 2019;17:100200.
15. Conroy T, Desseigne F, Ychou M, Bouché O, Guimbaud R, Bécouarn Y, et al. FOLFIRINOX versus gemcitabine for metastatic pancreatic cancer. *N Engl J Med*. 2011;364(19):1817-25.
16. Thibodeau S, Voutsadakis IA. FOLFIRINOX Chemotherapy in Metastatic Pancreatic Cancer: A Systematic Review and Meta-Analysis of Retrospective and Phase II Studies. *J Clin Med*. 2018;7(1).
17. Suker M, Beumer BR, Sadot E, Marthey L, Faris JE, Mellon EA, et al. FOLFIRINOX for locally advanced pancreatic cancer: a systematic review and patient-level meta-analysis. *Lancet Oncol*. 2016;17(6):801-10.
18. Chen DS, Mellman I. Oncology meets immunology: the cancer-immunity cycle. *Immunity*. 2013;39(1):1-10.
19. Whatcott CJ PR, Von Hoff DD, et al. . Desmoplasia and chemoresistance in pancreatic cancer.2012.

20. Lin JH, Huffman AP, Wattenberg MM, Walter DM, Carpenter EL, Feldser DM, et al. Type 1 conventional dendritic cells are systemically dysregulated early in pancreatic carcinogenesis. *J Exp Med*. 2020;217(8).
21. Hegde S, Krishawan VE, Herzog BH, Zuo C, Breden MA, Knolhoff BL, et al. Dendritic Cell Paucity Leads to Dysfunctional Immune Surveillance in Pancreatic Cancer. *Cancer Cell*. 2020;37(3):289-307 e9.
22. Jang JE, Hajdu CH, Liot C, Miller G, Dustin ML, Bar-Sagi D. Crosstalk between Regulatory T Cells and Tumor-Associated Dendritic Cells Negates Anti-tumor Immunity in Pancreatic Cancer. *Cell Rep*. 2017;20(3):558-71.
23. Yamamoto K, Venida A, Yano J, Biancur DE, Kakiuchi M, Gupta S, et al. Autophagy promotes immune evasion of pancreatic cancer by degrading MHC-I. *Nature*. 2020;581(7806):100-5.
24. Väyrynen SA, Zhang J, Yuan C, Väyrynen JP, Dias Costa A, Williams H, et al. Composition, Spatial Characteristics, and Prognostic Significance of Myeloid Cell Infiltration in Pancreatic Cancer. *Clin Cancer Res*. 2021;27(4):1069-81.
25. Vonderheide RH, Bear AS. Tumor-Derived Myeloid Cell Chemoattractants and T Cell Exclusion in Pancreatic Cancer. *Front Immunol*. 2020;11:605619.
26. Steele NG, Carpenter ES, Kemp SB, Sirihorachai VR, The S, Delrosario L, et al. Multimodal mapping of the tumor and peripheral blood immune landscape in human pancreatic cancer. *Nature Cancer*. 2020;1(11):1097-112.
27. Dougan M, Ingram JR, Jeong HJ, Mosaheb MM, Bruck PT, Ali L, et al. Targeting Cytokine Therapy to the Pancreatic Tumor Microenvironment Using PD-L1-Specific VHHs. *Cancer Immunol Res*. 2018;6(4):389-401.
28. Wang P, Li X, Wang J, Gao D, Li Y, Li H, et al. Re-designing Interleukin-12 to enhance its safety and potential as an anti-tumor immunotherapeutic agent. *Nature Communications*. 2017;8(1):1395.
29. Nywening TM, Wang-Gillam A, Sanford DE, Belt BA, Panni RZ, Cusworth BM, et al. Targeting tumour-associated macrophages with CCR2 inhibition in combination with FOLFIRINOX in patients with borderline resectable and locally advanced pancreatic cancer: a single-centre, open-label, dose-finding, non-randomised, phase 1b trial. *Lancet Oncol*. 2016;17(5):651-62.
30. Steele CW, Karim SA, Leach JDG, Bailey P, Upstill-Goddard R, Rishi L, et al. CXCR2 Inhibition Profoundly Suppresses Metastases and Augments Immunotherapy in Pancreatic Ductal Adenocarcinoma. *Cancer Cell*. 2016;29(6):832-45.
31. Ye J, Mills BN, Zhao T, Han BJ, Murphy JD, Patel AP, et al. Assessing the Magnitude of Immunogenic Cell Death Following Chemotherapy and Irradiation Reveals a New Strategy to Treat Pancreatic Cancer. *Cancer Immunol Res*. 2020;8(1):94-107.
32. Araki H, Tazawa H, Kanaya N, Kajiwara Y, Yamada M, Hashimoto M, et al. Oncolytic virus-mediated p53 overexpression promotes immunogenic cell death and efficacy of PD-1 blockade in pancreatic cancer. *Mol Ther Oncolytics*. 2022;27:3-13.
33. Ino Y, Yamazaki-Itoh R, Shimada K, Iwasaki M, Kosuge T, Kanai Y, et al. Immune cell infiltration as an indicator of the immune microenvironment of pancreatic cancer. *Br J Cancer*. 2013;108(4):914-23.
34. Balachandran VP, Łuksza M, Zhao JN, Makarov V, Moral JA, Remark R, et al. Identification of unique neoantigen qualities in long-term survivors of pancreatic cancer. *Nature*. 2017;551(7681):512-6.
35. Lupinacci RM, Goloudina A, Buhard O, Bachet JB, Maréchal R, Demetter P, et al. Prevalence of Microsatellite Instability in Intraductal Papillary Mucinous Neoplasms of the Pancreas. *Gastroenterology*. 2018;154(4):1061-5.
36. Humphris JL, Patch AM, Nones K, Bailey PJ, Johns AL, McKay S, et al. Hypermutation In Pancreatic Cancer. *Gastroenterology*. 2017;152(1):68-74 e2.
37. Le DT, Durham JN, Smith KN, Wang H, Bartlett BR, Aulakh LK, et al. Mismatch repair deficiency predicts response of solid tumors to PD-1 blockade. *Science*. 2017;357(6349):409-13.
38. Hiraoka N, Ino Y, Yamazaki-Itoh R, Kanai Y, Kosuge T, Shimada K. Intratumoral tertiary lymphoid organ is a favourable prognosticator in patients with pancreatic cancer. *Br J Cancer*. 2015;112(11):1782-90.

39. Poschke I, Faryna M, Bergmann F, Flossdorf M, Lauenstein C, Hermes J, et al. Identification of a tumor-reactive T-cell repertoire in the immune infiltrate of patients with resectable pancreatic ductal adenocarcinoma. *Oncoimmunology*. 2016;5(12):e1240859.
40. Stromnes Ingunn M, Schmitt Thomas M, Hulbert A, Brockenbrough JS, Nguyen Hieu N, Cuevas C, et al. T Cells Engineered against a Native Antigen Can Surmount Immunologic and Physical Barriers to Treat Pancreatic Ductal Adenocarcinoma. *Cancer Cell*. 2015;28(5):638-52.
41. Wedén S, Klemp M, Gladhaug IP, Møller M, Eriksen JA, Gaudernack G, et al. Long-term follow-up of patients with resected pancreatic cancer following vaccination against mutant K-ras. *International Journal of Cancer*. 2011;128(5):1120-8.
42. Leidner R, Sanjuan Silva N, Huang H, Sprott D, Zheng C, Shih YP, et al. Neoantigen T-Cell Receptor Gene Therapy in Pancreatic Cancer. *N Engl J Med*. 2022;386(22):2112-9.
43. Hwang RF, Moore T, Arumugam T, Ramachandran V, Amos KD, Rivera A, et al. Cancer-associated stromal fibroblasts promote pancreatic tumor progression. *Cancer Res*. 2008;68(3):918-26.
44. Feig C, Jones JO, Kraman M, Wells RJ, Deonarine A, Chan DS, et al. Targeting CXCL12 from FAP-expressing carcinoma-associated fibroblasts synergizes with anti-PD-L1 immunotherapy in pancreatic cancer. *Proc Natl Acad Sci U S A*. 2013;110(50):20212-7.
45. Kraman M, Bambrough PJ, Arnold JN, Roberts EW, Magiera L, Jones JO, et al. Suppression of antitumor immunity by stromal cells expressing fibroblast activation protein- $\alpha$ . *Science*. 2010;330(6005):827-30.
46. Winograd R, Byrne KT, Evans RA, Odorizzi PM, Meyer AR, Bajor DL, et al. Induction of T-cell Immunity Overcomes Complete Resistance to PD-1 and CTLA-4 Blockade and Improves Survival in Pancreatic Carcinoma. *Cancer Immunol Res*. 2015;3(4):399-411.
47. Byrne Katelyn T, Vonderheide Robert H. CD40 Stimulation Obviates Innate Sensors and Drives T Cell Immunity in Cancer. *Cell Rep*. 2016;15(12):2719-32.
48. Beatty GL, Chiorean EG, Fishman MP, Saboury B, Teitelbaum UR, Sun W, et al. CD40 agonists alter tumor stroma and show efficacy against pancreatic carcinoma in mice and humans. *Science*. 2011;331(6024):1612-6.
49. O'Hara MH, O'Reilly EM, Varadhachary G, Wolff RA, Wainberg ZA, Ko AH, et al. CD40 agonistic monoclonal antibody APX005M (sotigalimab) and chemotherapy, with or without nivolumab, for the treatment of metastatic pancreatic adenocarcinoma: an open-label, multicentre, phase 1b study. *Lancet Oncol*. 2021;22(1):118-31.





# CHAPTER 2

---

Het pancreascarcinoom: toch niet immuun voor therapie?  
Ontwikkelingen in de immunotherapie voor ductaal adenocarcinoom  
van het pancreas

Pancreatic cancer: immune for therapy? Advances in immunotherapy  
for pancreatic ductal adenocarcinoma

Sai Ping Lau  
Floris Dammeijer  
Casper H.J. van Eijck

## **SAMENVATTING**

Het pancreas ductaal adenocarcinoom (PDAC) staat bekend om zijn resistentie voor de huidige therapeutische behandelingen en zijn slechte prognose. Chirurgie en nieuwe chemotherapeutische ontwikkelingen zijn niet in staat om de overleving sterk te verbeteren. Alhoewel immuuntherapie spectaculaire resultaten heeft geleverd in verschillende typen kankers, blijven de successen bij PDAC uit. Tumor-intrinsieke factoren die specifiek zijn voor PDAC dragen bij aan de agressieve aard van de tumor en kunnen verklaring bieden voor de resistentie van immuuntherapie. In dit overzichtsartikel worden de tumorbiologie van PDAC besproken en wordt uitgelegd hoe immuuntherapie bij dit type tumor succesvol zou kunnen worden geïmplementeerd.

## **SUMMARY**

Pancreatic ductal adenocarcinoma (PDAC) is notorious for its therapeutic resistance and dismal prognosis. Surgery and new chemotherapeutic strategies are not capable to significantly improve survival. Although immunotherapy yields striking results in various malignancies, clinical responses in pancreatic cancer have been disappointing. Tumor intrinsic factors specific for PDAC contribute to the aggressive nature of the tumor and could explain its relative resistance to immunotherapy. In this overview article we will discuss the tumor biology driving PDAC and demonstrate how immunotherapy can be successfully implemented in this type of cancer.

## INLEIDING

Ductaal adenocarcinoom van de pancreas (PDAC) is één van de meest agressieve en lethale tumoren en wordt traditioneel behandeld met chirurgie, chemotherapie of een combinatie van beide. PDAC is op dit moment de derde en vierde grootste oorzaak van kanker-gerelateerde dood in respectievelijk Europa en de Verenigde Staten met een verwachte mortaliteit van 88.900 en 44.330.<sup>1,2</sup> Deze getallen stijgen en in 2030 wordt PDAC waarschijnlijk de op één na grootste oorzaak van kanker-gerelateerde dood.<sup>3</sup> In Nederland krijgen jaarlijks 3.500 mensen de diagnose pancreascarcinoom.<sup>4</sup> De 5-jaarsoverleving van alle stadia is beperkt en ligt onder 10%.<sup>1</sup> Patiënten bij wie de tumor kan worden geresecteerd hebben een betere prognose. Helaas ontwikkelt 30% van alle geopereerde patiënten binnen een jaar een recidief.<sup>5</sup> Met de toepassing van de huidige chemotherapeutische regimes wordt de prognose langzaam beter. In eerste instantie met de introductie van gemcitabine in combinatie met capecitabine dat een zeer bescheiden overlevingswinst gaf.<sup>6</sup> Meer recentelijk demonstreerden Conroy *et al.* dat geresecteerde patiënten met een adjuvant gemodificeerd FOLFIRINOX (5-fluorouracil, leucovorine, irinotecan en oxaliplatine)-regime een verbeterde mediane algehele overleving (mOS) hadden van 54,4 maanden, in vergelijking met 35,0 maanden in de gemcitabine-monotherapiegroep.<sup>5</sup> Dit is voor het pancreascarcinoom zeer veelbelovend. Het overgrote gedeelte van de patiënten presenteert zich echter niet met een resectabel pancreascarcinoom. Voor patiënten met gemetastaseerde ziekte wordt afgewogen tussen 'best supportive care' alleen of gecombineerd met palliatieve systeemtherapie met FOLFIRINOX of gemcitabine + nab-paclitaxel waarbij de mediane winst van deze behandeling in maanden uit te drukken is.<sup>7,8</sup> Langetermijnoverlevenden komen nauwelijks voor en genezing is zelden aan de orde. Er valt dus nog veel winst te behalen in de behandeling en overleving van PDAC. Gezien de beperkte meerwaarde van chemotherapie bij PDAC gaat veel onderzoek uit naar de ontwikkeling van innovatieve methoden om deze tumor gevoelig te maken voor therapie. Immunotherapie heeft het afgelopen decennium in verschillende voorheen (chemo)therapieresistente maligniteiten indrukwekkende resultaten laten zien en is in enkele gevallen al eerstelijnsbehandeling in de gemetastaseerde setting.<sup>9-11</sup> Met deze vorm van therapie wordt een anti-tumorrespons bewerkstelligd door het eigen immuunsysteem, voornamelijk T-cellen, te stimuleren dan wel te ondersteunen in het elimineren van kankercellen. Ondanks dat de aanwezigheid van intratumorale T-cellen bij PDAC-patiënten gecorreleerd is met een betere prognose, blijven successen met immunotherapie voor deze vorm van kanker uit.<sup>12</sup> Recente inzichten in de immunobiologie van PDAC bieden echter handvatten die succesvolle toepassing van immunotherapie voor pancreaskanker op den duur mogelijk kunnen maken. In dit overzichtsartikel worden de unieke immuno-oncologische aspecten van PDAC besproken, hoopvolle immunotherapeutische strategieën aangestipt en onze kijk gegeven op hoe immunotherapie bij dit type tumor succesvol zou kunnen worden geïmplementeerd.

## DE TUMORBIOLOGIE VAN PDAC

### TUMOR-IMMUNOGENICITEIT EN T-CELSTATUS

PDAC staat berucht als een weinig immunogene, immunologisch 'koude' tumor die weinig gevoelig is voor behandelingen die erop gericht zijn om een bestaande immuunrespons te versterken. Zo waren er in onderzoeken die het effect van mono- of combinatietherapie met immuun-'checkpoint'-remmers zoals 'anti-cytotoxic T-lymphocyte-associated protein 4' (CTLA-4; ipilimumab, tremelimumab) en/of anti-PD-(ligand)1 (pembrolizumab, durvalumab) onderzochten vrijwel geen responders (zie Tabel 1).<sup>13-15</sup> Recente aanwijzingen in de PDAC-literatuur onderschrijven echter enkele basale benodigheden die van essentieel belang zijn om deze tumoren toch gevoelig te maken voor het immuunsysteem. Effector-T-cellen staan centraal in de anti-tumorrespons en hebben de capaciteit om tumorcellen gericht te elimineren. Helaas bezit PDAC relatief weinig intratumorale T-lymfocyten.<sup>16</sup> Intrinsieke eigenschappen van de tumorcel verklaren deze bevinding ten dele. PDAC-cellen discrimineren zich van andere tumoren zoals melanoom en longkanker door weinig DNA-mutaties, wat verband houdt met de afwezigheid van sterke mutagene risicofactoren als UV-straling en tabaksrook.<sup>17</sup> De omvang van het aantal mutaties per megabase DNA, ook wel 'tumor mutational burden' (TMB) genoemd, gaat gepaard met de ontwikkeling van kanker-specifieke neo-antigenen, die op hun beurt robuuste T-celreacties kunnen uitlokken. Balachandran *et al.* demonstreerden dat zeldzame langetermijnoverlevers van PDAC in het bezit zijn van T-cellen gericht tegen specifieke neo-antigenen, waaronder het MUC16-eiwit.<sup>12</sup> Verdere ondersteuning voor het belang van neo-antigenen en immunogeniciteit komt uit een beperkte subpopulatie van PDAC-patiënten ( $\pm 1-2\%$ ) met tumordefecten in DNA-reparatie-eiwitten ('mismatch-repair'-deficiënt; dMMR), waardoor deze tumoren microsatellietinstabiel (MSI) en zeer mutatierijk worden. Recentelijk rapporteerden Le *et al.* dat progressief gemetastaseerde patiënten met dMMR, ongeacht het type tumor, gevoelig zijn voor anti-PD-1-blokkade.<sup>18</sup> In dit onderzoek waren zes evalueerbare dMMR-PDAC-patiënten opgenomen die allen respondeerden op pembrolizumab. Dit bevestigt dat het aantal mutaties gecorreleerd is aan de tumorimmunogeniciteit en verklaart ten dele waarom mutatierijke tumoren zoals niet-kleincelling longkanker en melanomen gevoelig kunnen zijn voor immuun-'checkpoint'-remmers.<sup>19,20</sup> Deze resultaten hebben ertoe geleid dat in mei 2017 de 'U.S. Food and Drug Administration' (FDA) de indicatie voor pembrolizumab (anti-PD-1) heeft verbreed naar MSI-high of dMMR-tumoren.<sup>21</sup> Het is dus voor het eerst dat niet naar het type tumor, maar naar de biologische eigenschap van een tumor wordt gekeken. Echter is maar 1-2% van alle PDAC-tumoren dMMR of MSI-high.<sup>22</sup> Naast de dMMR-subgroep zijn er mogelijk andere moleculair definieerbare subgroepen van PDAC-patiënten die gevoelig zouden kunnen zijn voor immuuntherapie. Zo beschrijven Bailey *et al.* en een jaar later Vonderheide een immunogeen/cytotoxisch T-cel-geïnfiltreerd type PDAC, met expressie van meerdere 'checkpoints'.<sup>23,24</sup> Het is vooralsnog onduidelijk of selectie van patiënten op basis van de moleculaire opmaak van de tumor ook werkelijk leidt tot betere responspercentages op

therapie. Aangezien het gros van de PDAC-patiënten geen dMMR-fenotype bezit, moet worden gezocht naar methoden om de immunogeniciteit van deze tumor te verhogen of de anti-tumorimmunitet verder te ondersteunen. Het is bekend dat chemo- of radiotherapie kan zorgen voor immunogene celdood en het aantal neo-antigenen in de tumor kan verhogen.<sup>25,26</sup> Tevens kunnen chemo- en radiotherapie zorgen voor directe tumordestructie waarbij tumorantigenen en immuun-activerende signaaleiwitten vrijkomen. Antigeen-presenterende cellen (zoals dendritische cellen) kunnen op hun beurt tumorantigenen aan effector-T-cellen presenteren, waardoor T-cellen in staat zijn om tumorcellen te herkennen.<sup>27</sup>

**TABEL 1.** Belangrijke uitgevoerde klinische onderzoeken met immuuntherapie bij ductaal adenocarcinoom van de pancreas.

Onderzoek	Fase	Aantal patiënten	Type immuuntherapie	Stadium PDAC	Resultaten (ORR)
Brahmer et al. (2012) <sup>13</sup>	1	14	Anti-PD-L1	IV	ORR 0%
Royal et al. (2010) <sup>14</sup>	2	27	Anti-CTLA-4	IV	ORR 0%
O'Reilly et al. (2019) <sup>72</sup>	2	64	Anti-CTLA-4 +/- anti-PD-L1	IV	Monotherapie (anti-CTLA-4): ORR 0% Combinatietherapie: ORR 3,2%
Le et al. (2017) <sup>18</sup>	2	8	Anti-PD-1	IV (dMMR)	6/8 evalueerbaar ORR 83%; 2 CR, 3 PR, 1 SD
Nywening et al. (2016) <sup>51</sup>	1b	39	Anti-CCR2 + FOLFIRINOX	III-IV	33/39 evalueerbaar ORR 49%; 16 PR, 16 SD, 1 PD
Hingorani et al. (2018) <sup>61</sup>	2	166	PEGPH20 + gemcitabine/ nab-paclitaxel	IV	139/166 evalueerbaar ORR 40%; 1 CR (hogere ORR in hoog-hyaluronan-positieve tumoren)
Beatty et al. (2011) <sup>64</sup>	1	21	CD40-agonist + gemcitabine	III-IV	19/21 evalueerbaar ORR 18%; 4 PR, 11 SD, 4 PD
Middleton et al. (2014) <sup>29</sup>	3	704	GV1001 + gemcitabine/ capecitabine (sequentieel of tegelijk)	IV	ORR 7,7%
Le et al. (2019) <sup>33</sup>	3	102	GVAX + CRS-207 + cyclofosfamide	IV	94/102 evalueerbaar ORR 1%; 1 PR, 22 SD
Beatty et al. (2018) <sup>39</sup>	1	6	Mesotheline-specifieke CAR-T-celtherapie	IV	ORR: 0%; 2 SD
Jiang et al. (2017) <sup>73</sup>	1/2	36	DC-CIK +/- S-1	III-IV	ORR: 0%; 25 SD

ORR='objective response rate', PD='progressive disease', SD='stable disease', PR='partial response', CR='complete response', DC-CIK='dendritic cell/cytokine-induced killer cell'.

'Checkpoint'-remmers	Immuunmodulatoren	Tumovaccins	Cellulaire therapie
----------------------	-------------------	-------------	---------------------

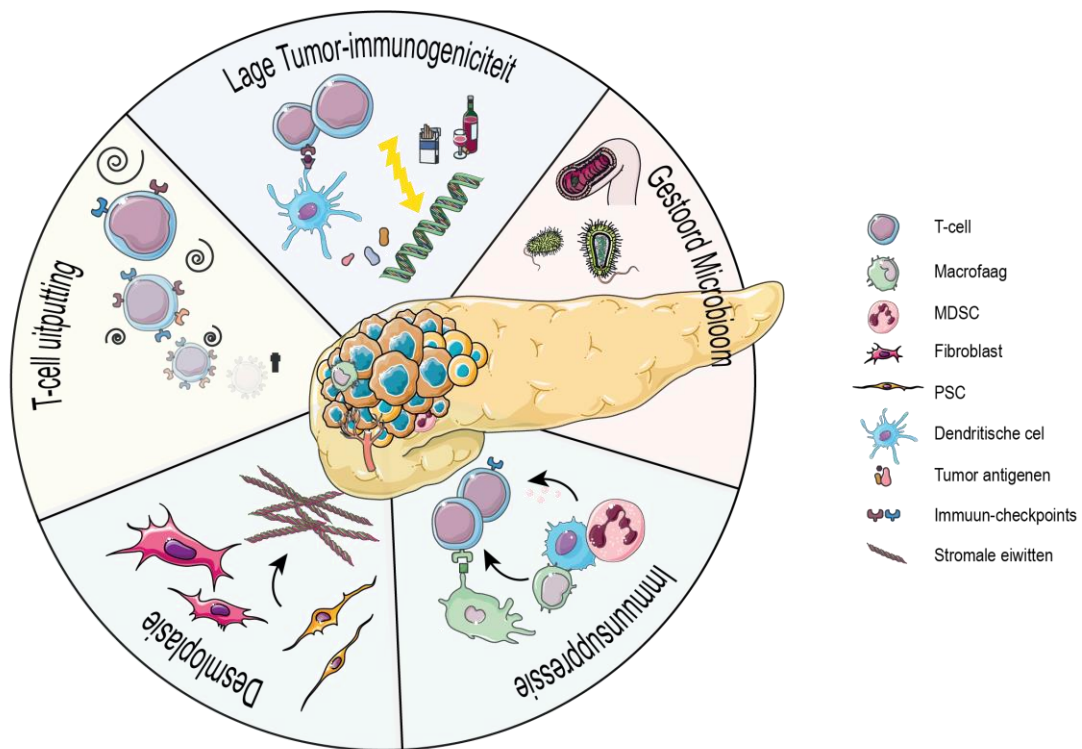
Een andere meer experimentele aanpak omvat het gebruik van oncolytische virussen om specifiek tumorcellen te infecteren en zo in een immunogene context anti-tumorimmunitet op te wekken. Deze aanpak is recentelijk onderzocht in een vroege fase van klinisch onderzoek bij melanoom en bleek effectief in het verhogen van T-celinfiltratie in tumoren en toonde op zijn beurt synergie met anti-PD-1-therapie.<sup>28</sup> Een in het verleden vaker toegepaste manier om de tumorspecifieke afweer te ondersteunen is het gebruik van peptidevaccins. Grote fase 3-onderzoeken met peptidevaccins zijn echter vroegtijdig gestaakt wegens tekort aan effectiviteit en laten tot nu toe bij PDAC-patiënten geen duidelijke overlevingswinst zien.<sup>29,30</sup> Een andere noemenswaardige vaccinatiestrategie voor PDAC is GVAX. Dit vaccin is gebaseerd op bestraalde allogene PDAC-tumorcellen, en gevaccineerde patiënten ontwikkelden mesotheline-specifieke effector-T-cellen die correleerden met verbeterende ziektevrije overleving.<sup>31</sup> In een onderzoek met gemetastaseerde PDAC-patiënten werd GVAX gecombineerd met ipilimumab (anti-CTLA-4). Dit leverde een 1-jaarsoverleving van 27% op in de combinatietherapiegroep versus 7% in de ipilimumabmonotherapiegroep.<sup>32</sup> Latere onderzoeken waarbij GVAX werd gecombineerd met chemotherapie lieten geen overlevingswinst zien.<sup>33</sup> Een andere manier om antigenpresentatie van tumor-antigenen te bespoedigen is door middel van dendritische cel (DC)-vaccinatie, waarbij DC's van de patiënt *ex vivo* worden beladen met (geselecteerde) tumorantigenen en vervolgens worden teruggegeven om dan direct T-cellen aan te zetten tot tumorherkenning en-destructie. Hierbij wordt de in potentie ineffectieve *in situ*-opname en verwerking van tumorantigenen door DC's en potentiële tolerantie omzeilt. Tot nu toe is er een tental fase 1/2-onderzoeken gedaan bij PDAC-patiënten waarbij gebruik wordt gemaakt van verschillende tumorantigenen (zoals MUC1, WT1, mesotheline, KRAS, hTERT, CEA) of lysaat van tumormateriaal.<sup>34</sup> Deze vorm van therapie is relatief veilig en partiële en complete responders zijn gerapporteerd, maar groter fase 3-onderzoek is nodig om effectiviteit aan te tonen. Een recentelijk gestart fase 2-onderzoek in het Erasmus MC onderzoekt de haalbaarheid van DC-therapie in de adjuvante setting na chirurgische resectie met als doel langdurige tumorsurveillance van het immuunsysteem te bewerkstelligen en de kans op een recidief te verlagen (NTR NL7432). Preklinische resultaten in translationale PDAC-modellen tonen effectiviteit van deze DC-therapie bij lage ziektelast. Of dit bij patiënten ook het geval is moet worden afgewacht (Lau *et al.*; manuscript in voorbereiding). Ten slotte kan direct op de T-cellen worden aangegrepen door genetisch gemodificeerde, tumorspecifieke T-cellen te injecteren die de tumor kunnen infiltreren en elimineren. Verschillende vormen van T-celtherapie, waaronder 'chimeric antigen receptor' (CAR)-T-cellen zijn mogelijk erg potent, maar ook potentieel toxisch wegens kruisreactiviteit tussen het beoogde neo-antigen en bijna-identieke eiwitten in gezond weefsel. Dit heeft in het verleden geleid tot neuro- en cardiotoxiciteit.<sup>35-37</sup> Alhoewel CAR-T-cellen bij hematologische maligniteiten als acute lymfatische leukemie en multipel myeloom veelbelovende resultaten opleveren, is het responspercentage bij solide tumoren vooralsnog laag.<sup>38</sup> Beatty *et al.* waren recentelijk in staat om mesotheline-specifieke CAR-T-cellen te genereren die bij chemotherapie-refractaire en gemetastaseerde PDAC-patiënten in staat bleken om anti-tumorimmunitet en klinische respons op te wekken.<sup>39</sup> Op het moment dat effectieve

anti-tumorimmunititeit wordt bewerkstelligd, is T-cel-uitputting een andere barrière die moet worden overwonnen. Onderzoeken laten zien dat de aanwezigheid van meerdere co-inhibitoire receptoren (zoals PD-1, CTLA-4, TIM-3, LAG-3, VISTA) sterk indicatief is voor T-cel-uitputting en disfunctie. Alhoewel we op dit moment met 'checkpoint'-remmers voornamelijk gefocust zijn op PD-(L)1 en CTLA-4, zijn er aanwijzingen dat T-cellen in PDAC-tumoren ook andere 'checkpoints' opreguleren die wellicht de rol van PD-1 en CTLA-4 kunnen overnemen (zoals VISTA).<sup>40</sup>

## DE IMMUUNSUPPRESSIEVE TUMOROMGEVING

PDAC-cellen zijn meester in camouflage en in staat het immuunsysteem naar hun hand te zetten. De tumorcellen zijn in staat verschillende cytokines en chemokines te produceren die leiden tot de rekrutering van verscheidene immuunsuppressieve cellen die vervolgens weer in staat zijn om T-cellen te remmen. De productie van chemokines als GM-CSF en CCL-2 kan zorgen voor aantrekking van 'myeloid-derived suppressor cells' (MDSC's), en CSF-1 en BAG-3 voor immuunsuppressieve macrofagen.<sup>41-43</sup> Cellen als MDSC's en macrofagen kunnen T-cellen direct onderdrukken door middel van opregulatie van PD-L1, en indirect door de productie van immuunsuppressieve stoffen zoals IL-6, IL-10 en indolamine-2,3-dioxygenase (IDO).<sup>44</sup> Ook regulatoire T-cellen zijn in staat om suppressieve cytokines zoals IL-10 en TGF $\beta$  te produceren en daarbij de anti-tumorimmunititeit te belemmeren en tumorgroei te bevorderen.<sup>45</sup> Daarnaast is aangetoond dat de tumorcellen ook effector-T-cellen kunnen excluderen door de productie van CXCL1.<sup>46</sup> Een aantal middelen is ontworpen om deze immuunsuppressieve cellen te depletieren of fundamenteel te wijzigen. De meeste onderzoeken zijn nog in vroeg-klinische fasen, waardoor het nut van deze therapieën moet worden afgewacht.<sup>47-49</sup> Bij muizen met PDAC zorgde blokkade van de receptor van CCL2 (CCR2) voor de depletie van intratumorale macrofagen en voor betere anti-tumorimmunititeit, verminderde tumorgroei en minder metastasen.<sup>50</sup> Bovendien hadden PDAC-patiënten met hoge intratumorale CCL-2-spiegels een slechtere overleving. Blokkade van CCR2 in combinatie met FOLFIRINOX bij niet-gemetastaseerde PDAC-patiënten zorgde voor een objectief radiografisch responspercentage van 49% (16/33) in tegenstelling tot 0% (0/5) voor de FOLFIRINOX-monotherapiegroep.<sup>51</sup> Naast immunogene celdood kan chemotherapie ook de immuuncelcompositie lokaal beïnvloeden. Gemcitabine en 5-FU (onderdeel van FOLFIRINOX) worden vaak gebruikt bij de behandeling van PDAC. In preklinische onderzoeken waren beide chemotherapeutica in staat om MDSC's effectief te depletieren.<sup>52,53</sup> Hoewel de aanwezigheid van intratumorale CD163+ macrofagen gecorreleerd is met slechtere overleving van PDAC-patiënten, zijn er tot nu toe nog geen klinische resultaten bekend met CSF1/CSF-1R-remmers.<sup>54</sup>





**Figuur 1.** De tumor-immunobiologie van PDAC. MDSC='myeloid-derived suppressor cells', PSC='pancreatic stellate cells'.

## DE DESMOPLASTISCHE REACTIE IN PDAC

De grootste component van PDAC bestaat vaak niet uit cellulair infiltraat, maar uit desmoplastisch stroma. Fibroblasten en 'pancreatic stellate cells' (PSC's) zijn rijk aanwezig in PDAC en moduleren de tumoromgeving en produceren verschillende extracellulaire matrixeiwitten, zoals collagenen en hyaluronzuur, die resulteren in een dichts tumorstroma.<sup>55</sup> De prominente aanwezigheid van tumorstroma verklaart deels de agressieve aard van PDAC; het fungeert als een fysieke barrière, beperkt de microvascularisatie en stimuleert een hypoxische omgeving, wat leidt tot de exclusie van effector-T-cellen en het falen van chemoradiatietherapie.<sup>55,56</sup> Er wordt dan ook veel onderzoek gedaan naar de preventie van stromavorming en stromalytische therapieën. Tumorcellen kunnen door CXCL12-productie kanker-geassocieerde fibroblasten (CAF's) rekruteren. In een muismodel lieten Fieg *et al.* zien dat CXCL12/CXCR4-blokkade zorgde voor verhoogde aantallen van intratumorale T-cellen en PDAC-tumoren gevoelig kan maken voor 'checkpoint'-therapie.<sup>57</sup> Er zijn ook verschillende therapieën om tumorstroma direct te lyseren. Hyaluronzuurremmers zorgden in muisonderzoeken voor de normalisering van de intratumorale druk, verbetering van de microcirculatie en daarbij ook betere penetrantie van geneesmiddelen.<sup>58,59</sup> In een fase 1/2-onderzoek werd gepegyleerd hyaluronidase (PEGPH20) in combinatie met chemotherapie toegepast bij patiënten met gemetastaseerd PDAC.<sup>60</sup> Patiënten met hoge hyaluronzuurwaarden hadden een OS van 13,0 maanden, terwijl bij patiënten met lage waarden een OS van 5,7 maanden werd gerapporteerd. In een groter fase 2-onderzoek was de progressievrije overleving significant verbeterd ten opzichte van de chemotherapiegroep.<sup>61</sup> Verder zijn CD40-agonisten

eveneens in staat gebleken om de tumor meer toegankelijk te maken voor het immuunsysteem. CD40 zit onder andere op tumorale macrofagen en bij binding aan deze receptor worden deze cellen geactiveerd om verschillende enzymen (zoals matrix-metallo-proteasen) te produceren die het stroma kunnen degraderen.<sup>62,63</sup> Beatty *et al.* lieten in een klein cohortonderzoek met niet-operabele PDAC-patiënten veelbelovende resultaten zien van CD40-agonistische antistoffen.<sup>64</sup> Op basis van de RECIST-criteria hadden vier van de 21 patiënten een partiële respons, 11 patiënten stabiele ziekte en vier patiënten waren progressief onder therapie. Grotere onderzoeken zijn gaande. Ook TGFβ zou mogelijk in de toekomst een potentieel doel kunnen zijn. Bij patiënten met gemetastaseerd urotheelcarcinoom was TGFβ-signalering in fibroblasten een belangrijke voorspeller voor klinische uitkomst. In muismodellen van urotheel en colorectaal carcinoom konden wetenschappers door middel van TGFβ-blokkering de tumor permeabel maken. Deze weinig-immunogene tumoren hadden na therapie verhoogde T-celinfiltraten en waren niet in staat om adequaat te groeien of te metastaseren.<sup>65,66</sup> Gezien het werkingsmechanisme op fibroblasten en collageenrijk stroma zou dit mogelijk ook voordelig kunnen zijn voor de behandeling van PDAC-patiënten.

Type immunotherapie	Stadium PDAC	Interim-resultaten	NTC-nummers
Anti-PD-L1 + anti-CSF1-R	IV	-	NCT02777710
Anti-PD-L1 + anti-CSF1-R + SBRT	III	-	NCT03599362
Anti-PD-L1 + GVAX + anti-CSF1-R + cyclofosfamide	III	-	NCT03153410
Anti-PD-L1 +/- FAK-remmer	I-II	-	NCT03727880
Anti-PD-L1 + FAK-remmer + gemcitabine	I-IV	-	NCT02546531
Anti-CD40 +/- Flt3L	III-IV	-	NCT03329950
Anti-CD40 + gemcitabine + nab-paclitaxel +/- anti-PD-1	IV	23/30 evalueerbaar ORR: 61%, 8 SD, 14 PR, 1 PD	NCT03214250
Anti-PD-1 + anti-CCR2/CCR5 + GVAX	III	-	NCT03767582
Anti-CXCR4	III-IV	-	NCT03277209
Neo-antigeen peptide vaccin + Poly ICLC	I, II	-	NCT03956056
Multi-antigeen specifieke T-cellen	I-IV	7/p evalueerbaar ORR: 43%, 3 SD, 2 PR, 1 CR, 1 PD	NCT03192462

**Tabel 2.** Noemenswaardige lpoende fase 1/2 (combinatie)immunotherapieonderzoeken bij het ductaal adenocarcinoom van de pancreas. ORR = objective response rate, PD = progressive disease, SD = stable disease, PR = partial response, CR = complete response, SBRT = stereotactic radiation therapy.

## HET MICROBIOOM

Alhoewel het microbioom een significante rol kan spelen in de effectiviteit van immunotherapie, is het pas sinds kort bekend dat het microbioom ook kan bijdragen aan immuunresistentie in PDAC.<sup>67</sup> Bacteriën kunnen immuunsuppressieve effecten uitoefenen op zowel de aangeboren als verworven anti-tumorimmunitet en bacteriële dysbiose kan de tumoromgeving nadelig beïnvloeden. Deze dysbiose is ook gevonden bij PDAC-patiënten, en bij muizen kan fecale

transplantatie tumorprogressie remmen.<sup>68,69</sup> Depletie van bepaalde bacteriële darmspecies zorgde voor minder MDSC-infiltratie en reprogramming van immuunsuppressieve macrofagen. Daarnaast waren de verhoogde aantallen van intratumorale T-cellen ook potenter in hun cytolytische capaciteit.<sup>69</sup> Er zijn ook bacteriën (zoals gammaproteobacteriën) gevonden die resideren in PDAC-tumoren en de effectiviteit van gemcitabine lokaal in de tumor kunnen verlagen.<sup>70</sup> Deze resultaten demonstreren de relevantie van het microbioom en geven aan dat specifieke bacterie-modulerende behandelingen wellicht de uitkomstmaten van immuuntherapieonderzoeken fundamenteel kunnen veranderen.

## **RATIONELE BEHANDELSTRATEGIEËN VOOR PDAC**

Het pancreascarcinoom staat bekend om zijn lage immunogeniciteit, afwezigheid van effector-T-cellen, een lokaal immuunsuppressief karakter en de prominente aanwezigheid van desmoplasie (Figuur 1). Een samenspel van bovenstaande mechanismen creëert een milieu dat bevorderlijk is voor tumorprogressie en metastasering. De resultaten met mono-immuuntherapieën bij PDAC blijven grotendeels uit en rationale combinatiestrategieën zijn op dit moment hard nodig om effectiviteit te genereren. Voor PDAC is er een aantal vereisten om tumordestructie te kunnen bewerkstelligen. Effectieve tumorspecifieke T-cellen dienen ten allereerste te worden gegenereerd. Dit kan door middel van (gepersonaliseerde) vaccinaties of door de immunogeniciteit van de tumor te verhogen. Eventueel moeten de effector-T-cellen worden ondersteund ter preventie van T-celdisfunctie door middel van beschikbare middelen (zoals anti-PD-(L)1) of remmers van nieuwere 'checkpoints'. Het moduleren van de tumoromgeving, ter facilitering van de T-cel-influx, is echter minstens zo belangrijk, zoals gebleken uit preklinische en klinische onderzoeken.<sup>32,49,57,71</sup> Zhu *et al.* demonstreerden dat het geven van chemotherapie, CSF-1R-blokkade en ICB kan leiden tot synergistische effecten. Dertig procent van de muizen met PDAC had een verlaging van 'tumor load' van 85% of meer.<sup>49</sup> Onlangs zijn twee fase 1-onderzoeken gestart met anti-CSF-1R-combinatietherapie bij PDAC (NCT03153410; NCT02777710, zie Tabel 2). Hetzelfde geldt voor combinatie onderzoeken met 'focal adhesion kinase' (FAK)-remmers (NCT03727880; NCT02758587; NCT02546531). FAK-remmers hebben op het tumorstroma een anti-fibrotische werking en in een preklinisch model waren FAK-remmers in staat om PDAC-tumoren gevoelig te maken voor 'checkpoint'-therapie.<sup>71</sup> Daarnaast zijn recentelijk de eerste onderzoeksresultaten gerapporteerd van gemetastaseerde PDAC-patiënten die werden behandeld met anti-CD40 in combinatie met anti-PD-1 en chemotherapie om de tumor vanuit meerdere invalshoeken aan te vallen (NCT03214250). Met dit regime respondeerden 20 van de 24 gemetastaseerde PDAC-patiënten (ASCO 2019, Abstract #8060), wat aantoont dat rationale behandelstrategieën potentieel in staat zijn om PDAC gevoelig te maken voor immuuntherapie.

## CONCLUSIE

Vooralsnog zijn de vereisten voor effectieve behandeling van niet-immunogene tumoren zoals PDAC nog niet geheel opgehelderd. Duidelijk is wel dat voor duurzame klinische effecten een multimodale en gepersonaliseerde behandelstrategie gewenst is, bestaande uit zowel conventionele als immuuntherapeutische behandelingen. Met het toenemende inzicht in de oorzaken van immuundisfunctie in PDAC en het veelvoud aan combinatiestrategieën dat nu wordt onderzocht, lijkt het pancreascarcinoom in de toekomst gevoelig en niet immuun te worden voor behandeling.

## AANWIJZINGEN VOOR DE PRAKTIJK

- 1 Met de komst van immuuntherapie is de behandeling voor veel vormen van kanker aanzienlijk veranderd en is de prognose verbeterd. Tot nu toe blijkt het ductaal adenocarcinoom van de pancreas (PDAC) echter verminderd gevoelig voor immuuntherapie.
- 2 Resistentie voor immuuntherapie bij PDAC kan worden verklaard door meerdere factoren, waaronder een tekort aan immunogene mutaties, een immuunsuppressieve tumoromgeving en een desmoplastisch stroma waardoor intratumorale T-lymfocyten spaarzaam zijn.
- 3 Nieuwe rationele combinatietherapieën waarbij meerdere punten van resistentie tegelijk worden aangepakt tonen echter aan dat PDAC niet immuun is voor immuuntherapie. De finale resultaten van deze onderzoeken worden afgewacht en zouden implicaties kunnen hebben voor de toekomstige behandeling van PDAC.

## REFERENTIES

1. Siegel RL, Miller KD, Jemal A. *CA Cancer J Clin* 2018;68:7-30.
2. Malvezzi M, Carioli G, Bertuccio P, et al. *Ann Oncol* 2018;29:1016-22.
3. Rahib L, Smith BD, Aizenberg R, et al. *Cancer Res* 2014;74:2913-21.
4. Fest J, Ruitter R, Van Rooij FJ, et al. *Eur J Cancer* 2017;72:186-91.
5. Conroy T, Hammel P, Hebbar M, et al. *N Engl J Med* 2018;379:2395-406.
6. Neoptolemos JP, Palmer DH, Ghaneh P, et al. *Lancet* 2017;389:1011-24.
7. Conroy T, Desseigne F, Ychou M, et al. *N Engl J Med* 2011;364:1817-25.
8. Von Hoff DD, Ervin T, Arena FP, et al. *N Engl J Med* 2013;369:1691-703.
9. Weber JS, D'Angelo SP, Minor D, et al. *Lancet Oncol* 2015;16:375-84.
10. Robert C, Long GV, Brady B, et al. *N Engl J Med* 2015;372:320-30.
11. Larkin J, Chiarion-Sileni V, Gonzalez R, et al. *N Engl J Med* 2015;373:23-34.
12. Balachandran VP, Luksza M, Zhao JN, et al. *Nature* 2017;551:512-6.
13. Brahmer JR, Tykodi SS, Chow LQ, et al. *N Engl J Med* 2012;366:2455-65.
14. Royal RE, Levy C, Turner K, et al. *J Immunother* 2010;33:828-33.
15. Patnaik A, Kang SP, Rasco D, et al. *Clin Cancer Res* 2015;21:4286-93.
16. Ino Y, Yamazaki-Itoh R, Shimada K, et al. *Br J Cancer* 2013;108:914-23.
17. Yarchoan M, Hopkins A, Jaffee EM. *N Engl J Med* 2017;377:2500-1.
18. Le DT, Durham JN, Smith KN, et al. *Science* 2017;357:409-13.
19. Rizvi NA, Hellmann MD, Snyder A, et al. *Science* 2015;348:124-8.
20. Snyder A, Makarov V, Merghoub T, et al. *N Engl J Med* 2014;371:2189-99.
21. <https://www.fda.gov/drugs/resources-information-approved-drugs/fda-grants-accelerated-approval-pembrolizumab-first-tissuesite-agnostic-indication>.
22. Dudley JC, Lin MT, Le DT, et al. *Clin Cancer Res* 2016;22:813-20.
23. Bailey P, Chang DK, Nones K, et al. *Nature* 2016;531:47.
24. Balli D, Rech AJ, Stanger BZ, et al. *Clin Cancer Res* 2017;23:3129-38.
25. Pfirschke C, Engblom C, Rickelt S, et al. *Immunity* 2016;44:343-54.
26. Brown JS, Sundar R, Lopez J. *Br J Cancer* 2018;118:312-24.
27. Chen DS, Mellman I. *Immunity* 2013;39:1-10.
28. Ribas A, Dummer R, Puzanov I, et al. *Cell* 2017;170:1109-19e10.
29. Middleton G, Silcocks P, Cox T, et al. *Lancet Oncol* 2014;15:829-40.
30. <https://www.fdanews.com/articles/87938-therion-reports-results-ofpanvac-vf-trial>.
31. Jaffee EM, Hruban RH, Biedrzycki B, et al. *J Clin Oncol* 2001;19:145-56.
32. Le DT, Lutz E, Uram JN, et al. *J Immunother* 2013;36:382-9.
33. Le DT, Picozzi VJ, Ko AH, et al. *Clin Cancer Res* 2019;25:5493-502.
34. Deicher A, Andersson R, Tingstedt B, et al. *Cancer Cell Int* 2018;18:85.
35. Hu Y, Sun J, Wu Z, et al. *J Hematol Oncol* 2016;9:70.
36. Cameron BJ, Gerry AB, Dukes J, et al. *Sci Transl Med* 2013;5:197ra103.
37. Linette GP, Stadtmauer EA, Maus MV, et al. *Blood* 2013;122:863-71.
38. Schmidts A, Maus MV. *Front Immunol* 2018;9:2593.
39. Beatty GL, O'Hara MH, Lacey SF, et al. *Gastroenterol* 2018;155:29-32.
40. Blando J, Sharma A, Higa MG, et al. *Proc Natl Acad Sci USA* 2019;116:1692-7.
41. Mitchem JB, Brennan DJ, Knolhoff BL, et al. *Cancer Res* 2013;73:1128-41.
42. Bayne LJ, Beatty GL, Jhala N, et al. *Cancer Cell* 2012;21:822-35.
43. Rosati A, Basile A, D'Auria R, et al. *Nature Comm* 2015;6:8695.
44. Martinez-Bosch N, Vinaixa J, Navarro P. *Cancers* 2018;10:6.
45. Hiraoka N, Onozato K, Kosuge T, et al. *Clin Cancer Res* 2006;12:5423-34.
46. Li J, Byrne KT, Yan F, et al. *Immunity* 2018;49:178-193.e7.
47. Seifert L, Werba G, Tiwari S, et al. *Gastroenterol* 2016;150:1659-72e5.
48. Steele CW, Karim SA, Leach JDG, et al. *Cancer Cell* 2016;29:832-45.

49. Zhu Y, Knolhoff BL, Meyer MA, et al. *Cancer Res* 2014;74:5057-69.
50. Sanford DE, Belt BA, Panni RZ, et al. *Clin Cancer Res* 2013;19:3404-15.
51. Nywening TM, Wang-Gillam A, Sanford DE, et al. *Lancet Oncol* 2016;17:651-62.
52. Suzuki E, Kapoor V, Jassar AS, et al. *Clin Cancer Res* 2005;11:6713-21.
53. Vincent J, Mignot G, Chalmin F, et al. *Cancer Res* 2010;70:3052-61.
54. Kurahara H, Shinchi H, Mataka Y, et al. *J Surg Res* 2011;167:e211-9.
55. Feig C, Gopinathan A, Neesse A, et al. *Clin Cancer Res* 2012;18:4266-76.
56. Yuen A, Diaz B. *Hypoxia (Auckl)* 2014;2:91-106.
57. Feig C, Jones JO, Kraman M, et al. *Proc Natl Acad Sci USA* 2013;110:20212-7.
58. Provenzano PP, Cuevas C, Chang AE, et al. *Cancer Cell* 2012;21:418-29.
59. Jacobetz MA, Chan DS, Neesse A, et al. *Gut* 2013;62:112-20.
60. Hingorani SR, Harris WP, Beck JT, et al. *Clin Cancer Res* 2016;22:2848-54.
61. Hingorani SR, Zheng L, Bullock AJ, et al. *J Clin Oncol* 2018;36:359-66.
62. Long KB, Gladney WL, Tooker GM, et al. *Cancer Discov* 2016;6:400-13.
63. Beatty GL, Winograd R, Evans RA, et al. *Gastroenterol* 2015;149:201-10.
64. Beatty GL, Chiorean EG, Fishman MP, et al. *Science* 2011;331:1612-6.
65. Tauriello DVF, Palomo-Ponce S, Stork D, et al. *Nature* 2018;554:538.
66. Mariathasan S, Turley SJ, Nickles D, et al. *Nature* 2018;554:544-8.
67. Helmink BA, Khan MAW, Hermann A, et al. *Nature Med* 2019;25:377-88.
68. Fan X, Alekseyenko AV, Wu J, et al. *Gut* 2018;67:120-7.
69. Pushalkar S, Hundeyin M, Daley D, et al. *Cancer Discov* 2018;8:403-16.
70. Geller LT, Barzily-Rokni M, Danino T, et al. *Science* 2017;357:1156-60.
71. Jiang H, Hegde S, Knolhoff BL, et al. *Nat Med* 2016;22:851-60.
72. O'Reilly EM, Oh D-Y, Dhani N, et al. *JAMA Oncol* 2019 Jul 18. doi: 10.1001/jamaoncol.2019.1588.
73. Jiang N, Qiao G, Wang X, et al. *Clin Cancer Res* 2017;23:5066-73.



# CHAPTER 3

---

Dendritic cell vaccination and CD40-agonist combination therapy licenses T cell-dependent antitumor immunity in a pancreatic carcinoma murine model

Sai Ping Lau

Nadine van Montfoort

Priscilla Kinderman

Melanie Lukkes

Larissa Klaase

Menno van Nimwegen

Mandy van Gulijk

Jasper Dumas

Dana A.M. Mustafa

Lysanne A. Lievense

Christianne Groeneveldt

Ralph Stadhouders

Ynlei Li

Andrew Stubbs

Koen A. Marijt

Heleen Vroman

Sjoerd H. van der Burg.

Joachim G. Aerts

Thorbald van Hall\*

Floris Dammeijer\*

Casper H.J. van Eijck\*

\* Shared last



## ABSTRACT

**Background:** Pancreatic ductal adenocarcinoma (PDAC) is notoriously resistant to treatment including checkpoint-blockade immunotherapy. We hypothesized that a bimodal treatment approach consisting of dendritic cell (DC) vaccination to prime tumor-specific T cells, and a strategy to reprogram the desmoplastic tumor microenvironment (TME) would be needed to break tolerance to these pancreatic cancers. As a proof of concept, we investigated the efficacy of combined DC vaccination with CD40-agonistic antibodies in a poorly immunogenic murine model of PDAC. Based on the rationale that mesothelioma and pancreatic cancer share a number of tumor associated antigens, the DCs were loaded with either pancreatic or mesothelioma tumor lysates. **Methods:** Immune-competent mice with subcutaneously or orthotopically growing *Kras*G12D/+;*Trp53*R172H/+;*Pdx-1*-Cre (KPC) PDAC tumors were vaccinated with syngeneic bone-marrow derived DCs loaded with either pancreatic cancer (KPC) or mesothelioma (AE17) lysate and consequently treated with FGK45 (CD40 agonist). Tumor progression was monitored and immune responses in TME and lymphoid organs were analyzed using multicolor flow cytometry and Nanostring analyses. **Results:** Mesothelioma-lysate loaded DCs generated cross-reactive tumor-antigen specific T-cell responses to pancreatic cancer and induced delayed tumor outgrowth when provided as prophylactic vaccine. In established disease, combination with stimulating CD40 antibody was necessary to improve survival, while anti-CD40 alone was ineffective. Extensive analysis of the TME showed that anti-CD40 monotherapy did improve CD8+ T-cell infiltration, but these essential effector cells displayed hallmarks of exhaustion, including PD-1, TIM-3 and NKG2A. Combination therapy induced a strong change in tumor transcriptome and mitigated the expression of inhibitory markers on CD8+ T cells. **Conclusion:** These results demonstrate the potency of DC therapy in combination with CD40-stimulation for the treatment of pancreatic cancer and provide directions for near future clinical trials.

## INTRODUCTION

Pancreatic adenocarcinoma is currently the fourth leading cause of cancer-related death in the United States and the third in Europe.<sup>1,2</sup> The incidence is rising and it is expected that pancreatic cancer will be the second leading cause of cancer-related death by 2030.<sup>3</sup> The current prognosis of a newly diagnosed pancreatic cancer patient is poor with a 5-year survival of 8.5%.<sup>1</sup> To date, surgical resection is the mainstay of curative treatment. However, this is usually not an option due to local vascular invasion or metastasis at diagnosis. Only 10-20% of all pancreatic cancer patients are eligible for surgical resection and relapse rates are high.<sup>4,5</sup> Adjuvant chemotherapy following surgical resection improves median overall survival, but even with new chemotherapy regimens cure is exceedingly rare.<sup>6</sup> Therefore, new treatment modalities are desperately needed in order to achieve durable disease control in pancreatic cancer patients.

Although immunotherapy yields striking results in numerous malignancies, clinical responses in pancreatic cancer have been disappointing.<sup>7-9</sup> Reasons for this poor clinical response are likely multifactorial. Pancreatic cancer has been considered an immunologically 'cold' tumor with rare infiltration of cytotoxic T cells, explaining the low response rates to immune checkpoint antibodies.<sup>10-12</sup> A highly immunosuppressive tumor microenvironment (TME) consisting of a plethora of cells including myeloid-derived suppressor cells, tumor associated macrophages (TAMs) and regulatory T cells (Tregs) in conjunction with a characteristic dense desmoplastic stroma has been reported to be responsible for the observed T-cell exclusion and dysfunction in established tumors.<sup>13</sup> Several therapeutic agents targeting the pancreatic TME have shown promising results.<sup>14, 15</sup> Seminal studies have investigated the potency of CD40-agonistic antibodies in modulating the TME and desmoplastic stroma of pancreatic cancers, thereby allowing T-cell infiltration and anti-tumor efficacy.<sup>16</sup> This was later shown to be dependent on stromalysis by TAM-precursors which, following upregulation of matrix metallo-proteases, degrade fibrosis and support the influx and anti-tumor efficacy of T cells.<sup>17, 18</sup> Although some clinical responses to CD40-agonistic antibodies have been reported, durable responses are limited. A lack of successfully presented and high-quality tumor-antigens has also been proposed to be involved in the lack of immune-reactivity to pancreatic cancers.<sup>19, 20</sup> Akin to this, observational patient studies have shown rare long-term post-resection pancreatic cancer survivors to have increased levels of tumor-reactive T cells in their peripheral blood and tumors.<sup>20, 21</sup> Dendritic cells (DCs) are the most potent T-cell activators of the immune system, and DC vaccination can successfully induce immune responses and clinical responses in various less-immunogenic malignancies when loaded with the appropriate tumor antigens.<sup>22</sup> Ideally, these antigens should be derived from the patient's own tumor. However, at this point in time, implementation of these personalized vaccines poses a logistical hurdle. An allogeneic 'off-the-shelf' strategy for tumor lysate could circumvent this issue and standardize treatment across patients. We have previously shown that treating mesothelioma patients with autologous DCs loaded with a allogeneic tumor lysate is feasible and induces immune responses and tumor

regressions in a subset of patients.<sup>22</sup> As several tumor-associated antigens (TAAs), such as cancer-testis antigens and tumor differentiation antigens, are shared across different tumor types, this vaccine could be effective in other tumors as well, including pancreatic cancer, which co-expresses several TAAs with mesothelioma tumors (*e.g.* mesothelin, WT-1, MUC1).

Here, we investigated the efficacy of DC vaccination in a representative murine model of human PDAC. We show that vaccination with mesothelioma lysate-loaded DCs yields tumor-specific immune responses against pancreatic cancer and decreases tumor progression. In established tumors, significant prolonged survival was only achieved when DC vaccination was combined with an agonistic CD40 antibody. Extensive analysis of the TME showed that whereas CD40-agonistic antibodies as monotherapy improved intratumoral T-cell infiltration, these cells displayed hallmarks of exhaustion. In the combination treatment, an improved T-cell phenotype lacking the high expression of various inhibitory receptors was observed. Therefore, CD40-agonistic antibody treatment may sensitize pancreatic tumors to tumor-specific immune responses induced by DC vaccination. These translational studies pave the way for future clinical trials investigating DC vaccination in occult disease or as part of combination immunotherapy in inoperable pancreatic cancer patients, some of which have already been initiated (REACTiVe trial).

## RESULTS

### *DC vaccination with mesothelioma lysate induces T-cell immunity and efficacy against pancreatic cancer*

We hypothesized that vaccination with DCs loaded with mesothelioma TAAs can generate a cross-reactive immune response against pancreatic cancer. We, therefore, evaluated whether pancreatic cancer (KPC3) lysate loaded-DCs or mesothelioma (AE17) lysate loaded-DCs induced protective immunity in mice challenged with KPC3 (Fig. 1a). Comparison of RNA-seq transcriptome profiles of KPC3 and AE17, based on a predefined list of validated TAAs, revealed that 63% of the TAAs were expressed by both AE17 and KPC3 (Fig. 1b, Table S1).<sup>23</sup> This supports the notion of shared antigens between the two cancer types. For a more unbiased approach, we also investigated the overlap in transcriptome profiles of KPC3, AE17 and two unrelated cell lines (B16F10, MC38) (Fig. S1). Shared transcripts could be found in all four tumor cell lines. Exposure of DCs to tumor lysates and CpG led to rapid upregulation of activation markers (*e.g.* CD40, CD80/86) (Fig. S2). Importantly, prophylactic vaccination of mice with DCs loaded with pancreatic or mesothelioma lysate was equally effective in delaying tumor growth and both had significant smaller tumor volumes compared to untreated mice at day 20 (Fig. 1c-d).

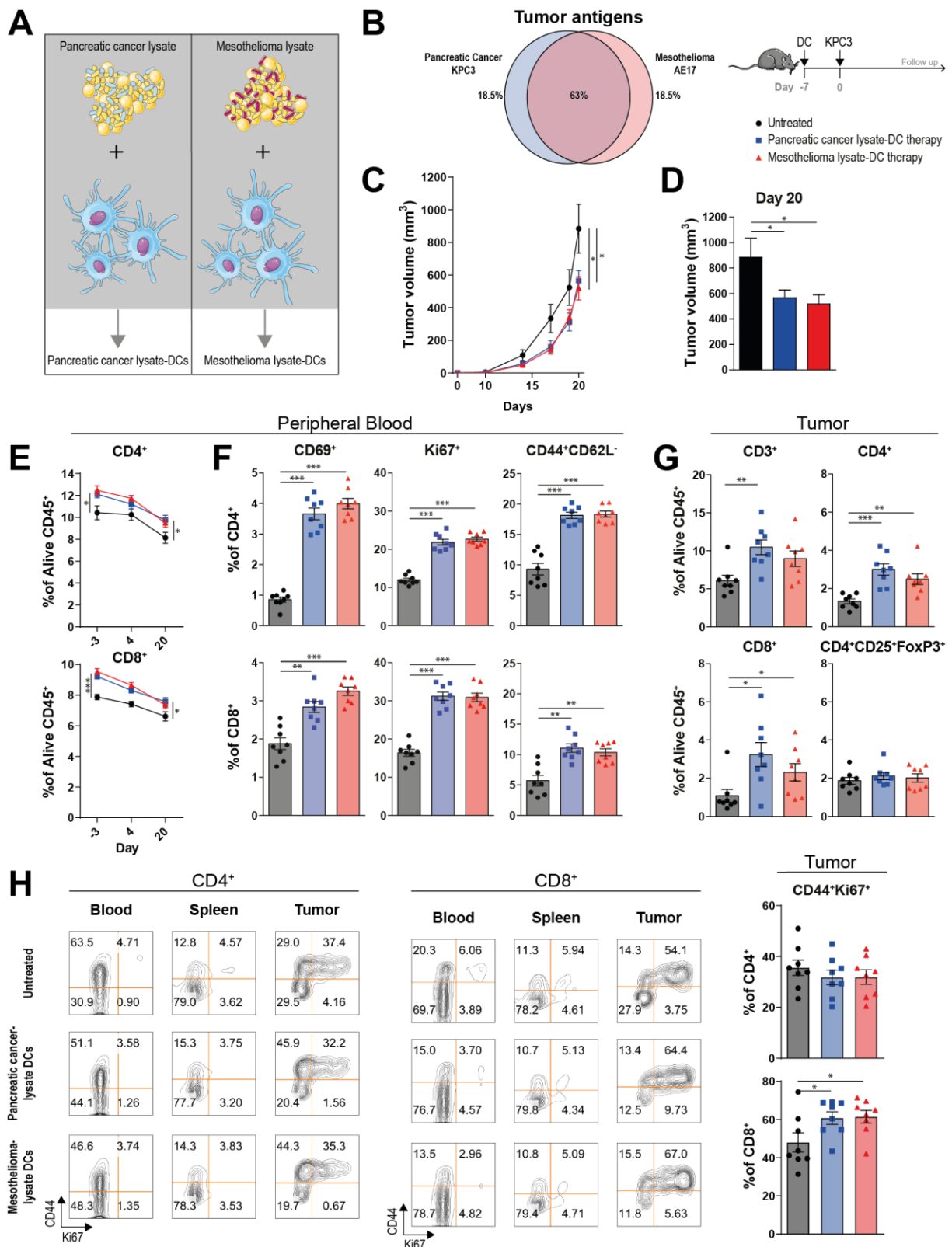


**Figure 1.** Mesothelioma lysate-DC vaccination is able to delay pancreatic tumor growth and induce strong T-cell immunity. (A) Dendritic cell vaccination study setup. (B) Expression of immunogenic tumor antigens as described by Cheever et al.<sup>23</sup> in the tumor cell line KPC3 and AE17. Percentages indicate amount of overlapping and non-overlapping genes. (C) Tumor volumes (with SEM) measured over time of untreated and treated mice. (D) Tumor size at the time of sacrifice (day 20 after tumor injection). (E) Circulating CD4<sup>+</sup> and CD8<sup>+</sup> T-cell frequencies at day -3, 4 and 20. (F) Percentage of CD69<sup>+</sup>, Ki67<sup>+</sup> and CD44<sup>+</sup>CD62L<sup>-</sup> subsets of CD4<sup>+</sup> and CD8<sup>+</sup> circulating T cells four days after DC vaccination. (G) CD3<sup>+</sup>,

CD4+, CD8+ and CD4+CD25+FoxP3+ TILs as a percentage of alive CD45+ cells at day 20 after tumor injection. (H) Expression of CD44 and Ki67 on CD4+ and CD8+ T cells at day 20 in blood, spleen and tumor. N=8 per group. Significance was determined using the non-parametric Mann-Whitney U test. Data presented as the mean±s.e.m. \*P<0.05, \*\*P<0.01, \*\*\*P<0.001.

To elucidate the mechanisms underlying DC therapy efficacy, we analyzed immune parameters in peripheral blood, spleen and tumors in both pancreatic cancer and mesothelioma lysate-loaded DC therapy treated mice. In vaccinated mice, increased frequencies of circulating CD3+, CD4+ and CD8+ T cells could be detected as early as four days after DC treatment (day-3 before tumor inoculation). These immune responses were durable and persisted over time until day of sacrifice (Fig. 1e). A more in-depth phenotypic analysis demonstrated that vaccinated mice had higher frequencies of activated (CD69+), proliferating (Ki-67+) and effector memory (CD44+CD62L-) CD4+ and CD8+ T cells in the peripheral blood compared to untreated mice. This did not differ between mesothelioma-lysate and pancreatic cancer-lysate DC-treated mice (Fig. 1f). In contrast to changes in T-cell frequencies, the expression of CD69+, Ki-67+ and CD44+CD62L- on circulating T cells of vaccinated mice waned over time (Fig. S3). Higher frequencies of intratumoral CD4+ and CD8+ T cells were noted, paralleling the delayed tumor growth observed after vaccination (Fig. 1g). CD8+ tumor infiltrating lymphocytes (TILs) of treated mice more often expressed the memory marker CD44 and the proliferation marker Ki-67, which was not observed in the spleen and peripheral blood at the time of sacrifice (Fig. 1h). This was also not observed for CD4+ TILs. Importantly, the frequencies of regulatory CD4+CD25+FoxP3+ TILs remained comparable between treated and untreated mice (Fig. 1g). Therefore, DC vaccination is able to induce the infiltration of PDAC tumors with activated, proliferating CD4+ and CD8+ T cells without concomitant Treg-induction.

#### *DC vaccination depends on tumor antigens and tumor-specific T cells*

We then assessed whether T-cell responses induced by mesothelioma lysate-loaded DCs were reactive to tumor antigens present on pancreas carcinoma cells. Mice treated with mesothelioma lysate-loaded DCs had significantly smaller tumors compared to untreated mice or those treated with non-loaded DCs, suggesting that the delay in tumor outgrowth was due to a TAA-reactive immune response (Fig. 2a). Indeed, CD8+ T cells isolated from vaccinated mice responded *in vitro* specifically to autologous pancreatic cancer lysate-loaded DCs, while T cells from untreated mice or those from non-loaded DC vaccinated mice did not (Fig. 2b). Upon stimulation, higher frequencies of CD8+ T cells from mesothelioma lysate-loaded DC treated mice expressed CD107a (being a marker of cytotoxic degranulation), Granzyme B, IFN $\gamma$  and TNF $\alpha$  compared to CD8+ T cells from untreated mice or mice treated with non-loaded DCs. This effect was not observed when CD8+ T cells were stimulated with DCs loaded with a control wild type tissue lysate (Fig. 2b), demonstrating that mesothelioma lysate-loaded DCs can generate tumor-antigen specific T cells reactive to antigens also expressed by pancreatic cancer cells. In these *in vitro* assays, CD8+ T cells from vaccinated mice also responded better than those from

untreated mice to DCs loaded with B16F10 melanoma lysate (Fig. S4), suggesting induction of immunity to shared tumor antigens across KPC3, AE17 and B16F10 as listed in Table S1.

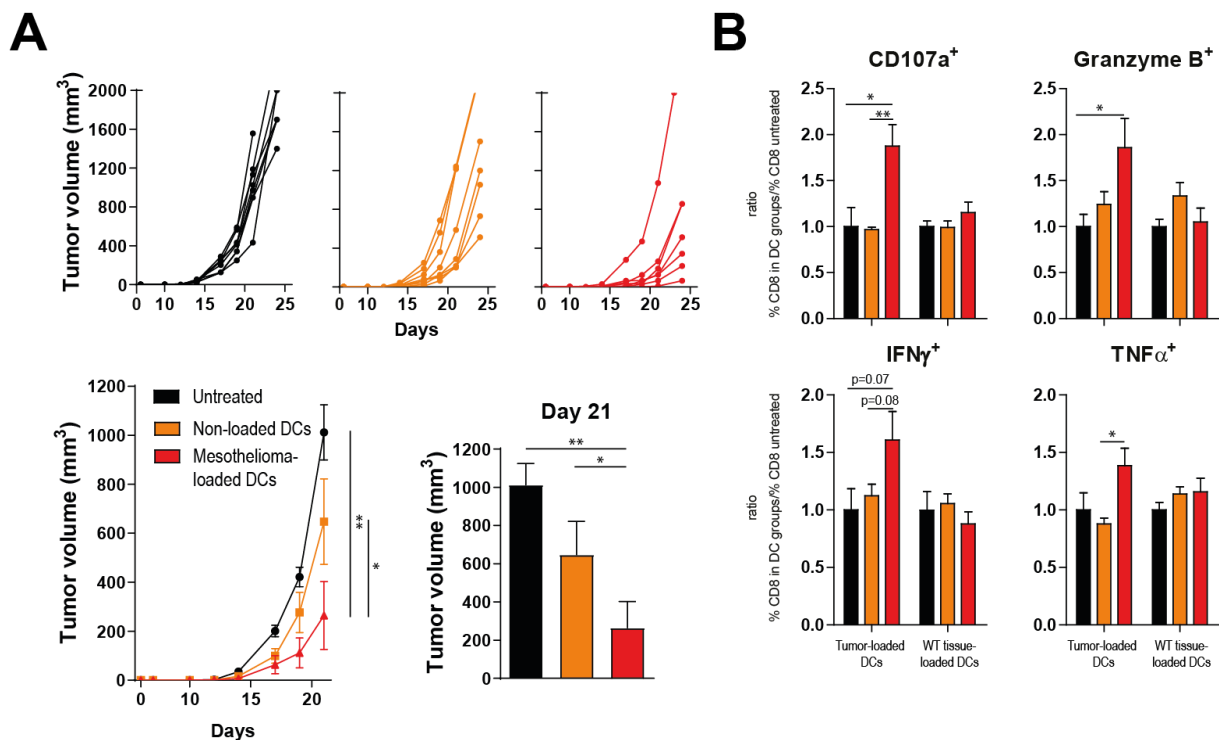


**Figure 2.** Tumor lysate DCs outperforms non-loaded DCs. (A) Tumor volume measured over time as individual tumor outgrowth curves and per group, and tumor size at day of sacrifice (day 21) of treated and untreated animals. (B) *In vitro* efficacy assay; Relative production of CD107a, Granzyme B, IFN $\gamma$  and TNF $\alpha$  by CD8<sup>+</sup> splenocytes of three treatment groups after stimulation with DCs loaded with autologous tumor lysate, or control lung lysate, normalized for untreated mice. N=8 per group. Significance was determined using the non-parametric Mann-Whitney U test. Data presented as the mean $\pm$ s.e.m. \*P<0.05, \*\*P<0.01.

### *CD40-agonistic antibody treatment sensitizes established pancreatic tumors to DC vaccination and improves efficacy*

As DC therapy generated systemic anti-tumor immune responses capable of stalling tumor growth when given prophylactically, we set out to test its capacity to control established KPC3 tumors. Although our pilot study demonstrated that tumor lysate-loaded DCs are capable of inducing systemic changes in T-cell subsets, as a single therapy it was unable to increase intratumoral T cells or delay tumor growth (Fig. S5). The lack of increased T-cell infiltration found in established tumors in the presence of a systemic immune response suggested that the PDAC TME might physically obstruct T cells from infiltrating the tumor. CD40-agonistic antibodies have previously been found to allow T-cell infiltration due to TME-reorganization in pancreatic cancer, offering a treatment rationale for combination therapy with DC vaccination.<sup>16</sup> As CD40 is also highly expressed on the tumor lysate-loaded DCs (Fig. S2), administering the antibody early following DC transfer might offer additional synergy between these treatments (Fig. S6a). Interestingly,  $\alpha$ CD40 combined with DC vaccination resulted in significant tumor growth control

when compared to untreated mice while monotherapy DC or  $\alpha$ CD40 did not (Fig. S6b).  $\alpha$ CD40 monotherapy was able to induce systemic and intratumoral responses (Fig. S6c-f). To show that the efficacy of this combination therapy was not limited to pancreatic cancer or the C57BL/6 mouse strain, we performed a comparable experiment in a mesothelioma tumor model (CBA/J background) yielding similar results (Fig. S7).

As treatment at day 5 after tumor cell injection still reflects minimal disease burden, we aimed at treating larger tumors (day 10) using an intensified treatment schedule (Fig. 3a). In this experimental setup, tumor growth and survival of mice treated with monotherapy DC vaccination or  $\alpha$ CD40 also did not significantly differ from untreated tumor-bearing mice (Fig. 3b-d, S8). The combination therapy, however, significantly delayed tumor growth (Fig. 3b), led to significantly smaller tumor volumes and improved survival (Fig. 3c-d). In order to elucidate the immunological prerequisites of therapeutic efficacy and to demonstrate if the observed anti-tumoral response is T-cell dependent, mice were depleted of CD4<sup>+</sup> and CD8<sup>+</sup> T cells before receiving treatment (Fig. S9). Anti-tumoral efficacy was retained in  $\alpha$ CD4 and isotype-treated mice receiving DC vaccination and  $\alpha$ CD40 (Fig. 3e-g). However, therapeutic responses were mitigated in mice depleted for CD8<sup>+</sup> T cells. Importantly, we assessed the efficacy of combination therapy in an orthotropic mouse model, in order to examine if our results could be replicated in a more translational model mimicking the anatomical location and phenotypic features of PDAC (Fig. 3h). Strikingly, 56% (5/9) of all combination therapy-treated mice were macroscopically free of tumor at the day of analysis (Fig. 3i, S10). In contrast, all untreated or monotherapy-treated mice bore tumors and tumor sizes were significantly larger compared to the remaining combination therapy-treated mice with tumor (Fig. 3j).

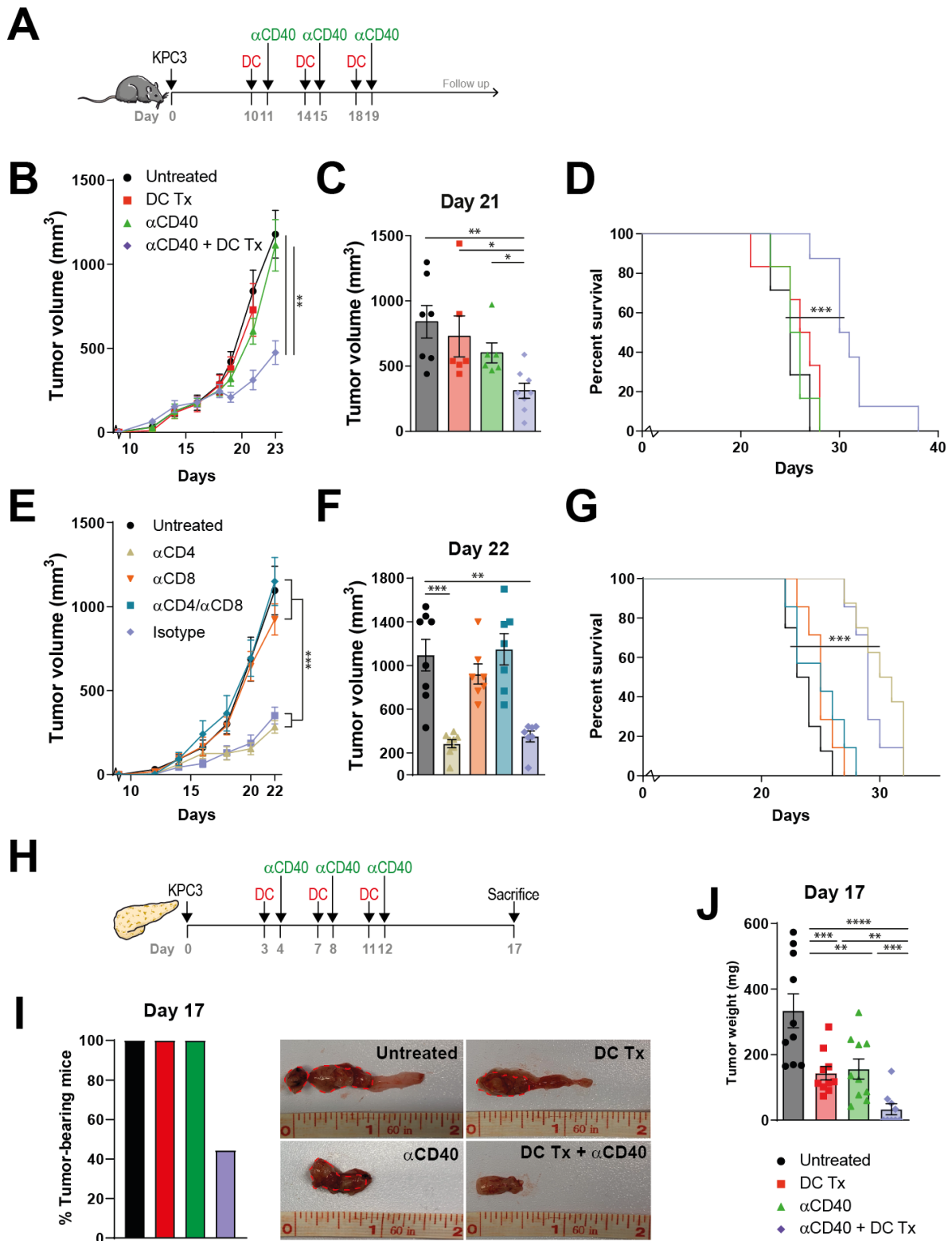


**Figure 3.** DC vaccination- $\alpha$ CD40 combination therapy improves survival of tumor-bearing mice. (A) Subcutaneous tumor model study setup. Mice were treated with AE17-lysate DCs and FGK45. (B) Tumor volumes measured over time. (C) Tumor size at day 21. (D) Kaplan-Meier analysis of treated and untreated animals. (E) Tumor volumes measured over time. (F) Tumor size at day 22. (G) Kaplan-Meier analysis of treated and untreated animals. (H) Orthotopic tumor model study setup. (I) Percentage of tumor bearing mice. (J) Tumor weight on day 17. N=8-10 per group. Significance was determined using the non-parametric Mann-Whitney U test or log-rank test. Data presented as the mean $\pm$ s.e.m. \* $P$ <0.05, \*\* $P$ <0.01, \*\*\* $P$ <0.001.



Interim peripheral blood analysis demonstrated that both monotherapy DC vaccination and  $\alpha$ CD40 treatment induced higher frequencies of CD69+, Ki-67+ and PD-1+ T cells. However, this effect was more confined to CD4+ T cells when mice were only treated with DC vaccination, and to CD8+ T cells for monotherapy  $\alpha$ CD40 (Fig. 4a). Combination therapy induced higher frequencies of CD69+, Ki-67+ and PD-1+ for both CD4+ and CD8+ T cells. Enrichment over time of Ki-67+ and PD-1+ T cells was detected in mice treated with either combination therapy or  $\alpha$ CD40 monotherapy. Furthermore, CD44+CD62L- effector memory T cells were significantly increased after both monotherapies and combination therapy (Fig. 4b). Over time, mice treated with combination therapy yielded the highest frequencies of effector memory T cells compared to mice treated with monotherapy or untreated mice. This was observed for both CD4+ and CD8+ T cells. The enrichment of effector memory T-cell frequencies was less prominent after single DC vaccination and subsequent  $\alpha$ CD40 treatment (Fig. S6d), promoting the role of multiple vaccinations.

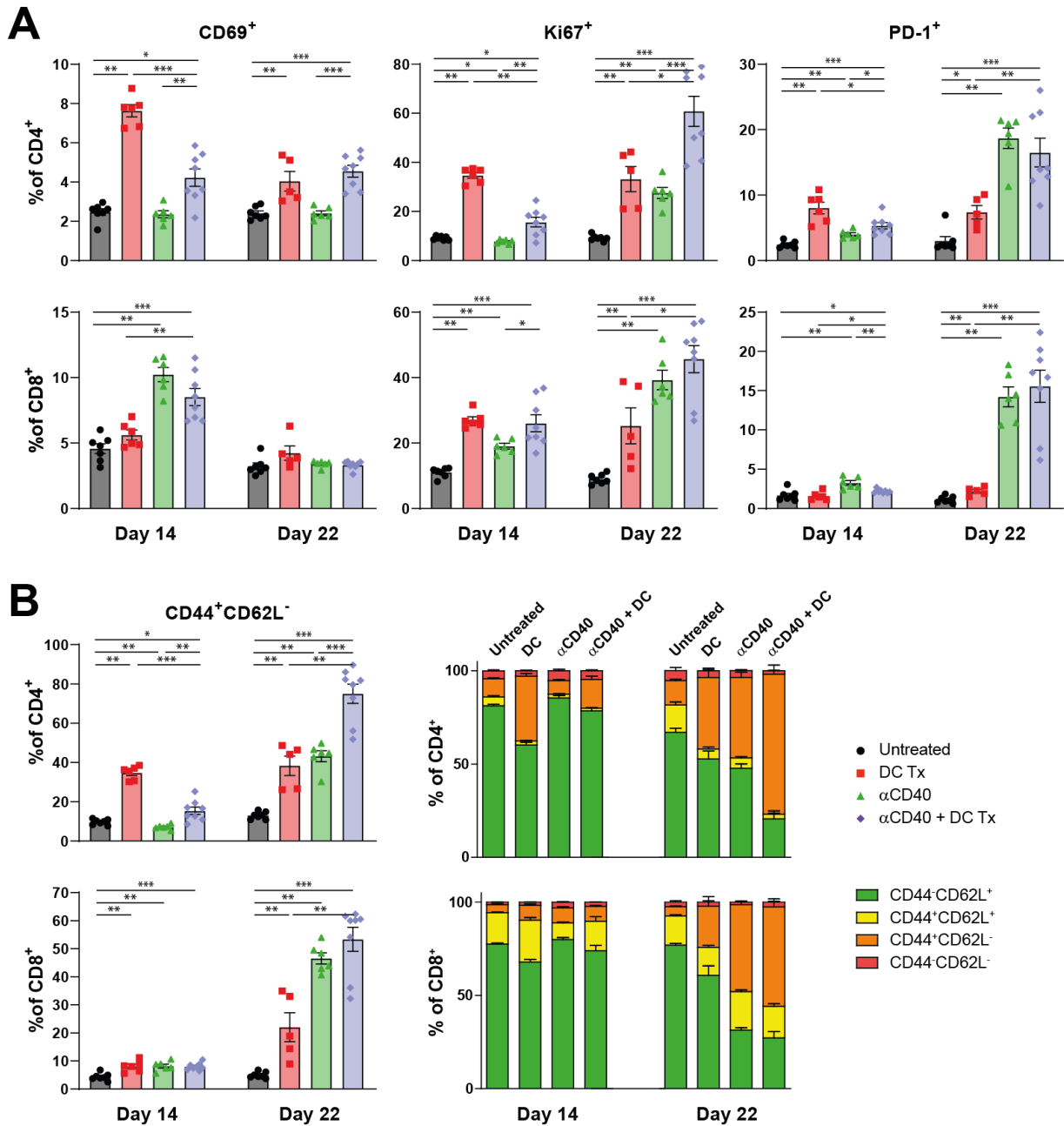


**Figure 4.** Immune activation in peripheral blood following AE17-lysate DC and FGK45 treatment. (A) Percentage of CD69<sup>+</sup>, Ki67<sup>+</sup> and PD-1<sup>+</sup> subsets of CD4<sup>+</sup> and CD8<sup>+</sup> circulating T cells at day 14 and 22. (B) Percentage of CD44<sup>+</sup>CD62L<sup>-</sup> effector memory subsets and memory status of CD4<sup>+</sup> and CD8<sup>+</sup> circulating T cells at day 14 and day 22. N=8 per group. Significance was determined using the non-parametric Mann-Whitney U test. Data presented as the mean $\pm$ s.e.m. \*P<0.05, \*\*P<0.01, \*\*\*P<0.001.

*Combining DC vaccination and  $\alpha$ CD40 remodels the tumor microenvironment, including T-cell exhaustion markers*

To further assess the mechanistic underpinnings of combination immunotherapy, we performed extensive analysis on the tumor and intratumoral immune cells, both numerically and phenotypically, using gene expression analysis and multicolor flow cytometry. Intratumoral analysis revealed increased T-cell numbers in treated mice (Fig. 5a). No distinct changes in myeloid subsets could be found (Fig. S11). However, DC therapy did induce a PD-L1 rich tumor

microenvironment (Fig. 5b). To get a more profound insight in the intratumoral immune changes induced by combination therapy, we applied NanoString gene-expression technology on tumors of treated and untreated mice. Unsupervised clustering of significantly different immune-related genes revealed that tumors of untreated or monotherapy-treated mice displayed a distinct gene expression profile as compared to mice treated with the combination therapy (Fig. 5c-d, S12), indicating a unique remodeling of the TME.

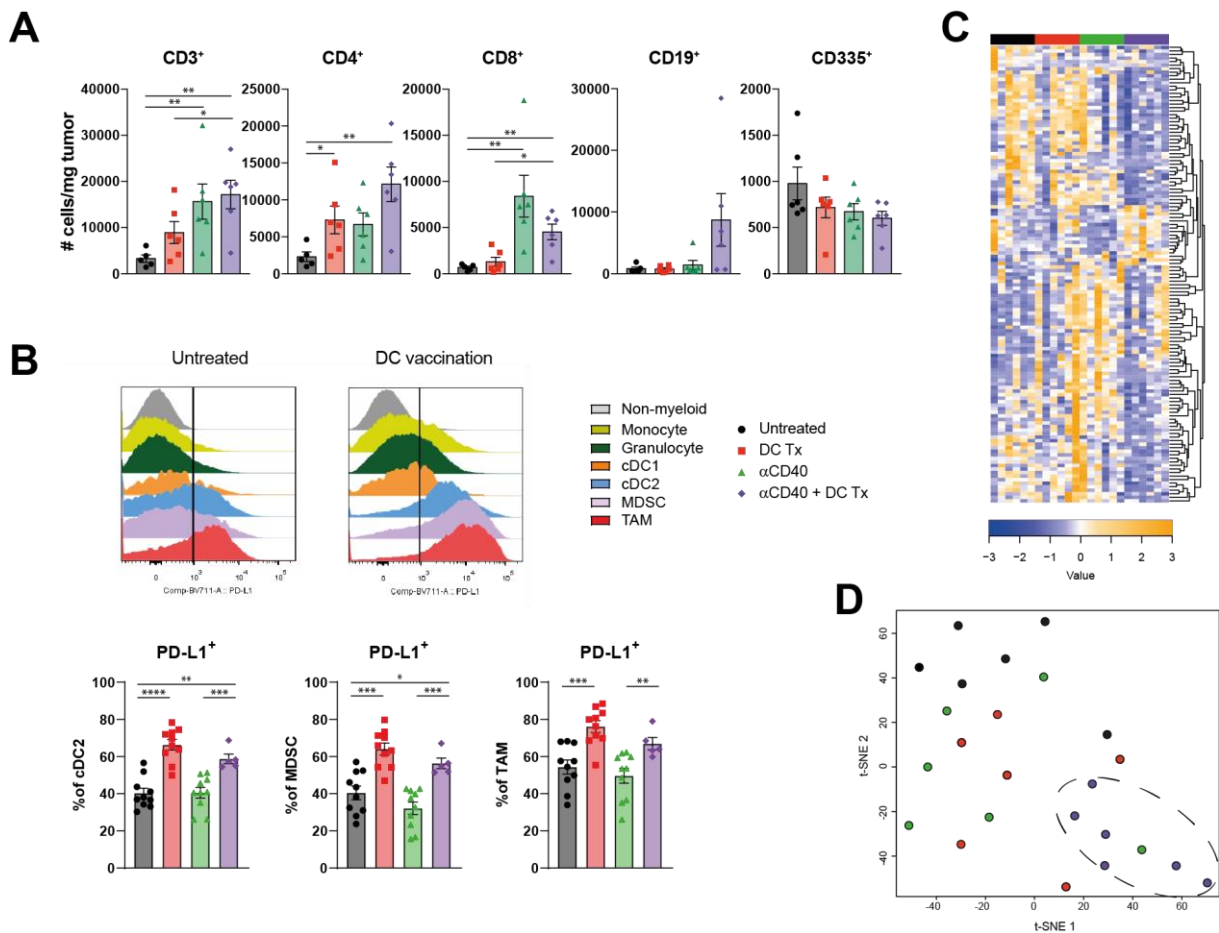


**Figure 5.** Tumors of combination therapy-treated mice displayed a distinct gene expression profile compared to tumors of untreated or monotherapy-treated mice (A) Number of CD3<sup>+</sup>, CD4<sup>+</sup>, CD8<sup>+</sup>, CD19<sup>+</sup> and CD335<sup>+</sup> TILs per mg tumor at end-stage disease. (B) PD-L1 MFI of non-myeloid (CD45<sup>-</sup>), monocyte (CD45+F4/80-CD11b+Ly6C+Ly6G<sup>-</sup>), granulocyte (CD45+F4/80-CD11b+Ly6C+Ly6G<sup>+</sup>), cDC1 (CD45+F4/80-CD11b+CD11c+MHCII+CD103<sup>+</sup>), cDC2 (CD45+F4/80-CD11b+CD11c+MHCII<sup>+</sup>), MDSC (CD45+F4/80-CD11b+Ly6C+Ly6G<sup>int</sup>) and TAM (CD45+F4/80+CD11b<sup>+</sup>) population, and percentage of PD-L1<sup>+</sup> subset of cDC2s, MDSCs and TAMs. (C) Unsupervised clustering of genes significantly different between groups. Downregulated genes are marked blue and upregulated genes are marked yellow. (D) t-SNE clustering of individual tumor samples based on genes significant different between groups. N=5-10 per group. Significance was determined using the non-parametric Mann-Whitney U test. Data presented as the mean±s.e.m. \*P<0.05, \*\*P<0.01, \*\*\*P<0.001 \*\*\*\*P<0.0001.

Mice treated with combination therapy had consistently lower transcript amounts of a wide range of inhibitory receptors, including *Pdcd1* (PD-1), *Ctla4*, *Entpd1* (CD39), *Vsir* (VISTA), *Cd244* (2B4), *Havcr2* (Tim-3) and *Tigit*, compared to monotherapy treated mice (Fig. 6a). Remarkably,

both monotherapies induced higher expression of various effector molecules like *Prf1* (perforin), *Gzma* & *Gzmb* (Granzymes) and *Ifng* (Interferon- $\gamma$ ). Differential gene expression analysis between monotherapy groups and the combination therapy confirmed significantly higher transcript levels of both inhibitory receptors and effector molecules in tumors of monotherapy treated mice (Fig. S13).

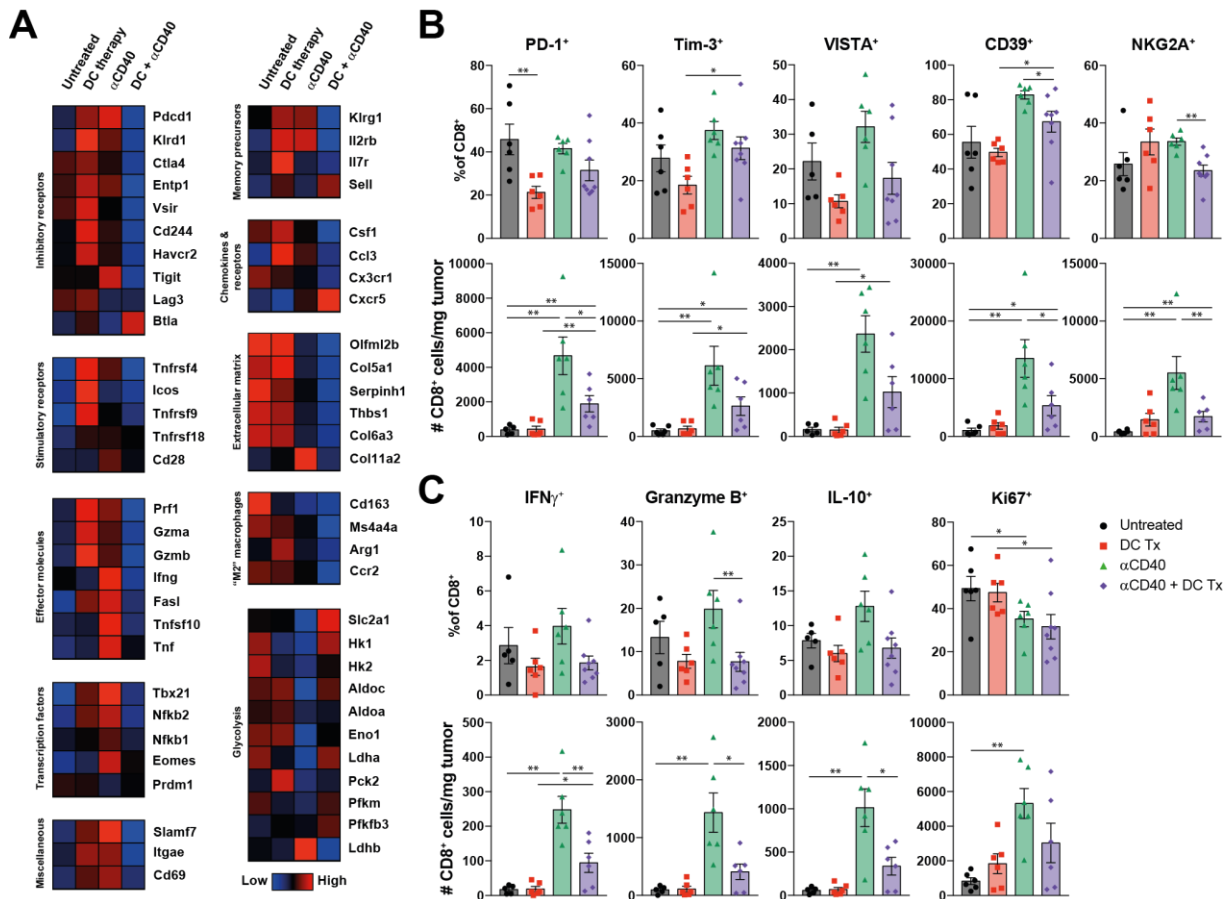


**Figure 6.** DC vaccination is able to reduce hallmarks of T-cell exhaustion. (A) Heatmap illustrating the average transcript expression of the indicated genes, grouped by function. Rows represent averaged z-scores. (B) Number and percentage of PD-1<sup>+</sup>, Tim-3<sup>+</sup>, VISTA<sup>+</sup>, CD39<sup>+</sup> and NKG2A<sup>+</sup> subsets of CD8<sup>+</sup> TILs. (C) Number and percentage of IFN $\gamma$ <sup>+</sup>, Granzyme B<sup>+</sup>, IL-10<sup>+</sup> and Ki67<sup>+</sup> subsets of CD8<sup>+</sup> TILs. N=7-8 per group. Significance was determined using the non-parametric Mann-Whitney U test. Data presented as the mean $\pm$ s.e.m. \*P<0.05, \*\*P<0.01, \*\*\*P<0.001.

Although the findings of increased effector molecules in the absence of clinical benefit may seem counterintuitive, similar cells displaying high levels of co-inhibitory and effector molecules were recently found to be consistent with a terminally exhausted T-cell phenotype.<sup>24-28</sup> In line with these findings, gene-set enrichment analysis (GSEA) revealed that gene transcripts associated with T-cell exhaustion were significantly enriched in tumors of  $\alpha$ CD40 therapy treated mice compared to combination therapy treated animals (Fig. S14a). This was not observed for DC therapy treated mice. As increased levels of co-inhibitory receptors and effector molecules may be linked to a more exhausted T-cell phenotype, we interrogated markers associated with this state. High expression of *Tbx21* (T-Bet) and *Klrg1* was found in both

monotherapies while high expression of the transcription factor *Eomes* was only found in  $\alpha$ CD40 treated mice (Fig. 6a). Interestingly, combination therapy induced higher expression of *Sell* (L-selectin) and the chemokine receptor *Cxcr5* in the tumor compared to other groups. Furthermore, we also found lower expression of genes related to various collagen markers and “M2” phenotype macrophages after  $\alpha$ CD40 therapy indicating TME remodeling. In order to confirm  $\alpha$ CD40-induced stromalysis, histochemical stainings were performed. Tumors of both  $\alpha$ CD40 monotherapy as combination therapy-treated mice showed decreased collagen content (Fig. S15). Strikingly, high mRNA expression of genes related to glycolysis were detected in tumors after combination therapy as compared to  $\alpha$ CD40 monotherapy (Fig. 6a). A glycolysis gene set enrichment analysis indeed revealed higher activity in the combination therapy treated mice compared to  $\alpha$ CD40 treated mice (Fig. S14b). Combination therapy was also able to significantly upregulate expression of *Vegfa*, *adm* and *Flt1* compared to  $\alpha$ CD40 treated mice (Fig. S13). This is indicative for angiogenesis and vascular formation and may promote immune cell infiltration into the tumor. When immunohistochemically stained for the endothelial marker CD31, tumors of combination therapy-treated mice did express more CD31 compared to untreated or monotherapy-treated mice (Fig. S16).

As gene expression analysis was performed on whole tumor material, inhibitory markers and effector molecules were further validated and quantified at the protein level on both CD4+ and CD8+ TILs (Fig. 6b-c, S17). Untreated and  $\alpha$ CD40 treated mice had the highest frequencies of CD8+ TILs expressing various inhibitory receptors (*i.e.* PD-1, Tim-3, VISTA, CD39, NKG2A) (Fig. 6b). However, only  $\alpha$ CD40 treated mice had the highest number of CD8+ TILs expressing co-inhibitory receptors. DC therapy was able to reduce the frequencies of PD-1+, Tim-3+, VISTA+, CD39+ TILs. A similar trend was also observed when co-expression of multiple inhibitory receptors was assessed (Fig. S17c-d). In addition, DC vaccinated and combination therapy treated mice had the highest frequencies of PD-1/Tim-3 double negative TIL, which have been described to exhibit the highest effector potential, whereas PD-1/TIM-3 double positive T cells are known to be severely dysfunctional.<sup>26</sup>  $\alpha$ CD40 mediated induction of IFN $\gamma$ + and granzyme B+ TILs came at the expense of increased numbers of cells producing IL-10 (Fig. 6c). Both the mRNA and protein-expression data point to a preferential induction of effector T cells expressing less multiple co-inhibitory receptors in the combination immunotherapy treated, as compared to CD40-agonistic monotherapy treated mice.

Recently, targeting NKG2A on T cells has been described as a novel approach to promote anti-tumor immunity and has been linked to T-cell dysfunction.<sup>29,30</sup> Interestingly,  $\alpha$ CD40 induced the highest numbers of NKG2A+ CD8+ TILs compared to combination therapy arm (Fig. 6b). Moreover, although  $\alpha$ CD40 therapy increased TIL numbers, the frequencies of proliferating TILs were lower compared to untreated mice suggesting that this is not explained by local expansion, but enhanced infiltration (Fig. 6c). Altogether, these findings offer an explanation for the observed efficacy of DC-CD40-agonist combination therapy where an influx of T cells exhibiting low levels of co-inhibitory checkpoints is associated with restricted tumor growth.

## DISCUSSION

Our data highlight that rationally combining immunotherapies in pancreatic cancer can lead to synergistic improvements in anti-tumor T-cell immunity and clinical responses. For these studies, we used immune-competent mice bearing PDAC tumors obtained from  $Kras^{G12D/+};Trp53^{R172H/+};Pdx-1-Cre$  (KPC) mice. This model mimics (immune) phenotypic features and the aggressiveness of human pancreatic adenocarcinoma.<sup>16, 31</sup> We mainly focused on DC-based therapy to strengthen the tumor-specific effector T-cell response. Previous trials in pancreatic cancer patients utilized single peptide or autologous tumor as a lysate source for DC therapy. We assessed the possibility of loading DCs with mesothelioma lysate based on the rationale that cross-reactive T cells would be generated due to expression of a number of shared TAAs by both mesothelioma and pancreatic cancer. The use of an allogeneic-tumor lysate offers an off-the-shelf approach which is not dependent on the identification of immunodominant epitopes and can be used irrespective of the patient's HLA type and exploits a broad spectrum of TAAs.<sup>32</sup> We found that mesothelioma-lysate DC therapy was able to delay pancreatic tumor growth, generate KPC-reactive T cells and induce TIL influx, confirming cross-reactivity. Although some efficacy was observed with non-loaded DCs, possibly by an unspecific inflammatory response that activates bystander T cells or during culture phagocytosed bovine serum proteins, the use of tumor lysate-loaded DCs had significant higher efficacy against the tumor *in vivo* and *in vitro* (Fig. 2). Interestingly, cross-reactivity could also be found *in vitro* when B16F10 lysate was used to load DCs but not to non-loaded DCs (Fig. S4), indicating the involvement of shared antigens (Table S1).

We also investigated if targeting CD40 is able to control tumor growth in established disease. CD40 can be found on B cells, DCs and macrophages and ligation leads to activation.<sup>33</sup>  $\alpha$ CD40 therapy may therefore also activate endogenous DCs that present tumor antigens and contribute to a monotherapy effect. Also, Schoenberger and Bennett *et al.* demonstrated that CD40-activated APCs might replace the requirement for CD4+ T helper-mediated licensing, thereby lowering the threshold for CD8+ effector T-cell priming. This could explain why CD4+ T-cell depletion prior combination immunotherapy did not affect efficacy.<sup>34, 35</sup> Alternatively, CD40 ligation may also license delivered DCs, thereby enhancing their capacity to prime CD8+ T cells.<sup>36, 37</sup> Indeed, when bone marrow-derived DCs were treated with  $\alpha$ CD40, increased IL-12 production could be detected (Fig. S18). Furthermore,  $\alpha$ CD40 therapy can also directly modulate the TME: targeting CD40 on macrophages can lead to phenotypic polarization from immunosuppressive "M2" into inflammatory "M1" macrophages, the latter being tumoricidal and capable of ablating tumor stroma.<sup>16, 38</sup> In line with this thought, our mRNA expression data and histochemical staining on tumors confirmed decreased collagen content after  $\alpha$ CD40 mono and combination therapy (Fig. 6a). Also, lower expression of mRNA levels related to M2 macrophages was found in tumors of mice treated with  $\alpha$ CD40 (Fig. 6a). Furthermore, it was shown that M2 macrophage-derived granulins contribute to CD8+ T cell exclusion and that this

process is driven by colony-stimulating factor-1 (CSF-1). It has been found that CSF-1 inhibition leads to desmoplasia depletion and sensitizes pancreatic cancer to immune checkpoint blockade therapy.<sup>39</sup> We were able to show lower *Csf1* mRNA levels in tumors after  $\alpha$ CD40 therapy and combination therapy (Fig. 6a). A recently reported combination therapy involving  $\alpha$ CD40 and  $\alpha$ PD-1 therapy showed promising results in preclinical PDAC models, and demonstrated that therapy reprograms the TME resulting in the increase of DCs and decrease of granulocytic-myeloid derived suppressor cells (MDSCs).<sup>40</sup> As we now focused on the T-cell phenotype responsible for slowing tumor progression following combination treatment, further in-depth studies immediately following  $\alpha$ CD40 therapy are likely required to formally dissect its spatiotemporal roles on macrophages and DCs in promoting anti-tumor immune responses.

Interestingly, despite the absence of clinical responses in monotherapy-treated animals in the established tumor model, both monotherapy and combination therapy-treated mice were able to increase total CD3+ TIL numbers. The effect of DC therapy was most pronounced on CD4+ T cells and less on CD8+ T cells whereas  $\alpha$ CD40 treatment displayed an inverse pattern. DC and  $\alpha$ CD40 treated mice showed improved survival and increased both CD4+ and CD8+ intratumoral T-cell numbers. However, we demonstrated that the clinical response was primarily driven by CD8+ T cells (Fig. 3e-g). The sensitizing role of DC vaccination may be mainly priming of MHC class I-restricted cytotoxic T lymphocytes. Even though CD40 agonistic antibodies significantly increased T-cell infiltration in established pancreatic tumors, clinical efficacy was lacking, prompting further phenotypic analysis of these cells. We observed high expression of various inhibitory receptors and effector molecules on TILs of  $\alpha$ CD40 monotherapy treated mice when compared to the other treatment groups. Studies only recently published have associated this phenotype with that of terminally exhausted T cells in both solid cancer and chronic viral infection settings.<sup>25, 41</sup> Although our mRNA expression data also demonstrated the expression of various inhibitory receptors in DC monotherapy treated mice, mRNA analysis was performed on whole tumor tissue, challenging the interpretation of our data as we were not able to assign specific markers to individual immune cell subsets. However, lower amounts of mRNA of various stimulatory receptors (*i.e.* CD28, ICOS, GITR, CD137, OX-40) and high expression of *Tbx21* (T-Bet) and *Eomes* found in  $\alpha$ CD40 monotherapy treated mice suggest that this phenotype is primarily restricted to these tumors. In addition, KLRG1<sup>hi</sup>IL7r<sup>lo</sup> CD8+ T cells have previously been described as dysfunctional.<sup>42</sup> We found that monotherapy with  $\alpha$ CD40 induced higher expression of *Klrg1* but not *Il7r*, whereas DC vaccination increased the levels of both *Klrg1* and *Il7r*. In accordance with the aforementioned phenotype, *Sell* (L-selectin), a marker associated with naïve-like memory T cells and T-cell homing, was particularly induced in mice treated with combination therapy.<sup>24, 25, 28</sup> Finally, the chemokine receptor CXCR5 has been recently found to mark a specific T-cell population capable of responding to PD-1 checkpoint blocking antibodies, which expresses lower levels of co-inhibitory receptors and effector molecules as compared to their CXCR5-negative counterparts.<sup>25, 26, 41</sup> We found that combination DC and  $\alpha$ CD40 therapy indeed induced higher *Cxcr5* expression in the tumor compared to other groups.

Flow cytometry analysis confirmed the reduced expression of various inhibitory markers on CD8+ TILs derived from combination therapy-treated mice compared to  $\alpha$ CD40-treated mice. In addition, the lower proliferation rate as evidenced by *ex vivo* measurements of Ki-67 in combination therapy treated animals also matches with an improved T-cell phenotype, as others have previously found these cells to persist in culture longer compared to their Ki-67-high counterparts.<sup>25</sup> As human cancers grow at a considerably slower pace than most murine tumor models, it is conceivable that longer T-cell persistence is crucial for durable tumor control.

The presence of low amounts of glycolysis-related gene transcripts following  $\alpha$ CD40 monotherapy fits with a more exhausted, terminally differentiated memory T-cell state, as has been proposed by others.<sup>43, 44</sup> Glut-1 (*Slc2a1*) was found to be essential for T-cell activation and *Slc2a1* was highly expressed in combination therapy treated mice.<sup>45</sup> However, as gene expression was performed on whole tumor material, it's unclear whether glycolysis-related transcripts originated from tumor cells or immune infiltrates. Further functional studies on our combination treated T-cell phenotype are needed to truly assess which factors determine their superior anti-tumor efficacy.

DCs loaded with allogeneic mesothelioma-tumor cell lysate have already proven to be feasible, with clinical efficacy in the absence of toxicity in patients with mesothelioma.<sup>22</sup> Following this, a phase II clinical trial examining whether this holds true for macroscopically disease-free, post-resection PDAC patients is currently being conducted (REACTiVe trial; Netherlands Trial Register NL7432). However, as the majority of pancreatic patients presents with irresectable or metastatic disease, rational and safe treatment combinations are needed to offer perspective for this group of patients too. Currently, several studies with combination strategies incorporating CD40 agonists in PDAC patients are ongoing and recruiting (NCT03214250; NCT02588443; NCT03329950). We have shown that DC-therapy pretreatment allows for proper CD40-agonist efficacy by precluding the formation of T cells associated with an exhaustion phenotype when administered alone. The lack of DC-therapy toxicity in patients is of particular importance since CD40-agonistic antibodies are associated with serious adverse events leading to premature termination of treatment in some patients.<sup>16, 46</sup> To assess the feasibility and safety of our combinatory approach we are currently in the process of initiating a trial involving DC-CD40-agonist combination therapy in metastatic disease. Since DC vaccination also induced a PD-L1 rich tumor microenvironment, future combination strategies with immune checkpoint blockers are warranted.

In conclusion, we have found pancreatic cancer and mesothelioma lysate-loaded DCs to be effective in restraining immunologically cold pancreatic tumors when administered prophylactically. In established tumors, effective intratumoral immunity was achieved when DC vaccination was combined with CD40-agonistic antibodies, generating non-redundant immunological effects capable of restraining tumor progression.



## METHODS

### *Mice*

C57BL/6 and CBA/J mice were purchased from Charles River Laboratories and Janvier respectively. All mice were housed in individually ventilated cages, maintained under specific pathogen-free conditions and used at 8-10 weeks of age. All mouse experiments were controlled by the animal welfare committee (IvD) of the Leiden University Medical Center (Leiden) or Erasmus University Medical Center (Rotterdam) and approved by the national central committee of animal experiments (CCD) under the permit numbers AVD116002015271 and AVD101002017867, in accordance with the Dutch Act on Animal Experimentation and EU Directive 2010/63/EU.

### *Mouse tumor cell lines*

The pancreatic cancer KPC3 cell line is derived from a primary tumor of a female KPC mouse.<sup>31</sup> AE17 and AC29 cell lines are derived from mesothelioma tumors in C57BL/6 and CBA/J mice and kindly provided by Professor Bruce W.S. Robinson (Queen Elizabeth II Medical Centre, Nedlands, Australia) and Professor Peter D. Katsikis (Erasmus Medical Center, Rotterdam, The Netherlands), respectively. KPC3, AE17 and AC29 tumor cell lines were cultured in RPMI 1640 containing glutamax-I (Gibco), 50 µg/mL gentamicin (Invitrogen), and 8% fetal bovine serum (FBS) (Gibco) at 37°C in a humidified atmosphere containing 5% CO<sub>2</sub>. Cell lines were assured to be free of rodent viruses and *Mycoplasma* by regular PCR analysis. Low passage number cultures from stock vials were used for all experiments. Transcriptomes of KPC3, AE17 and B16F10 cells from stock vials were analyzed by Macrogen NGS Services (Macrogen Inc., Seoul, Republic of Korea). Illumina platform was used with TruSeq Stranded Total RNA LT Sample Prep Kit (Human Mouse Rat) Library. MC38 transcriptome data was previously published<sup>47</sup> and downloaded from Sequence Read Archive (SRA) SRX6812144.

### *Generation of DC vaccination*

Bone-marrow derived cells seeded in 100mm Petri dishes (day 0) and cultured in 10 mL DC culture medium: RPMI 1640 containing glutamax-I (Gibco), 50 µg/mL gentamicin (Invitrogen), 5% FBS (Gibco), 50 mol/L mercaptoethanol (Sigma-Aldrich) and 20 ng/mL recombinant murine granulocyte macrophage-colony-stimulating factor (GM-CSF, kindly provided by Prof. B. Lambrecht, VIB Ghent, Belgium). Cells were cultured at 37°C in a humidified atmosphere containing 5% CO<sub>2</sub>. At day 3 and 6 fresh DC culture medium was added. Tumor cell lysate was prepared by freeze-thawing and subsequent sonication for 3x10 seconds with an amplitude of 10mm, using a Soniprep 150 ultrasonic disintegrator equipped with a microtip (Sanyo Gallenkamp). After 9 days of culture, tumor cell lysate was added to the DC cultures, to the equivalent of three tumor cells per DC. After 8 hours, 10 g/mL CpG (ISS-ODN 1668, Invitrogen) was added to the culture to allow complete maturation while incubated overnight. The next

day, DCs were harvested and washed three times in PBS. The quality of the DC preparation was determined by cell counting, morphology and cell surface marker expression by flow cytometry, as previously described.<sup>48</sup>

#### *In vivo experiments*

Cultured tumor cells were harvested at 70% confluency. The pancreatic cancer model was generated by injecting 100,000 KPC3 cells in 100ul PBS/0.1% BSA subcutaneously in the flank of the mice or by injecting 10,000 KPC3 cells in 20ul PBS/0.1% BSA orthotopically in the pancreas. The mesothelioma model was generated by injecting  $20 \times 10^6$  AC29 cells in 200l PBS intraperitoneally. Subcutaneous tumors were measured 3-7 times a week in three dimensions using a caliper. Mice were treated with DC immunotherapy at day-7 (seven days before tumor injection) or day 5. Repeated DC vaccination occurred at day 10, 14 and 18 in mice with subcutaneous pancreatic tumors and at day 3, 7 and 11 in mice with orthotopic pancreatic tumors. One day after DC vaccination, FGK45 or isotype IgG2a was administered intraperitoneally (BioXCell, 70 $\mu$ g/dose). Mice with AC29 tumors were DC vaccinated on day 10 followed by FGK45 on day 10, 12 and 14. For CD4+ and CD8+ T-cell depletion, mice were injected i.p. two days before treatment and every 6 days onward with GK1.5 and/or 2.42 or isotype IgG2b (BioXCell, 100 $\mu$ g/dose). Peripheral blood samples for interim analysis were collected 4 days after DC vaccination and were immediately stained (see Flow cytometry). Mice were sacrificed at the pre-defined experimental endpoint (Fig. 1, 2 and 3h-j) or when tumors reached a volume of 1000 or 1500mm<sup>3</sup>.

#### *Cell preparation and flow cytometry*

Whole blood or single-cell suspensions of spleen and tumor were prepared for flow cytometry. Spleens were passed through a 100 $\mu$ m mesh with RPMI 1640 containing glutamax-I (Gibco) and collected through centrifugation. Lymph nodes were excluded during tumor collection and tumors were dissociated using a validated tumor dissociation system (Miltenyi Biotec). To assess cytokine production, lymphoid cells were stimulated for 4 hours at 37°C using PMA and ionomycin supplemented with GolgiStop (BD Biosciences). Intracellular cytokine and transcription factor staining was performed using PFA/Saponin protocol and Foxp3 Transcription Factor Staining Buffer Kit (eBioscience) respectively. Cell surface staining was performed after blocking Fc II/III receptor using anti-mouse 2.4G2 antibody (kindly provided by L. Boon, Bioceros, Utrecht, the Netherlands) by incubating cells with fluorescently conjugated mAbs directed against murine CD3e (145-2C11), CD4 (GK1.5), CD8a (53-67), CD11b (M1/70), CD11c (N418), CD19 (1D3), CD25 (PC61), CD40 (1C10), CD44 (IM7), CD45 (30-F11), CD62L (MEL-14), CD69 (H1.2F3), CD80 (16-20A2), CD86 (GL1), CD103 (2E7), CD107a (1D4B), CD335 (29A1.4), F4/80 (BM8), FoxP3 (FJK-16s), Granzyme B (NGZB), IFN $\gamma$  (XMG1.2), IL-2 (JES6-5H4), IL-10 (JES5-16E3), Ki-67 (SolA15), LAG-3 (eBioC9B7W), Ly6C (AL-21), Ly6G (RB6.8C5), MHCII (M5/114.15.2), NKG2A (16a11), PD1 (J43) PDL1 (MIH5), TIM3 (8B.2C12), TNF $\alpha$  (MP6-XT22), VISTA (MH5A). Cells were in addition stained for viability using fixable LIVE/DEAD aqua cell stain (Thermo Fisher

Scientific). Data were acquired using an LSR-II flow cytometer (BD Biosciences) and analyzed by FlowJo v10.0.7 (Treestar).

#### *In vitro experiments*

*Tumor antigen specific T-cell detection assay:* Dissected subcutaneous tumors from treated mice and lungs from wild-type C57BL/6 mice were beads homogenized in 150µl Milli-Q for four cycles of 1 minute. A Bradford assay was performed in order to assess the protein concentration. Bone-marrow derived DCs were generated as described above, and loaded with 70µg tumor lysate or 200µg lung lysate/mL DC suspension. Tumor cell line lysate loaded DCs were prepared as described above. Tumor loaded DCs were in *in vitro* co-cultured with paired splenocytes at a ratio of 1:10 for 4 hours at 37°C supplemented with GolgiStop (BD Biosciences). After 4 hours, intra-cellular cytokine expression was assessed by flow cytometry as described above.

IL-12p40 detection: Bone-marrow derived DCs were cultured as described above. At day 9, FGK45 (BioXCell, 30µg/mL) or isotype IgG2b (BioXCell, 30µg/mL) was added to the DC culture. After 24 hours, supernatant was collected and a sandwich ELISA assay was performed as previously described.<sup>37</sup>

#### *(Immuno)histochemistry*

Immunohistochemistry was performed with an automated, validated and accredited staining system (Ventana Benchmark Discovery ULTRA, Ventana Medical Systems, USA) using Omnimap anti-rabbit or mouse and the universal DAB detection Kit. In brief, following deparaffinization and heat-induced antigen retrieval the tissue samples were incubated according to their optimized time with CD31 (Abcam; polyclonal). Incubation was followed by hematoxylin II counter stain for 8 minutes and then a blue coloring reagent for 8 minutes according to the manufacturer's instructions. Tonsil tissue was used as positive control. Trichrome blue was stained using optimized protocol provided in the fully automated Ventana Benchmark Special staines system. Sirius Red was stained by hand, in brief, following deparaffinization slides were rehydrated by passage through decreasing ethanol series, 5 minutes predifferentiation step using 0,2% fosformolybdeen-acid followed by 45 minutes incubation with 0,1% Sirius Red solution. Slides were analyzed using polarization method.

#### *mRNA expression analysis*

NanoString nCounter Technologies was applied on 120µm of Tissue-Tek(Sakura)-embedded fresh frozen tumor samples using the PanCancer IO 360™ Panel. To identify the differentially expressed genes, raw data was normalized using the values of the most stable 15 housekeeping genes selected by applying the geNorm algorithm. Unsupervised clustering of normalized gene expression values (row Z-scores) was performed using the complete linkage method with Euclidean distance measure or standard PCA/t-SNE functions in R (through RStudio v 1.1.463). For the volcano plots, Mann-Whitney U test was conducted to compare the normalized count values in two groups (*i.e.* monotherapy vs. combination therapy) for each of the 750 markers.

The original  $p$ -values were adjusted for multiple testing using Benjamini-Hochberg procedure. All calculation and the volcano plots were done in program R.

Gene set enrichment analysis was performed by ranking all genes based on difference of means scaled by the standard deviation (signal-to-noise).<sup>49</sup> Previously reported gene sets M9480 and M5937 were used for exhausted phenotype and glycolysis enrichment analysis<sup>50</sup>, respectively. The false-discovery rate adjusted  $p$ -values (q-value) was considered significant when  $<0.05$ .

#### *Statistical analysis*

Difference between groups of interest were statistically analyzed with the non-parametric Mann-Whitney U test. Data are displayed as means with the standard error of the mean and analyzed using GraphPad Prism software (Graphpad, v7.0a). Survival data were plotted as Kaplan–Meier survival curves. The non-parametric log-rank test (Mantel-Cox test) was used to compare the survival distribution of groups of mice. In all cases a  $p$ -value of 0.05 and below was considered significant (\*),  $p<0.01$ (\*\*) and  $p<0.001$  (\*\*\*) as highly significant.

## REFERENCES

1. Siegel RL, Miller KD, Jemal A. Cancer statistics, 2018. *CA Cancer J Clin* 2018;68:7-30.
2. Carioli G, Malvezzi M, Bertuccio P, et al. European cancer mortality predictions for the year 2018 with focus on colorectal cancer. *Annals of Oncology* 2018;29:1016-1022.
3. Rahib L, Smith BD, Aizenberg R, et al. Projecting cancer incidence and deaths to 2030: the unexpected burden of thyroid, liver, and pancreas cancers in the United States. *Cancer Res* 2014;74:2913-21.
4. Matsumoto I, Murakami Y, Shinzeki M, et al. Proposed preoperative risk factors for early recurrence in patients with resectable pancreatic ductal adenocarcinoma after surgical resection: A multi-center retrospective study. *Pancreatology* 2015;15:674-680.
5. Paniccia A, Hosokawa P, Henderson W, et al. Characteristics of 10-Year Survivors of Pancreatic Ductal Adenocarcinoma. *JAMA Surg* 2015;150:701-10.
6. Neoptolemos JP, Palmer DH, Ghaneh P, et al. Comparison of adjuvant gemcitabine and capecitabine with gemcitabine monotherapy in patients with resected pancreatic cancer (ESPAC-4): a multicentre, open-label, randomised, phase 3 trial. *Lancet* 2017;389:1011-1024.
7. Weber JS, D'Angelo SP, Minor D, et al. Nivolumab versus chemotherapy in patients with advanced melanoma who progressed after anti-CTLA-4 treatment (CheckMate 037): a randomised, controlled, open-label, phase 3 trial. *Lancet Oncol* 2015;16:375-84.
8. Robert C, Long GV, Brady B, et al. Nivolumab in previously untreated melanoma without BRAF mutation. *N Engl J Med* 2015;372:320-30.
9. Larkin J, Chiarion-Sileni V, Gonzalez R, et al. Combined Nivolumab and Ipilimumab or Monotherapy in Untreated Melanoma. *N Engl J Med* 2015;373:23-34.
10. Brahmer JR, Tykodi SS, Chow LQ, et al. Safety and activity of anti-PD-L1 antibody in patients with advanced cancer. *N Engl J Med* 2012;366:2455-65.
11. Patnaik A, Kang SP, Rasco D, et al. Phase I Study of Pembrolizumab (MK-3475; Anti-PD-1 Monoclonal Antibody) in Patients with Advanced Solid Tumors. *Clin Cancer Res* 2015;21:4286-93.
12. Jan N, Dagmar M, Hans L, et al. Systemic treatment with anti-PD-1 antibody nivolumab in combination with vaccine therapy in advanced pancreatic cancer. *Journal of Clinical Oncology* 2016;34:3092-3092.
13. Whatcott CJ PR, Von Hoff DD, et al. . Desmoplasia and chemoresistance in pancreatic cancer., 2012.
14. Stromnes IM, Brockenbrough JS, Izeradjene K, et al. Targeted depletion of an MDSC subset unmasks pancreatic ductal adenocarcinoma to adaptive immunity. *Gut* 2014;63:1769-1781.
15. Zhu Y, Knolhoff BL, Meyer MA, et al. CSF1/CSF1R blockade reprograms tumor-infiltrating macrophages and improves response to T-cell checkpoint immunotherapy in pancreatic cancer models. *Cancer Res* 2014;74:5057-69.
16. Beatty GL, Chiorean EG, Fishman MP, et al. CD40 agonists alter tumor stroma and show efficacy against pancreatic carcinoma in mice and humans. *Science* 2011;331:1612-6.
17. Long KB, Gladney WL, Tooker GM, et al. IFN $\gamma$  and CCL2 Cooperate to Redirect Tumor-Infiltrating Monocytes to Degrade Fibrosis and Enhance Chemotherapy Efficacy in Pancreatic Carcinoma. *Cancer Discovery* 2016.
18. Beatty GL, Winograd R, Evans RA, et al. Exclusion of T Cells From Pancreatic Carcinomas in Mice Is Regulated by Ly6C(low) F4/80(+) Extratumoral Macrophages. *Gastroenterology* 2015;149:201-210.
19. Tjomsland V, Sandström P, Spångeus A, et al. Pancreatic adenocarcinoma exerts systemic effects on the peripheral blood myeloid and plasmacytoid dendritic cells: an indicator of disease severity? *BMC Cancer* 2010;10:87.
20. Dallal RM, Christakos P, Lee K, et al. Paucity of dendritic cells in pancreatic cancer. *Surgery* 2002;131:135-8.
21. Balachandran VP, Łuksza M, Zhao JN, et al. Identification of unique neoantigen qualities in long-term survivors of pancreatic cancer. *Nature* 2017;551:512.

22. Aerts JG, de Goeje PL, Cornelissen R, et al. Autologous dendritic cells pulsed with allogeneic tumor cell lysate in mesothelioma: From mouse to human. *Clin Cancer Res* 2017.
23. Cheever MA, Allison JP, Ferris AS, et al. The prioritization of cancer antigens: a national cancer institute pilot project for the acceleration of translational research. *Clin Cancer Res* 2009;15:5323-37.
24. Canale FP, Ramello MC, Nunez N, et al. CD39 Expression Defines Cell Exhaustion in Tumor-Infiltrating CD8(+) T Cells. *Cancer Res* 2018;78:115-128.
25. Miller BC, Sen DR, Al Abosy R, et al. Subsets of exhausted CD8+ T cells differentially mediate tumor control and respond to checkpoint blockade. *Nature Immunology* 2019;20:326-336.
26. Kurtulus S, Madi A, Escobar G, et al. Checkpoint Blockade Immunotherapy Induces Dynamic Changes in PD-1(-)CD8(+) Tumor-Infiltrating T Cells. *Immunity* 2019;50:181-194 e6.
27. Li H, van der Leun AM, Yofe I, et al. Dysfunctional CD8 T Cells Form a Proliferative, Dynamically Regulated Compartment within Human Melanoma. *Cell* 2019;176:775-789 e18.
28. Duhén T, Duhén R, Montler R, et al. Co-expression of CD39 and CD103 identifies tumor-reactive CD8 T cells in human solid tumors. *Nature Communications* 2018;9:2724.
29. van Montfoort N, Borst L, Korner MJ, et al. NKG2A Blockade Potentiates CD8 T Cell Immunity Induced by Cancer Vaccines. *Cell* 2018;175:1744-1755 e15.
30. Andre P, Denis C, Soulas C, et al. Anti-NKG2A mAb Is a Checkpoint Inhibitor that Promotes Anti-tumor Immunity by Unleashing Both T and NK Cells. *Cell* 2018;175:1731-1743 e13.
31. Lee JW, Komar CA, Bengsch F, et al. Genetically Engineered Mouse Models of Pancreatic Cancer: The KPC Model (LSL-Kras(G12D/+);LSL-Trp53(R172H/+);Pdx-1-Cre), Its Variants, and Their Application in Immuno-oncology Drug Discovery. *Current protocols in pharmacology* 2016;73:14.39.1-14.39.20.
32. Neller MA, Lopez JA, Schmidt CW. Antigens for cancer immunotherapy. *Semin Immunol* 2008;20:286-95.
33. Vonderheide RH, Bajor DL, Winograd R, et al. CD40 immunotherapy for pancreatic cancer. *Cancer Immunol Immunother* 2013;62:949-54.
34. Schoenberger SP, Toes RE, van der Voort EI, et al. T-cell help for cytotoxic T lymphocytes is mediated by CD40-CD40L interactions. *Nature* 1998;393:480-3.
35. Bennett SRM, Carbone FR, Karamalis F, et al. Help for cytotoxic-T-cell responses is mediated by CD40 signalling. *Nature* 1998;393:478.
36. Cella M, Scheidegger D, Palmer-Lehmann K, et al. Ligation of CD40 on dendritic cells triggers production of high levels of interleukin-12 and enhances T cell stimulatory capacity: T-T help via APC activation. *J Exp Med* 1996;184:747-52.
37. Schuurhuis DH, Laban S, Toes RE, et al. Immature dendritic cells acquire CD8(+) cytotoxic T lymphocyte priming capacity upon activation by T helper cell-independent or-dependent stimuli. *J Exp Med* 2000;192:145-50.
38. Buhtoiarov IN, Lum H, Berke G, et al. CD40 ligation activates murine macrophages via an IFN-gamma-dependent mechanism resulting in tumor cell destruction in vitro. *J Immunol* 2005;174:6013-22.
39. Schmid MC, Quaranta V, Rainer C, et al. Macrophage-derived granulins drives resistance to immune checkpoint inhibition in metastatic pancreatic cancer. *Cancer Research* 2018.
40. Ma HS, Poudel B, Torres ER, et al. A CD40 Agonist and PD-1 Antagonist Antibody Reprogram the Microenvironment of Nonimmunogenic Tumors to Allow T-cell-Mediated Anticancer Activity. *Cancer Immunology Research* 2019;7:428-442.
41. Im SJ, Hashimoto M, Gerner MY, et al. Defining CD8+ T cells that provide the proliferative burst after PD-1 therapy. *Nature* 2016;537:417-421.
42. Wherry EJ, Kurachi M. Molecular and cellular insights into T cell exhaustion. *Nature Reviews Immunology* 2015;15:486.
43. Siska PJ, Rathmell JC. T cell metabolic fitness in antitumor immunity. *Trends Immunol* 2015;36:257-64.
44. Phan AT, Goldrath AW, Glass CK. Metabolic and Epigenetic Coordination of T Cell and Macrophage Immunity. *Immunity* 2017;46:714-729.

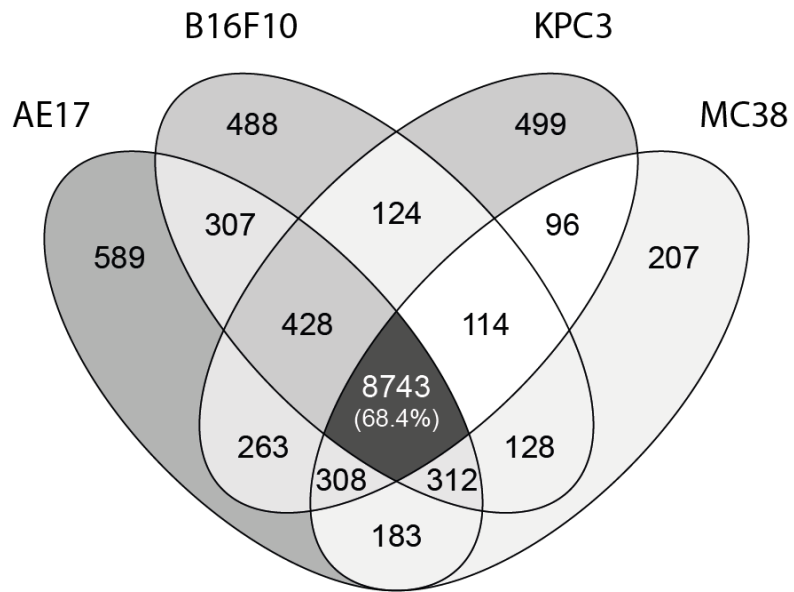
45. Macintyre AN, Gerriets VA, Nichols AG, et al. The glucose transporter Glut1 is selectively essential for CD4 T cell activation and effector function. *Cell Metab* 2014;20:61-72.
46. Vonderheide RH, Glennie MJ. Agonistic CD40 Antibodies and Cancer Therapy. *Clinical Cancer Research* 2013;19:1035-1043.
47. Hos BJ, Camps MGM, Bulk Jvd, et al. Identification of a neo-epitope dominating endogenous CD8 T cell responses to MC-38 colorectal cancer. *OncolImmunology* 2019:1673125.
48. Hegmans JP, Hemmes A, Aerts JG, et al. Immunotherapy of murine malignant mesothelioma using tumor lysate-pulsed dendritic cells. *Am J Respir Crit Care Med* 2005;171:1168-77.
49. Doering TA, Crawford A, Angelosanto JM, et al. Network analysis reveals centrally connected genes and pathways involved in CD8+ T cell exhaustion versus memory. *Immunity* 2012;37:1130-44.
50. Subramanian A, Tamayo P, Mootha VK, et al. Gene set enrichment analysis: A knowledge-based approach for interpreting genome-wide expression profiles. *Proceedings of the National Academy of Sciences* 2005;102:15545-15550.



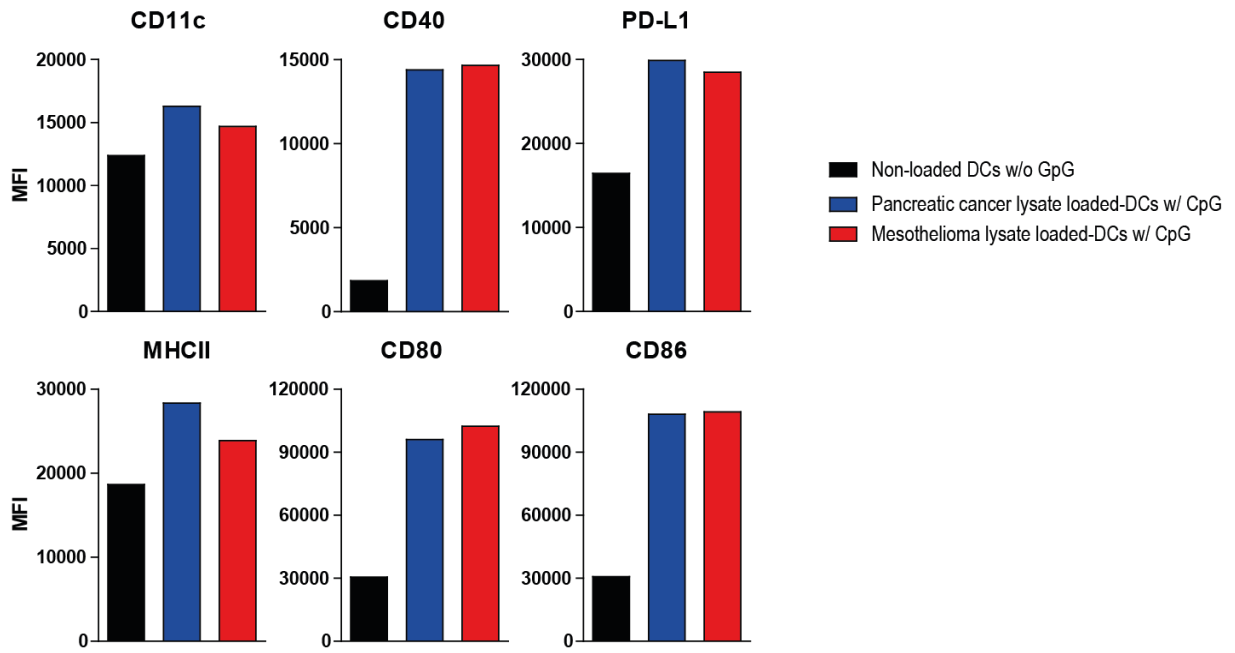


Tumor antigen (Hu) (Cheevers <i>et al.</i> )	MGI Symbol	AE17 (RPKM)	KPC-3 (RPKM)	B16F10 (RPKM)
B7H3	Cd276	10,453	5,128	1,836
Carbonic anhydrase IX	Car9	0,877	1,723	0,728
Cyclin B1	Ccnb1	33,524	49,515	79,788
CYP1B1	Cyp1b1	0,469	1,83	0,148
EGFR	Egfr	15,562	4,443	0,009
EphA2	Epha2	13,012	68,084	0,5
ETV6-AML	Etv6	7,635	4,272	4,298
Fos-related antigen 1	Fosl1	1,58	14,79	0,133
GD2	B4galnt1	2,647	5,119	0,096
HER-2/neu	Erb2	6,633	7,248	1,947
hTERT	Tert	0,621	1,516	1,038
Legumain	Lgmn	57,026	15,997	19,044
LMP2	Psmb9	5,375	0	0,686
Mesothelin	Msln	1,613	188,694	0,166
Mlana	Mlana	0,137	0,029	962,142
MUC1	Muc1	0,187	31,107	0,008
p53	Trp53	40,636	72,406	23,872
PAP	Acpp	1,667	0,014	5,093
PAX3	Pax3	1,097	0,027	22,599
PDGFR- $\beta$	Pdgfrb	19,265	0,012	2,071
Pmel	Pmel	0,315	0,098	1322,953
Proteinase3 (PR1)	Tmem37	12,497	0,511	0,086
PSCA	Psca	0,036	6,192	0
Ras	kras	9,478	7,068	9,674
RhoC	Rhoc	59,806	76,701	36,765
Sarcoma translocation breakpoints	Ewsr1	53,468	65,421	74,243
SART3	Sart3	10,381	15,07	12,161
Spa17	Spa17	0,011	0,417	1,094
SSX2	Rab3ip	8,145	7,677	7,988
Survivin	Birc5	33,091	50,658	76,914
Tyr	Tyr	0	0,006	58,169

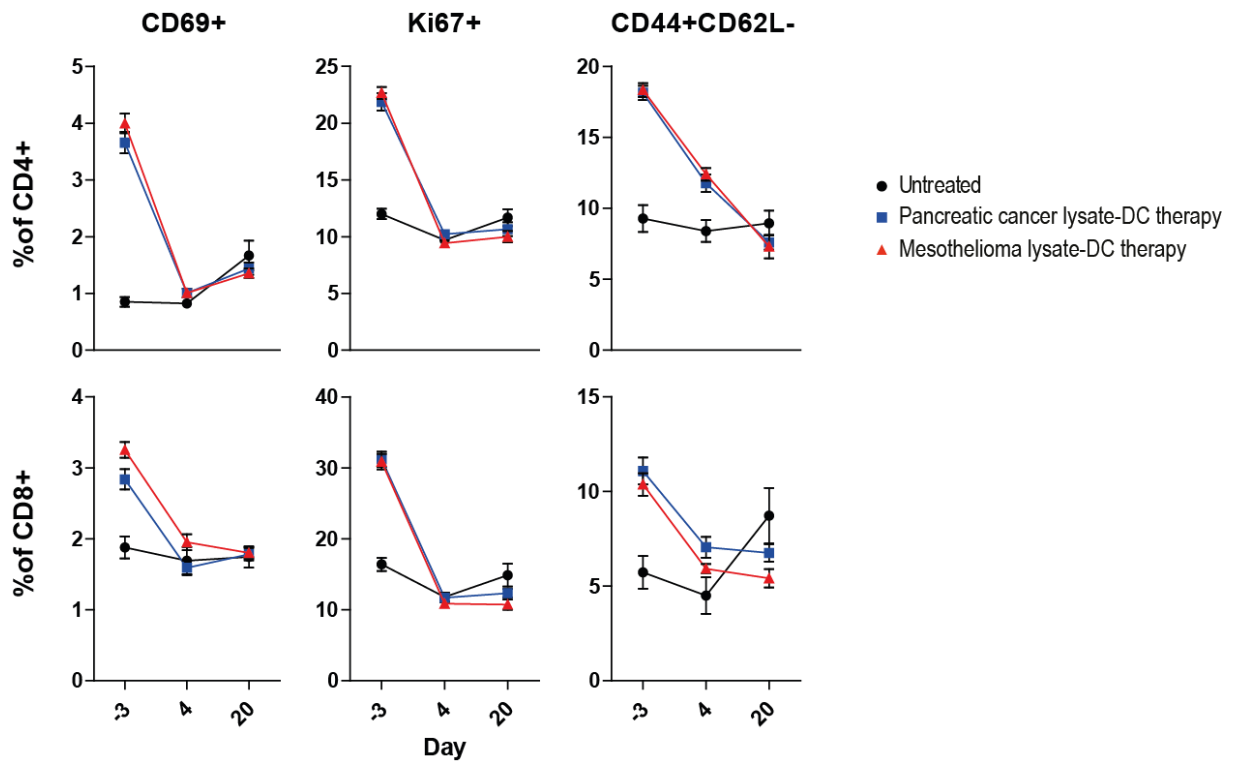
**Supplementary Table 1.** Expression levels of immunogenic tumor antigens as reported by Cheevers *et al.* translated to murine gene names (Mouse Genome Informatics) in KPC3, AE17 and B16 with a minimal threshold of 1 RPKM (reads per kilo base per million mapped reads).



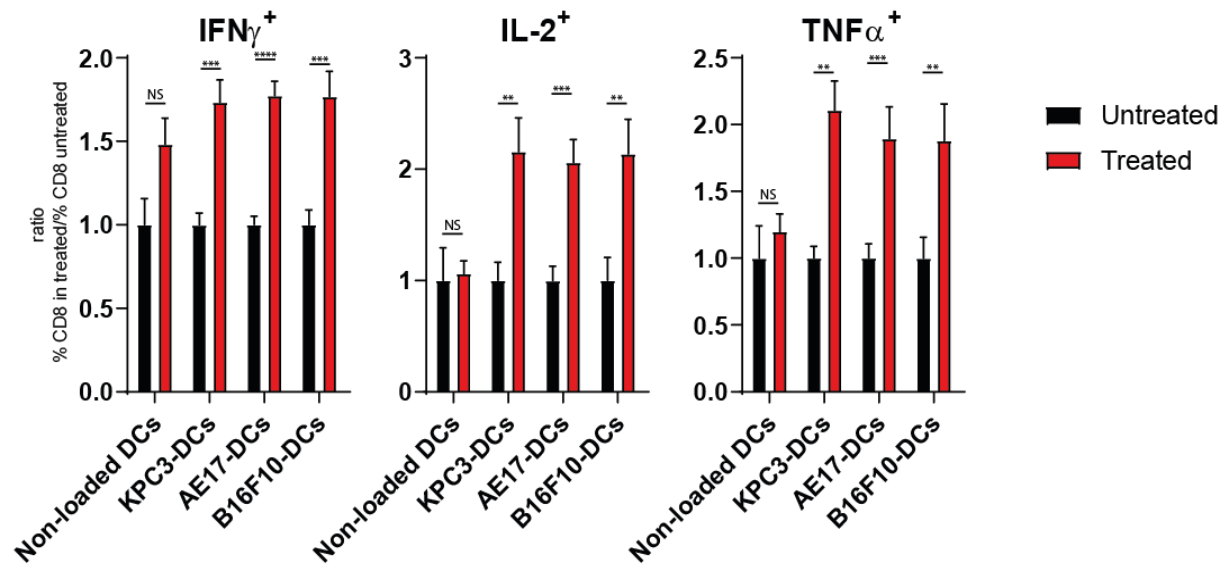
**Supplementary Figure 1.** Venn diagram illustrating overlapping and non-overlapping genes of the tumor cell lines KPC3 (pancreatic cancer), AE17 (mesothelioma), B16F10 (melanoma) and MC38 (colon adenocarcinoma).



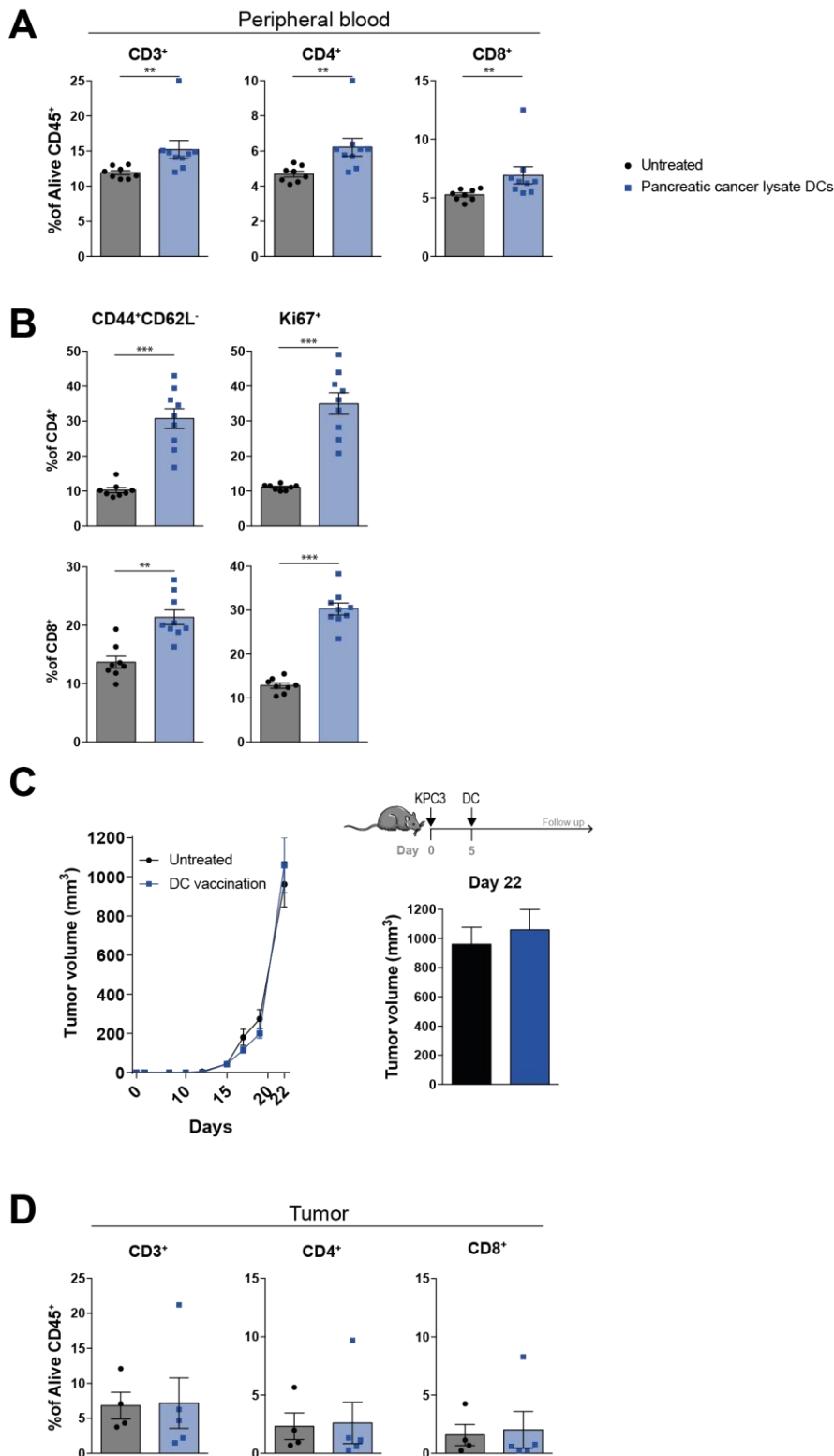
**Supplementary Figure 2:** MFI of CD11c, CD40, PD-L1, MHCII, CD80 and CD86 on cultured DCs for vaccination. Control non-loaded DCs were not stimulated with CpG.



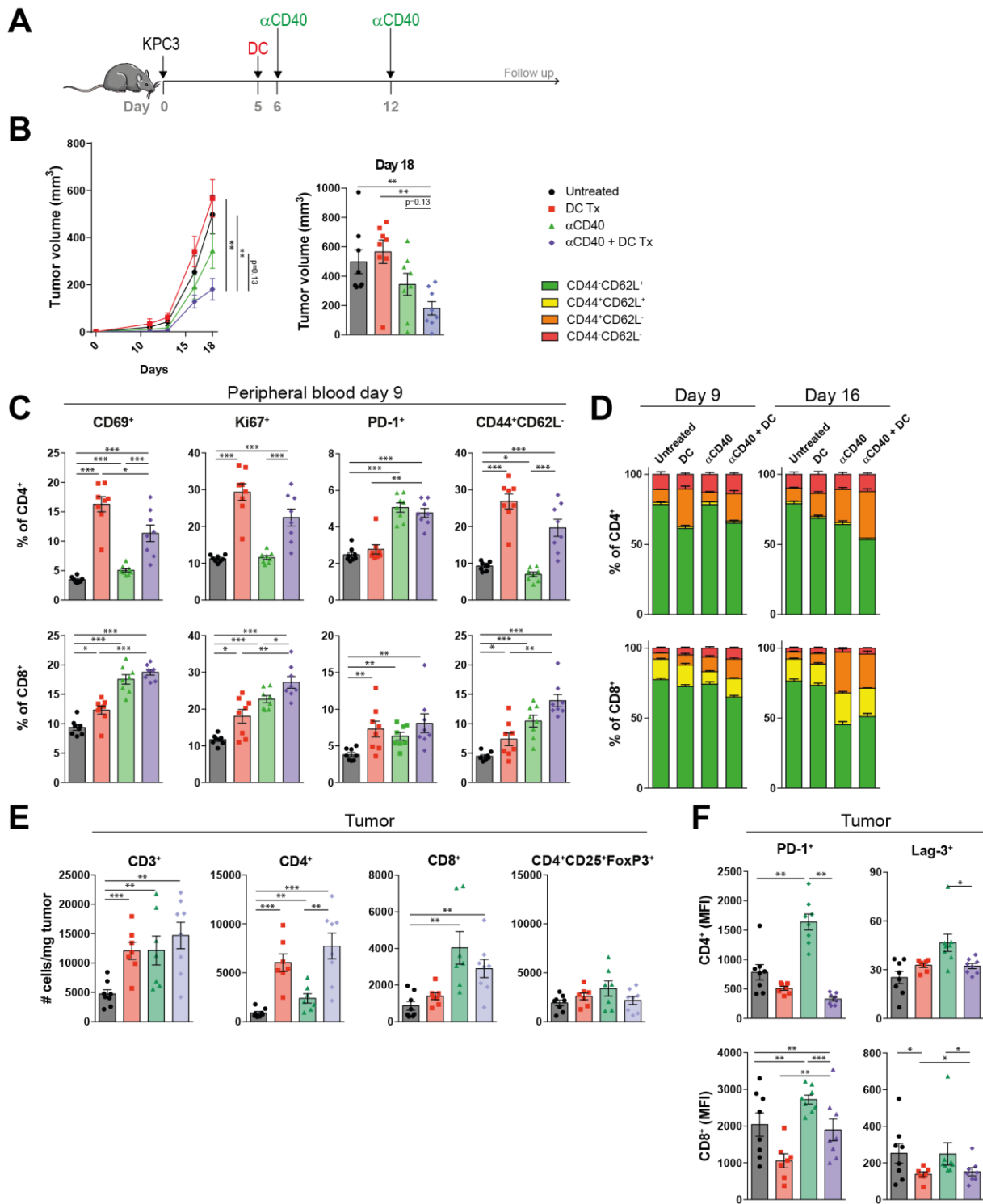
**Supplementary Figure 3.** Percentage of CD69+, Ki67+ and CD44+CD62L- subsets of circulating CD4+ and CD8+ T cells at day-3, 4 and 20. N=8 per group. Significance was determined using the non-parametric Mann-Whitney U test. Data presented as the mean  $\pm$  s.e.m. \*P<0.05.



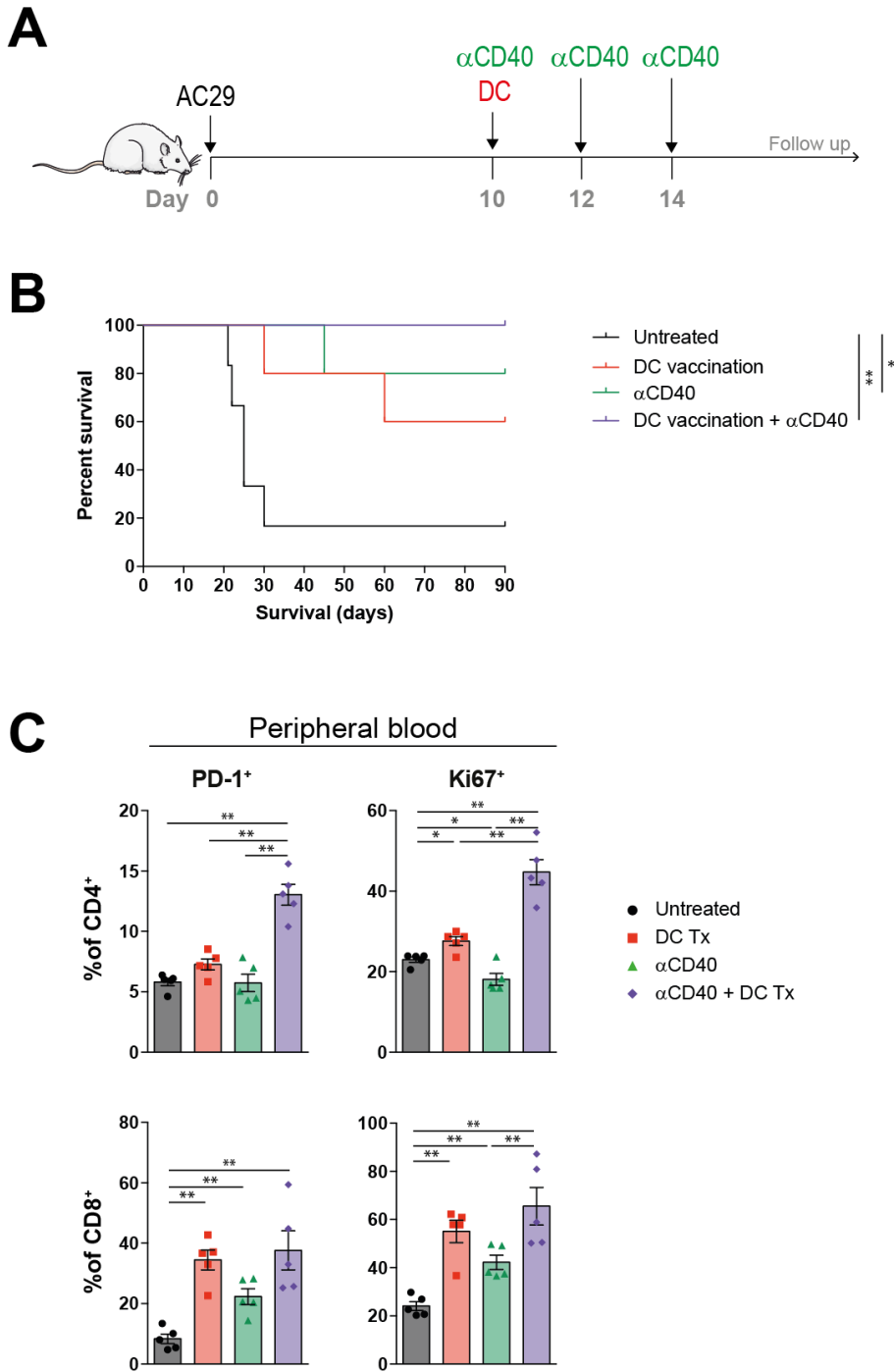
**Supplementary Figure 4.** Relative production of IFN $\gamma$ , IL-2 and TNF $\alpha$  by CD8<sup>+</sup> splenocytes of AE17 lysate-DC/ $\alpha$ CD40-treated and untreated after stimulation with DCs loaded with KPC3, AE17 or B16F10, or non-loaded DCs, normalized for untreated mice. N=6-10 per group. Significance was determined using the non-parametric Mann-Whitney U test. Data presented as the mean $\pm$ s.e.m. \*\*P<0.01, \*\*\*P<0.001, \*\*\*\*P<0.0001.



**Supplementary Figure 5.** Lysate-DC is not effective as monotherapy in tumor-bearing mice. (A) CD3<sup>+</sup>, CD4<sup>+</sup> and CD8<sup>+</sup> circulating T cells as a percentage of alive CD45<sup>+</sup> cells, four days after DC vaccination. (B) Percentage of CD44<sup>+</sup>CD62L<sup>-</sup> and Ki67<sup>+</sup> subsets of CD4<sup>+</sup> and CD8<sup>+</sup> circulating T cells, four days after DC vaccination. (C) Tumor volume measured over time, and tumor size at the day of sacrifice (day 22). (D) CD3<sup>+</sup>, CD4<sup>+</sup> and CD8<sup>+</sup> TILs as a percentage of alive CD45<sup>+</sup> cells. N=5-9 per group. Significance was determined using the non-parametric Mann-Whitney U test. Data presented as the mean  $\pm$  s.e.m. \*P<0.05, \*\*P<0.01, \*\*\*P<0.001.

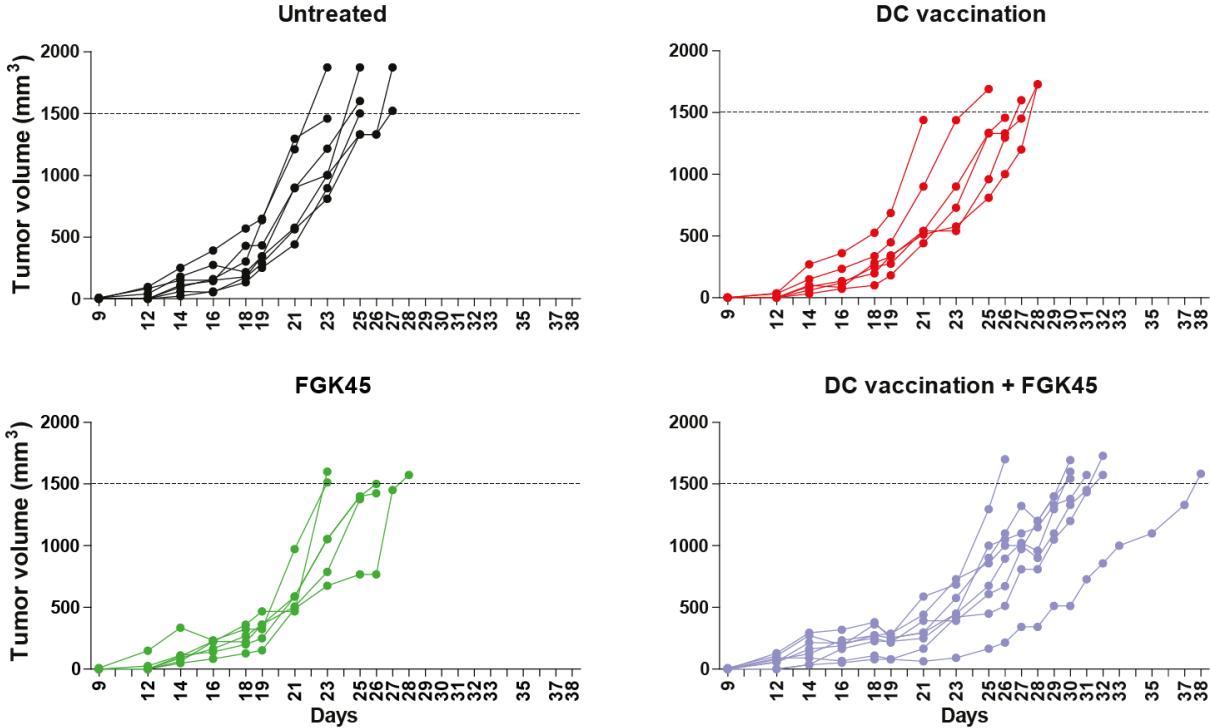


**Supplementary Figure 6.** (A) Study setup (B) Tumor volume measured over time, and tumor size at day of sacrifice (day 18). (C) Percentage of CD69<sup>+</sup>, Ki67<sup>+</sup>, PD-1<sup>+</sup> and CD44<sup>+</sup>CD62L<sup>-</sup> subsets of CD4<sup>+</sup> and CD8<sup>+</sup> circulating T cells, four days after treatment initiation. (D) Memory status of CD4<sup>+</sup> and CD8<sup>+</sup> circulating T cells at day 9 and day 16. (E) Number of CD3<sup>+</sup>, CD4<sup>+</sup>, CD8<sup>+</sup>, CD4<sup>+</sup>CD25<sup>+</sup>FoxP3<sup>+</sup> TILs per mg tumor. (F) MFI of PD-1 and Lag-3 of CD4<sup>+</sup> and CD8<sup>+</sup> TILs. N=7-8 per group. Significance was determined using the non-parametric Mann-Whitney U test. Data presented as the mean  $\pm$  s.e.m. \*P<0.05, \*\*P<0.01, \*\*\*P<0.001.

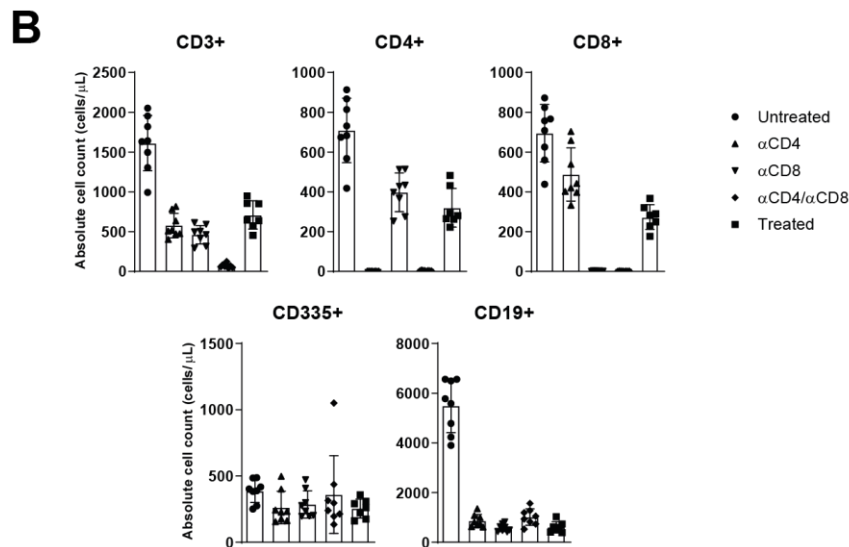
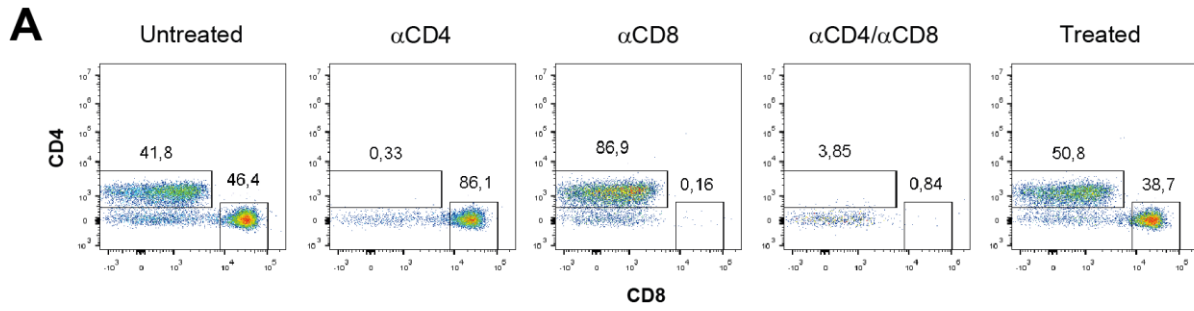


**Supplementary Figure 7.** (A) Study setup in mesothelioma model. (B) Kaplan-Meier analysis of treated and untreated animals. (C) Percentage of PD-1+ and Ki67 subsets of CD4+ and CD8+ circulating T cells, on day 16. N=5 per group. Significance was determined using the non-parametric Mann-Whitney U test. Data presented as the mean  $\pm$  s.e.m. \*P<0.05, \*\*P<0.01.

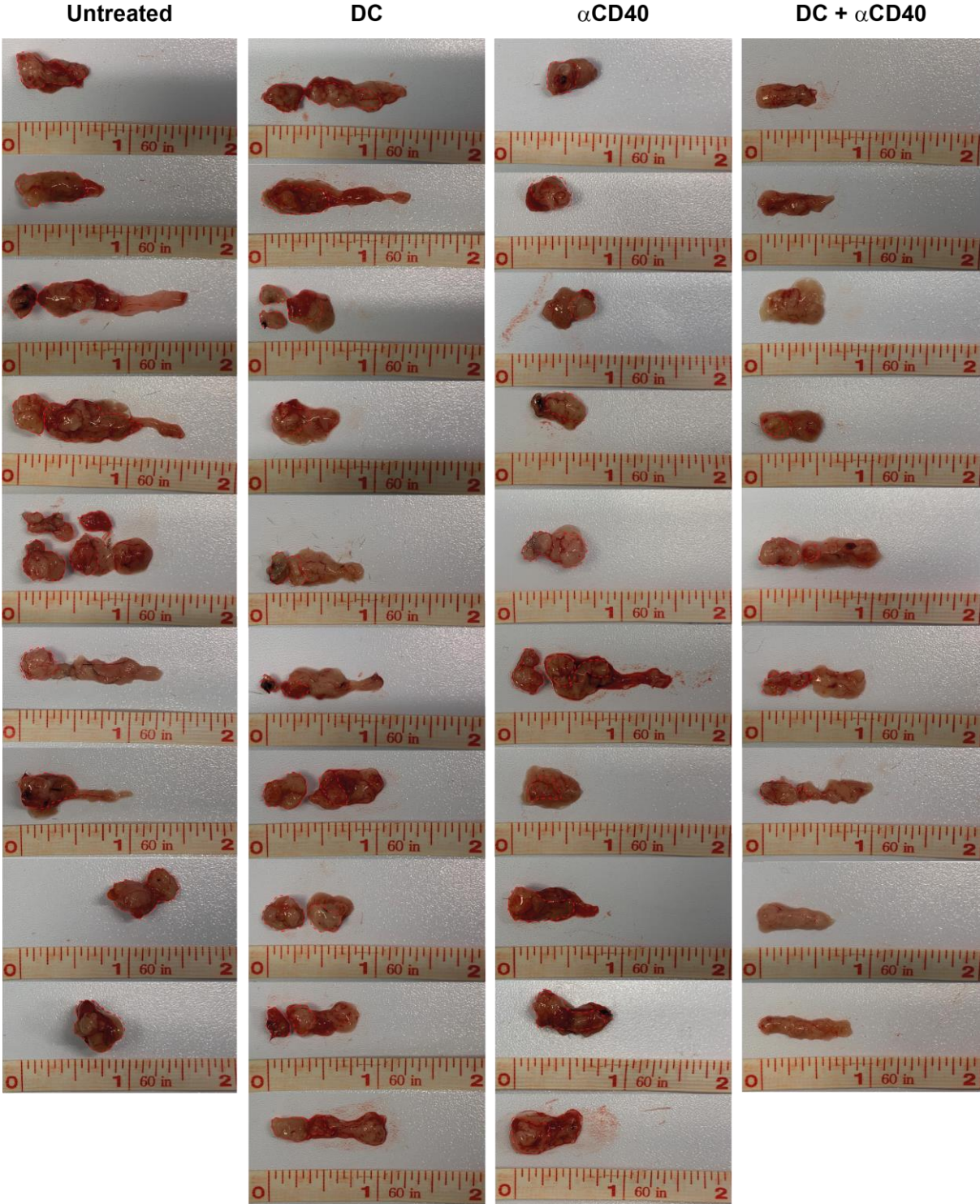




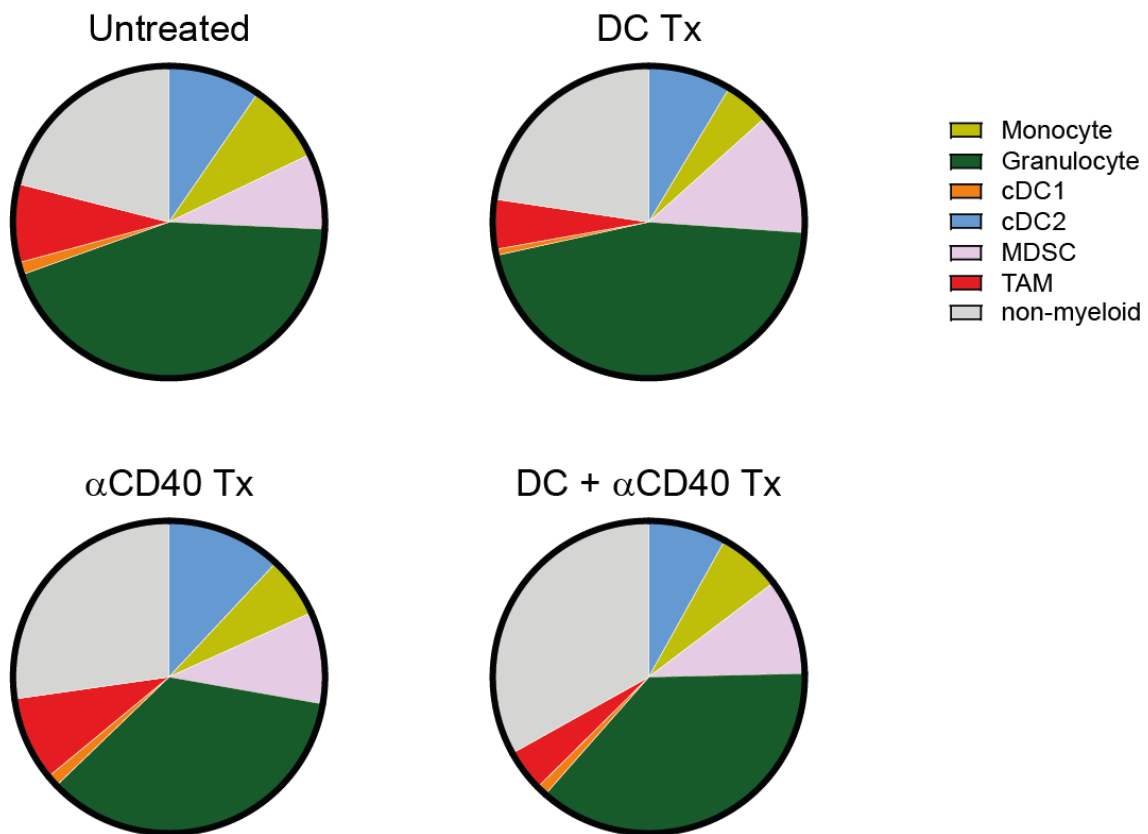
Supplementary Figure 8. Tumor outgrowth curves of treated and untreated tumor-bearing mice.



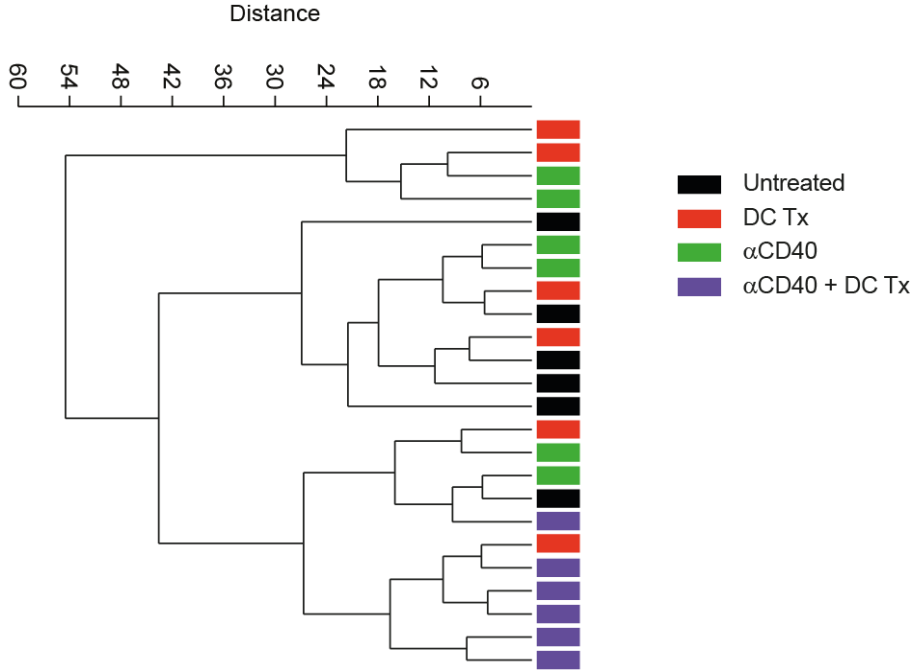
**Supplementary Figure 9.** (A) Interim blood analysis on day 14. Percentage of CD4+ and CD8+ of CD3+ T cells. (B) Absolute number of CD3+, CD4+, CD8+, CD335+ and CD19+ cells per  $\mu\text{L}$  blood drawn on day 14.



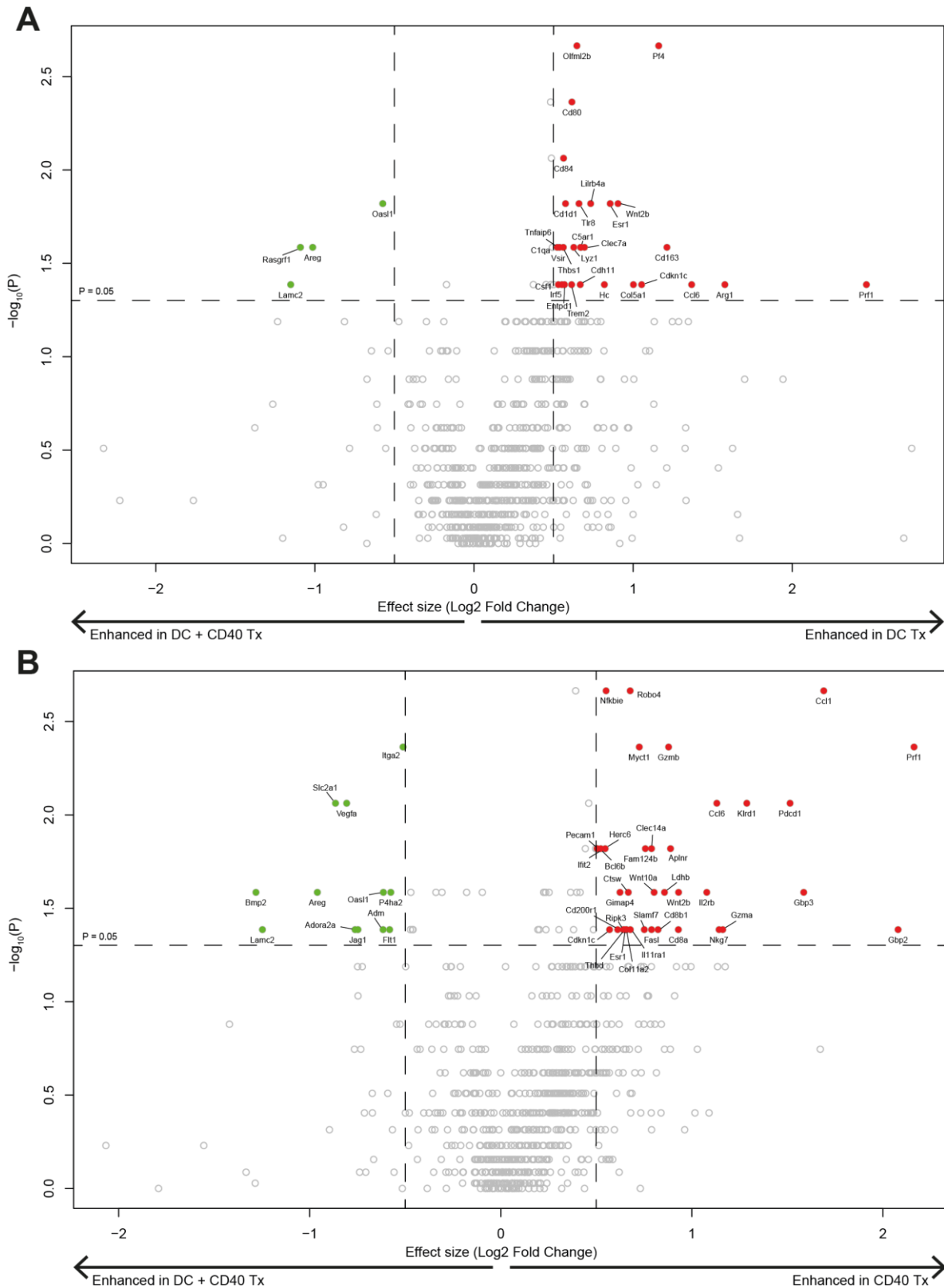
Supplementary Figure 10. Orthotopic tumors taken out on day 17.



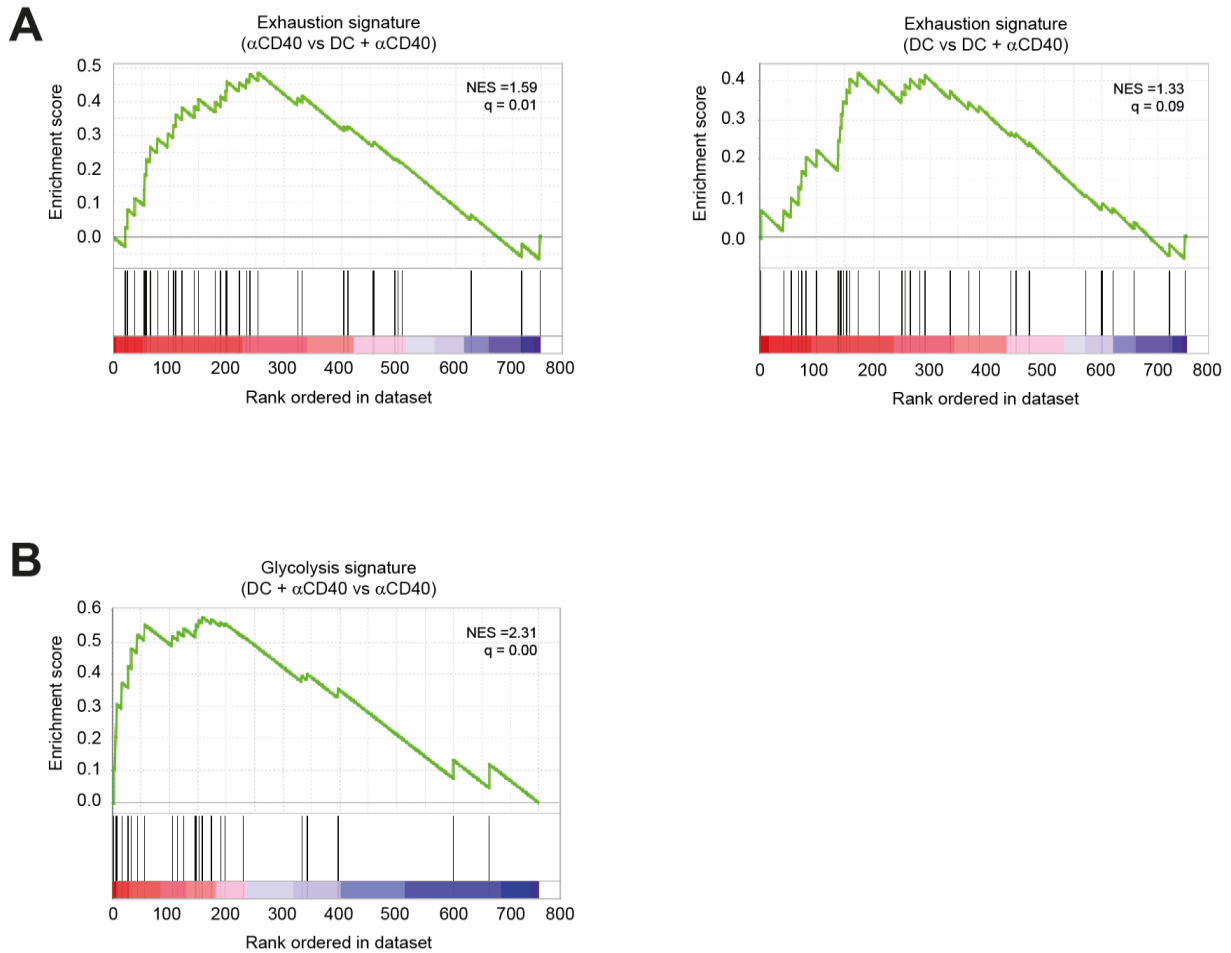
**Supplementary Figure 11.** Fraction of non-myeloid (CD45<sup>-</sup>), monocyte (CD45<sup>+</sup>F4/80-CD11b+Ly6C+Ly6G<sup>-</sup>), granulocyte (CD45<sup>+</sup>F4/80-CD11b+Ly6C-Ly6G<sup>+</sup>), cDC1 (CD45<sup>+</sup>F4/80-CD11b+CD11c+MHCII+CD103<sup>+</sup>), cDC2 (CD45<sup>+</sup>F4/80-CD11b+CD11c+MHCII<sup>+</sup>), MDSC (CD45<sup>+</sup>F4/80-CD11b+Ly6CintLy6Gint) and TAM (CD45<sup>+</sup>F4/80+CD11b<sup>+</sup>) as part of a whole of treated and untreated tumors.



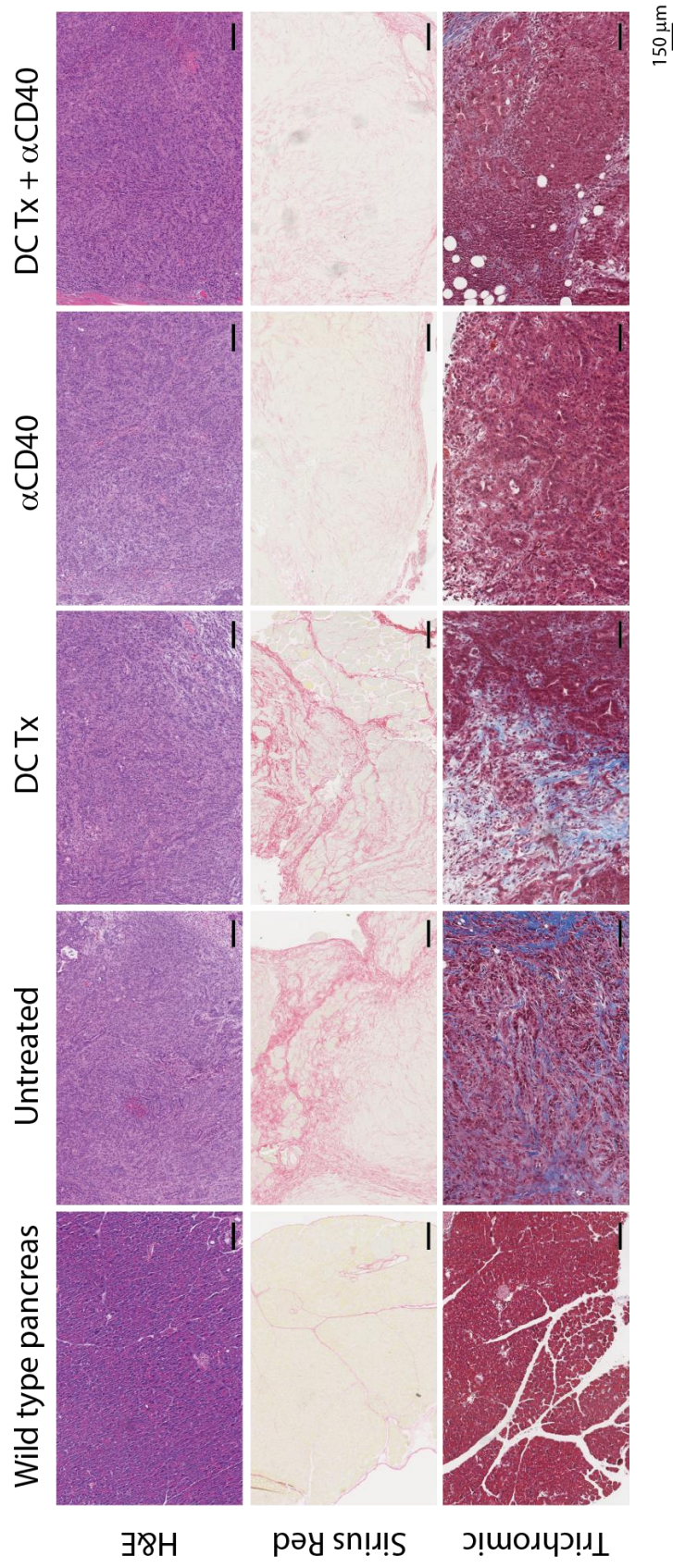
**Supplementary Figure 12.** Hierarchical clustering of individual tumor samples based on genes significantly different between groups.



**Supplementary Figure 13.** Volcano plots of differentially expressed genes between DC vaccination vs combination therapy (A) or  $\alpha$ CD40 vs combination therapy (B). The X-axis is log<sub>2</sub> fold change and the Y-axis is  $-\log_{10}$  of the original p-value. Markers with p-values < 0.05 and log<sub>2</sub> fold change > 0.5 are marked in red, while markers with p-values < 0.05 and log<sub>2</sub> fold change < -0.5 are marked in green. The two vertical lines indicate the log<sub>2</sub> fold change threshold of 0.5 and -0.5. The horizontal line indicates the original p-value threshold of 0.05.

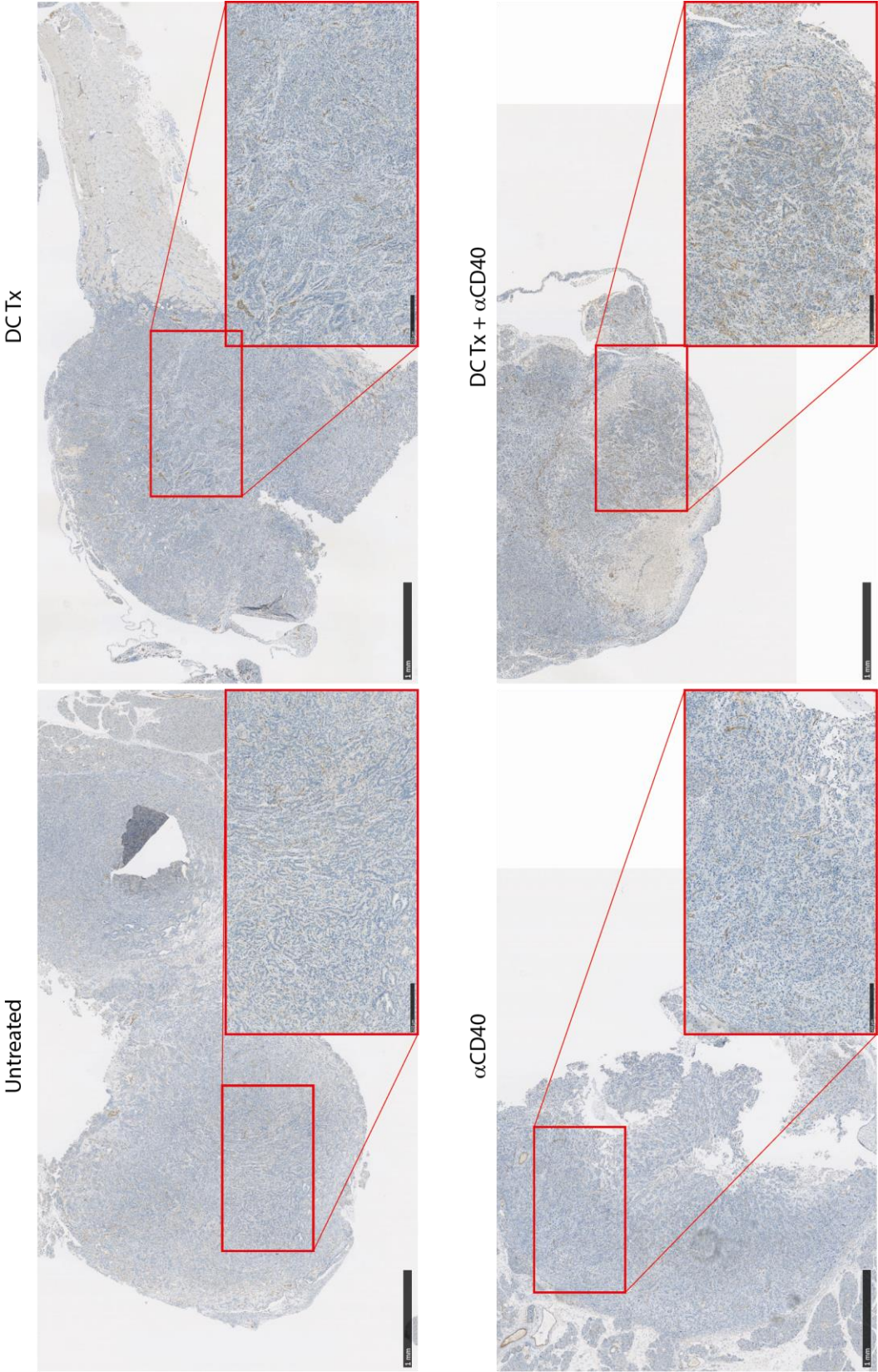


**Supplementary Figure 14.** (A) GSEA of T-cell exhaustion gene sets in tumors of  $\alpha$ CD40 or DC therapy versus combination therapy treated mice, presented as the normalized enrichment score (NES). (B) GSEA of T-cell exhaustion and glycolysis gene sets in tumors of combination therapy versus  $\alpha$ CD40 treated mice, presented as the normalized enrichment score (NES).

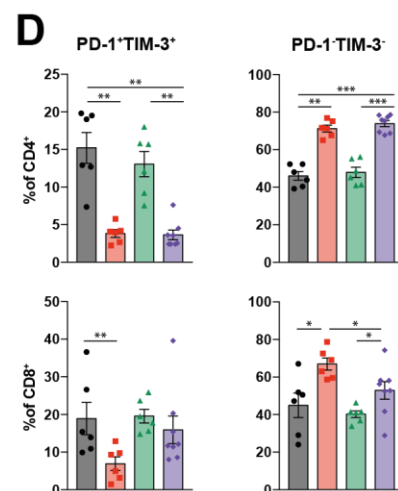
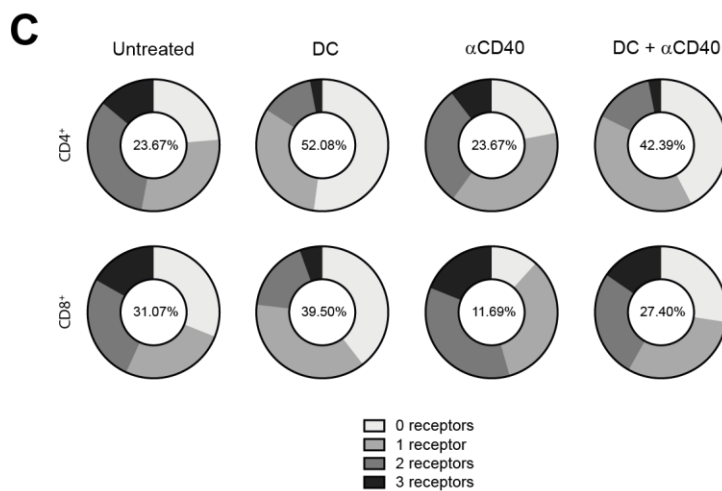
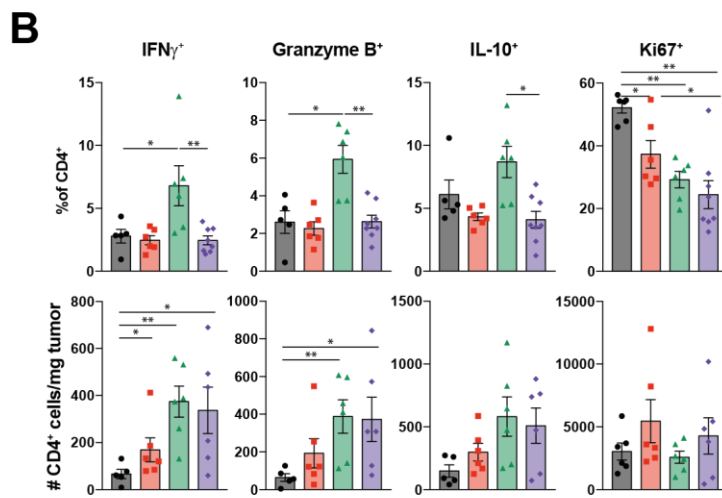
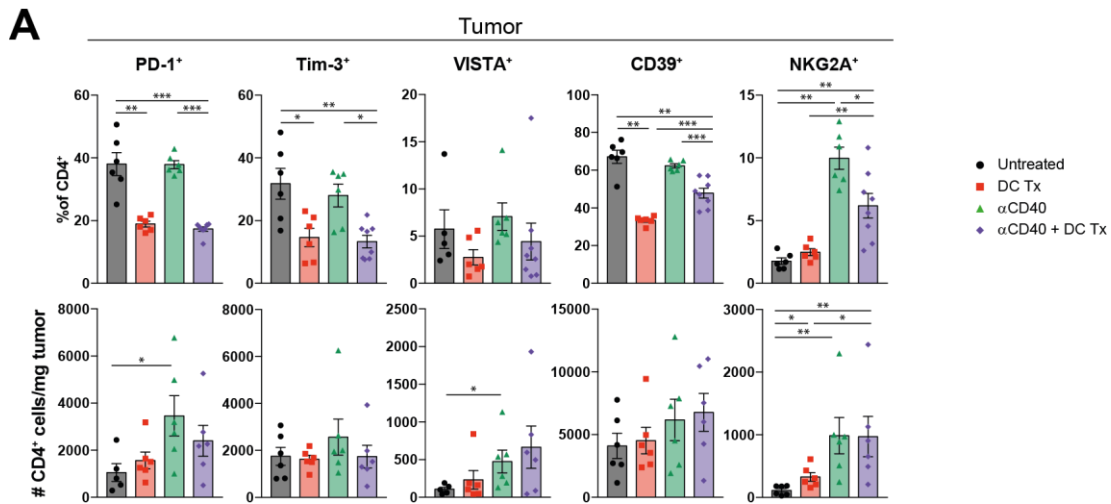


Supplementary Figure 15. Hematoxylin and Eosin, Sirius Red and Trichromic staining on tumor tissue.

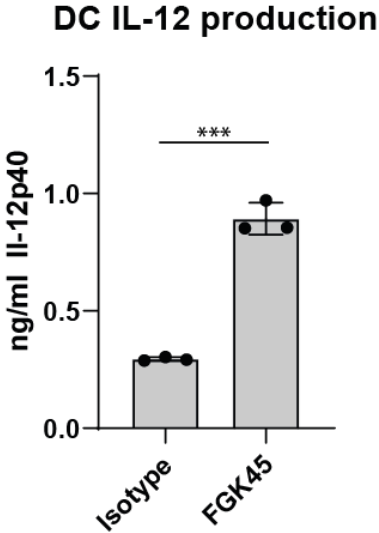




Supplementary Figure 16. CD31 immunohistochemistry staining on tumor tissue of treated and untreated mice.



**Supplementary Figure 17.** (A) Number and percentage of PD-1+, Tim-3+, VISTA+, CD39+ and NKG2A+ subsets of CD4+ TILs. (B) Number and percentage of IFN $\gamma$ +, Granzyme B+, IL-10+ and Ki67+ subsets of CD4+ TILs. (C) Detection of co-expression of inhibitory receptors (PD-1, Tim-3 and CD39) on CD4+ and CD8+ TILs. Numbers within circles represent percentage of TILs with 0 inhibitory receptors. (D) Percentage of PD-1/TIM-3 double positive and negative cells of CD4+ and CD8+ TILs. N=7-8 per group. Significance was determined using the non-parametric Mann-Whitney U test. Data presented as the mean  $\pm$  s.e.m. \*P<0.05, \*\*P<0.01, \*\*\*P<0.001.



Supplementary Figure 18. ELISA-based IL-12p40 detection in supernatant of bone-marrow derived DCs stimulated with FGK45 or isotype. Significance was determined using the Student's t-test. Data presented as the mean ± s.e.m. \*\*\*P<0.001.





# CHAPTER 4

---

Autologous dendritic cells pulsed with allogeneic tumor cell lysate induce tumor-reactive T-cell responses in pancreatic cancer patients: a phase I study

Sai Ping Lau

Larissa Klaase

Madelief Vink

Jasper Dumas

Koen Bezemer

Anneloes van Krimpen

Ruud van der Breggen

Leonoor V. Wismans

Michael Doukas

Willem de Koning

Andrew P. Stubbs

Dana A.M. Mustafa

Heleen Vroman

Ralph Stadhouders

Joana B. Nunes

Christoph Stingl

Noel F.C.C. de Miranda

Theo M. Luider

Sjoerd H. van der Burg\*

Joachim G. Aerts\*

Casper H.J. Van Eijck\*

\* *Shared last*

## ABSTRACT

**Background:** Pancreatic ductal adenocarcinoma (PDAC) is notorious for its poor prognosis even after curative resection. Responses to immunotherapy are rare and related to inadequate T-cell priming. We previously demonstrated the potency of allogeneic lysate-dendritic cell (DC) vaccination in a preclinical model. Here we translate this concept to patients. **Methods:** In this phase I study, patients with resected PDAC were included when they demonstrated no radiologic signs of recurrence after standard-of-care treatment. Allogeneic tumor lysate-loaded autologous monocyte-derived DCs were injected at weeks 0, 2, 4 and at months 3 and 6. Objectives are feasibility, safety and immunogenicity of allogeneic tumor-DCs. The presence of tumor antigens shared between the vaccine and patient tumors was investigated. Immunological analyses were performed on peripheral blood, skin and tumor. **Results:** Ten patients were included. DC production and administration were successful. All patients experienced a grade 1 injection-site and infusion-related reaction. Two patients experienced a grade 2 fever and 1 patient a grade 3 dyspnea. No vaccine-related serious adverse events were observed. Shared tumor antigens were found between the vaccine and patient tumors. All evaluated patients displayed a vaccine-induced response indicated by increased frequencies of Ki67+ and activated PD-1+ circulating T cells. In addition, treatment-induced T-cell reactivity to autologous tumor of study patients was detected. Seven out of ten patients have not experienced disease recurrence or progression at a median follow-up of 25 months (15- 32 months). **Conclusion:** Allogeneic tumor lysate-DC treatment is feasible, safe and induces immune reactivity to PDAC expressed antigens.

## INTRODUCTION

Pancreatic ductal adenocarcinoma (PDAC) is one of the leading causes of cancer-related death and its incidence is rising.(1-3) Prognosis is poor and the 5-year survival is less than 10%.(1) The majority of PDAC patients present with either locally advanced or metastatic disease, with only 10-20% of patients eligible for curative-intent surgery.(4,5) However, even after surgical resection long-term survival is exceptional in the majority of patients.(6-8) Therefore adjuvant chemotherapy is now considered standard of care. However, the median overall survival of patients with resected PDAC after receiving adjuvant gemcitabine treatment is 19.8 months.(9) However, this regimen is nowadays considered out of date as the ESPAC-4 trial demonstrated that adjuvant gemcitabine with capecitabine is superior to gemcitabine monotherapy.(10) In 2018, the PRODIGE-24/CCTG PA.6 trial showed that adjuvant FOLFIRINOX is superior to adjuvant gemcitabine.(11) In the era of these improved multi-agent systemic therapy improvements in survival have been achieved, however still 70-80% of patients will develop tumor recurrence within 5-years and therefore novel treatment modalities are still urgently needed.(12) Although immunotherapy demonstrated impressive results in various malignancies, immune-checkpoint inhibitors like PD-1 failed to show improvement of survival(8,13,14) and as such PDAC is considered a non-immunogenic tumor.(15-17) Recent seminal studies implementing rational immunotherapeutic strategies achieved disease control in PDAC demonstrating the importance of resurrecting immunogenicity.(18,19) In PDAC, T-cell dysfunction and exclusion have been proposed to be paramount.(20,21)

Dendritic cells (DCs) are potent activators of the immune system and can successfully be used to induce tumor immunity.(22) DC paucity in PDAC leads to dysfunctional immune surveillance, and it has been shown that restoring DC numbers in early PDAC lesions reinvigorates anti-tumor T-cell immunity.(23) Several DC-vaccination trials have previously demonstrated clinical and immunological responses in PDAC.(24-26) These DC-based vaccines exploit synthetic peptides, purified proteins or DNA/RNA making the detection of immunodominant epitopes imminent. We have demonstrated the rationale, safety and clinical efficacy of an allogeneic-tumor lysate based DC therapy (MesoPher) in patients with malignant mesothelioma (MM).(22) An allogeneic tumor lysate has several advantages as this is an off-the-shelf source of various tumor-associated antigens that can be shared across different tumor types, it eliminates the need for obtaining autologous tumor material, a known major logistical hurdle, and it provides treatment standardization across patients. Also, the use of lysate containing a broad repertoire of tumor associated antigens including cancer-testis and tumor-differentiation antigens may avoid tumor-immune escape which has been described for single-peptide strategies.(27,28) The MesoPher platform consists of autologous DCs loaded with an allogenic tumor cell lysate generated from MM cell lines.(22) It has been demonstrated that PDAC and MM share tumor antigens like mesothelin, WT1, Survivin.(29-31) We recently showed that the mesothelioma lysate-loaded DCs induced clinically effective tumor-specific T-cell responses in a murine PDAC



model due to shared tumor antigens across MM and PDAC.(32) Therefore, in this study we investigated this allogeneic lysate-DC strategy for feasibility and immunogenicity in patients with PDAC.

Immunologically, the detrimental survival of PDAC is markedly accounted by the formation of ubiquitous acellular matrix present in the solid tumor. The desmoplastic stroma is able to physically exclude and impair trafficking of T cells, thereby impeding its effector function.(33) We postulate that DC therapy is able to induce adequate anti-tumor immunity against occult metastatic disease before the process of desmoplasia has been initiated. Therefore, in this study we exclusively focused on patients with surgically resected PDAC who are clinically and radiologically free of local disease recurrence.

Here, we report on feasibility, safety and immune-reactivity of MesoPher treatment in resected PDAC patients. We determined overlap in tumor antigens between MesoPher and the autologous tumors of resected PDAC patients. Furthermore, we analyzed therapy-induced T-cell activation, and an *in vitro* co-culture assay was performed to assess the induction of autologous tumor-specific T cells.

## METHODS

### *Study design and participants*

The REACTiVe (Rotterdam pancrEatic Cancer Vaccination) trial is a single-center, non-randomized, open-label safety phase I study for patients aged 18 years or older with surgically resected and histologically proven PDAC who have completed standard-of-care treatment. Additional eligibility criteria were an Eastern Cooperative Oncology Group performance status score of 0–2, normal organ function and adequate bone marrow reserve (absolute neutrophil count  $>1.0 \times 10^9/L$ , platelet count  $>100 \times 10^9/L$ , and Hb  $>6.0$  mmol/L), and a positive DTH skin test (induration  $>2$  mm after 48 hours) against the positive control antigen tetanus toxoid. Patients were excluded if: residual disease was present at the time of inclusion, previously treated with immunomodulatory anticancer drugs, a history of autoimmune disease, organ allograft, malignancy (except adequately treated basal cell or squamous cell skin cancer, superficial or in situ bladder cancer or other cancer for which the patient has been 5-years disease-free) or used immunosuppressive therapy. A detailed list of inclusion and exclusion criteria can be found in the clinical trial protocol attached in the supplementary material.

The study was approved by the Central Committee on Research involving Human Subjects (NL67169.000.18) as defined by the Medical Research Involving Human Subjects Act. Procedures followed were in accordance with the ethical standards of these committees on human experimentation and with the Helsinki Declaration of 1975, as revised in 2008. The trial is registered with the Netherlands Trial Register, NL7432. An informed written consent was obtained from each subject.

### *Procedures*

Monocytes for DC (mo-DC) production were retrieved via leukapheresis. Every vaccination consists of  $25 \times 10^6$  autologous mo-DCs pulsed with the allogeneic tumor cell line lysate PheraLys, all produced under Good Manufacturing Practice (GMP)-certified conditions, as described previously.(22) MesoPher is injected 3 times every 2 weeks. After the 3rd injection, a DTH skin test was performed with MesoPher ( $4 \times 10^6$  DCs), and booster vaccinations are given after 3 and 6 months. Therapy is administered two-thirds intravenously and one-third through intradermal injection, as proposed earlier (34). Blood draws for immunomonitoring done before every main vaccination and one week after the first vaccination and 2 weeks after the third vaccination (Fig. 1A).

Tumor load was radiographically assessed with a CT-thorax/abdomen every three months starting from screening until the end of the study by the radiologist and reported per RECIST v1.1 criteria. Patients underwent follow-up using CT scans examinations every six months, or when recurrence was suspected. Safety assessments were done at each study visit including vital signs and laboratory testing. Adverse events were graded according to the National Cancer Institute Common Terminology Criteria for Adverse Events (NCI-CTCAE) v4.03.

### *Outcomes*

The primary objective is feasibility of MesoPher vaccination, as determined by the success of leukapheresis and MesoPher production, and the ability to vaccinate according to the predefined study schedule. Secondary objectives were clinical outcome as determined by overall and progression-free survival, safety according to NCI-CTCAE, and immunogenicity as detected by DTH skin reactions, peripheral blood T-cell activation, and the capacity of T cells to respond to stimulation with MesoPher and/or autologous tumor cell-derived antigens.

### *Statistical analysis*

The primary objective was feasibility. The study was considered positive when eight out of ten patients were able to undergo the whole treatment. Paired Wilcoxon signed-ranks tests were used to test for significance between baseline measurements and other time points. Flow-cytometry data were normalized for baseline. Figures were made using GraphPad Prism software v8.0. Gene-expression data was corrected for multiple testing using Benjamini-Hochberg procedure. Progression-free and overall survival were calculated from inclusion to the first documented event. Survival data were plotted as Kaplan–Meier survival curves, and log-rank testing was performed to compare cohorts. In all cases, a p-value of 0.05 and below was considered significant (\*),  $p < 0.01$  (\*\*) and  $p < 0.001$  (\*\*\*) as highly significant.

Material and methods concerning the immunological experiments can be found in the supplementary.

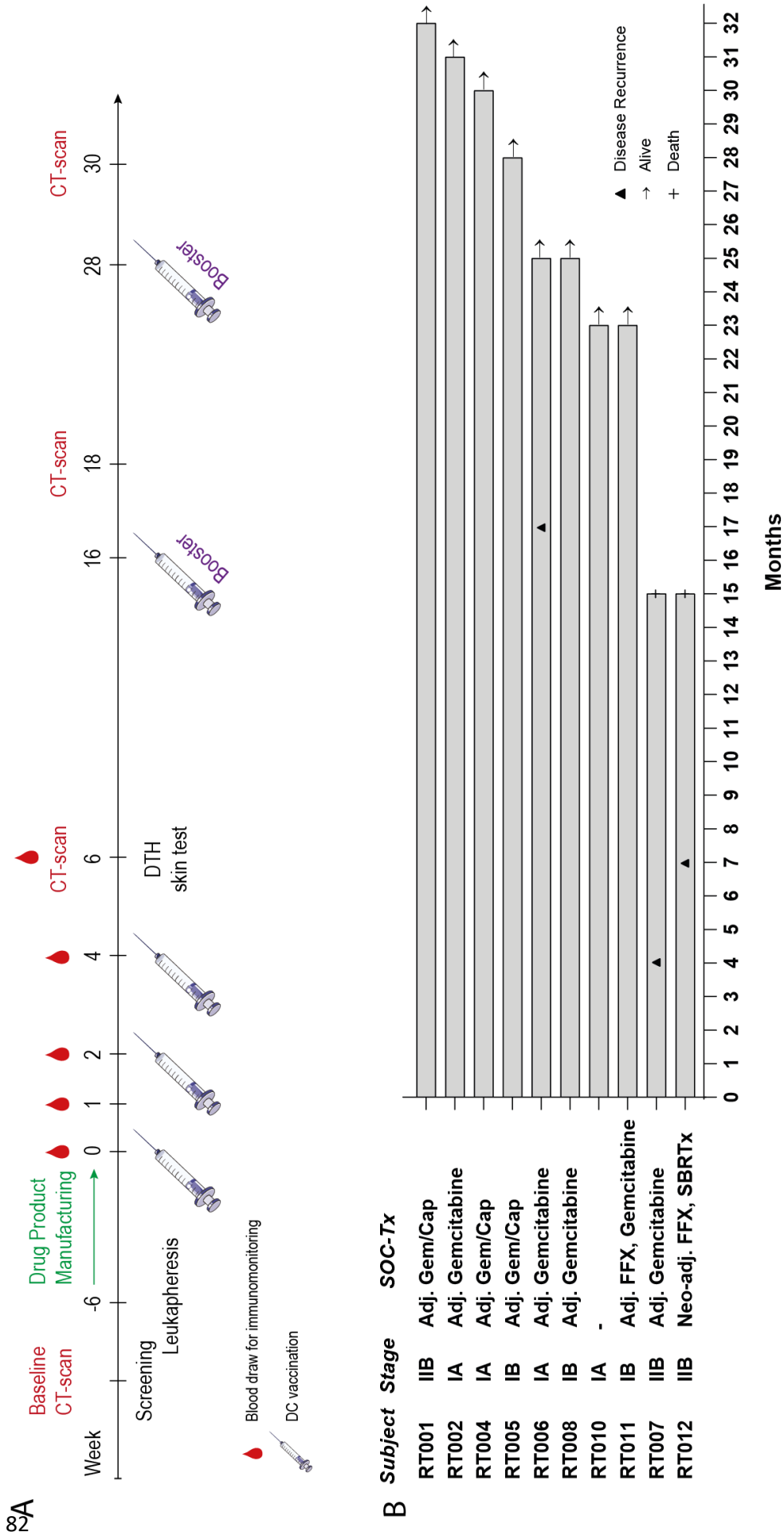


**Figure 1.** Treatment schedule REACTiVe Trial and swimmer plot of study patients. (A) Red droplets indicate blood draws for immunomonitoring. Syringes indicate DC vaccination. Blood draws were taken before immunotherapy. (B) Swimmer plot representing survival of patients since date of inclusion. Tumor stage according to the AJCC Cancer Staging Manual (8th Edition) and standard-of-care treatment is presented per individual patient. Stable disease is depicted as a square, disease recurrence with a triangle, death with a cross and alive with an arrow. Abbreviations: SOC-Tx, standard-of-care treatment; Adj., adjuvant; Neo-adj., neo-adjuvant; Gem/Cap, gemcitabine/capecitabine; FFX, FOLFIRINOX; SBRTx, stereotactic-body radiotherapy.

## RESULTS

### *Patient Characteristics*

Ten patients with surgically resected PDAC who had completed standard-of-care treatment were recruited between February 2019 and February 2020. Study patients were treated as indicated in Fig. 1a. Patient characteristics are summarized in Table 1. The median age at study entry was 64 years (range 47- 81 years). In eight of ten patients the performance status score was 0, and two others had a performance status score of 1 and 2. All patients had a tumor stage of I or II, and all except one patient had a microscopically margin-negative (R0) resection. Eight patients received adjuvant chemotherapy and one neoadjuvant chemoradiation therapy. One patient did not receive (neo)adjuvant treatment as she was deemed unfit for chemotherapy by the treating oncologist. The median time from finalizing standard-of-care treatment to inclusion was 3.5 months (range 1- 12 months).

### *Feasibility*

Feasibility was assessed for all ten patients. For eight of the ten patients, one leukapheresis was required to produce all five MesoPher vaccinations. In two patients (RT002, RT004), the first leukapheresis had to be interrupted because of venous flow problems. RT002 required a third leukapheresis to produce the 4th and 5th vaccine. All drug products passed quality control and sterility testing (Sup. Table 4). Also, intravenous, and intradermal administration of study drug were performed successfully (Sup. Table 5). Nine of the ten patients received all five treatments. RT012 received four vaccinations due to disease progression.

### *Safety and Toxicity*

Safety and toxicity were assessed for all ten patients. No significant clinical changes in vital signs within two hours after MesoPher administration were observed (Sup. Fig. 1). In some patients, a non-clinically relevant drop in systolic or diastolic blood pressure was observed. This was potentially due to the two hours of obligatory inactive observation period. No complaints or clinical signs of distress were reported during vaccination or in the observation period. After vaccination, all patients experienced a grade 1 injection-site reaction (ISR) consisting of erythema (100%), local pruritus (60%), local pain (10%), skin induration (100%), and/or warmth (20%) (Sup. Table 6). All patients also experienced an infusion-related reaction (IRR). Grade 1 IRRs consisted of chills (80%), fatigue (100%), fever (70%), headache (10%), hot flashes (10%), malaise (20%), myalgia (50%), pruritus (10%), vertigo (10%), vomiting (10%). One patient experienced grade 3 dyspnea following study treatment. Two patients had a grade 2 fever after vaccination. In general, ISR and IRR events lasted for 1-2 days.

No serious adverse events (SAE) related to MesoPher treatment were reported during the study. One patient experienced a study treatment-unrelated SAE (dyspnea) requiring

hospitalization. The patient is known with a history of chronic obstructive pulmonary disease (COPD) and the event (exacerbation of COPD) occurred between study treatments. All adverse events during the study are listed in Sup. Table 6.

Characteristics	Patients (N = 10)
Age (yr)	
Median	64
Range	47- 81
Gender (N)	
Male	4
Female	6
Ethnicity (N)	
Caucasian	9
Arab-Berbers	1
ECOG performance status score (N)	
0	8
1	1
2	1
Tumor stage (N)	
IA	4
IB	3
IIA	0
IIB	3
Pancreatic tumor location (N)	
Head	6
Body	1
Tail	3
CA 19-9 at time of inclusion (N)	
≤90 U/ml	10
≥90 U/mL	0
Surgery (N)	
Pancreaticoduodenectomy	7
Distal pancreatectomy and splenectomy	3
Status of surgical margins (N)	
R0	9
R1	1
Additional treatment (N)	
Neo-adj. FOLFIRINOX/SBRTx	1
Adj. Gemcitabine	4
Adj. Gemcitabine/Capecitabine	3
Adj. Gemcitabine/FOLFIRINOX	1
Time since SOC treatment (mos.)	
Median	3.5
Range	1- 12

**Table 1.** Demographic and baseline characteristics of patients in the study population. Abbreviations: ECOG, Eastern Cooperative Oncology Group; CA19-9, Carbohydrate antigen 19-9; FOLFIRINOX, 5-fluorouracil + leucovorin + irinotecan + oxaliplatin; SBRTx, Stereotactic Body Radiation Therapy; SOC, Standard-of-Care. Tumor stage was assessed according to the AJCC Cancer Staging Manual, 8th Edition.

### *Clinical Outcome*

Median overall survival and progression-free survival were not reached at the time of data cut-off (November 2021). No local disease recurrence or any tumor progression was observed in seven of the ten patients with a median follow-up of 25 months (range 15- 32 months). Eight patients were disease-free at 12 months (Fig. 1b). Three patients experienced recurrence of disease at the time of data cut-off. RT007 and RT012 died 11 and 8 months after disease progression, respectively. RT006 is alive 8 months after progression without subsequent treatment. During follow-up of RT002, after completing MesoPher treatment, a solitary pulmonary nodule with a diameter of 7.2mm was found for which a resection was performed. Retrospectively, this nodule was present at baseline with a diameter of 2.3mm. Pathological examination revealed that this lesion was a metastatic lesion. Currently, 12 months after video assisted thoracic surgery, RT002 shows no evidence of recurrent disease.

### *MesoPher and PDAC share known tumor antigens.*

To explore the presence of shared tumor antigens between the drug product and PDAC, we compared the mRNA expression of known tumor antigens (Sup. Table 2) between the five mesothelioma cell lines utilized in MesoPher and autologous tumor cells of study subjects. A total of 111 known tumor antigens were detected (Fig. 2a, Sup. Table 7), 42 of which were shared between the cell lines and patient tumors. Subsequently, the presence of shared tumor antigens was evaluated at protein level analyzing MesoPher and PDAC samples of nine patients. The presence of 51 known tumor antigens (Fig. 2b; Sup. Table 8) within 163 identified peptide sequences (Sup. Fig. 2) was detected. In total, 39 of the 51 proteins were shared between autologous tumors and MesoPher (Fig. 2b right column), confirming the potential of the vaccine to induce PDAC-reactive immune reactivity.

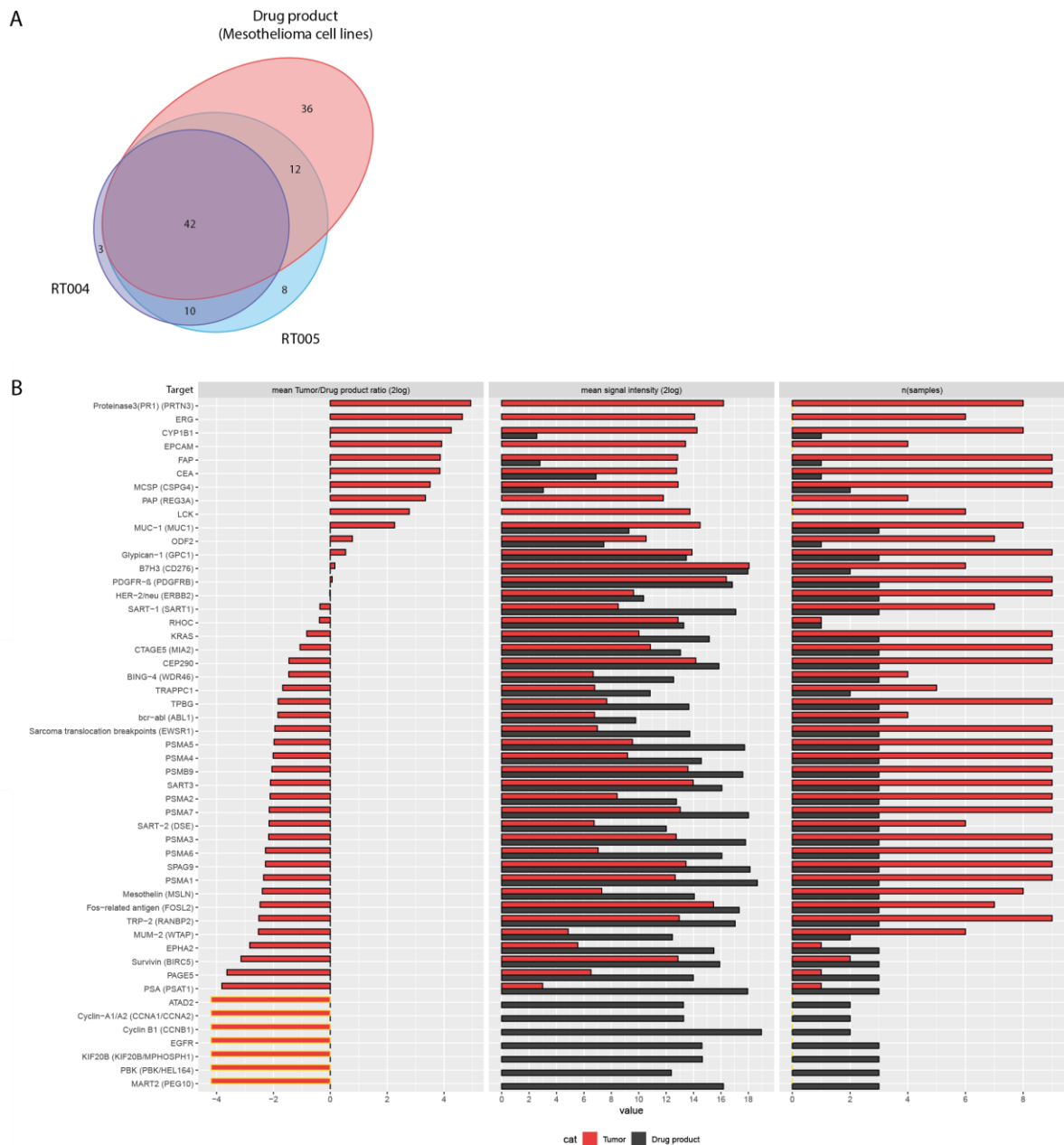


**Figure 2.** Autologous tumors of study patients and MesoPher demonstrated shared tumor antigens. (A) Venn diagram of number of identified tumor antigens on transcriptome level between RT004, RT005, and mesothelioma tumor cell lines used in MesoPher. (B) Mass spectrometry analysis on nine tumor samples; Waterfall plot of mean Tumor lysate/Drug product ratio (left), mean measured signal intensity of the tumor antigen (mid), and number of samples in which tumor antigens was identified (right). Yellow marking indicates that no peptide of the tumor antigen was detected above the threshold of  $S/N \geq 10$  for PDAC samples.

*MesoPher vaccination induces T-cell activation.*

All patients developed a positive delayed-type hypersensitivity skin reaction to MesoPher post-vaccination (Fig. 3).

We first performed broad gene-expression profiling of peripheral blood cells to evaluate the induction of specific immune responses following therapy. This demonstrated the upregulation of various T-cell activation markers (e.g. CD28, ICOS, TNFRSF4) after the first vaccination (Fig.

4a, b). Other genes upregulated two weeks after treatment include CCR4, TCF7, USP9Y, JAK3, CCR7, FLT3LG, and IL11RA. To confirm the presence of T-cell activation at protein level, we performed multi-parameter flow cytometry in circulating immune cells at multiple time points (Sup. Fig. 3). A transient increase in absolute numbers of CD3+ and CD4+ T cells was observed after DC vaccination (Fig. 4c). The percentages of CD4+ non-regulatory T cells expressing HLA-DR+, ICOS+, Ki67+ and/or PD-1+Ki67+ frequencies increased early after vaccination (Fig. 4d), while the percentage of CD4+ T cells expressing markers of T-cell inhibition (*i.e.*, TIM-3, CTLA-4, LAG-3) did not (Sup. Fig. 4). No overt changes were found in the proportions of naïve, memory, and effector-cell subpopulations (Fig. 4e). To demonstrate vaccine-specific activation, analysis of T cell receptor (TCR)- $\beta$  repertoires of the T cells isolated from both MesoPher-challenged skin and blood at week 5 of 3 patients was performed. This revealed an increase in the fraction of shared TCRs post vaccination. Although not observed in CD8+ T cells, an enrichment of shared TCRs was found in the CD4+PD-1+ (activated T cells) non-Treg compartment as compared to CD4+PD-1- T-cell fractions (Fig. 4f; Sup. Table 9).

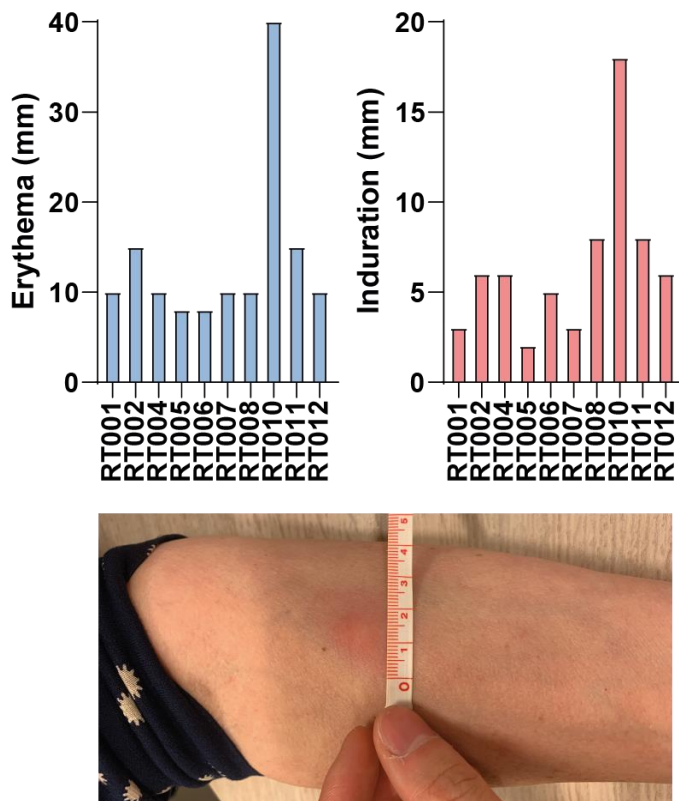


**Figure 3.** Positive Delayed-Type Hypersensitivity skin test following DC vaccination. A DTH skin test with MesoPher is performed after the third DC vaccination. Bar graphs display erythema and induration following DTH skin test per patient in mm. Photograph illustrates a positive reaction.



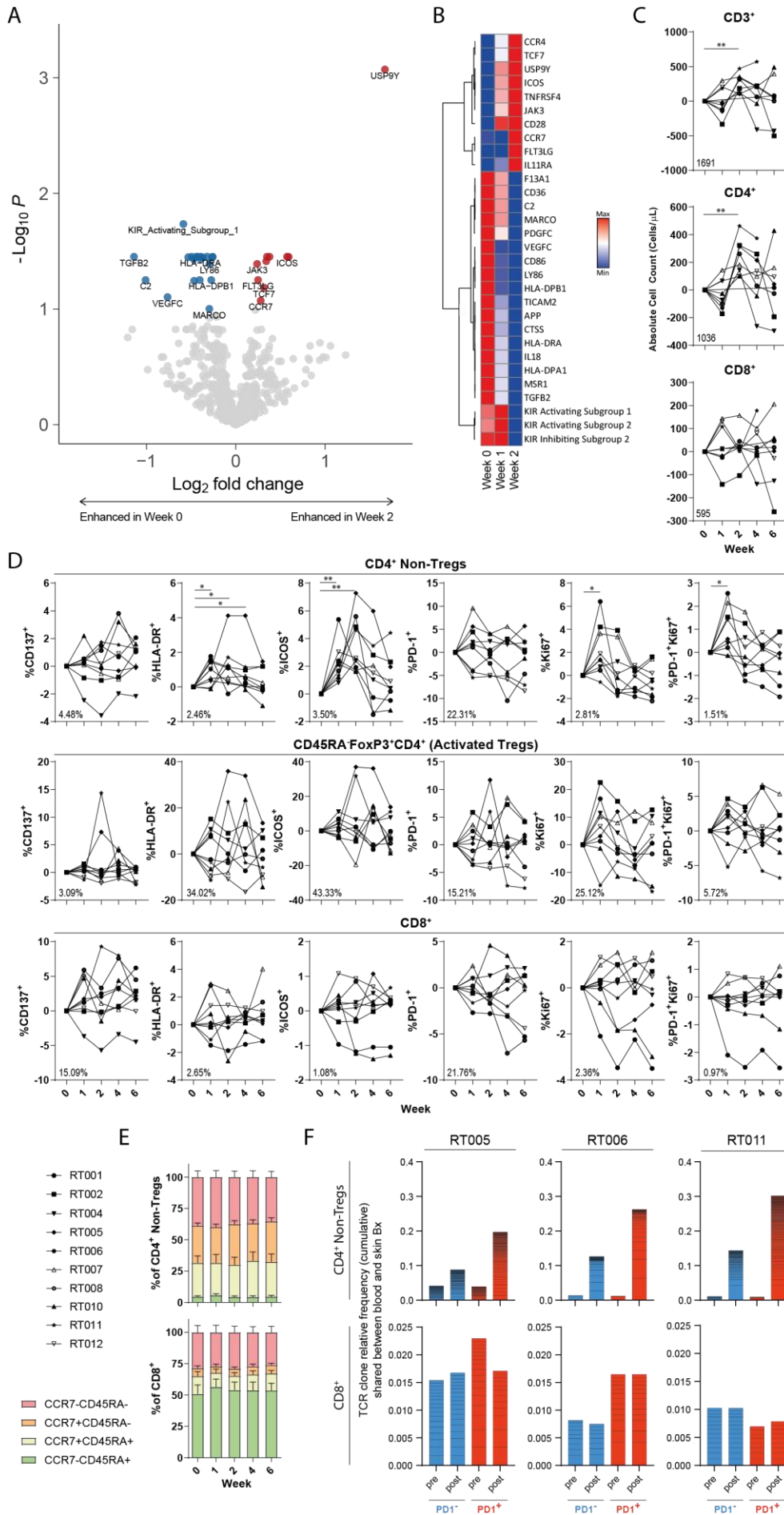
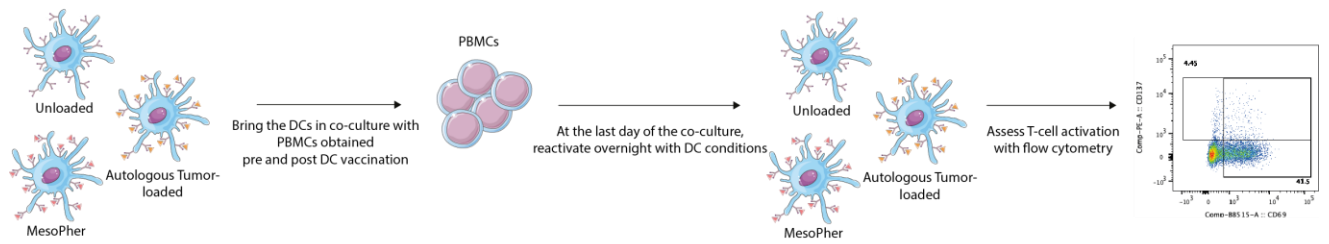


**Figure 4.** MesoPher vaccination induces T-cell activation. (A) Volcano plot demonstrating genes upregulated at baseline versus 2 weeks after vaccination. Genes with an BH-corrected P-value < 0.1 were highlighted. (B) Significantly differentially expressed genes (BH-corrected P-value < 0.1) between baseline, week 1 and week 2 are visualized. (C) Number of CD3+, CD4+ and CD8+ T cells per uL blood. (D) Percentage of CD137+, HLA-DR+, ICOS+, PD-1+, Ki67+ and PD-1+Ki67+ subsets of CD4+ Non-Tregs, CD45RA-FOXP3+CD4+ Tregs, and CD8+ cells. N= 10 per group. Data is normalized for baseline (week 0) and paired per patient. Percentage in left corner represent the average frequency at baseline. Significance was determined using the paired Wilcoxon signed-rank test. \*P<0.05, \*\*P<0.01, \*\*\*p<0.001. (E) Percentage of CCR7-CD45RA-, CCR7+CD45RA-, CCR7+CD45RA+ and CCR7-CD45RA+ subsets of CD4+ Non-Tregs and CD8+ T cells in peripheral blood. (F) Detection in skin biopsies of TCR $\beta$  clones corresponding to PD-1+ and PD-1- cells in the CD4+ and CD8+ T cell compartment shared with blood before (week 0) and after treatment (5 weeks).

*MesoPher stimulated T cells recognize autologous tumor-derived antigens.*

Six patients had sufficient study material (*i.e.*, mo-DCs, PBMCs, and autologous tumor material) to perform an *in vitro* co-culture assay to assess treatment-directed T-cell responses (Fig. 5a). To investigate vaccine and tumor-reactivity induced by study treatment, peripheral blood lymphocytes isolated before and after treatment were stimulated *in vitro* with MesoPher, autologous tumor lysate-loaded DCs or with non-loaded DCs, and reactivated overnight with DCs. It has been demonstrated that CD137 accurately identifies tumor-specific T cells.(35,36) In all six tested patients, a MesoPher-specific CD4+ T-cell response, indicated by increased frequencies of CD137+ cells, was detected post-therapy (*i.e.* week 2, 6) but not before vaccination (*i.e.* week 0) when peripheral blood lymphocytes were co-cultured with MesoPher and reactivated overnight with MesoPher compared to reactivation with control non-loaded DCs (Fig. 5b). Also, MesoPher-specific CD8+ T-cell responses were detected in four out of six patients (RT005, RT006, RT008, RT009). When post-treatment PBMCs were co-cultured with MesoPher or autologous tumor-loaded DCs, increased CD137+ frequencies could be observed in three out of five patients (RT006, RT008, RT009) when reactivated with autologous tumor-DCs compared to reactivation with non-loaded DCs. In none of the patients such a response was observed in the pre-treatment samples, or when post-treatment PBMCs were co-cultured with control non-loaded DCs before they were reactivated with autologous tumor-DCs, underlining the presence of a tumor-specific T-cell response.

A



B

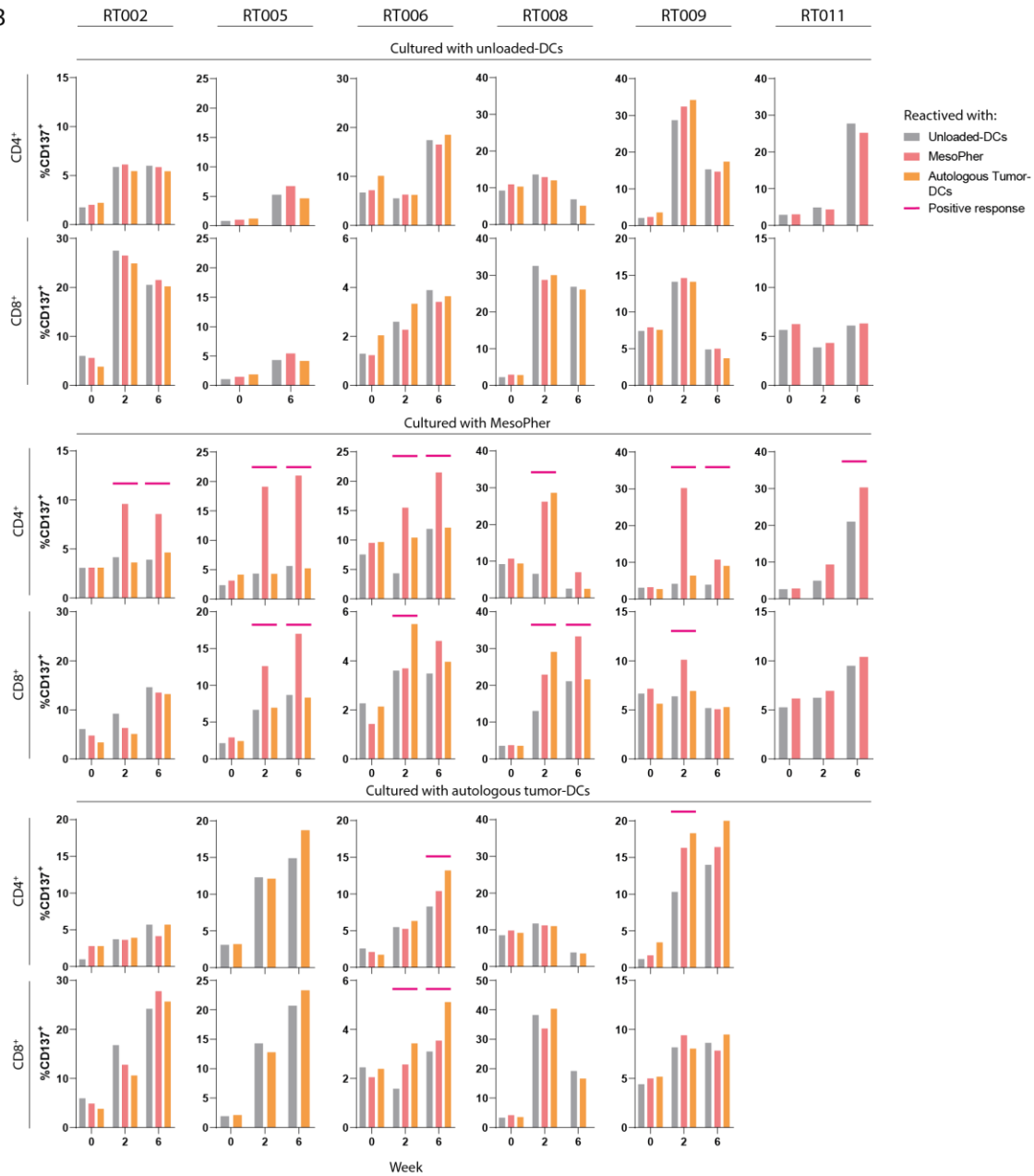


**Figure 5.** MesoPher and autologous tumor-directed responses can be measured *in vitro*. (A) Schematic overview of the *in vitro* co-culture system. PBMCs were co-cultured with various DC conditions at start and reactivated with various DC conditions to assess specific responses. (B) Percentages of CD137+ subsets of CD4+ and CD8+ circulating T cells at baseline (week 0) and post-treatment (week 2, 6) after stimulation with unloaded DCs, MesoPher or autologous tumor-loaded DCs and reactivated overnight with unloaded DCs, MesoPher or autologous tumor-loaded DCs in RT002, RT005, RT006, RT008, RT009, and RT011. Autologous tumor reactivity was not evaluated for RT011 due to lack of material. A positive

response to DCs with the antigen indicated is defined as a 50% or higher increase in the percentage of T cells expressing the indicated activation marker when compared to antigen-control cells (unloaded-DC). Positive responses are marked with a red stripe. A vaccine-induced response is defined as a positive response after vaccination which was not present before vaccination and not present when cultured with unloaded-DCs at start.

## DISCUSSION

This is the first-in-human clinical trial, driven by preclinical observations, treating PDAC patients after surgical resection with allogeneic tumor lysate-DC vaccination. MesoPher vaccination therapy was found to be feasible and safe, in line with the previously reported safety data of MesoPher in mesothelioma patients.(22) The primary endpoint was reached as all patients were able to receive the three DC vaccinations as planned. This opened the way to an expansion cohort which is currently enrolling to formally assess clinical efficacy [NL67169.000.18].

Next to feasibility, treatment-induced immunological responses were assessed. MesoPher vaccination was reactogenic as indicated by a positive DTH skin reaction to MesoPher in all patients. Comprehensive multicolor flow cytometry of peripheral blood showed increases in the frequencies of predominantly activated CD4+ T cells.(37) We also revealed that various memory T-cell subsets displayed a vaccine-induced increase in PD-1+Ki67+ cell frequencies, which may potentially be clinically beneficial as this double-positive population correlates with clinical outcome after immunotherapy.(38) The central memory CD4+ non-regulatory T-cell compartment showed the strongest response to vaccination. This is favorable in the context of tumor vaccines since central memory T cells can sustain the activation of new effector cells.(39,40) Notably, the upregulation of TCF7 post-vaccination may indicate the formation of T cells with stem-like properties which are sensitive for immune checkpoint blockade.(41) The combination of FLT3LG, CCR7 and, JAK3 upregulated post-therapy may indicate maturation and migration of DCs.(42) DCs capture, process and (cross-)present tumor antigens and are critical for robust T-cell immunity.(43) Among the different types of DCs that can be distinguished, specifically the rare population of cDC1's seems indispensable for the induction of proper tumor-reactive T-cell responses in the cancer immune cycle during different types of cancer therapies.(44) Although it is possible to successfully use low numbers of cDC1's for vaccine therapy in murine models(44), it yet is still difficult to translate this to the clinic and a reason for us to utilize mo-DCs as antigen-presenting cells. Also, the activation of mo-DC, when correctly triggered, is sufficient to induce effective tumor immunity.(44) This is also stressed by studies showing that disrupting differentiation of mo-DCs leads to diminished effect of chemo and immunotherapy.(45)

Shared clones between skin-test infiltrating activated (PD-1+) T cells and post-vaccination circulating activated CD4+PD-1+ T cells were also detected, suggesting that the MesoPher-driven changes in circulating activated CD4+ T-cell frequencies reflect the response of MesoPher-specific T cells. These analyses at transcriptome and protein level back-to-back substantiate the presence of a bona fide T-cell responses specifically induced by treatment.

The REACTiVe Trial was initiated on the promises that mesothelioma and PDAC share tumor characteristics and antigens. Indeed, identification of a selection of known tumor antigens on both transcriptome as protein level on the drug product and autologous tumors derived from study patients showed a large overlap. As only known antigens were analyzed by targeted mass spectrometry, a greater repertoire of shared tumor antigens is not unlikely. Indeed, our *in vitro* co-cultures showed that MesoPher vaccination was able to activate CD4+ and/or CD8+ T cells able to respond to autologous tumor-lysate loaded DCs, which was also found in a preclinical PDAC tumor model.(32)

Limitations common to phase I trials should be noted, including small sample size, lack of control group, and potential selection bias. Our study population consisted of patients with an ECOG performance status score of 0-2, tumor stage I-II, and free of local disease, representing a population with a potential advantageous clinical outcome compared to resected patients who finished standard-of-care treatment.

With all caveats of the small sample, median progression-free and overall survival have not been reached, and seven out the ten patients have not yet experienced local disease recurrence or new metastatic lesions at a median follow-up of 25 months (range 15- 32 months). The study cohort had a favorable survival compared patients with resected pancreatic cancer who survived for at least 1 year.(46) Furthermore, PDAC patients with disease recurrence usually results in poor prognosis and rapid death. Interestingly, the study patients with disease recurrence did not demonstrate rapid tumor dissemination or early death. This has also been described for cancer vaccines in other malignancies.(47)

In established PDAC disease, immunotherapy may offer new treatment opportunities if one takes into account the hurdles posed by the intricate tumor microenvironment(48) as demonstrated in recent trials with rationally combined treatment strategies.(18,19) We have previously demonstrated that improved systemic T-cell immunity following DC therapy, was able to restrain murine PDAC tumor growth when given prophylactically but not therapeutically, unless DC therapy was combined with CD40 agonistic antibody therapy.(32)

In conclusion, we demonstrated feasibility and safety of MesoPher in PDAC patients and showed that the MesoPher vaccine induced a T-cell response. Furthermore, shared tumor antigens between the vaccine and PDAC, allowing MesoPher to induce PDAC-reactive T cells. Future results in larger cohorts must demonstrate whether MesoPher-induced immune responses translate into robust clinical efficacy of dendritic cell vaccination in resected pancreatic cancer patients after standard-of-care systemic treatment.

## REFERENCES

1. Siegel RL, Miller KD, Jemal A. Cancer statistics, 2020. *CA Cancer J Clin* 2020;70(1):7-30.
2. Rahib L, Smith BD, Aizenberg R, Rosenzweig AB, Fleshman JM, Matrisian LM. Projecting cancer incidence and deaths to 2030: the unexpected burden of thyroid, liver, and pancreas cancers in the United States. *Cancer Res* 2014;74(11):2913-21.
3. Carioli G, Bertuccio P, Boffetta P, Levi F, La Vecchia C, Negri E, et al. European cancer mortality predictions for the year 2020 with a focus on prostate cancer. *Ann Oncol* 2020;31(5):650-8.
4. Matsumoto I, Murakami Y, Shinzeki M, Asari S, Goto T, Tani M, et al. Proposed preoperative risk factors for early recurrence in patients with resectable pancreatic ductal adenocarcinoma after surgical resection: A multi-center retrospective study. *Pancreatology* 2015;15(6):674-80.
5. Paniccia A, Hosokawa P, Henderson W, Schulick RD, Edil BH, McCarter MD, et al. Characteristics of 10-Year Survivors of Pancreatic Ductal Adenocarcinoma. *JAMA Surg* 2015;150(8):701-10.
6. Schnelldorfer T, Ware AL, Sarr MG, Smyrk TC, Zhang L, Qin R, et al. Long-term survival after pancreatoduodenectomy for pancreatic adenocarcinoma: is cure possible? *Ann Surg* 2008;247(3):456-62.
7. Nishio K, Kimura K, Amano R, Yamazoe S, Ohira G, Nakata B, et al. Preoperative predictors for early recurrence of resectable pancreatic cancer. *World J Surg Oncol* 2017;15(1):16.
8. Brahmer JR, Tykodi SS, Chow LQ, Hwu WJ, Topalian SL, Hwu P, et al. Safety and activity of anti-PD-L1 antibody in patients with advanced cancer. *N Engl J Med* 2012;366(26):2455-65.
9. Versteijne E, van Dam JL, Suker M, Janssen QP, Groothuis K, Akkermans-Vogelaar JM, et al. Neoadjuvant Chemoradiotherapy Versus Upfront Surgery for Resectable and Borderline Resectable Pancreatic Cancer: Long-Term Results of the Dutch Randomized PREOPANC Trial. *J Clin Oncol* 2022;JCO2102233.
10. Neoptolemos JP, Palmer DH, Ghaneh P, Psarelli EE, Valle JW, Halloran CM, et al. Comparison of adjuvant gemcitabine and capecitabine with gemcitabine monotherapy in patients with resected pancreatic cancer (ESPAC-4): a multicentre, open-label, randomised, phase 3 trial. *Lancet* 2017;389(10073):1011-24.
11. Conroy T, Hammel P, Hebbar M, Ben Abdelghani M, Wei AC, Raoul J-L, et al. FOLFIRINOX or Gemcitabine as Adjuvant Therapy for Pancreatic Cancer. *New England Journal of Medicine* 2018;379(25):2395-406 doi 10.1056/NEJMoa1809775.
12. Groot VP, Rezaee N, Wu W, Cameron JL, Fishman EK, Hruban RH, et al. Patterns, Timing, and Predictors of Recurrence Following Pancreatectomy for Pancreatic Ductal Adenocarcinoma. *Ann Surg* 2018;267(5):936-45.
13. Patnaik A, Kang SP, Rasco D, Papadopoulos KP, Ellassaiss-Schaap J, Beeram M, et al. Phase I Study of Pembrolizumab (MK-3475; Anti-PD-1 Monoclonal Antibody) in Patients with Advanced Solid Tumors. *Clin Cancer Res* 2015;21(19):4286-93.
14. Nesselhut J, Marx D, Lange H, Regalo G, Cillien N, Chang RY, et al. Systemic treatment with anti-PD-1 antibody nivolumab in combination with vaccine therapy in advanced pancreatic cancer. *Journal of Clinical Oncology* 2016;34(15\_suppl):3092- doi 10.1200/JCO.2016.34.15\_suppl.3092.
15. Weber JS, D'Angelo SP, Minor D, Hodi FS, Gutzmer R, Neyns B, et al. Nivolumab versus chemotherapy in patients with advanced melanoma who progressed after anti-CTLA-4 treatment (CheckMate 037): a randomised, controlled, open-label, phase 3 trial. *Lancet Oncol* 2015;16(4):375-84.
16. Larkin J, Chiarion-Sileni V, Gonzalez R, Grob JJ, Cowey CL, Lao CD, et al. Combined Nivolumab and Ipilimumab or Monotherapy in Untreated Melanoma. *N Engl J Med* 2015;373(1):23-34.
17. Robert C, Long GV, Brady B, Dutriaux C, Maio M, Mortier L, et al. Nivolumab in previously untreated melanoma without BRAF mutation. *N Engl J Med* 2015;372(4):320-30.
18. Brandon George S, Benjamin Leon M, Spyridoula V, Manik K, Ayumi W, Catherine R, et al. A phase I trial targeting advanced or metastatic pancreatic cancer using a combination of standard chemotherapy and adoptively transferred nonengineered, multiantigen specific T cells in the first-line setting

- (TACTOPS). *Journal of Clinical Oncology* 2020;38(15\_suppl):4622- doi 10.1200/JCO.2020.38.15\_suppl.4622.
19. O'Hara MH, O'Reilly EM, Varadhachary G, Wolff RA, Wainberg ZA, Ko AH, et al. CD40 agonistic monoclonal antibody APX005M (sotigalimab) and chemotherapy, with or without nivolumab, for the treatment of metastatic pancreatic adenocarcinoma: an open-label, multicentre, phase 1b study. *Lancet Oncol* 2021;22(1):118-31.
  20. Steele NG, Carpenter ES, Kemp SB, Sirihorachai VR, The S, Delrosario L, et al. Multimodal mapping of the tumor and peripheral blood immune landscape in human pancreatic cancer. *Nature Cancer* 2020;1(11):1097-112 doi 10.1038/s43018-020-00121-4.
  21. Beatty GL, Winograd R, Evans RA, Long KB, Luque SL, Lee JW, et al. Exclusion of T Cells From Pancreatic Carcinomas in Mice Is Regulated by Ly6C(low) F4/80(+) Extratumoral Macrophages. *Gastroenterology* 2015;149(1):201-10.
  22. Aerts J, de Goeje PL, Cornelissen R, Kaijen-Lambers MEH, Bezemer K, van der Leest CH, et al. Autologous Dendritic Cells Pulsed with Allogeneic Tumor Cell Lysate in Mesothelioma: From Mouse to Human. *Clin Cancer Res* 2018;24(4):766-76.
  23. Hegde S, Krisnawan VE, Herzog BH, Zuo C, Breden MA, Knolhoff BL, et al. Dendritic Cell Paucity Leads to Dysfunctional Immune Surveillance in Pancreatic Cancer. *Cancer Cell* 2020;37(3):289-307 e9.
  24. Lepisto AJ, Moser AJ, Zeh H, Lee K, Bartlett D, McKolanis JR, et al. A phase I/II study of a MUC1 peptide pulsed autologous dendritic cell vaccine as adjuvant therapy in patients with resected pancreatic and biliary tumors. *Cancer Ther* 2008;6(B):955-64.
  25. Thomas AM, Santarsiero LM, Lutz ER, Armstrong TD, Chen YC, Huang LQ, et al. Mesothelin-specific CD8(+) T cell responses provide evidence of in vivo cross-priming by antigen-presenting cells in vaccinated pancreatic cancer patients. *J Exp Med* 2004;200(3):297-306.
  26. Shindo Y, Hazama S, Maeda Y, Matsui H, Iida M, Suzuki N, et al. Adoptive immunotherapy with MUC1-mRNA transfected dendritic cells and cytotoxic lymphocytes plus gemcitabine for unresectable pancreatic cancer. *J Transl Med* 2014;12:175.
  27. Ahmad M, Rees RC, Ali SA. Escape from immunotherapy: possible mechanisms that influence tumor regression/progression. *Cancer Immunology, Immunotherapy* 2004;53(10):844-54 doi 10.1007/s00262-004-0540-x.
  28. Nelde A, Rammensee H-G, Walz JS. The Peptide Vaccine of the Future. *Mol Cell Proteomics* 2021;20:100022- doi 10.1074/mcp.R120.002309.
  29. Hassan R, Thomas A, Alewine C, Le DT, Jaffee EM, Pastan I. Mesothelin Immunotherapy for Cancer: Ready for Prime Time? *J Clin Oncol* 2016;34(34):4171-9 doi 10.1200/jco.2016.68.3672.
  30. Naitoh K, Kamigaki T, Matsuda E, Ibe H, Okada S, Oguma E, et al. Immunohistochemical Analysis of WT1 Antigen Expression in Various Solid Cancer Cells. *Anticancer Res* 2016;36(7):3715-24.
  31. Garg H, Suri P, Gupta JC, Talwar GP, Dubey S. Survivin: a unique target for tumor therapy. *Cancer Cell International* 2016;16(1):49 doi 10.1186/s12935-016-0326-1.
  32. Lau SP, van Montfoort N, Kinderman P, Lukkes M, Klaase L, van Nimwegen M, et al. Dendritic cell vaccination and CD40-agonist combination therapy licenses T cell-dependent antitumor immunity in a pancreatic carcinoma murine model. *J Immunother Cancer* 2020;8(2).
  33. Whatcott CJ, Posner RG, Von Hoff DD, Han H. Desmoplasia and chemoresistance in pancreatic cancer. 2012.
  34. Adema GJ, de Vries IJ, Punt CJ, Figdor CG. Migration of dendritic cell based cancer vaccines: in vivo veritas? *Curr Opin Immunol* 2005;17(2):170-4.
  35. Ye Q, Song DG, Poussin M, Yamamoto T, Best A, Li C, et al. CD137 accurately identifies and enriches for naturally occurring tumor-reactive T cells in tumor. *Clin Cancer Res* 2014;20(1):44-55.
  36. Melero I, Shuford WW, Newby SA, Aruffo A, Ledbetter JA, Hellström KE, et al. Monoclonal antibodies against the 4-1BB T-cell activation molecule eradicate established tumors. *Nature Medicine* 1997;3(6):682-5 doi 10.1038/nm0697-682.
  37. de Goeje PL, Klaver Y, Kaijen-Lambers MEH, Langerak AW, Vroman H, Kunert A, et al. Autologous Dendritic Cell Therapy in Mesothelioma Patients Enhances Frequencies of Peripheral CD4 T Cells Expressing HLA-DR, PD-1, or ICOS. *Front Immunol* 2018;9:2034.

38. Kamphorst AO, Pillai RN, Yang S, Nasti TH, Akondy RS, Wieland A, et al. Proliferation of PD-1+ CD8 T cells in peripheral blood after PD-1-targeted therapy in lung cancer patients. *Proc Natl Acad Sci U S A* 2017;114(19):4993-8.
39. Harris NL, Watt V, Ronchese F, Le Gros G. Differential T cell function and fate in lymph node and nonlymphoid tissues. *J Exp Med* 2002;195(3):317-26.
40. Hengel RL, Thaker V, Pavlick MV, Metcalf JA, Dennis G, Jr., Yang J, et al. Cutting edge: L-selectin (CD62L) expression distinguishes small resting memory CD4+ T cells that preferentially respond to recall antigen. *J Immunol* 2003;170(1):28-32.
41. Utzschneider DT, Charmoy M, Chennupati V, Pousse L, Ferreira DP, Calderon-Copete S, et al. T Cell Factor 1-Expressing Memory-like CD8(+) T Cells Sustain the Immune Response to Chronic Viral Infections. *Immunity* 2016;45(2):415-27.
42. Rivas-Caicedo A, Soldevila G, Fortoul TI, Castell-Rodríguez A, Flores-Romo L, García-Zepeda EA. Jak3 is involved in dendritic cell maturation and CCR7-dependent migration. *PLoS One* 2009;4(9):e7066.
43. Chen Daniel S, Mellman I. Oncology Meets Immunology: The Cancer-Immunity Cycle. *Immunity* 2013;39(1):1-10 doi <https://doi.org/10.1016/j.immuni.2013.07.012>.
44. Keirsse J, Van Damme H, Van Ginderachter JA, Laoui D. Exploiting tumor-associated dendritic cell heterogeneity for novel cancer therapies. *J Leukoc Biol* 2017;102(2):317-24.
45. Sharma MD, Rodriguez PC, Koehn BH, Baban B, Cui Y, Guo G, et al. Activation of p53 in Immature Myeloid Precursor Cells Controls Differentiation into Ly6c(+)CD103(+) Monocytic Antigen-Presenting Cells in Tumors. *Immunity* 2018;48(1):91-106 e6.
46. Latenstein AEJ, van Roessel S, van der Geest LGM, Bonsing BA, Dejong CHC, Groot Koerkamp B, et al. Conditional Survival After Resection for Pancreatic Cancer: A Population-Based Study and Prediction Model. *Annals of Surgical Oncology* 2020;27(7):2516-24 doi 10.1245/s10434-020-08235-w.
47. Hollingsworth RE, Jansen K. Turning the corner on therapeutic cancer vaccines. *npj Vaccines* 2019;4(1):7 doi 10.1038/s41541-019-0103-y.
48. Ho WJ, Jaffee EM, Zheng L. The tumour microenvironment in pancreatic cancer- clinical challenges and opportunities. *Nat Rev Clin Oncol* 2020;17(9):527-40.



## SUPPLEMENTARY MATERIAL AND METHODS

### *RNA sequencing and Mass Spectrometry*

For transcriptome analysis, fresh-frozen autologous tumors were shredded in lysis buffer (QIAGEN) using an Ultra-Turrax T25 homogenizer (Janke & Kunkel). RNA isolation was performed with the RNeasy® Micro Kit (QIAGEN) and isolated RNA was prepared with the TruSeq Stranded mRNA Library Prep Kit (Illumina). The resulting RNA libraries were sequenced according to the Illumina TruSeq Rapid v2 protocol on an Illumina HiSeq2500 sequencer. Reads were generated from 50 base pairs in length. RNA sequencing of the five mesothelioma cell lines present in MesoPher was outsourced to BGI Genomics and was performed using the Illumina HiSeq 4000 platform. Adapter sequences were trimmed and mapped against the human genome for the pancreas lysate using HiSat2 (version 2.1.0). A minimal threshold of 1 FPKM (fragments per kilobase of transcript per million mapped reads) was taken.

To generate tumor lysate for Mass Spectrometry (MS), fresh-frozen autologous tumors were bead-homogenized in Milli-Q for four cycles of 3 minute. A Bradford assay was performed to determine protein content of the tumor. Hundred µg lysate were reduced, alkylated, and digested with trypsin by filter-aided sample preparation.(1) Thirty ug of each digest were labeled with TMTsixplex isobaric labels and labeled samples were then grouped and combined into 3 pools (Sup. Table 1) for two types of MS measurements. Pools were fractionated into 24 fractions by high-pH reversed phase chromatography. First, all fractions were measured with an untargeted method optimized for sensitivity. Acquired MS2 spectra data were subjected to a Mascot database search against the combined human subset of Swiss-Prot/TrEMBL database and further analyzed with the software package Scaffold for protein grouping and FDR filtering. The selected tumor antigens of interest (Sup. Table 2) where used as targets for the subsequent MS measurement. For accurate and multiplexed detection, the peptides in lysates we applied a sequential precursor selection MS3 method that used parent mass lists for specific selection of peptide species (MS2 precursors) and peptide species fragments (MS3 precursors) to reduce unspecific interference and ratio distortion, and to enhance quantitative confidence. Acquired MS3 reporter ions were extracted, assigned to the identifying MS2 spectra, and quantitative properties, *e.g.* intensity and signal-to-noise ratio (S/N), determined. Proteins and peptides were reported as detected if the S/N of an associated peptide species was above 10. The raw data is publicly available on the ProteomeXchange Consortium with the identifier PXD025210.(2)

### *NanoString gene-expression profiling*

NanoString nCounter Technologies was applied on PBMCs using the PanCancer Immune Profiling Panel. To identify the differentially expressed genes, raw data was normalized using the values of the most stable 15 housekeeping genes selected by applying the geNorm algorithm. The original p values were adjusted for multiple testing using Benjamini-Hochberg procedure.

Volcanoplots were generated using the R-package EnhancedVolcano (v1.8.0). Heatmaps were generated using the Z-score of normalized count data and visualized using web-based tool Morpheus.

#### *Flow cytometry immuno-monitoring*

For enumeration of immune subsets, whole blood was freshly stained for flow cytometry. In addition, longitudinal immuno-monitoring was performed on liquid nitrogen stored peripheral blood mononuclear cells. Cell surface staining was done after blocking Fc receptors by incubating cells with fluorescently conjugated mAbs directed against specific epitopes (Sup. Table 3). Intracellular transcription factor staining was performed using the FoxP3 Staining Buffer Set (eBioscience). Cells were in addition stained for viability using fixable LIVE/DEAD aqua cell stain. Data were acquired using the Symphony flow cytometer (BD Biosciences) and analyzed with FlowJo v10.7 (Treestar).

#### *TCR- $\beta$ sequencing*

For the comprehensive analysis of TCR- $\beta$  repertoires in blood and tissue samples, PBMCs from baseline and post-therapy (week 5) were sorted for CD3+, CD4+CD127+CD25-PD1-, CD4+CD127+CD25-PD1+, CD8+PD1-, and CD8+PD1+ subsets with the Aria (BD Biosciences), and cells from MesoPher-challenged DTH skin test biopsies were isolated and cultured for seven days with culture medium (100 IU/ml IL-2, RPMI, 7% human serum). DNA was isolated with the NucleoSpin Tissue Kit (Machery-Nagel) according to the manufacturer's instructions. TCR- $\beta$  DNA libraries were constructed with the Ion AmpliSeq™ Library Kit Plus (#4488990) and the OncoPrint™ TCR $\beta$  SR Assay (#A39072) according to the OncoPrint™ Human Immune Repertoire user guide (MAN0017438). The individual libraries were quantified using the Ion Library TaqMan™ Quantitation Kit (#4468802), pooled and normalized to 25pM. Final libraries were templated on ION 530™ Chips (#A27764) using the Ion Chef™ System and sequenced on the Ion Genestudio™ S5 Series System with the Ion 510™ & Ion 520™ & Ion 530™ Kit- Chef (#A34461) by GenomeScan BV (Leiden, the Netherlands) according to the user guide references (MAN0016854). All kits and equipment used, unless stated otherwise, are from ThermoFisher Scientific.

The diversity analysis was performed with the IonReporter 5.14 software using the OncoPrint™ TCR- $\beta$  -SR- w1.2- DNA- Single Sample (version 5.12) workflow with default settings. Subsequent analysis including the investigation of clonal relations between tissues were performed with in-house developed scripts in R-studio (4.0.4). Analysis was focused on clones with a relative frequency of, at least, 0.05%.

#### *In vitro co-culture assay*

MesoPher DCs were generated from liquid-nitrogen stored CD14+ monocytes according to a 10-day culture protocol.(3) In addition, autologous tumor lysate-loaded DCs were generated by loading with an equivalent amount of 70  $\mu$ g autologous tumor lysate per 500.000 mo-DCs. DCs

were co-cultured *in vitro* with PBMCs at a ratio of 1:10 for 7 days in culture medium (RPMI 1640, 50 µg/mL gentamicin, 5% FCS, 50 mmol/L mercaptoethanol) at 37°C 5% CO<sub>2</sub>. After 7 days, PBMCs were washed and replated in culture medium supplemented with IL-2 (1000U/mL). When most cells became phenotypically round, PBMCs were reactivated overnight with MesoPher or autologous tumor lysate-loaded DCs. Unloaded DCs were used as control. Following overnight stimulation, cells were freshly stained for flow cytometry.

## REFERENCES

1. Wiśniewski JR, Zougman A, Nagaraj N, Mann M. Universal sample preparation method for proteome analysis. *Nat Methods*. 2009;6:359-62.
2. Perez-Riverol Y, Csordas A, Bai J, Bernal-Llinares M, Hewapathirana S, Kundu DJ, et al. The PRIDE database and related tools and resources in 2019: improving support for quantification data. *Nucleic Acids Res*. 2019;47:D442-D50.
3. Aerts J, de Goeje PL, Cornelissen R, Kaijen-Lambers MEH, Bezemer K, van der Leest CH, et al. Autologous Dendritic Cells Pulsed with Allogeneic Tumor Cell Lysate in Mesothelioma: From Mouse to Human. *Clin Cancer Res*. 2018;24:766-76.

Sample	Category	TMT-label	Pool
RT002	TUMOR LYSATE	TMT6-127	POOL1
RT003	TUMOR LYSATE	TMT6-129	POOL1
RT004	TUMOR LYSATE	TMT6-130	POOL1
Drug product	Drug product	TMT6-131	POOL1
RT006	TUMOR LYSATE	TMT6-127	POOL2
RT007	TUMOR LYSATE	TMT6-128	POOL2
Drug product	Drug product	TMT6-129	POOL2
RT008	TUMOR LYSATE	TMT6-131	POOL2
Drug product	Drug product	TMT6-126	POOL3
Drug product	Drug product	TMT6-127	POOL3
RT010	TUMOR LYSATE	TMT6-128	POOL3
RT011	TUMOR LYSATE	TMT6-130	POOL3

**Supplementary Table 1.** List of samples and corresponding TMT-labels and pools used in mass spectrometry analysis.

## Chapter 4

Antigens of Interest		
ACRBP	GM3	PBK
ACTL8	gp100	PDGFR-β
ADAM2	HER-2/neu	PIWIL2
ADAM29	HORMAD1	PLAC1
AFP	HSPB9	PRAME
AKAP3	hTERT	Proteinase3 (PR1)
AKAP-4	IDO1	PRSS54
ALK	JARID1B	PSA
Androgen receptor	KK-LC-1	PSCA
ARMC3	KM-HN-1	PSMA
ATAD2	KRAS	RAB38/NY-MEL-1
B7H3	LCK	RAGE-1/MOK
BAGE-1	LDHC	RBM46
BAGE-2	Legumain	RGS5
BAGE-3	LEMD1	RhoC
BAGE4	LIPI	ROPN1
BAGE5	LMP2	SAGE-1
bcr-abl	LUZP4	Sarcoma translocation breakpoints
BING-4	LY6K	SART-1
BRDT	MAGE-A1	SART-2
CABYR	MAGE-A10	SART3
CAGE	MAGE-A11	SLCO6A1
Carbonic anhydrase IX	MAGE-A12	SOX10
CCDC33	MAGE-A2	SPA17
CCDC36	MAGEA2B	SPACA3
CEA	MAGE-A3	SPAG9
CEP290	MAGE-A4	SPANXA1
COX6B2	MAGE-A5	SPANXA2
CPXCR1	MAGE-A6	SPANXB1
CRISP2	MAGE-A7	SPANXC
CSAG1	MAGE-A8	SPANXD
CSAG2	MAGE-A9	SPANXN5
CTAG1A	MAGEB1	SPINLW1
CTAG2	MAGEB2	SPO11
CTAGE1	MAGEB3	SSX1
CTAGE5	MAGEB4	SSX2
CTCF	MAGEB5	SSX2
CTNNA2	MAGEB6	SSX3
CXorf48	MAGE-C1	SSX4
Cxorf61	MAGE-C2	SSX5
Cyclin B1	MAGEC3	SSX6
Cyclin-A1	MAGED4	SSX7
CYP1B1	MART2	SSX9
DDX43	MC1R	Survivin
DIRC2	MCSF	SYCE1
DKKL1	MelanA/MART1	SYCP1
DSCR8	Mesothelin	TAF7L
EGFRvIII	ML-IAP	TAG-1
EpCAM	MMP7	TAG-2
EphA2	MORC1	TDRD1
ERG	MPHOSPH1	TDRD6
FAM133A	MUC1	TEX14
FAP	MUM-1	TEX15
FATE1	MUM-2	TFDP3
FGF5	MYCN	THEG
FMR1NB	NA88-A	Tie 2
Fos-related antigen 1	NLRP4	TPBG
FTHL17	NXF2	TPTE
GAGE1-2	NY-BR-1	TRAG-3
GAGE2A	NY-ESO-1/LAGE-1	TRP-1
GAGE2B	OA1	TRP-2
GAGE2C	ODF2	TSGA10
GAGE3	OIP5	TSP50
GAGE4	p53	TSPY3
GAGE5	PAGE1	TSSK6
GAGE6	PAGE2	TTK
GAGE7	PAGE2B	TULP2
GAGE8	PAGE3	Tyrosinase
GD2	PAGE4	VEGFR2
GD3	PAGE5	WT1
glypican-1	PAP	XAGE1B
glypican-2	PASD1	XAGE2
	PAX3	XAGE3
	PAX5	XAGE5
		ZNF165

**Supplementary Table 2.** Tumor antigens of interest used in our RNA sequencing and mass spectrometry analysis to determine shared antigens.

Antibody	Clone	Source	Identifier
CCR7-BV421	043H7	Biolegend	Cat#: 353208
CD137/4-1BB-PE	4B4-1	BD	Cat#: 555956
CD137/4-1BB-PerCP-Cy5.5	4B4-1	Biolegend	Cat#: 309814
CD28-PE-Cy7	CD28.2	Biolegend	Cat#: 302926
CD39-BV711	TU66	BD	Cat#: 563680
CD3-APC-eFluor 780	UCHT1	Thermo Fisher Scientific	Cat#: 47-0038-42
CD3-PE-CF594	UCHT1	BD	Cat#:562286
CD45RA-PE-TXR	MEM-56	Thermo Fisher Scientific	Cat#: MHCD45RA17
CD4-BV786	SK3	BD	Cat#: 563877
CD56-BV605	NCAM16.2	BD	Cat#: 562780
CD8-AF700	SK1	Biolegend	Cat#: 344724
CD8-BV421	RPA-T8	BD	Cat#: 562428
CTLA-4-PerCP-eFluor 710	14D3	Thermo Fisher Scientific	Cat#: 46-1529-42
FOXP3-PE	236A/E7	Thermo Fisher Scientific	Cat#: 12-4777-42
Granzyme B-FITC	QA16A02	Biolegend	Cat#: 372206
HLA-DR-BV711	G46-6	BD	Cat#: 563696
ICOS-BV650	DX29	BD	Cat#: 563832
IFN $\gamma$ -BV711	B27	BD	Cat#: 564039
IL-10-PE-Cy7	JES3-9D7	Biolegend	Cat#: 501420
IL2-BV650	5344,111	BD	Cat#: 563467
KI-67-FITC	20Raj1	Thermo Fisher Scientific	Cat#: 11-5699-42
LAG-3-PE-Cy7	11C3C65	Biolegend	Cat#: 369310
PD1-APC	EH12.2H7	Biolegend	Cat#: 329908
TIM-3-BV650	F38-2E2	Biolegend	Cat#: 345027
TNF $\alpha$ -PerCP-Cy5.5	MAb11	Thermo Fisher Scientific	Cat#: 45-7349-42

**Supplementary Table 3.** Fluorescently conjugated monoclonal antibodies directed against specific epitopes used for flow cytometry.

Study ID	Quantity		Phenotype		Potency		Safety	
	Mature DCs (x10 <sup>8</sup> )	Viability (Spec: >80%)	CD11c <sup>+</sup> HLA-DR <sup>-</sup> (Spec: >90%)	CD11c <sup>+</sup> HLA-DR <sup>-</sup> CD80 <sup>+</sup> (Spec: >80%)	CCL19 (Spec: >30%)	CCL21 (Spec: >30%)	Sterility	Mycoplasma Endotoxin
RT001	1,98	94,0	97,7	92,9	90,5	77,1	Sterile	Negative
RT002	1,19	95,3	97,1	86,7	30,4	30,9	Sterile	Negative
RT002 (2)	1,12	93,2	96,9	93,4	31,6	32,7	Sterile	Negative
RT004	1,90	93,8	97,8	93,8	39,2	54,7	Sterile	Negative
RT005	2,11	94,8	98,8	97,2	81,3	78,4	Sterile	Negative
RT006	2,09	95,9	97,9	93,1	73,0	70,2	Sterile	Negative
RT007	1,85	96,3	98,6	97,9	34,8	55,9	Sterile	Negative
RT008	1,80	86,8	94,6	80,3	36,3	38,9	Sterile	Negative
RT010	2,22	91,6	98,4	98,7	30,7	48,1	Sterile	Negative
RT011	2,53	96,9	97,9	98,6	44,0	64,1	Sterile	Negative
RT012	2,10	94,6	99,6	95,7	69,3	77,2	Sterile	Negative

**Supplementary Table 4.** MesoPher production. A batch should reach a specification of 1.65x10<sup>8</sup> mature DCs in order to be released as a full production consisting of 5 vaccinations. Each vaccine was frozen down at 30x10<sup>6</sup> DCs. In addition, 3 vials of 5x10<sup>6</sup> DCs were frozen down for DTH skin testing, migrations and retention assay. Potency was determined with a migration assay for the chemokines CCL19 and CCL21. Safety testing was done externally by Eurofins Scientific. Abbreviations: DC, dendritic cell; Spec, specification.

MesoPher Vaccination															
Study ID	1			2			3			4			5		
	Cells	Viability	i.v./i.d.	Cells	Viability	i.v./i.d.	Cells	Viability	i.v./i.d.	Cells	Viability	i.v./i.d.	Cells	Viability	i.v./i.d.
RT001	35,8	100	Yes/Yes	25,4	96,9	Yes/Yes	29,4	100	Yes/Yes	28,6	97,8	Yes/Yes	28,3	97,8	Yes/Yes
RT002	25,8	97,5	Yes/Yes	25,9	97,6	Yes/Yes	24,9	96,8	Yes/Yes	22,3	95,1	Yes/Yes	27,7	96,6	Yes/Yes
RT004	27,9	97,7	Yes/Yes	29,2	98,3	Yes/Yes	24,3	96,3	Yes/Yes	35,3	98,6	Yes/Yes	29,6	97,9	Yes/Yes
RT005	31,45	100	Yes/Yes	26,9	98,2	Yes/Yes	30,08	96,9	Yes/Yes	28,8	96,8	Yes/Yes	30,7	96,4	Yes/Yes
RT006	24,7	93,3	Yes/Yes	25	98,7	Yes/Yes	26,4	95,8	Yes/Yes	21,6	93,7	Yes/Yes	28,3	96,7	Yes/Yes
RT007	30,6	99,5	Yes/Yes	22,4	96,6	Yes/Yes	28,16	96,2	Yes/Yes	22,4	93,9	Yes/Yes	23,5	92,5	Yes/Yes
RT008	20	91,9	Yes/Yes	22,4	89,5	Yes/Yes	21,9	98,5	Yes/Yes	26	90,4	Yes/Yes	27	89,9	Yes/Yes
RT010	24,8	93,2	Yes/Yes	29,9	92,6	Yes/Yes	25,8	93,6	Yes/Yes	28,1	94,4	Yes/Yes	26,9	95,3	Yes/Yes
RT011	28,2	97,2	Yes/Yes	22,9	96	Yes/Yes	20,6	97,7	Yes/Yes	24,3	96,2	Yes/Yes	27	99,4	Yes/Yes
RT012	33	96,2	Yes/Yes	25,6	90,4	Yes/Yes	26,6	96,4	Yes/Yes	29,9	100	Yes/Yes	-	-	No/No

**Supplementary Table 5.** MesoPher administration. Abbreviations: i.v./i.d., intravenous/intradermal. MesoPher administration. Cells are in millions and viability in percentages.



Event	Grade 1	Patients (N = 10)	
		Grade 2	Grade 3-4
<b>Injection site reaction (ISR)</b>			
Erythema	100%	-	-
Local pruritus	60%	-	-
Pain	10%	-	-
Skin induration	100%	-	-
Warmth	20%	-	-
<b>Infusion related reaction (IRR)</b>			
Chills	80%	-	-
Dyspnea	-	-	10%
Fatigue	100%	-	-
Fever	70%	20%	-
Headache	10%	-	-
Hot flashes	10%	-	-
Malaise	20%	-	-
Myalgia	50%	-	-
Pruritus	10%	-	-
Vertigo	10%	-	-
Vomiting	10%	-	-
<b>Non ISR/IRR-related event</b>			
Abdominal pain	10%	-	-
Back pain	10%	-	-
Chills	10%	-	-
Constipation	10%	-	-
Cough	10%	-	-
Diarrhea	20%	-	-
Dyspnea	10%	10%	10%
Esthesia	10%	-	-
Fatigue	30%	-	-
Fever	10%	-	-
Flu like symptoms	10%	-	-
Headache	20%	-	-
Hematoma	20%	-	-
Hematuria	10%	-	-
Hypertension	10%	-	-
Laryngeal inflammation	10%	-	-
Localized edema	10%	-	-
Nausea	10%	-	-
Non-cardiac chest pain	10%	-	-
Pain	20%	-	-
Psoriasis	10%	-	-
Urinary retention	-	10%	-
Urinary tract infection	-	10%	-
Vertigo	10%	-	-
Vomiting	10%	-	-
Wound complication	20%	-	-
<b>Hematologic event</b>			
Anemia	50%	20%	-
Hypokalemia	10%	-	-
<b>Biochemical events</b>			
Decreased platelet count	30%	-	-
Elevated ALP level	80%	-	-
Elevated ALT level	20%	-	-
Elevated AST level	40%	-	-
Elevated GGT level	30%	10%	-
Elevated serum amylase level	10%	-	-
Hyperglycemia	10%	-	-

**Supplementary Table 6.** Adverse events during study follow-up. Abbreviations: ALT, alanine aminotransferase; AST, aspartate aminotransferase; ALP, alkaline phosphatase; GGT, gamma-glutamyltransferase. Adverse event grading was performed using the Common Terminology Criteria for Adverse Events (CTCAE) v4.03.

Gene	Differentiation antigens	Cancer Testis antigens	Overexpressed/Others	RT004	RT005	Thorr 1	Thorr 2	Thorr 3	Thorr 5	Thorr 6
ACRBP		ACRBP		1,05	2,41	0,04	0,00	0,15	0,22	0,05
ACTL8			ACTL8	0,00	0,00	0,00	0,11	0,00	0,08	0,00
AFP		AFP		0,03	0,10	0,88	0,02	0,11	0,00	0,00
AKAP3			AKAP3	0,27	0,35	0,05	0,28	0,03	0,26	0,14
ALK				0,07	0,07	0,00	0,12	0,00	0,02	0,04
AR			Androgen receptor	0,71	1,59	2,88	0,00	0,01	0,00	0,04
ARMC3			ARMC3	0,05	0,12	0,02	0,00	0,51	0,00	0,00
ATAD2			ATAD2	0,97	2,29	9,86	26,26	17,83	22,88	19,19
CD276			B7H3	9,63	23,61	24,95	36,36	25,47	8,29	20,08
BAGE		BAGE-1		0,00	0,00	0,00	0,00	1,59	0,00	0,00
BAGE2		BAGE-2		0,00	0,00	0,01	0,00	2,63	0,00	0,00
BAGE3		BAGE-3		0,00	0,00	0,01	0,00	2,62	0,00	0,00
BAGE4		BAGE4		0,00	0,00	0,01	0,00	2,73	0,00	0,00
BAGE5		BAGE5		0,00	0,00	0,01	0,00	2,73	0,00	0,00
BCR	bcr-abl			3,29	7,41	6,81	14,01	4,45	3,33	7,66
WDR46			BING-4	10,94	21,47	0,05	1,08	0,10	0,13	0,24
CABYR			CABYR	0,42	1,72	2,12	1,49	4,30	1,04	5,80
DDX53		CAGE		0,02	0,00	0,00	0,00	3,27	0,00	0,00
CA9			Carbonic anhydrase IX	4,78	3,96	1,27	1,20	6,69	1,99	0,00
CCDC33		CCDC33		0,03	0,32	0,00	0,00	0,00	0,00	0,00
CEACAM5	CEA			8,97	51,78	0,00	0,00	0,00	0,00	0,00
CEP290		CEP290		0,68	2,35	0,35	1,24	1,73	6,97	2,34
COX6B2		COX6B2		0,28	0,67	0,06	0,23	0,34	7,01	0,21
CRISP2			CRISP2	1,41	0,13	0,00	0,00	0,00	0,00	0,00
CSAG1		CSAG1		0,00	0,09	0,00	0,00	25,60	0,00	0,00
CTAG2		CTAG2		0,08	0,00	0,00	0,00	0,87	0,00	0,00
CTAGE1		CTAGE1		0,01	0,00	0,00	0,00	0,00	0,00	0,06
MIA2		CTAGE5		9,75	11,56	5,04	9,64	6,55	3,54	13,03
CTCFL		CTCFL		0,00	0,00	0,00	0,07	0,00	0,02	0,00
CTNNA2		CTNNA2		0,15	0,73	0,01	0,00	0,84	0,04	0,01
CT55		CXorf48		0,00	0,06	0,00	0,00	0,06	0,03	0,00
CT83		Cxorf61		0,00	1,01	0,00	0,00	0,40	0,00	0,00
CCNB1			Cyclin B1	1,74	3,35	86,77	79,72	90,34	57,26	76,09
CCNA1		Cyclin-A1		0,10	0,44	8,42	3,92	1,07	1,74	0,61
CYP1B1			CYP1B1	2,46	11,68	19,11	12,21	13,44	2,06	0,27
DDX43			DDX43	0,49	0,60	2,82	0,00	3,50	0,03	0,04
SLC49A4			DIRC2	3,07	4,04	5,55	9,60	3,92	3,30	4,42
DKKL1		DKKL1		0,00	0,21	0,12	0,00	0,82	0,12	0,00
DSCR8			DSCR8	0,00	0,00	0,06	0,00	8,60	0,00	0,00
EGFR			EGFRvIII	3,95	7,21	14,66	45,95	10,94	42,97	39,53
EPCAM	EpCAM			46,37	77,15	0,00	0,09	0,30	0,04	0,00
EPHA2			EphA2	5,51	12,55	33,06	101,87	25,46	62,07	166,35
ERG			ERG	2,03	4,08	0,68	0,00	0,03	0,03	0,00
FAM133A		FAM133A		0,00	0,07	0,00	0,00	3,90	0,06	0,02
FAP			FAP	2,89	23,35	0,19	3,61	3,94	0,00	0,06
FATE1		FATE1		0,00	0,05	0,00	0,00	0,00	0,00	0,00
FGF5			FGF5	0,03	0,06	1,02	4,63	28,08	0,04	1,54
FMR1NB		FMR1NB		0,00	0,00	0,00	0,00	0,05	0,08	0,00
FOSL1	Fos-related antigen 1			2,31	2,51	14,97	50,51	163,13	263,75	54,62
GAGE1		GAGE1-2		0,00	0,00	0,38	0,00	0,02	0,00	0,00
GAGE2A		GAGE2A		0,00	0,00	5,28	0,00	1,52	0,00	0,00
GAGE2B		GAGE2B		0,00	0,00	0,10	0,00	3,91	0,00	0,00
GAGE2C		GAGE2C		0,00	0,00	0,19	0,00	0,00	0,00	0,00
GAGE4		GAGE4		0,00	0,00	0,00	0,00	0,10	0,00	0,00
GAGE5		GAGE5		0,00	0,00	0,00	0,00	0,10	0,00	0,00
GAGE7		GAGE7		0,00	0,00	0,00	0,00	0,10	0,00	0,00
B4GALNT1	GD2			0,42	3,12	3,96	1,44	3,85	14,16	8,42
ST8SIA1	GD3			0,05	0,28	0,05	0,01	0,00	0,06	0,01
GPC1			glypican-1	10,03	23,52	134,86	30,79	44,55	92,37	66,26
GPC2			glypican-2	0,18	1,32	0,05	0,00	1,75	1,54	1,71
ST3GAL5	GM3			2,71	7,93	8,09	22,61	9,00	3,34	11,69
PMEL	gp100			0,54	1,11	0,71	0,03	0,31	42,68	0,45
ERBB2			HER-2/neu	13,78	28,13	19,37	12,02	15,40	16,31	23,53
HORMAD1		HORMAD1		0,06	0,31	0,00	0,00	0,00	0,00	0,00
HSPB9		HSPB9		0,21	0,74	0,00	0,00	0,00	0,00	0,09
TERT	hTERT			0,00	0,03	1,13	0,29	0,06	0,00	0,11
IDO1			IDO1	0,74	2,36	0,19	0,67	0,19	0,00	0,16
KDM5B			JARID1B	2,75	5,59	12,79	7,60	20,99	3,67	11,37
CCDC110		KM-HN-1/CCDC110		1,68	0,24	0,50	0,27	0,02	0,19	0,00
KRAS			KRAS	3,12	4,87	6,38	7,94	14,54	15,26	7,67
LCK			LCK	2,65	13,55	0,00	0,00	0,00	0,00	0,00
LDHC		LDHC		0,09	0,05	0,00	0,88	0,08	0,04	0,08
LGMN			Legumain	20,88	45,78	21,19	12,32	14,81	28,52	20,68
LEMD1		LEMD1		0,52	3,32	0,08	0,00	0,00	0,26	0,00
PSMB9			LMP2	8,83	24,26	0,00	0,05	0,00	0,05	0,05
LUZP4		LUZP4		0,00	0,04	0,00	0,00	0,00	0,00	0,00
LY6K		LY6K		0,03	2,62	0,24	1,16	0,29	30,51	0,54
MAGEA1		MAGE-A1		0,00	0,00	0,00	0,00	32,32	0,03	0,00
MAGEA11		MAGE-A11		0,00	0,00	0,00	0,00	1,37	0,00	0,00
MAGEA12		MAGE-A12		0,00	0,00	0,03	0,03	49,00	0,00	0,00
MAGEA2		MAGE-A2		0,00	0,00	0,00	0,00	0,10	0,00	0,00
MAGEA2B		MAGEA2B		0,00	0,00	0,00	0,00	0,09	0,00	0,00

Chapter 4

MAGEA3		MAGE-A3		0,03	0,07	0,12	0,00	1,96	0,00	0,00
MAGEA6		MAGE-A6		0,00	0,00	0,29	0,00	13,16	0,00	0,00
MAGEB2		MAGEB2		0,00	0,00	0,09	0,06	0,00	52,73	0,03
MAGEB6		MAGEB6		0,00	0,00	0,00	0,11	0,29	0,03	0,10
MAGEC2		MAGE-C2		0,03	0,00	0,00	0,15	0,08	0,00	0,00
MAGEC3		MAGEC3		0,00	0,10	0,00	0,00	0,00	0,00	0,00
MAGED4		MAGED4		0,25	0,85	0,04	0,00	0,12	0,02	0,04
HHAT			MART2	1,30	2,21	0,43	0,55	2,85	0,55	1,27
MC1R			MC1R	1,28	3,88	1,10	0,38	2,90	0,24	0,91
CSPG4	MCSP			1,68	3,82	0,07	8,95	1,29	0,12	0,21
MLANA	MelanA/MART1			0,00	0,00	0,01	0,04	0,19	0,05	0,02
MSLN			Mesothelin	9,56	17,38	42,29	53,28	72,37	148,19	118,04
BIRC7			ML-IAP	0,27	1,23	0,00	0,02	0,00	0,18	0,00
MMP7			MMP7	144,22	479,57	0,29	0,00	0,00	0,00	0,00
KIF20B		MPHOSPH1		0,14	0,43	4,05	5,87	9,19	7,39	7,77
MUC1	MUC1			101,61	126,44	11,05	13,61	12,15	18,75	14,18
IRF4			MUM-1	0,36	1,62	0,00	0,00	0,00	0,00	0,00
TRAPPC1			MUM-2	27,19	71,68	142,61	91,76	139,01	79,70	140,81
MYCN	MYCN			0,10	0,17	0,00	0,12	0,00	0,00	0,00
NXF2		NXF2		0,00	0,00	0,00	0,00	0,04	0,00	0,00
ANKRD30A	NY-BR-1			0,00	0,00	0,00	0,00	0,13	0,00	0,00
GPR143			OA1	0,59	1,66	0,52	5,71	0,03	0,00	0,09
ODF2		ODF2		4,76	10,54	11,82	6,31	23,25	10,28	11,81
OIP5		OIP5		0,10	0,21	4,19	15,87	6,51	5,39	5,15
TP53			p53	8,28	17,22	54,73	67,27	88,41	24,68	37,83
PAGE1		PAGE1		0,00	0,00	0,23	0,00	5,67	0,00	0,00
PAGE2		PAGE2		0,11	0,00	0,23	0,00	1,05	0,00	0,00
PAGE2B		PAGE2B		0,11	0,00	0,00	0,00	1,82	0,00	0,19
PAGE5		PAGE5		0,00	0,00	8,33	0,00	12,18	0,00	0,00
REG3A	PAP			979,24	754,98	0,00	0,00	0,00	0,00	0,00
PAX5			PAX5	0,15	1,02	0,00	0,04	0,00	0,00	0,00
PBK		PBK		0,39	0,29	14,50	14,21	33,91	18,95	14,20
PDGFRB			PDGFR-β	12,77	71,34	25,17	17,18	8,71	1,79	26,78
PIWIL2		PIWIL2		2,34	0,91	0,02	0,01	0,02	0,02	0,02
PLAC1			PLAC1	0,05	0,06	0,04	0,18	0,22	2,94	0,00
PRAME			PRAME	0,00	0,15	0,00	0,02	0,00	1,45	0,00
PRTN3	Proteinase3 (PR1)			0,00	0,00	0,00	0,00	0,00	0,10	0,00
PRSS54		PRSS54		0,43	0,68	0,97	0,03	0,29	0,83	0,73
KLK3	PSA		PSA	0,00	0,13	0,00	0,00	0,00	0,00	0,00
PSCA	PSCA			4,58	23,26	0,10	0,52	0,31	16,74	0,44
FOLH1			PSMA	0,13	0,29	0,00	0,00	0,00	0,08	0,00
RAB38			RAB38/NY-MEL-1	0,87	1,09	2,58	0,11	0,55	0,00	0,21
MOK			RAGE-1/MOK	3,47	6,96	1,59	9,73	50,41	327,28	51,43
RBM46	RBM46			0,02	0,03	0,00	0,00	0,00	0,00	0,00
RGS5			RGS5	12,79	25,96	7,67	0,82	0,10	0,07	0,50
RHOC			RhoC	65,86	134,10	719,44	216,48	139,28	197,05	120,02
SAGE1		SAGE-1		0,00	0,10	0,00	0,00	0,00	0,00	0,00
EWSR1			Sarcoma translocation break	32,88	75,40	49,29	61,98	72,48	57,46	64,00
SART1			SART-1	6,88	14,10	12,65	19,44	48,18	24,62	20,16
DSE			SART-2	1,27	3,10	38,68	67,14	9,94	10,86	0,91
SART3			SART3	5,20	12,09	12,80	19,50	23,10	23,63	23,48
SOX10			SOX10	0,99	1,64	0,00	0,00	0,00	0,00	0,00
SPA17		SPA17		2,07	3,60	12,12	3,21	3,07	2,20	4,67
SPACA3		SPACA3		5,74	1,54	0,00	0,00	0,00	0,00	0,00
SPAG9		SPAG9		6,43	8,13	11,92	9,82	10,95	34,66	30,36
SPANXA1		SPANXA1		0,00	0,00	0,12	0,00	0,12	0,00	0,00
SPANXA2		SPANXA2		0,00	0,00	0,12	0,00	0,13	0,00	0,00
SPANXC		SPANXC		0,00	0,00	0,00	0,00	0,57	0,00	0,00
SPANXD		SPANXD		0,00	0,00	0,00	0,00	0,45	0,00	0,00
SSX1		SSX1		0,00	0,00	20,28	0,00	1,93	0,00	0,04
SSX6P		SSX6		0,00	0,00	0,00	0,00	0,00	0,00	0,24
BIRC5			Survivin	0,53	1,26	47,65	41,78	48,87	36,57	20,88
SYCE1		SYCE1		0,59	0,84	9,01	0,00	0,00	0,00	0,00
TAF7L		TAF7L		0,03	0,03	0,00	0,00	0,00	0,00	0,11
CNTN2			TAG-1	0,15	0,22	0,01	0,00	0,01	0,03	0,00
TDRD1		TDRD1		0,03	0,08	0,00	0,00	0,00	0,00	0,00
TEX14		TEX14		0,06	0,18	0,11	0,13	0,01	0,69	0,11
TEX15		TEX15		0,00	0,00	0,00	0,00	0,00	0,08	0,00
TEK			Tie 2	2,50	4,92	0,04	0,12	2,41	0,00	0,02
TPBG			TPBG	4,50	7,40	19,26	54,67	16,29	5,09	8,98
TPTE		TPTE		0,00	0,00	0,00	0,00	1,39	0,00	0,00
TYRP1	TRP-1			0,55	0,08	4,43	1,39	0,42	0,07	2,47
DCT	TRP-2			0,18	0,24	0,00	0,00	0,02	0,04	0,00
TSGA10		TSGA10		0,75	1,38	0,21	0,27	0,87	0,21	0,11
PRSS50		TSP50		1,16	4,14	0,00	0,00	0,00	0,00	0,00
TSSK6		TSSK6		0,21	0,48	0,15	0,15	1,00	0,53	0,57
TTK			TTK	0,12	0,35	13,16	11,36	13,25	11,63	12,51
TULP2	TULP2			0,00	0,03	0,00	0,00	0,00	0,00	0,00
KDR			VEGFR2	1,20	4,58	3,11	16,50	0,01	0,18	0,45
WT1			WT1	0,30	1,05	6,72	30,18	0,44	0,24	15,11
XAGE1A		XAGE1B		0,00	0,00	0,00	0,00	0,11	0,00	0,00
XAGE2		XAGE2		0,09	0,00	0,00	0,00	0,00	0,00	0,00
ZNF165		ZNF165		1,74	1,24	0,55	0,37	0,29	0,65	1,06

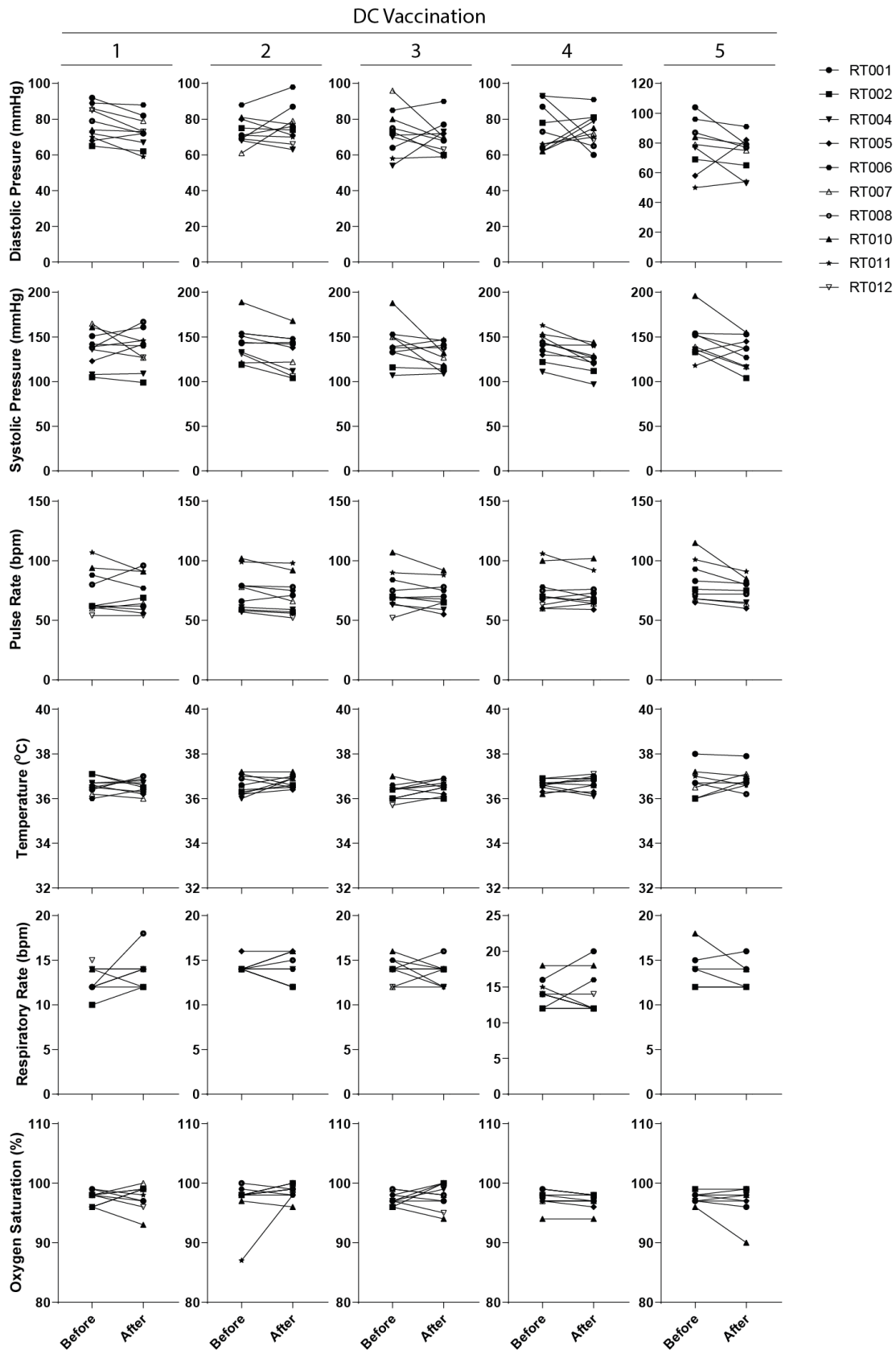
**Supplementary Table 7.** Transcriptome of autologous tumor from RT004, RT005 and the five mesothelioma cell lines use in Mesopher with expression values in FPKM. Tumor antigens with a FPKM >1 are highlighted and categorized in differentiated, cancer testis, and overexpressed/other tumor antigen.



**Supplementary Table 8.** List of found tumor antigens with mass spectrometry and the individual targets with gene name, accession number, primary name, alternative genes, alternative accession numbers and names. Download supplementary file when a higher resolution is desired; [https://www.ejancer.com/article/S0959-8049\(22\)00159-9/fulltext](https://www.ejancer.com/article/S0959-8049(22)00159-9/fulltext)

Sample	# cell sorted	# clones detected	# clones detected $\geq 0.05\%$ relative frequency	Shannon Diversity	Evenness
RT005_Baseline_CD3+	2000000	7005	149	10,7966	0,8452
RT005_Baseline_CD8+PD1+	284686	1976	243	8,096	0,7395
RT005_Baseline_CD8+PD1-	991021	1533	118	5,7962	0,5477
RT005_Baseline_CD4+PD1+	913745	8086	211	11,7826	0,9077
RT005_Baseline_CD4+PD1-	2570901	9694	145	12,4046	0,9367
RT005_Week5_CD3+	500000	6397	120	9,8077	0,7757
RT005_Week5_CD8+PD1+	14641	717	344	7,4484	0,7852
RT005_Week5_CD8+PD1-	66328	1380	85	5,2467	0,503
RT005_Week5_CD4+PD1+	51519	2909	626	10,2671	0,8923
RT005_Week5_CD4+PD1-	110483	7564	167	12,1379	0,942
RT005_Cells from Skin Bx	400000	4337	309	10,3799	0,8591
RT006_Baseline_CD3+	2000000	8894	91	11,2868	0,8604
RT006_Baseline_CD8+PD1+	361843	2468	253	8,4142	0,7467
RT006_Baseline_CD8+PD1-	1761394	6434	102	9,754	0,771
RT006_Baseline_CD4+PD1+	304619	4699	105	8,2023	0,6724
RT006_Baseline_CD4+PD1-	1596269	8208	49	12,6174	0,9704
RT006_Week5_CD3+	400000	7273	92	11,2259	0,8751
RT006_Week5_CD8+PD1+	18323	1382	296	8,1957	0,7856
RT006_Week5_CD8+PD1-	107449	7471	98	10,1639	0,7899
RT006_Week5_CD4+PD1+	16921	1825	477	7,8749	0,7269
RT006_Week5_CD4+PD1-	80303	11682	30	13,1158	0,9707
RT006_Cells from Skin Bx	130000	2193	144	7,3245	0,6599
RT011_Baseline_CD3+	2000000	8989	73	11,1408	0,8482
RT011_Baseline_CD8+PD1+	1500000	1787	143	5,9709	0,5527
RT011_Baseline_CD8+PD1-	500000	3119	83	6,2744	0,5406
RT011_Baseline_CD4+PD1+	2000000	9186	131	11,6224	0,8828
RT011_Baseline_CD4+PD1-	2200000	9890	95	12,7221	0,9586
RT011_Week5_CD3+	518156	7609	91	10,6403	0,8252
RT011_Week5_CD8+PD1+	17249	525	196	6,0437	0,6688
RT011_Week5_CD8+PD1-	93139	2306	87	5,9286	0,5307
RT011_Week5_CD4+PD1+	41183	5741	199	11,3561	0,9094
RT011_Week5_CD4+PD1-	76259	9882	107	12,6145	0,9506
RT011_Cells from Skin Bx	450000	5642	260	11,2557	0,9032

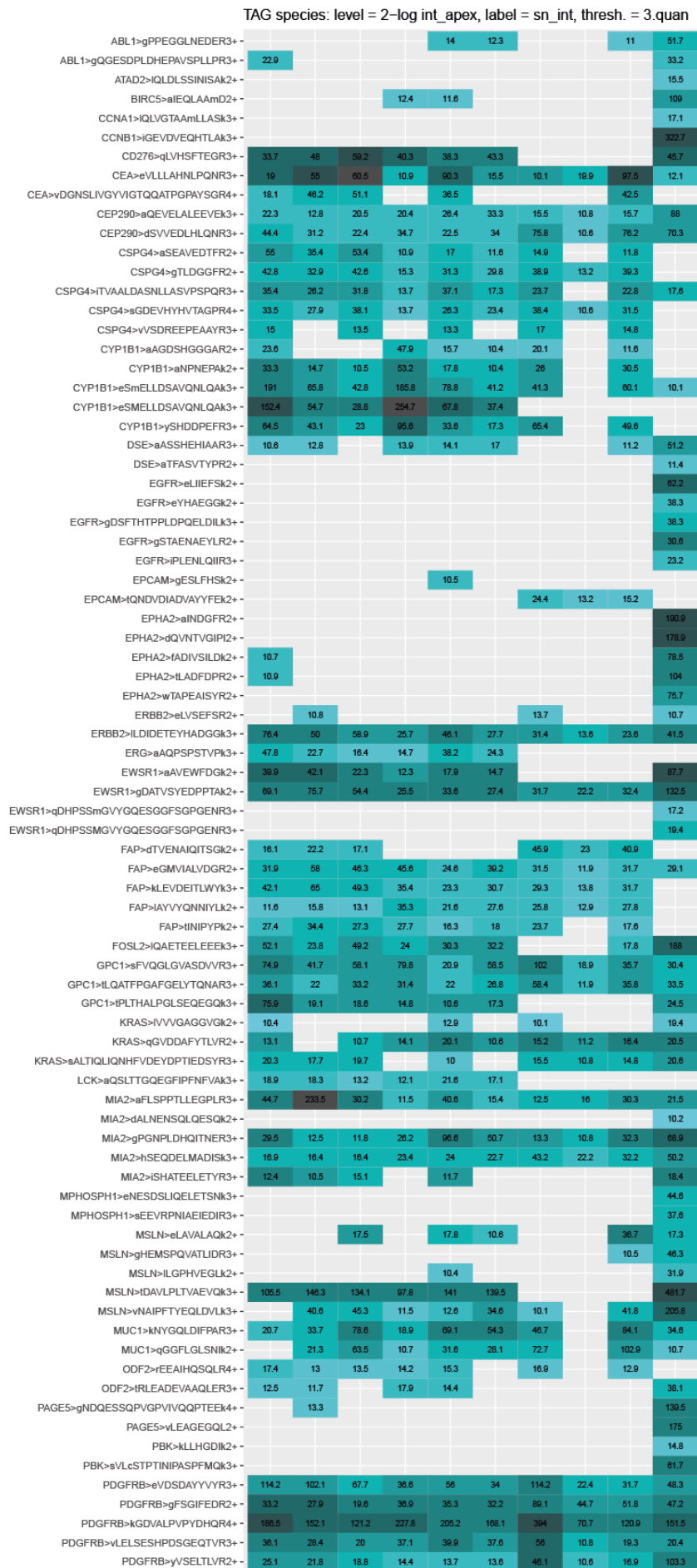
**Supplementary Table 9.** Metadata concerning cell populations used for TCRv $\alpha$  sequencing. Number of sorted cells, number of clones detected, number of clones detected with a relative frequency of  $\geq 0.05\%$ , Shannon diversity, and evenness are given per cell population.



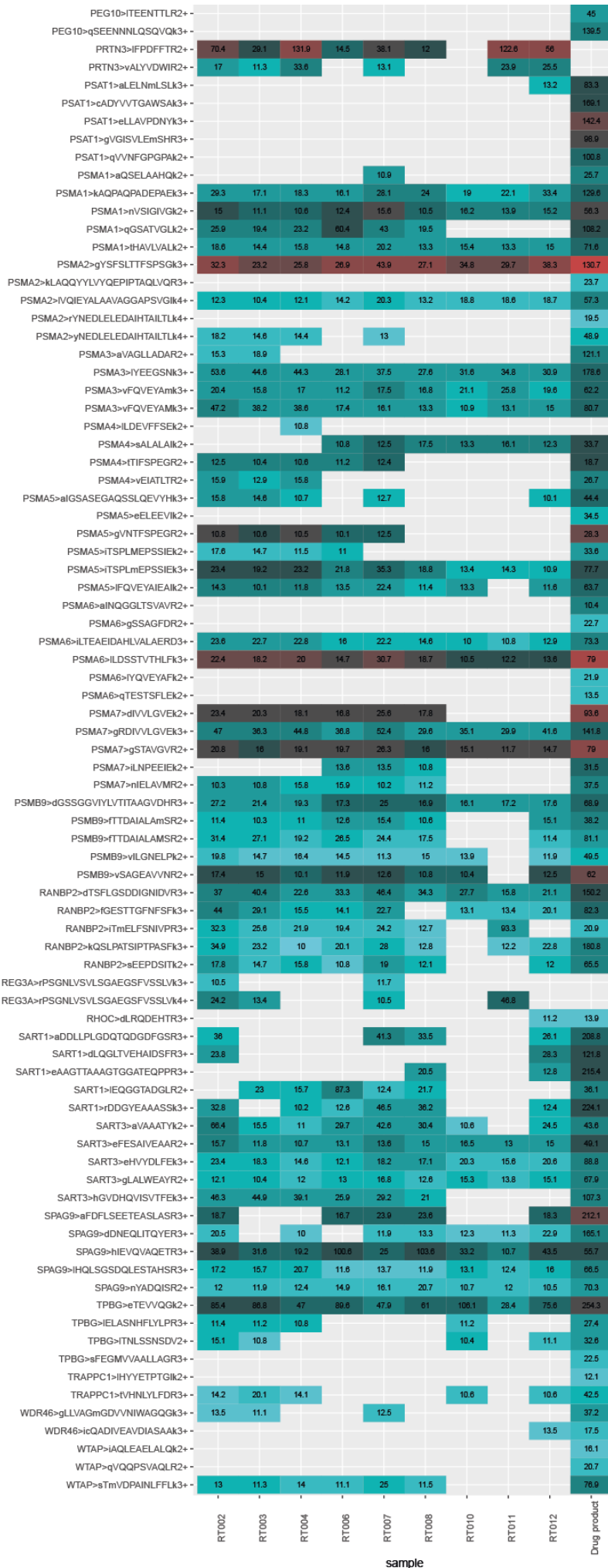
**Supplementary Figure 1.** Vital parameters at the time of DC vaccination. Abbreviations: mmHg, millimeter of mercury; bpm, beats per minute; °C, degrees Celsius.



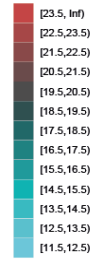
Chapter 4



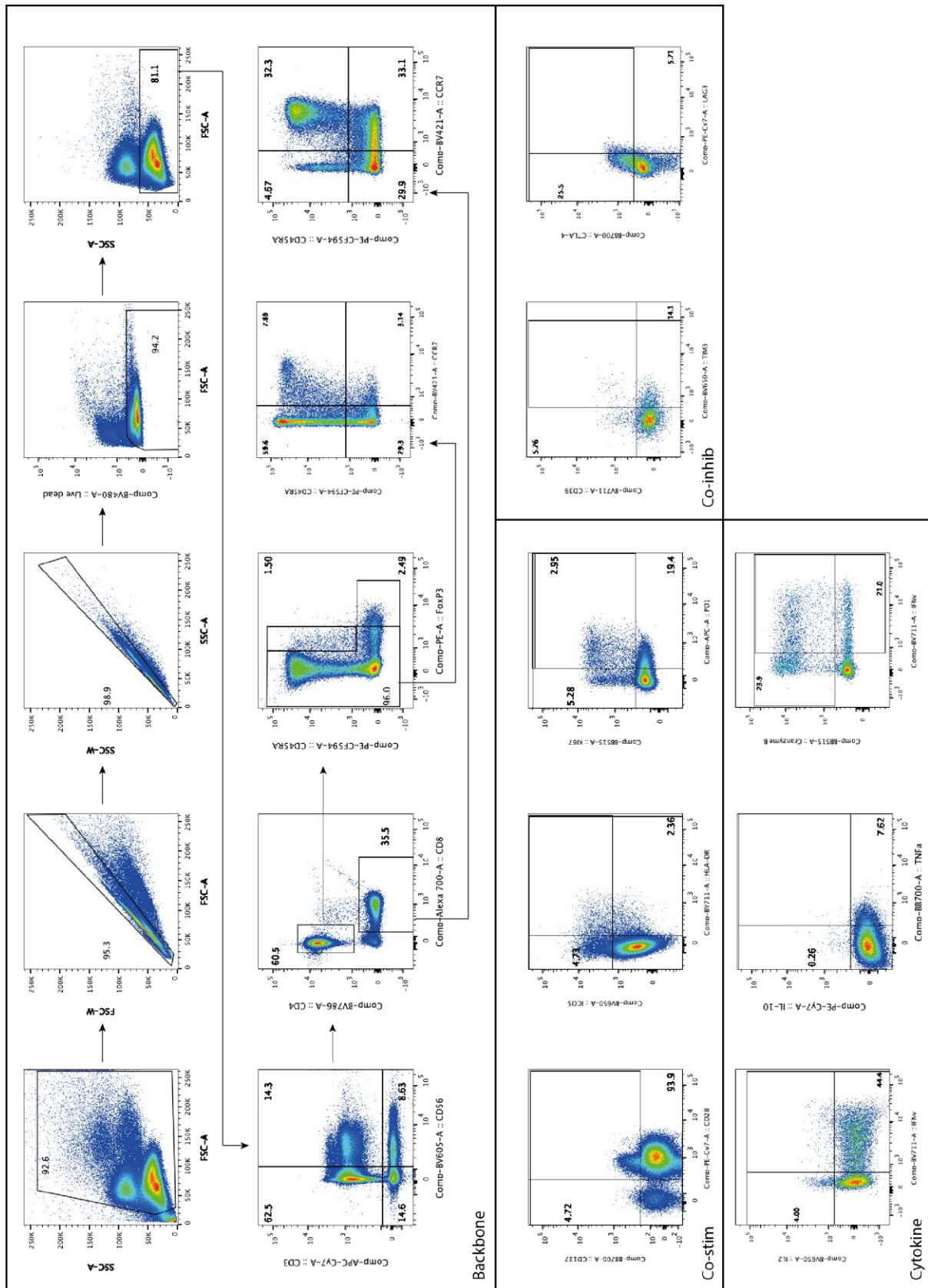
target



level

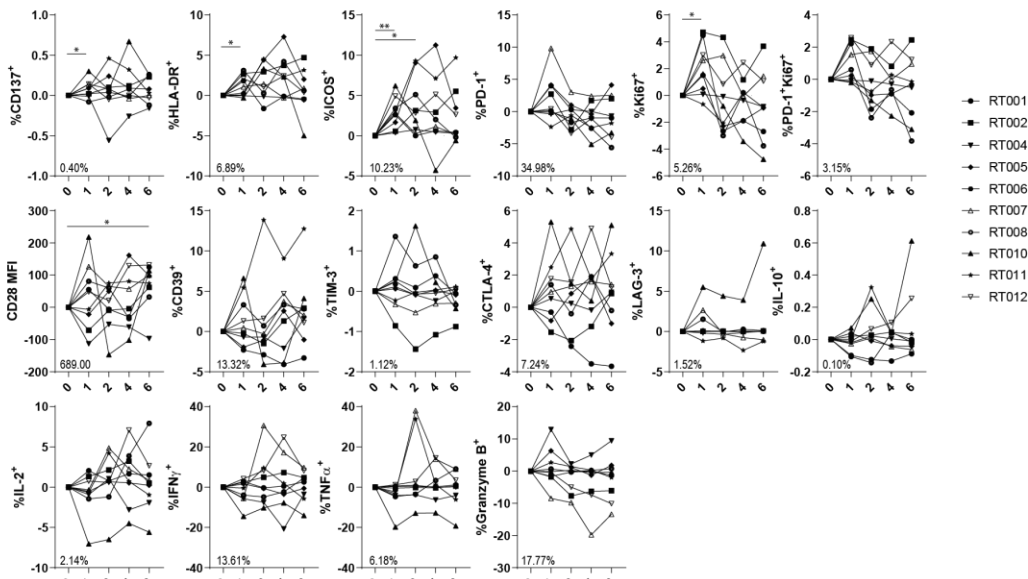


**Supplementary Figure 2.** Heat map of tumor antigen peptide species identified in tumor tissue lysates and drug product. Color of the heat map fields expresses the abundance (legend = intensity level,  $^2\log$ , of (arbitrary) reporter ion count) and number in heat map fields show the S/N of the peptide species in the corresponding sample. Lower case letters in the peptide sequence indicate modified amino acids (TMT label reagent or methionine oxidation). Download supplementary file when a higher resolution is desired; [https://www.ejancer.com/article/S0959-8049\(22\)00159-9/fulltext](https://www.ejancer.com/article/S0959-8049(22)00159-9/fulltext)

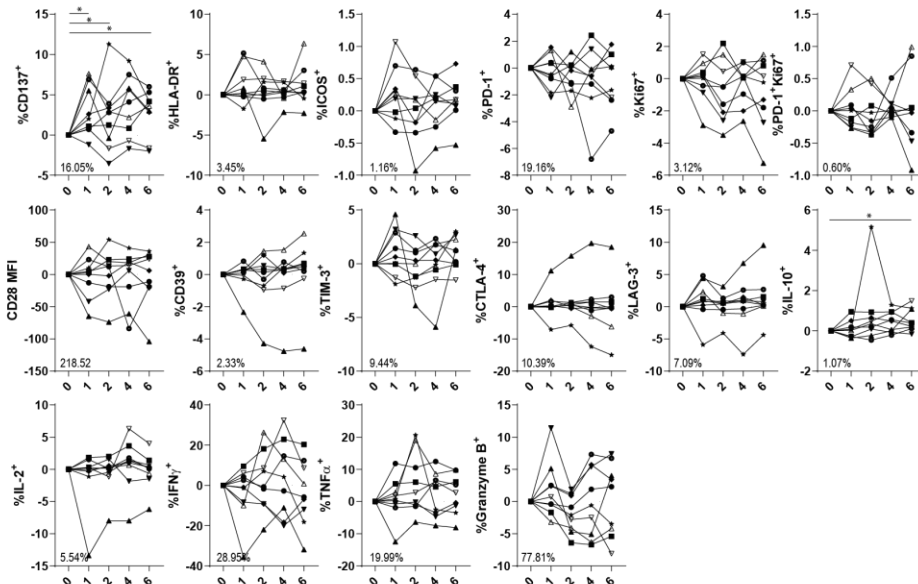


**Supplementary Figure 3.** Gating strategy FACS immuno-monitoring. Three FACS panels were used to characterize T cells. CD137, CD28, ICOS, HLA-DR, Ki67, PD-1 were included in the co-stimulatory panel. CD19, TIM-3, CTLA-4, LAG-3 were included in the co-inhibitory panel. IL-2, IL-10, IFN $\gamma$ , TNF $\alpha$ , Granzyme B were included in the cytokine panel. Abbreviations: Co-stim, co-stimulatory; co-inhib, co-inhibitory.

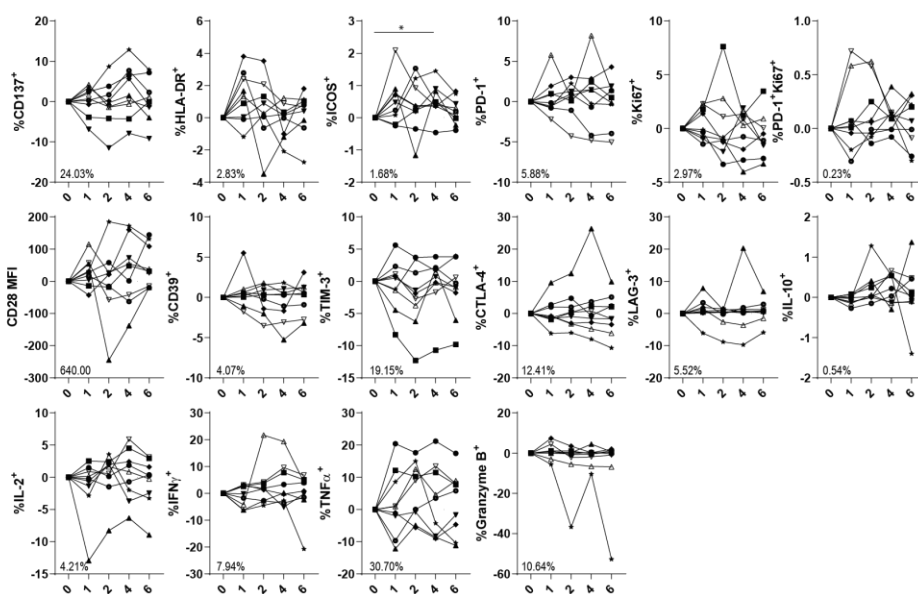
**D** CCR7<sup>+</sup>CD45RA<sup>-</sup> | Effector Memory CD4<sup>+</sup> Non-Tregs

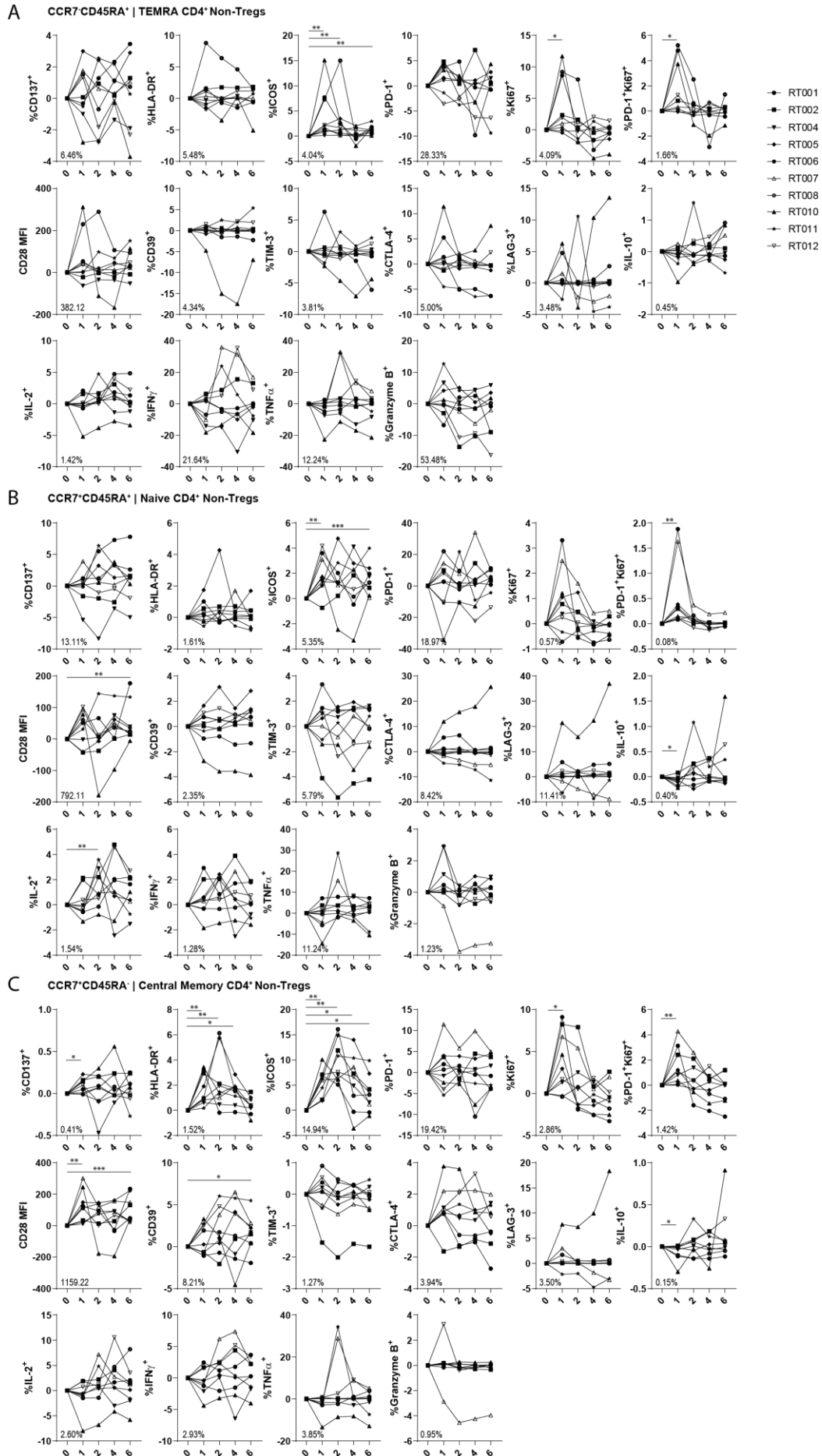


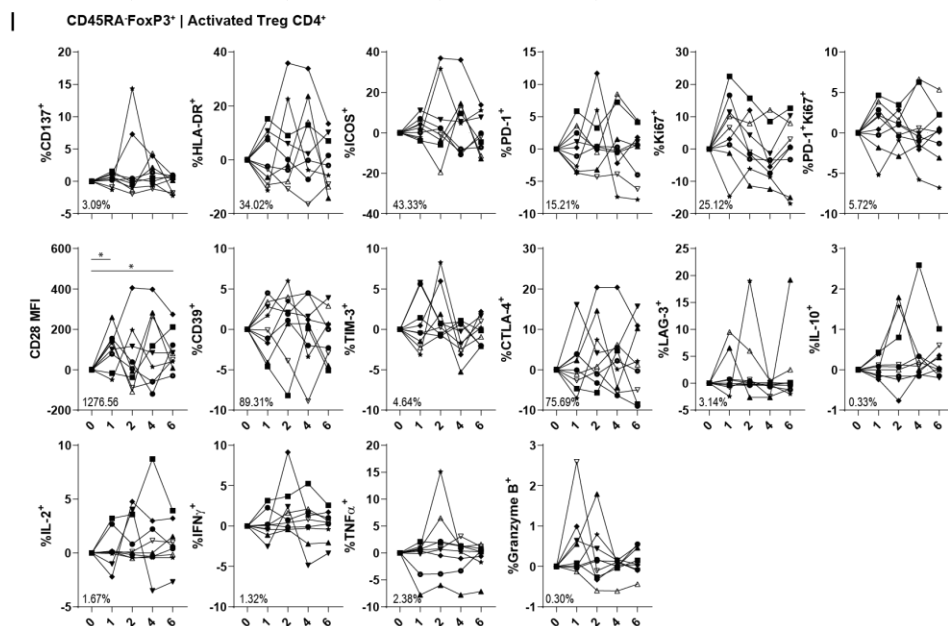
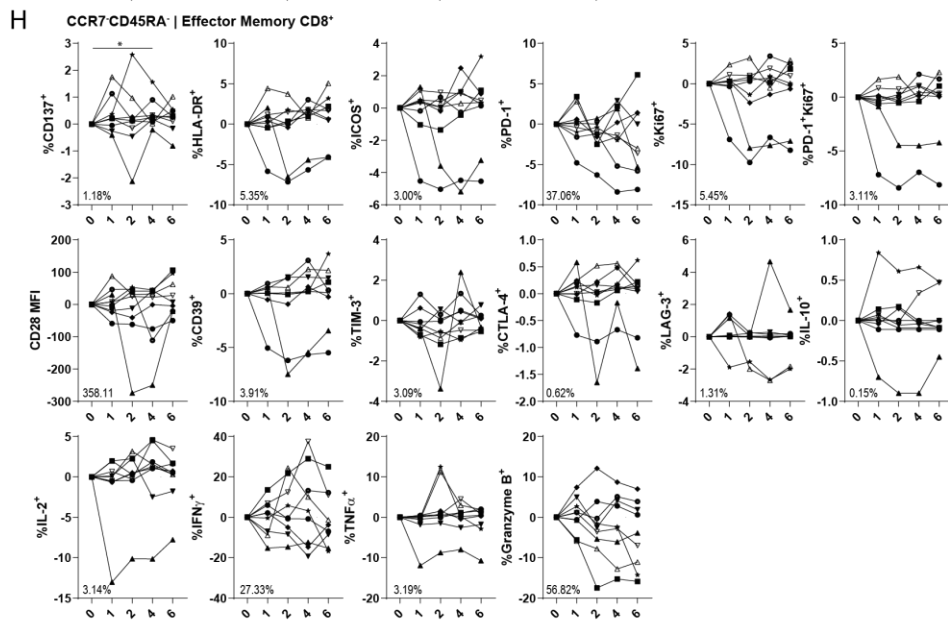
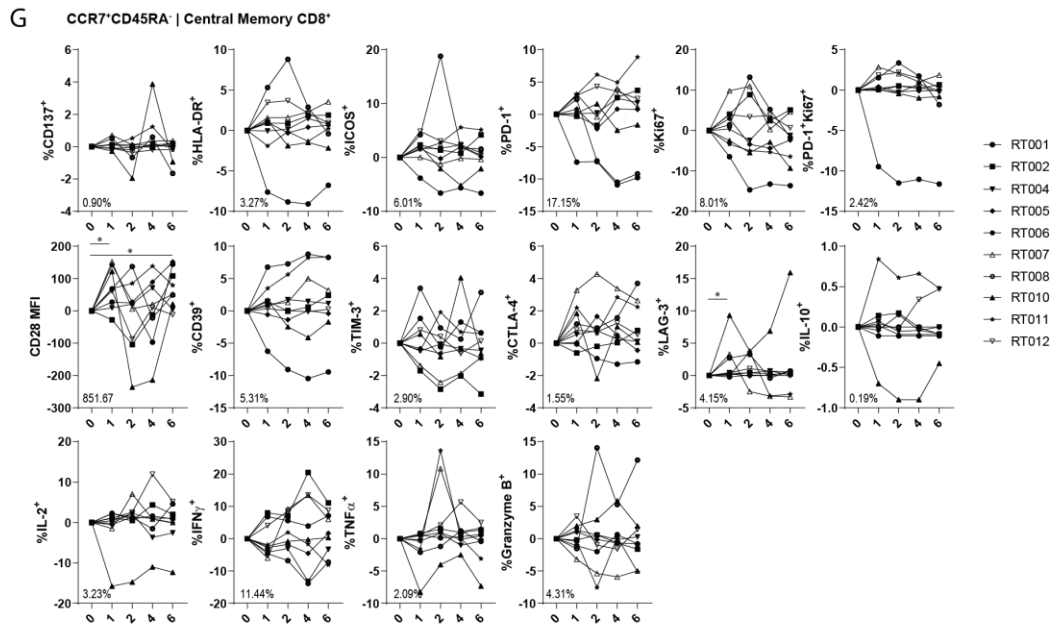
**E** CCR7<sup>+</sup>CD45RA<sup>+</sup> | TEMRA CD8<sup>+</sup>

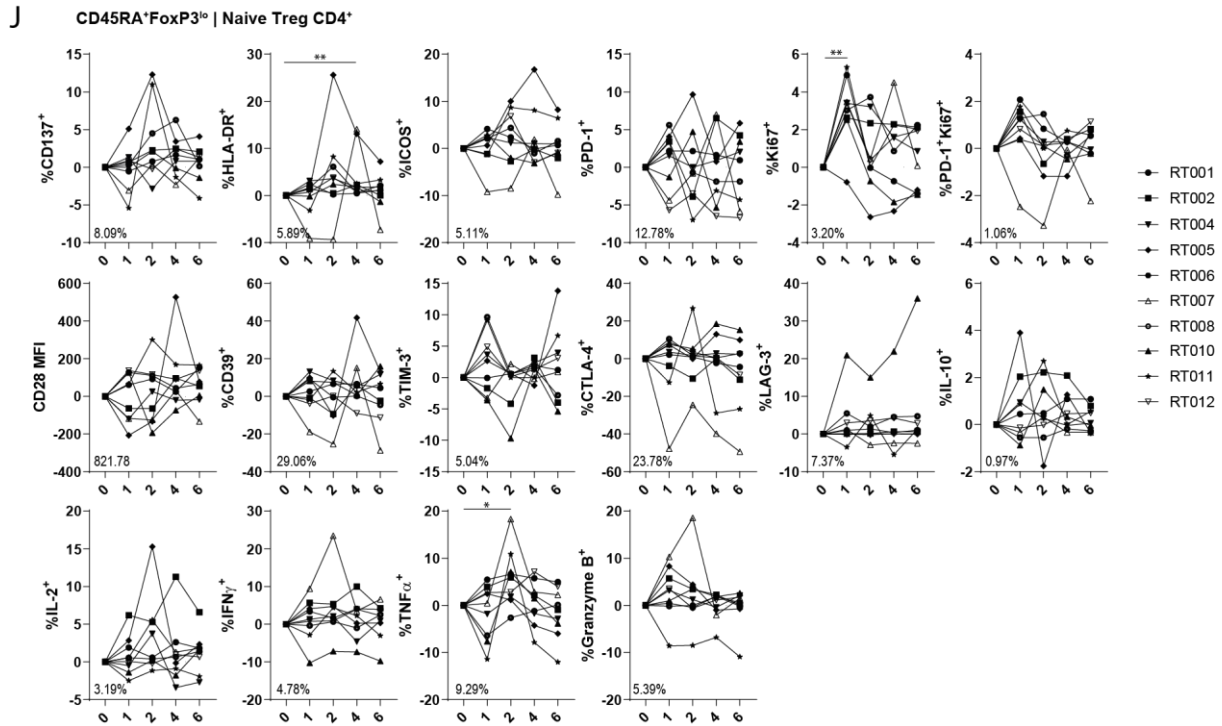


**F** CCR7<sup>+</sup>CD45RA<sup>+</sup> | Naive CD8<sup>+</sup>









**Supplementary Figure 4.** Comprehensive analysis of circulating T-cell memory subsets. (A) CCR7-CD45RA<sup>+</sup> TEMRA CD4<sup>+</sup> Non-Tregs. (B) CCR7+CD45RA<sup>+</sup> Naïve CD4<sup>+</sup> Non-Tregs. (C) CCR7+C45RA<sup>-</sup> Central Memory CD4<sup>+</sup> Non-Tregs. (D) CCR7-CD45RA<sup>-</sup> Effector Memory CD4<sup>+</sup> Non-Tregs. (E) CCR7-CD45RA<sup>+</sup> TEMRA CD8<sup>+</sup>. (F) CCR7+CD45RA<sup>+</sup> Naïve CD8<sup>+</sup>. (G) CCR7+C45RA<sup>-</sup> Central Memory CD8<sup>+</sup>. (H) CCR7-CD45RA<sup>-</sup> Effector Memory CD8<sup>+</sup>. (I) CD45RA-FoxP3<sup>+</sup> Activated CD4<sup>+</sup> Tregs. (J) CD45RA-FoxP3<sup>low</sup> Naïve CD4<sup>+</sup> Tregs. Most of the vaccine-induced changes in frequencies of activated T cells were detected among the CD4<sup>+</sup> central-memory (CM) T cells, and increase of CD137<sup>+</sup> and CD28<sup>+</sup> frequencies were also observed in CD4<sup>+</sup> effector-memory (EM) compartment. These changes were not observed in CD45RA-FoxP3<sup>+</sup>CD4<sup>+</sup> immunosuppressive T-regulatory cells. Subset analysis within CD8<sup>+</sup> T cells demonstrated increased frequencies of CD137<sup>+</sup>CD8<sup>+</sup> EM T cells re-expressing CD45RA (TEMRA). N= 10 per group. Data is normalized for baseline (week 0) and paired per patient. Percentage in left corner represent the average frequency at baseline. Significance was determined using the paired Wilcoxon signed-rank test. \*P<0.05, \*\*P<0.01, \*\*\*p<0.001.





# CHAPTER 5

---

Dataset from a proteomics analysis of tumor antigens shared between an allogenic tumor cell lysate vaccine and pancreatic tumor tissue.

Christoph Stingl\*

Sai Ping Lau\*

Sjoerd H. van der Burg

Joachim G. Aerts

Casper H.J. van Eijck<sup>#</sup>

Theo M. Luider<sup>#</sup>

*\* Shared first*

*# Shared last*

## ABSTRACT

The data described was acquired as part of a clinical study with the aim to investigate the potential of tumorreactive T-cell response as response to vaccination of pancreatic cancer patients with an allogeneic tumor cell lysate vaccine [1]. Proteomics analysis was carried out to identify tumor antigens that are shared between the allogeneic tumor cell lysate used for the vaccine and pancreatic ductal adenocarcinoma (PDAC) tissue samples. To this objective, cell lysates of the vaccine and of nine tissue samples were enzymatically digested and isotopically labeled with tandem mass tags (TMT) in a so-called six-plex manner (Thermo Fisher Scientific). Three pools were prepared by mixing the samples according to their TMT-labels. Subsequently, the three sample pools were fractionated into 24 fractions with high-pH reversed phase chromatography. These fractions were first analyzed on a nano-liquid chromatography (LC) system online coupled to a high-resolution Eclipse Orbitrap mass spectrometer (MS) equipped with a high-field asymmetric-waveform ion-mobility spectrometry (FAIMS) source using a data-dependent MS2 shotgun method. Overall, 126,618 unique peptide sequences, on basis of 768,638 peptide spectra matches and corresponding to 7,597 protein groups, were identified in the total sample set including 61 tumor antigens that were prioritized by Cheever and co-workers as vaccine target antigens on basis a of a series of objective criteria [2]. In the second phase of the experiment, this set of tumor antigens was targeted using a serial precursor selection (SPS) MS3 method. From this data, ion trap MS2 and Orbitrap MS3 fragment spectra were extracted for peptide identification (protein sequence database-dependent search) and relative quantification using the TMT labels, respectively. The dataset ultimately allowed the identification and quantification of 51 proteins and 163 related peptide precursors with the TMT labels (see Figure 2B and Supplemental Table 8, Lau *et al.* 2022).

## SPECIFICATIONS TABLE

Subject	Omics: Proteomics (Biological sciences) and Oncology (Health and medical sciences)
Specific subject area	Targeted proteomic analysis to determine antigens shared between pancreatic ductal adenocarcinoma and an allogenic cell lysate vaccine combining TMT labelling, highpH preparative LC, and FAIMS Eclipse Orbitrap MS.
Type of data	Table; Figure
How the data were acquired	Two-dimensional chromatography with high pH and reverse phase chromatography (Ultimate 3000 and preparative fractionation). Ultimate 3000 nano RSLC (Thermo Fisher Scientific, Germering, Germany) coupled to an Orbitrap Eclipse Tribrid Mass Spectrometer equipped with a High Field Asymmetric Waveform Ion Mobility Spectrometry (FAIMS) interface (Thermo Fisher Scientific, San Jose, CA, USA).
Data format	Raw and Analyzed
Description of data collection	Data-dependent ion trap MS2 shotgun method for deep proteome analysis (PXD032800) and targeted SPS-MS3 (Orbitrap) method for the targeted quantitative analysis (PXD025210) on selected tumor antigen candidates.
Data source location	Erasmus University Medical Center, Department of Neurology, Rotterdam, The Netherlands
Data accessibility	All MS data (raw), including detailed information about the targeted method, fragment spectra (mgf) used for database search and TMT quantification, and results of database search (mzident) have been made public available via ProteomeXchange with the following identifiers PXD025210 ( <a href="https://www.ebi.ac.uk/pride/archive/projects/PXD025210/private">https://www.ebi.ac.uk/pride/archive/projects/PXD025210/private</a> ) and PXD032800 ( <a href="https://www.ebi.ac.uk/pride/archive/projects/PXD032800/private">https://www.ebi.ac.uk/pride/archive/projects/PXD032800/private</a> ).[3]
Related research article	Lau SP <i>et al.</i> , " Autologous dendritic cells pulsed with allogenic tumor cell lysate induce tumor-reactive T-cell responses in pancreatic cancer patients: a phase I study ", European Journal of Cancer, In Press, 2022.

## VALUE OF THE DATA

- o The data provides a comprehensive compilation of TMT-labelled peptides identified in cell lysate and tumor tissue (N=9) with mass spectrometry and is additionally annotated with chromatographic measures under low and high-pH reversed phase chromatography conditions (retention times and fraction numbers, respectively) and FAIMS ion mobility information (individual compensation voltage ranges).
- o The dataset can be beneficial for further development of liquid chromatography and mass spectrometry methods for identification and quantification, such as the selection of peptides suitable for targeted measurements (*e.g.* PRM) or fractionation strategies for deep-proteome profiling.
- o The dataset may serve as basis (trainings set) for in-silico studies of modelling and predicting peptide properties and behaviors.
- o The dataset provides information about peptides of tumor antigen candidates [1,2] that were quantified with a data-dependent shotgun method using pre-defined inclusions list of peptide precursors and peptide fragments for SPS-MS3 TMT quantification.
- o The data can be used for further development of analysis and acquisition software to analyze SPS-MS3 spectra and FAIMS data.

Column Name	Description
sample	Name of the analytical samples, composed of pool number and fraction number; ( <i>e.g.</i> POOL1-f01 means fraction 1 of pool 1).
file	Raw file name, as uploaded to the repository.
scan	scan index of raw file.
pepseq	Peptide sequence; lower case letters specify the following modifications: m = oxidation of methionine, c = carbamidomethylation of cysteine, k = TMT-labelled Lysine, any N-terminal amino acid = TMT-labelling of N-terminus.
score	Mascot score.
prec_mz	m/z ratio of peptide precursor.
charge	charge state of peptide precursor.
rt	Retention time of MS/MS spectra
CV	FAIMS compensation voltage of MS scan.
genes	Gene identifier related to peptide (derived from accession number reported in database search result).
accnrs	Protein accession number related to peptide (Uniprot/Swissprot format).

**Table 1.** Column names and description used in peptide-spectra-matches tables uploaded to ProteomeXchange repository PXD032800.

## DATA DESCRIPTION

We describe two datasets that were acquired in order to detect and quantify shared tumor antigens between an allogeneic tumor cell line lysate (PheraLys) and tissue samples from pancreatic ductal adenocarcinoma (PDAC) of 9 patients as described by Lau and colleagues. [1]

Prior to the LC-MS measurements, all samples were enzymatically digested with trypsin, TMT-labelled, pooled in six-plex, and fractionated into 24 fractions with high-pH reversed phase preparative chromatography. Hence, basis for the LC-MS measurements was a set of 72 analytical samples (24 fractions of 3 pools). The first dataset (ProteomeXchange ID PXD032800) contains spectra of data-dependent shotgun measurements that were set up to identify as many peptides and proteins as possible. To that aim, MS/MS scans were detected in the ion-trap for highest scan speed and sensitivity. In total, these measurements yielded 768,638 peptide-spectra-matches, 126,618 unique peptide sequences and 7,597 proteins groups (protein FDR < 1% and peptide FDR < 0.1%). A complete list of all peptide-spectramatches identified, annotated with FAIMS compensation voltages and LC retention time and fraction numbers, respectively, is publicly available on ProteomeXchange repository PXD032800. Column characteristics are described in Table 1. Corresponding to this, the numbers of identification per individual fraction and related distributions of peptide charges, peptide length and FAIMS CV fractions are shown in Figure 1. The second dataset (PXD025210) was acquired for peptide quantification using TMT reporter ions. For this purpose, we applied a serial-precursor selection (SPS) Orbitrap MS3 method in order to reduce non-specific background signal that potentially generates interferences and leads to biased quantifications.[4,5] To compensate for reduced scan speed and sensitivity of the Orbitrap SPS-MS3 method compared to the ion trap MS2 method, we restricted the data-dependent shotgun method using a precursor inclusion list that just allowed MS2 and MS3 precursor selection of predefined peptide precursors and fragments, respectively.



**Figure 1.** Bar-chart of number of peptide-spectra-matches (PSM) and unique peptide sequences identified in 24 fractions of pool 1, 2, and 3 (A). Distribution of peptide charges (B), peptide length (C) and FAIMS compensation voltage (D) plotted per fraction and pool. Download image when a higher resolution is desired; [https://ars.els-cdn.com/content/image/1-s2.0-S2352340922006849-gr1\\_lrg.jpg](https://ars.els-cdn.com/content/image/1-s2.0-S2352340922006849-gr1_lrg.jpg)

## EXPERIMENTAL DESIGN, MATERIALS AND METHODS

### *Sample digest and labelling*

Volumes corresponding to 100 µg protein amount (Bradford assay) were dissolved in 2% Sodium deoxycholate (SDC), 100 mM Triethylammonium bicarbonate (TEAB), and 10 mM 1,4-Dithiothreitol and filled up with water to a total of 229 µL. Samples were heated for 2 minutes at 95 °C, intensively sonicated (Branson cup sonification device) for 2 minutes at 70% intensity, and incubated for a further 30 minutes at 56 °C and mildly shaken. Then, samples were loaded in an Amicon Ultra-0.5 Centrifugal Filter Unit with an Ultracel-30 regenerated cellulose membrane and washed three times with 0.5% SDC, 5% acetonitrile (ACN), and 100 mM TEAB. Next, 15 mM Iodoacetamide was added, samples were incubated at darkness for 30 minutes and then washed twice with 0.5% SDC, 5% ACN and 100 mM TEAB, and additionally washed twice with 200 mM TEAB. For sample digestion, 4 µg trypsin (Trypsin Gold, Promega) was added and samples were incubated at 37 °C over-night (approx. 14 h). Finally, the digest solution was spun down and a small aliquot of 1.8 µL was acidified and diluted (10x), centrifuged and used for nano-LC test runs, during which UV absorbance was detected to determine total peptide abundance. For peptide labeling with Tandem Mass Tags (TMT), a normalized volume corresponding to 30 µg digest was taken and filled up with 200 mM TEAB to a total volume of 75 µL. Then, TMT six-plex reagents were diluted in 100 µL ACN and 31 µL label reagent was added to each sample according to the scheme in Table 2. Samples were incubated for 1 hour at 20 °C with mild shaking, and thereafter reaction was quenched by the addition of 2.7 µL 5% hydroxylamine. Finally labelled samples were combined into three pools according to the scheme in Table 2, acidified, dried (speedvac concentrator), resuspended in 2% ACN/0.5% TFA and transferred to LC vials for the following preparative fractionation. If not noted otherwise, all reagents were purchased from Sigma-Aldrich/Merck.

#	Sample ID	Patient	TMT reporter ion	Pool	Category
1	RT002	Pat1	126	POOL1	non-tumor tissue*
2	RT002	Pat1	127	POOL1	tumor lysate
3	RT003	Pat2	128	POOL1	non-tumor tissue*
4	RT003	Pat2	129	POOL1	tumor lysate
5	RT004	Pat3	130	POOL1	tumor lysate
6	Drug product	(vaccine)	131	POOL1	Drug product
7	RT004	Pat3	126	POOL2	non-tumor tissue*
8	RT006	Pat4	127	POOL2	tumor lysate
9	RT007	Pat5	128	POOL2	tumor lysate
10	Drug product	(vaccine)	129	POOL2	Drug product
11	RT008	Pat6	130	POOL2	non-tumor tissue*
12	RT008	Pat6	131	POOL2	tumor lysate
13	Drug product	(vaccine)	126	POOL3	Replicate
14	Drug product	(vaccine)	127	POOL3	Drug product
15	RT010	Pat7	128	POOL3	tumor lysate
16	RT011	Pat8	129	POOL3	non-tumor tissue*
17	RT011	Pat8	130	POOL3	tumor lysate
18	RT012	Pat9	131	POOL3	tumor lysate

**Table 2.** Sample table of three TMT-sixplex pools. \* non-tumor tissue: no applicable for study.



### *High-pH reversed phase fractionation*

Preparative chromatography was conducted on an Ultimate 3000 LC system (Thermo Fisher Scientific) equipped with C18 reversed phase column (Kinetex EVO, 2.1 mm x 150 mm, PN 00F-4725-AN, Phenomenex) operated at an oven temperature of 40 °C. Peptides were separated by a binary gradient from 4% to 38% solvent B in 8 minutes at a flow rate of 450 µL/min, whereby solvent A was composed of 10 mM ammonium formate buffer pH 10 and solvent B was 80% ACN and 10 mM ammonium formate pH 10. Twenty-four fractions of 200 µL (collection period of 26 seconds) were collected in a 96 well-plate (PN P-96-450V-C, Axygen/Thermo Fisher Scientific), dried (speedvac concentrator), resuspended in 2% ACN/0.1% TFA, split in two aliquots and transferred to a heatsealed 384 well-plate, where it was stored at 4 °C until subsequent LC-MS analysis.

### *LC-MS measurements*

LC-MS measurements were performed on a nano-LC system (Ultimate 3000 RSLC, Thermo Fisher Scientific, Germering, Germany) coupled to an Orbitrap Eclipse Tribrid Mass Spectrometer equipped with a High Field Asymmetric Waveform Ion Mobility Spectrometry (FAIMS) interface (Thermo Fisher Scientific, San Jose, CA, USA). Twenty-four µL peptide fraction were injected and transferred on a trap column (C18 PepMap, 300 µm ID x 5 mm; Thermo Fisher Scientific) using 0.1% trifluoroacetic acid at a flow rate of 20 µL/min, and further eluted and separated on a 50 cm analytical nano-LC column (PepMap C18, 75 µm ID x 500 mm, 2 µm, 100 Å; Thermo Fisher Scientific) using a binary 3 hours gradient from 4% to 24% solvent B in 120 minutes and further increasing to 45% B in 60 minutes, whereby solvent A was 0.1% formic acid, solvent B 80% acetonitrile and 0.08% formic acid, and a flow rate 300 nL/min and a column temperature of 40°C was applied. For electrospray ionization we used coated silica nano electro-spray emitters (New Objective, Woburn, MA, USA) at a spray voltage of 2.2 kV. FAIMS was setup to collect ion mobility fractions at compensation voltages (CV) of -40, -60 and -80 V. For the untargeted survey experiment (with the aim to identify as many tumor antigens as possible), a data dependent acquisition MS method was used with an Orbitrap survey scan (range 375- 1500 m/z, resolution of 120,000, AGC target 400,000), followed by consecutively isolation (isolation with = 0.7 amu), fragmentation (HCD, 35% NCE) and detection (ion trap, AGC 10,000) of the peptide precursors detected in the survey scan until a duty cycle time of 1 seconds per FAIMS CV fraction was exceeded. Precursor masses that were selected once for MS/MS were excluded for subsequent fragmentation for 60 seconds. In total, 16 fractions of 3 pools (fractions 6 to 23; 54 runs) were measured with this method. Additionally, four early fractions (fraction 1,2, 5, and 8) and the last fraction (fraction 24) that showed in general comparable low peptide amounts, were measured by a shorter 60 minutes gradient, with otherwise identical parameters.

Thereafter, a targeted SPS-MS3 methods was developed to specifically acquired MS3 reporter ion spectra with enhanced accuracy and selectivity, whereby a targeted inclusion list for TAG related peptides (MS2 precursor masses) and fragments (MS3 precursors masses; using

fragments with relative intensities greater 10%) were prepared on the basis of the results of the preceding survey experiment. The initial list of tumor antigens was derived from a preceding RNA sequencing analysis and literature research [2] and is shown in Lau *et al.* 2022 (Supplemental Table 2[1]). Each peptide was specified by the expected m/z ratio, retention time, compensation voltage, and high-pH fraction. For each fraction in which TAG peptides were targeted (fractions 6 to 23), a specifically adapted method (parent mass list table) was prepared containing the expected peptides, but also of the preceding and following fractions to compensate for variation of elution during preparative LC. Up to 10 MS2 fragment masses were allowed for sequential precursor selection (SPS), the MS2 isolation width was 3 m/z (fixed) and HCD collision energy set to 55%. SPS-MS3 scans were acquired in the Orbitrap at a resolution of 50,000, AGC target of 250,000 and maximum injection time of 200 ms. In total we measured 16 fractions of 3 pools with this approach, whereby 2 measurements (fraction 18 and 19 of pool 3) did not yield suitable data because of a hardware failure.

#### *Mass spectrometry data analysis*

Acquired RAW data of both, survey experiment and targeted SPS-MS3 runs, were processed with MSaccess and MSconvert (proteowizard version 3.0.19263)[6] to extract scan meta information and fragment ion peak lists as MGF files, respectively. For peptide and protein identification we conducted a Mascot fragment ion database search (v.2.301; Matrix Science) and subsequent carried out determination of the false-discovery rates, protein grouping and exporting of results (spectra report) using the software package Scaffold (version 4.11.1; Proteome Software), whereby following settings were applied: combined human subsets of Swiss-Prot and TrEMBL (download: January 18th 2021, 194,237 entries), decoy search, carbamidomethylation (+57.021 u) of cysteine and TMT6plex labelling (+229) of lysin and the peptide N-terminus as fixed modification, oxidation (+ 15.995 u) of methionine, 10 ppm precursor ion tolerance and 0.5 Da fragment ion tolerance, and 1% peptide and 0.1% protein false discovery rate threshold. Results were exported (via a scaffold spectra report) from the runs of the survey experiment and compared to the list of TAGs described above to derive a list of targeted TAG peptides for targeted SPS-MS3 measurements. From the targeted SPS-MS3 data, MS3 reporter ions were extracted from the peak lists (mgf files) and assigned to the MS2 spectra identified. The noise level of each MS3 spectra was estimated as the median overall fragment intensity, and for each peptide species and pool the scan with the highest overall reporter ion intensity was selected for quantification. From these scans the ratio of intensity in tissue lysate to PheraLys, the individual intensities and signal to noise ratio (S/N) of the signal were derived for each reporter ion. Peptides were reported as positively detected and quantified in a sample if the S/N of the reporter ion was above 3 and 10, respectively. At a maximum, the five most suitable peptides per proteins were reported and used to calculate quantitative protein properties. Protein intensities were calculated as the sum of peptide intensity normalized by the total number of peptide intensities of reported peptides. For data

extraction we used adjusted and in-house written Perl programs[7], and for data analysis and plotting the statistical software package R[8].

## REFERENCES

1. Lau SP, Klaase L, Vink M, et al. Autologous dendritic cells pulsed with allogeneic tumor cell lysate induce tumorreactive T-cell responses in pancreatic cancer patients: a phase I study. *Eur J Cancer*. 2022;In Press.
2. Cheever MA, Allison JP, Ferris AS, et al. The prioritization of cancer antigens: a national cancer institute pilot project for the acceleration of translational research. *Clin Cancer Res*. 2009;15:5323–37.
3. Vizcaíno JA, Csordas A, del-Toro N, et al. 2016 update of the PRIDE database and its related tools. *Nucleic Acids Res*. 2016;44:D447–56.
4. McAlister GC, Nusinow DP, Jedrychowski MP, et al. MultiNotch MS3 enables accurate, sensitive, and multiplexed detection of differential expression across cancer cell line proteomes. *Anal Chem*. 2014;86:7150—7158.
5. Erickson BK, Jedrychowski MP, McAlister GC, et al. Evaluating multiplexed quantitative phosphopeptide analysis on a hybrid quadrupole mass filter/linear ion trap/orbitrap mass spectrometer. *Anal Chem*. 2015;87:1241–9.
6. Chambers MC, Maclean B, Burke R, et al. A cross-platform toolkit for mass spectrometry and proteomics. *Nat Biotechnol*. 2012;30:918–20.
7. Köcher T, Pichler P, Schutzbier M, et al. High precision quantitative proteomics using iTRAQ on an LTQ Orbitrap: a new mass spectrometric method combining the benefits of all. *J Proteome Res*. 2009;8:4743–52.
8. R Core Team. *R: A Language and Environment for Statistical Computing*. Vienna, Austria: R Foundation for Statistical Computing; 2013.



# CHAPTER 6

---

Rationally combining immunotherapies to improve efficacy of immune checkpoint blockade in solid tumors

Sai Ping Lau\*

Floris Dammeijer\*

Casper H.J. van Eijck

Sjoerd H. van der Burg

Joachim G.J.V. Aerts

*\* These authors contributed equally to this work.*

## ABSTRACT

With the widespread application of immune checkpoint blocking antibodies (ICBs) for the treatment of advanced cancer, immunotherapy has proven to be capable of yielding unparalleled clinical results. However, despite the initial success of ICB-treatment, still a minority of patients experience durable responses to ICB therapy. A plethora of mechanisms underlie ICB resistance ranging from low immunogenicity, inadequate generation or recruitment of tumor-specific T cells or local suppression by stromal cells to acquired genetic alterations leading to immune escape. Increasing the response rates to ICBs requires insight into the mechanisms underlying resistance and the subsequent design of rational therapeutic combinations on a per patient basis. In this review, we aim to establish order into the mechanisms governing primary and secondary ICB resistance, offer therapeutic options to circumvent different modes of resistance and plea for a personalized medicine approach to maximize immunotherapeutic benefit for all cancer patients.

## INTRODUCTION

For many years, directing our immune system to target cancer was minimally effective in generating durable clinical responses. T-cell responses induced by often inferiorly formulated and designed vaccines were not powerful enough to overcome the many barriers posed by advanced solid tumors [1,2]. However, following the unprecedented results of ‘re-invigorating’ T cells in a proportion of metastatic cancer patients by blocking immune inhibitory checkpoints, tumor immunotherapy has regained its position at the forefront of cancer treatment today [3]. To this date, the most studied and manipulated immune checkpoints on T cells are the receptors T lymphocyte associated antigen 4 (CTLA-4) and programmed cell death protein 1 (PD-1). Targeting CTLA-4 and the PD-1-PD-L1-axis with antagonistic antibodies has proven to be highly efficacious in a proportion of cancer patients (Fig. 1). The finding that a subgroup of patients has a pre-existing but dysfunctional anti-tumor immune response that can be therapeutically restored, prompts further investigation into what constitutes tumor immunity and precludes response to immunotherapy.

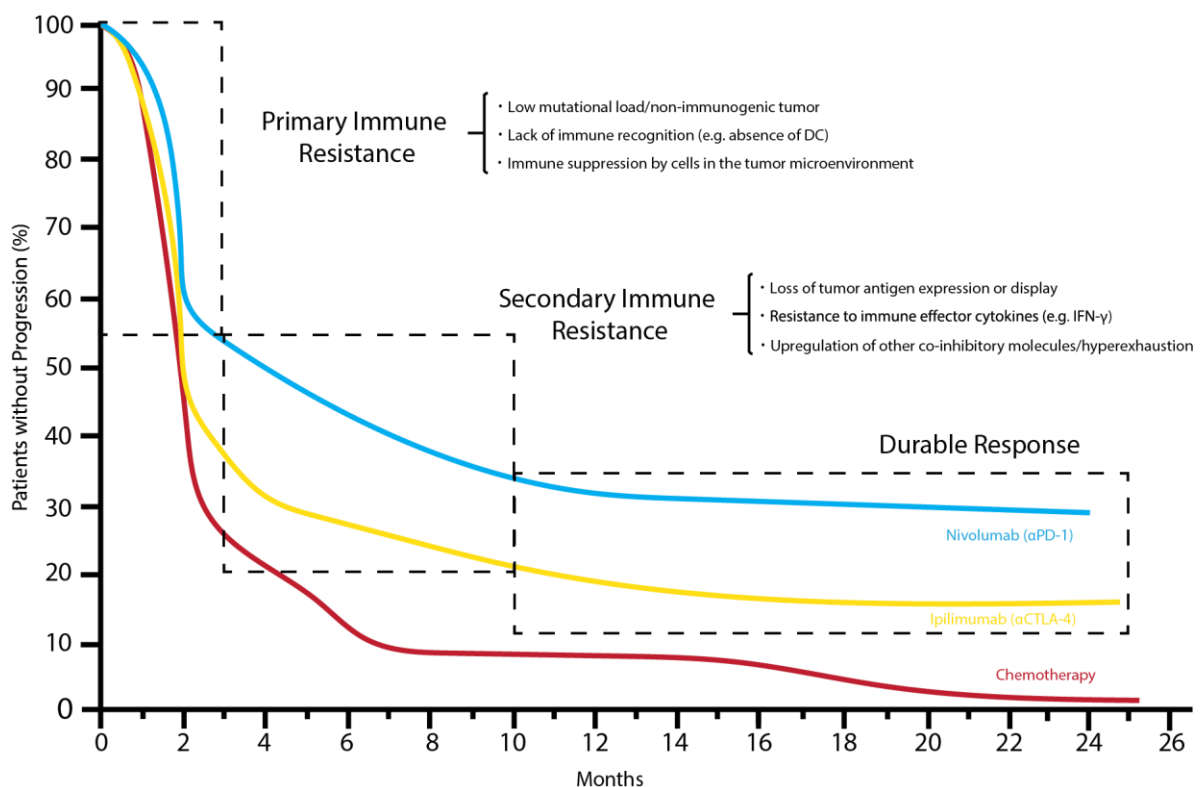


**Figure 1.** Progression-free survival curves for chemotherapy, anti-PD-1- and anti-CTLA-4- checkpoint blockers; primary and secondary resistance to immune checkpoint blockade (ICB) therapy precludes patients from achieving durable responses and long-term survival. When patients do not respond to ICBs immediately following start of treatment they experience primary immune resistance. When patients do respond initially but relapse over time, secondary resistance to ICB-treatment has developed. PFS-curves have been derived from the following clinical trials investigating ICB-efficacy in metastatic melanoma: Robert et al. NEJM 2011, Schachter et al. ASCO #9504 2016.



## CURRENT STATE OF IMMUNE CHECKPOINT BLOCKADE IN ADVANCED CANCER

Immune checkpoints are receptors expressed by T cells that upon ligation by their respective ligands regulate immune cell effector functions and proliferation thereby maintaining tolerance to self-antigens and ensure immune homeostasis [4,5]. Blocking inhibitory checkpoints using antagonistic antibodies may 'release the brakes' on T cells, including those cells specific for tumor antigens.

CTLA-4 is upregulated by T cells following recognition of cognate antigen by antigen presenting cells (APCs) in the lymph node [6]. The structure of CTLA-4 is nearly identical to the costimulatory receptor CD28 but interacts with much higher affinity for its ligands CD80/CD86 (B7-1/B7-2) expressed by the APC [7]. In contrast to CD28 stimulation, CTLA-4 has an inhibitory effect on effector T cells by causing cell cycle arrest [6,7]. Additionally, regulatory T cells (Tregs) constitutively express high levels of CTLA-4 on their cell surface, further facilitating their immune suppressive potential [8]. Antibodies directed towards CTLA-4 may therefore also act by decreasing Treg frequencies in blood and tumor via antibody dependent cytotoxicity (ADCC) [9,10].

Besides CTLA4, activated T cells express PD-1, and the coupling of PD-1 to programmed cell death ligand 1 (PD-L1, also called B7-H1) or PD-L2 (B7-DC) restrains T-cell effector function and proliferation [11]. PD-L1 is expressed on tumor cells (constitutively due to oncogenic signaling or in response to interferons), myeloid cells including APCs, and PD-L2 is solely expressed by APCs [12]. It has recently been shown that both PD-L1 on host myeloid cells and on tumor cells is a prerequisite for anti-PD-1-therapy efficacy [13]. PD-1 was previously thought to attenuate T-cell receptor (TCR)-signaling but recent insights have firmly established the inhibitory role of PD-1 on downstream CD28-signalling in T cells, further emphasizing the importance of proper (local) co-stimulation for T-cell function [14,15].

Thus far, four ICBs are FDA approved; anti-CTLA-4 (ipilimumab), anti-PD-1 (pembrolizumab and nivolumab) and anti-PD-L1 monoclonal antibodies (atezolizumab). Response rates vary between 11 and 40% depending on tumor type with PD-1 blockade yielding superior responses at a more favorable toxicity profile compared to CTLA-4 inhibition [16–20]. It has been suggested that the discrepancy in toxicities between ICBs can be explained by the time of checkpoint engagement in the T-cell response. The PD-1/PD-L1 axis has been proposed to operate later during the effector phase of a T cell, resulting in a more confined response whereas CTLA-4 acts on the lymph node during T-cell priming [21]. These temperospatial differences between ICBs are being exploited by combining anti-CTLA-4 and anti PD-1/PD-L1 in the clinic. Combining ipilimumab (anti-CTLA4) and nivolumab (anti-PD-1) in BRAF wild-type melanoma patients was efficacious in reaching its primary endpoint of progression free survival [22]. Although primary analysis showed a significant advantage of combination therapy over both monotherapies, recent follow-up data report a 2-year survival rate of 64% in the

combination treated group compared to 59% survival in  $\alpha$ PD-1 monotherapy treated patients. Notably, the difference in serious adverse event rate was considerable (58% vs 21%) suggesting limited clinical value of this immunotherapy combination [23]. In other solid tumors including non-small-cell lung cancer (NSCLC) and renal cell carcinoma, response rates of ICB monotherapy are more modest ranging from 15 to 20% [24–29]. Reasons underlying this heterogeneity in response rates shall be further addressed in the following sections.

Despite the significant progress that has been made with ICB across multiple tumor types, still much remains to be gained. Recent insights into tumors from initial and durable responders and non-responders to ICB have offered novel insights into tumor-immune interactions and the prerequisites for establishing effective and durable anti-tumor immunity. A complete understanding of these processes is still lacking but with knowledge of basic (tumor-)immunological principles and the implementation of innovative diagnostics, rational therapeutic combinations can be designed to improve ICB response rates in advanced cancer patients.

## **MECHANISMS UNDERLYING PRIMARY AND SECONDARY RESISTANCE TO ICB**

Despite the success of ICBs, only a minority of patients experience durable responses to ICB therapy. The remainder of patients do not respond at all (primary resistance) or initially respond but relapse over time (secondary resistance) (Fig. 1). A plethora of mechanisms underlie ICB resistance. Primary as well as secondary resistance to ICB results from an intricate interplay between immune cells, other stromal cells (*e.g.* cancer associated fibroblasts (CAF), endothelial cells) and tumor cells, all together composing the tumor microenvironment (TME). In general, primary resistance occurs when tumors lack an endogenous adaptive and functional immune infiltrate (this includes the pre-existence of an irreversibly ‘hyper-exhausted’ T-cell response incapable of responding to ICB). Secondary resistance recapitulates all the adaptive mechanisms which takes place subsequently to therapeutic pressure resulting in the failure to maintain an effective anti-tumor response. It has to be noted that the proposed distinction between primary and secondary immune resistance is pragmatic and useful in most causes of resistance but in reality, multiple opposing phenomena may be at play and some (such as an immune suppressive TME) may act throughout the course of ICB treatment.

### *Primary resistance to ICB*

Primary resistance to ICB can result from the absence of a functional immune response to poorly immunogenic tumor (Fig. 2). Tumors with a high non-synonymous mutational load are more likely to display neo-antigens that could be considered foreign to the immune system and thus possibly immunogenic [30,31]. Therefore, it is not surprising that cancer types with the highest mutational loads generally have high response rates to ICB (melanoma, NSCLC) [32]. Also, subtypes of tumors characterized by deficiencies in mismatch repair genes, as is the case

for microsatellite instable colon cancers, respond markedly better to ICB compared to their microsatellite stable counterparts [33]. However, even within the same tumor type, high mutational load in tumors was shown to at least partially predict response to both anti-PD1- and CTLA4-inhibition further supporting the importance of tumor mutational landscape and concomitant immunogenicity in determining ICB efficacy [31,34,35]. But does an increased neo-antigen load also necessarily lead to enhanced cytolytic T-cell responses in tumors? A seminal study by Rooney *et al.* shows that increased neo-antigen load, and in some tumors the presence of viral genes, was indeed associated with enhanced cytotoxic T-cell activity [36]. In line with these findings, positive correlations between anti-CTLA-4 therapy efficacy and the presence of a pre-existing immune response together with a high mutational and neo-antigen load in melanoma have been found [35]. A similar prerequisite for ICB-efficacy was found in melanoma patients where a pre-existing CD8+ PD1+ T-cell infiltrate in the invasive tumor margin and center predicted response to pembrolizumab (anti-PD-1 antibody) treatment [37]. High mutational load and/or expression of neo-antigens alone does not seem to fully predict response to ICB, and others have shown that expression of other antigens such as cancer testis antigens and tumor associated (overexpressed) antigens may also contribute to tumor immuno-genicity [38]. These data demonstrate that endogenous immune reactivity characterized by cytolytic T cells in the tumor constitutes a basic requirement for ICB efficacy.

Another major reason for primary ICB resistance is the immune-privileged tumor micro-environment, characterized by the paucity of infiltrating tumor-specific T cells. The existence of this so-called 'non-inflamed' tumor derives from the inadequate generation or recruitment of tumor-specific T cells, or the physical inability of immune cells to reach the tumor. In order to induce a functional immune response, innate immune recognition and subsequent priming of tumor-antigen specific T cells in the lymph node is imperative [39,40]. Interrogation of the the TCGA database by Gajewski and colleagues to identify factors associated with a T-cell inflamed tumor phenotype failed to detect an association between a T-cell inflamed tumor and mutational burden [41]. However, they did find strong positive correlations between T-cell infiltration and presence of DC-related genes emphasizing the importance of DC-mediated anti-tumor immunity over solely tumor antigenicity. In accordance with these data, others have found intratumoral DCs to be critical for establishing tumor immunity, with tumors being capable of actively subverting DC-accumulation or function *in vivo* [42]. One such cause of immune ignorance that could be at play is a mutated b-catenin/Wnt-signaling pathway in tumor cells, which causes a decrease in chemokines known to be crucial for DC-homing to the tumor [43]. Such mutations could present a significant downside to having a high mutational burden, and could provide an explanation for the heterogeneity observed in ICB efficacy in high mutation tumors [41]. Interestingly, other mutations in key oncogenic pathways are currently being identified that impede immune cell-infiltration and/or function in the tumor (*e.g.* mutations in PTEN, MYC etc.) [44,45]. Re-establishing immune surveillance by skewing myeloid precursors to the DC-fate, targeting oncogenic pathways or promoting DC-function may be essential in sensitizing patients to ICB.

Moreover, the amount of intratumoral T effector cells could determine the potential of ICB therapy to induce robust anti-tumor response. T effector cells can be mechanically excluded by a physical barrier consisting of thick extracellular matrix produced by stromal cells (*e.g.* CAFs) [46]. CAFs can also exclude T cells through coating of cancer cells with CXC chemokine ligand-12 (CXCL12) [47]. Furthermore, the abnormal vasculature in the TME expressing high endothelial Fas-ligand promotes intravascular T cell apoptosis [48]. In addition, effector T cells will need to express the proper integrins in order to bind to the tumor endothelium, egress and exert their function. Changing the route of vaccination was shown to modulate integrin expression on T cells and improve homing to the tumor tissue [49].

Finally, immune resistance can also be achieved by the preferred attraction of immune inhibitory cells to the TME. Tregs, tumor associated macrophages (TAMs) and myeloid derived suppressor cells (MDSCs) often populate the TME where they exert several immune inhibitory properties, making it difficult for T cells to sustain their anti-tumor effector responses, especially in the setting of ICB [50].

Tumors can recruit, induce and expand Tregs capable of suppressing (ICB-induced) anti-tumor T cells via competition for key survival factors (CD80/86 co-stimulatory signals, IL-2) and suppressive cytokines (*e.g.* IL-10, TGF- $\beta$ , IL-35). As Tregs are much more potent in binding these survival factors by means of constitutive CTLA-4 and IL-2-receptor (CD25) expression, CD8+ T cells are shortly outcompeted. Tregs were found to be involved in limiting  $\alpha$ PD-1-efficacy as depletion of these cells improved responses to therapy in several solid tumor mouse models [51].

TAMs contribute to a majority cancer hallmarks including neo-angiogenesis, metastasis, chronic inflammation and immune suppression [52]. Skewing or depleting TAMs could therefore affect multiple critical steps in oncogenesis and abrogate different modes of immune resistance [53]. TAMs display an alternatively activated 'M2'-phenotype known to be critical in controlling tissue homeostasis and wound healing [52]. In the tumor, however, this phenotype is undesirable as it enables potent T-cell inhibition via cytokines (*e.g.* IL-10), depletion of key metabolites (expression of arginase, IDO) or by contact inhibition (*e.g.* via PD-L1) [52]. This TAM-phenotype is also critical in determining ICB efficacy as an innate 'wound healing' and immune suppressive gene signature was found to optimally predict non-responders prior to  $\alpha$ PD-1 treatment [54]. Recently, Arlauckas *et al.* identified another mechanism whereby TAMs can limit  $\alpha$ PD-1 therapy efficacy. They found TAMs to capture PD-1 targeting antibodies on the T-cell surface thereby considerably limiting the duration of drug efficacy [55].

Similar to TAMs, MDSCs can potently inhibit T-cell function but they can also indirectly contribute to an immune suppressive TME by differentiating into TAMs or skewing them to an M2-phenotype [56]. MDSCs are the epitome of chronic and systemic immune modulation by a tumor that secretes numerous molecules capable of skewing myelopoiesis (*e.g.* GM-CSF, IL-6, VEGF etc.) [56].

The presence of these immune inhibitory cells in most patients tumors suggests that a balance exists whereby ICB-responsive anti-tumor T cells are in equilibrium with immune suppressive

cells in the TME [57]. In line with this hypothesis is data from  $\alpha$ PD-1 and  $\alpha$ CTLA-4-treated patients tumors showing increased presence of memory T cell- and (activated) DC gene signatures in ICB responders, in contrast to MDSC, Treg and monocyte signatures in the non-responding patients [58]. Findings ways to shift this balance preferably from both sides will be key in improving ICB responsiveness.

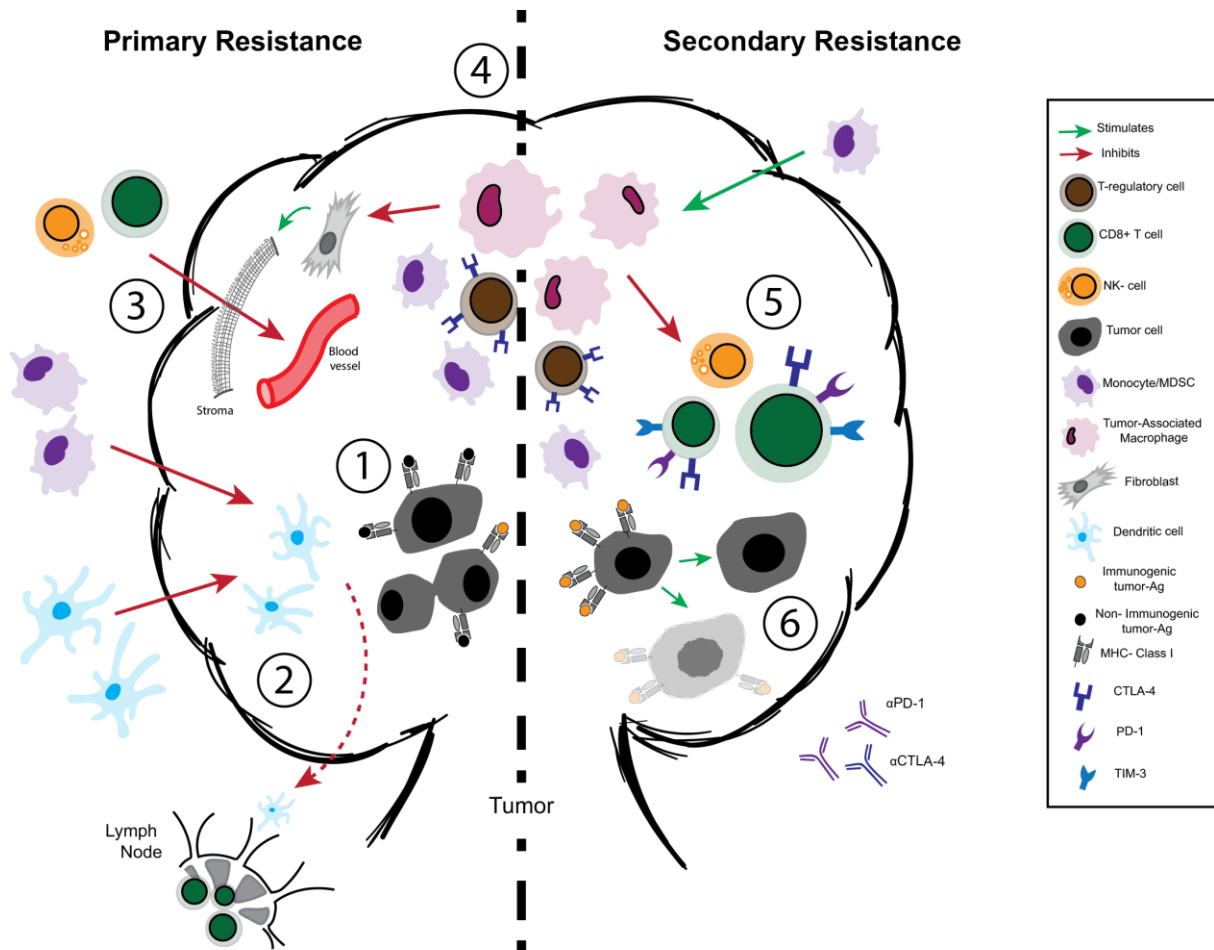


**Figure 2.** Different processes underlying primary and/or secondary resistance to checkpoint blocking antibodies in solid tumors; Primary resistance can result from the absence of a functional immune response to a poorly immunogenic tumor. The magnitude of resistance is influenced by differences in: (1) non-synonymous mutational load and neo-antigen expression, (2) the presence of intratumoral dendritic cells capable of antigen trafficking and presentation, (3) the generation or recruitment of tumor-specific T cells and (4) immune inhibition by inhibitory immune cell populations in the TME. Continuous therapeutic pressure may result in the development of secondary (acquired) resistance. Mechanisms include (5) upregulation of other co-inhibitory molecules and (6) loss of tumor (neo)antigen expression.

### *Secondary ICB resistance*

Over time, relapse will occur in a majority of patients initially responsive to ICB therapy. A possible phenomenon underlying secondary resistance are new mutations acquired by tumor cells that have expanded under continuous therapeutic pressure (immune editing) and have eventually grown out (immune evasion) (Fig. 2).

Tumor intrinsic mutations that have evolved over the course of ICB-treatment can have highly variable consequences to tumor-immune interactions. It has been known for several years that loss of antigen display by tumor cells due to mutations in the antigen-processing machinery (*e.g.* TAP) or proteins involved in antigen presentation (β2-microglobulin, HLA) can cause lack of recognition by CD8+ T cells following immunotherapy [59]. Recently, similar mutations were detected in patients who relapsed following αPD-1 ICB [60]. Another pathway that can be silenced by mutations following ICB is the interferon-gamma receptor (IFNGR) pathway, consisting of the IFNGR, JAK1/JAK2 and STAT1 which promotes transcription of interferon-induced genes [61]. The cytokine IFN-γ is known to have dichotomous immunological properties by inducing apoptosis of tumor cells, blood vessel disruption and upregulation of MHC-expression on the one hand, but expression of IDO, PD-L1 and other co-inhibitory markers on the other hand [61–64]. These co-inhibitory molecules including LAG-3 and TIM-3 synergize with CTLA-4 and PD-1 in promoting T-cell exhaustion [65,66] and are known to be upregulated following initiation of ICB therapy [67]. Inactivating mutations in the IFNGR-pathway have been documented in patients and are hypothesized to occur in settings of checkpoint blockade which leaves tumors cells exposed only to the anti-tumor properties of IFN-γ, causing selective pressure [60,63]. Paradoxically, chronic exposure to interferons including IFN-γ was found to also induce immune resistance due to PD-L1-dependent and independent mechanisms [64]. This may occur in settings of chronic (ICB-induced) inflammation where the pro-tumor functions of IFNs prevail over the anti-tumor ones, leading to immune resistance.

Besides specific mutations in immune-related pathways, tumors may lose neo-antigens and thereby escape immune control. In two melanoma patients, immunogenic neo-antigens were lost during tumor progression indicating immune-editing [68]. Immune editing was also reported in NSCLC patients whose lesion(s) initially responded to PD-1-inhibition but later progressed. The relapsed tumors were devoid of several mutations encoding for neo-antigens that were present prior to treatment [69].

## **THERAPEUTIC INTERVENTIONS AIMED AT (RE-)SENSITIZING TUMORS TO ICB**

Increasing the response rates to ICB will require rational combinations of conventional anti-cancer therapies and other immunotherapies on a per patient basis to optimally prime the tumor for ICBs to have effect. As many of these therapies act by alleviating both primary and secondary forms of immune resistance they shall be addressed per individual class of therapy (Fig. 3).

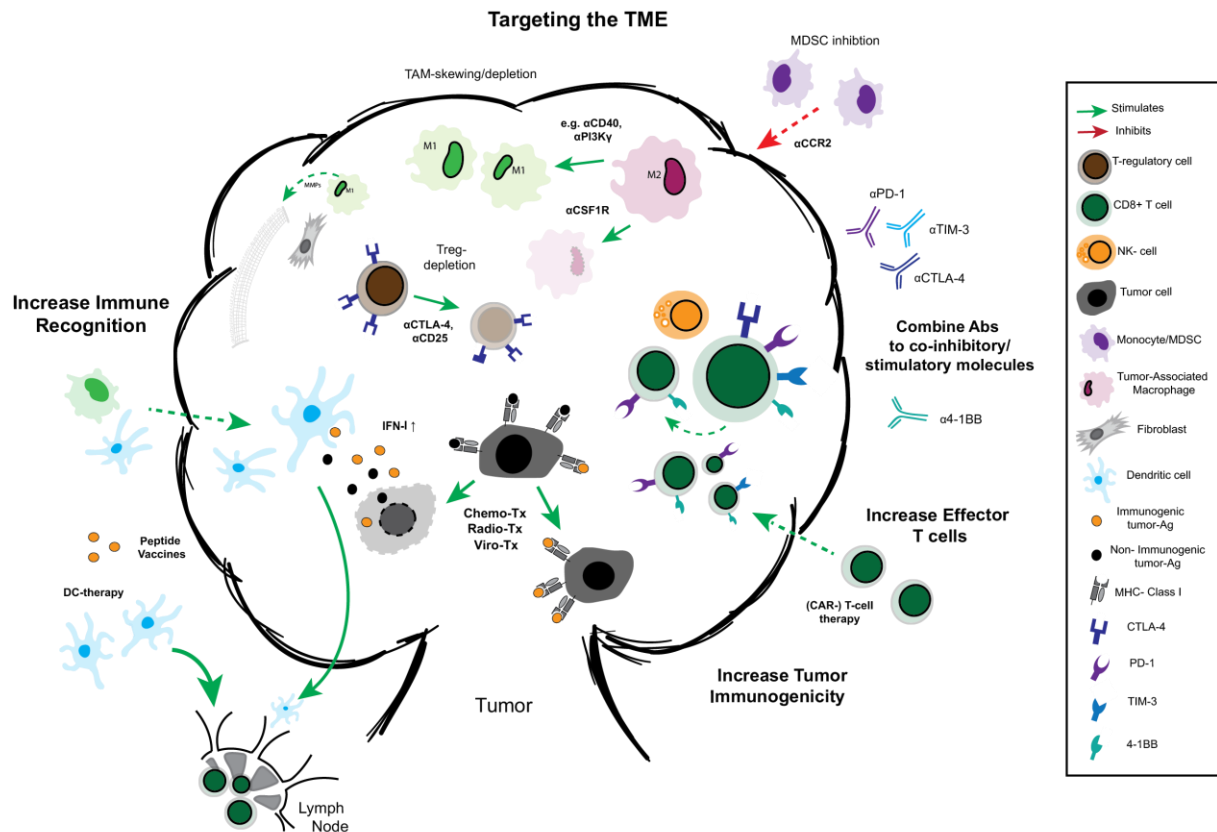


**Figure 3.** Therapeutic options to target immune resistance; sensitizing tumors to checkpoint blockade therapy can be achieved by increasing immune recognition, targeting the TME to remove immune suppression, combining antibodies to co-inhibitory/stimulatory molecules on T cells, increasing effector T cells and by increasing tumor immunogenicity.

#### *Modulating the T cell: novel immune checkpoints involving co-inhibition/co-stimulation*

Following the discovery of PD-1 and CTLA-4, numerous other co-inhibitory molecules on the T-cell surface have been characterized and shown to contribute to T-cell exhaustion [5]. It could therefore be beneficial or even necessary to target multiple inhibitory molecules at the same time to attempt reversal of exhaustion [70]. It should be noted, however, that T-cell dysfunction in cancer is a multifactorial process depending on many factors besides co-inhibitory receptor signaling [5]. Moreover, co-expression of multiple inhibitory molecules besides PD-1, including LAG-3 and TIM-3 indicates a state of ‘hyperexhaustion’ that is not recoverable by ICB-treatment [71]. Upregulation of co-inhibitory molecules has been shown to occur in mice and humans following PD-1-inhibition (TIM-3, LAG-3) [67] and in case of anti-CTLA-4-treatment (VISTA, PD-L1) [72]. These findings provide a clinical incentive to combine different ICB-therapies to potentially sensitize tumors previously thought to be ICB-resistant (e.g. prostate cancer). Paradoxically, dysfunctional T cells in the TME are known to express co-stimulatory receptors simultaneously with co-inhibitory molecules such as 4-1BB (CD137), ICOS and OX40, suggesting a possible balance that can be therapeutically exploited [72,73]. Preliminary data from pre-clinical mouse models indeed show benefit of combining agonistic antibodies to co-stimulatory

molecules with antagonistic antibodies targeting co-inhibitory molecules [73,74]. It may therefore be beneficial to ‘push the pedal’ by targeting co-stimulatory molecules on the hand, and ‘release the brakes’ using co-inhibitory checkpoint blocking antibodies on the other hand to fully exploit T-cell effector function.

*Chemotherapy, radiotherapy and oncolytic viruses: aiming to re-establish anti-tumor immunity*

Many conventional anti-cancer therapies such as chemo and radiotherapy, including oncolytic viral therapy was previously thought to principally act by arresting tumor cell proliferation and causing cell death. However, novel insights have led to a change in paradigm where many of these ‘traditional’ anti-cancer treatment strategies are now appreciated to function at least partially by modulating the immune system [75,76]. As mentioned before, a major contributor to primary ICB-resistance is lack of functional DCs in the tumor capable of priming T cells in lymphoid organs. Both radiotherapy and certain classes of chemotherapy, but also several oncolytic viruses are capable of causing immunogenic cell death (ICD) which increases antigen availability to dendritic cells in the TME [76]. Besides releasing antigens, tumors cells release damage associated molecular patterns (DAMPs) that are capable of attracting and stimulating innate immune cells to subsequently phagocytose cellular debris and present antigen to tumor-specific T cells [75–78]. A thorough appraisal of the various immune modulating functions of the different classes of chemotherapy, and to a lesser extend radiotherapies, is beyond the scope of this review. However, it is important to note that even drugs within the same class of chemotherapies *e.g.* oxaliplatin and cisplatin, may have different effects on the immune system, be it ICD or enhanced expression of co-stimulatory markers on APCs, respectively [77,79].

Chemo and radiotherapy have also been shown to upregulate type I interferons in the tumor microenvironment, thereby attracting T cells by increased chemokine production in case of anthracyclines [80], or by activating dendritic cells critical for adaptive immune induction [81]. Therapy elicited type I interferons can also improve responses in the setting of secondary ICB resistance where MHC-molecules on the tumor cell surface are downregulated, but can be potently re-expressed when exposed to type I interferon [82]. Reinstating immunity following primary or secondary immune resistance by conventional therapies has been shown to (re-)sensitize tumors to ICB therapy [83,84]. In a study by Twyman-Saint Victor *et al.*, melanoma patients received radiation on one index lesion followed by systemic CTLA-4-blocking antibodies. Besides a few responses including one patient with abscopal responses (regression of unirradiated distant tumors), the majority of patients progressed [10]. They went on further to show that upregulation of PD-L1 on the tumor following radio-immunotherapy significantly abrogated effective immune responses, which could be reversed by administering PD-1-inhibiting antibodies. Similar phenomena also occur in the setting of oncolytic viral therapy where virus treatment is able to inflame immunologically silent tumors and upregulate immune checkpoints that could be targeted by ICB [85,86]. It has to be noted that several studies have also reported negative effects of radiotherapy on anti-tumor immunity including the increase of immune suppressing cells in the TME (Tregs, MDSCs and TAMs) [75]. Also, in patients



receiving radiotherapy, immune monitoring of blood showed increased myeloid cell and decreased lymphoid cell counts and immune reactivity following radiotherapy in contrast to standard chemotherapy [87,88]. Some of these discrepancies may be caused by opposing biological pathways underlying different radiation regimens as was recently reported by Demaria *et al.*, showing that multiple low-dose irradiation cycles synergized with  $\alpha$ CTLA-4 antibodies in contrast to one single higher dose of radiotherapy in pre-clinical tumor models. Lower doses of radiation induced local type I IFN-production and concomitant recruitment of DCs, whereas high dose irradiation activated a cytosolic DNA-degradation pathway, preventing immune induction [89]. Novel mechanisms underlying these divergent effects of radiotherapy will have to be addressed and may involve modification of the treatment schedule and dose (fractionated or high dose) and the requirement for future combination strategies (*e.g.* TME targeted depletion, ICB).

*Cytoreduction by surgery: an (neo-)adjuvant role for ICB in treating locally advanced disease?*

The addition of immunotherapy to conventional cytoreductive surgery may improve patient survival by extending recurrence free survival following (incomplete) tumor resection. From an immunological perspective, the major advantage of surgery is the reduction of tumor and associated antigen load. Chronic antigen exposure is known to be a main contributor to exhaustion of effector T cells and occurs already early in tumorigenesis [90]. The persistence of T-cell exhaustion could eventually lead to the irreversibility to reinvigorate T-cell function with ICB therapy [71,90]. Moreover, increased tumor size correlates with extended immune suppression [91], suggesting that manually reducing tumor size could alleviate immune inhibition and T-cell exhaustion. Whether ICB should be administered in an adjuvant or neo-adjuvant setting has been recently investigated in murine breast cancer models. In these models Liu *et al.* showed superiority of neo-adjuvant anti-PD-1 therapy over adjuvant treatment in the context of surgery [92]. Mice treated with neo-adjuvant ICB had significantly longer recurrence free survival due to higher frequencies of circulating tumor-specific memory T cells capable of surveying the body for micro-metastasis [92]. The reported immune response kinetics resemble what is observed in the setting of acute infection, where a decrease in antigen load following clearance of the pathogen supports induction of a proper memory T-cell pool [93]. Furthermore, recent insights into biomarkers associated with response to  $\alpha$ PD-1 therapy have implicated elevated CD8<sup>+</sup> PD1<sup>+</sup> T-cell proliferation in a setting of low tumor load to be predictive of response [94]. It is possible that in the future, surgery may fulfil a pivotal role in establishing such a setting in the case of extensive tumor burden. However, it should be noted that surgery may also induce the influx of immunosuppressive cells abrogating T-cell function as part of a systemic 'wound healing response' [95] (De Goeje, Aerts, unpublished results).

*Immunotherapy: passive and active immunization approaches to induce novel immune responses*

Primary immune resistance to ICB can result from the inability or lack of endogenous DCs capable of priming anti-tumor T cells (non-inflamed tumor) or the presence of tumor infiltrating T cells that are either irreversibly exhausted or not specific for tumor-antigens [21,71]. In these cases, novel immune responses need to be induced that in time can be further enhanced by checkpoint blockade.

Tumor vaccines enable induction of novel immune responses or reinstate pre-existing immune responses towards a specific or wide array of tumor antigens formulated in the vaccine [1]. Although cancer vaccines offer significant advantages including high specificity, a favorable safety profile, of-the-shelf applicability and the premise of life-long anti-tumor immunity, clinical efficacy is often limited in overt cancer [2]. Several studies have highlighted the importance and power of neo-antigen specific immune responses in establishing tumor control [30,96]. Exploiting novel tools from the field of cancer immunogenomics enables the characterization of immunogenic neo-antigens that can be subsequently produced and incorporated into personalized vaccines [97,98]. Several trials are underway investigating the safety and clinical efficacy of these personalized vaccines [97].

Besides peptide vaccines, it is possible to circumvent endogenous antigen presentation and expose *in vitro* cultured autologous dendritic cells to tumor antigens and stimuli [99]. This form of immunotherapy called DC-therapy was found to be safe, capable of inducing anti-tumor immune responses and effective in a subgroup of advanced cancer patients [2,100]. Additionally, DC-immunotherapy was shown to induce epitope spreading, eliciting novel T-cell responses specific to antigens not formulated in the vaccine, and capable of inducing both CD8+ and CD4+ T-cell responses *in vivo* [101]. Both forms of active immunization were found to synergize with checkpoint blockade therapy in pre-clinical tumor models, possibly by eliciting a new pool of T cells that is susceptible to re-invigoration in a (PD-L1 high) tumor [102,103]. In case of tumors lacking a functional antigen-presentation pathway (mutations in TAP, low MHC-I; secondary immune resistance), it may be possible in the future to vaccinate with TEIPPs (T cell epitopes associated with impaired peptide processing), as these antigens are selectively presented in settings of abnormal antigen processing such as cancer [104].

Instead of actively inducing endogenous anti-tumor T-cell responses using (DC-)vaccines, one can directly infuse large numbers of tumor antigen-specific T cells derived from resected tumor tissue (TIL-therapy) or from PBMCs following genetic modification TCR-engineered or chimeric antigen receptor (CAR) T-cell therapy [105]. These forms of therapy are currently revolutionizing the field of hemato-oncology with the implementation of CD19-specific T cells, and have yielded anecdotal results in solid tumors [106]. However, as the majority of cancer patients are not eligible for TIL-therapy, and safe and effective targets for engineered T cells are still lacking as well as the challenges in T-cell penetration and persistence for most solid tumors, T-cell therapy still has a long road ahead.

*Targeting key players of the tumor microenvironment – making an example of TAMs*

We recently identified TAMs to be critically involved in determining the exhaustion status of vaccine-induced T cells, as tumor infiltrating T cells expressed lower levels of the co-inhibitory molecules PD-1, LAG-3 and TIM-3 following M-CSFRi-mediated TAM-depletion [127]. As this PD-1 low/intermediate expressing phenotype is particularly sensitive to re-invigoration by PD-1-blocking antibodies [71], M-CSFR-inhibition enhanced the efficacy of ICB in mouse models of pancreatic cancer [107].

Besides depleting TAMs (*e.g.* by targeting the M-CSF-receptor or homing receptors such as CCR2), skewing of TAMs to a more pro-inflammatory 'M1' phenotype may be even more efficacious in inducing tumor regression. Skewing of TAMs by CD40-agonistic antibodies was shown to result in loss of desmoplasia and induction of tumor regression in combination with gemcitabine in pancreatic cancer patients and pre-clinical models of PDAC [108,109]. Similar observations were made following pharmacological inhibition of PI3K in multiple tumor models, where PI3K was identified as a key molecular switch governing the M2-macrophage phenotype [110,111]. Skewing of TAMs could therefore ameliorate primary immune resistance caused by mechanical obstruction of T-cell infiltration by the collagen-rich stroma [112]. In support of this are the markedly increased T-cell numbers in tumors treated with PI3K-inhibition or CD40-agonistic antibodies [111,113]. Importantly, resistance to ICB in pre-clinical models could be overcome by combination with both TAM-skewing compounds, highlighting the role of myeloid cells in perturbing anti-tumor immunity and ICB-efficacy [114,115]. As PD-1 is thought to act primarily on T cells at the effector site, it is tempting to speculate whether skewing of TAMs to a M1-phenotype could provide B7-costimulatory molecules capable of binding CD28 on T cells in the tumor. As PD-1-blockade could enable proper signaling through the CD28-B7-axis, this could provide another explanation for the observed synergy between these different forms of immunotherapy.

The composition of the TME varies extensively between different tumor types, requiring tailored approaches to target specific immune populations [116]. Besides TAMs, other myeloid cells such as neutrophils, MDSCs and tolerogenic DCs but also regulatory T cells can pose significant obstacles to the generation of effective anti-tumor immunity. In line with TAM-targeting therapies, strategies aimed at depleting MDSCs (*e.g.* anti-CXCR2 or CCR2 antibodies, multikinase inhibitors *e.g.* cabozantinib) [117–119] or Tregs (Fc-optimized aCD25-antibodies) [120] all synergize with ICB-therapies.

## **A PERSONALIZED MEDICINE APPROACH TO OPTIMALLY STRATIFY AND TREAT CANCER PATIENTS WITH ICB**

At present, the identification of predictive factors determining the response to ICB treatment has remained difficult. Extensively reviewed biomarkers such as PD-L1 on tumor and myeloid cells have failed to deliver robust results across multiple cancers [121]. Similar to PD-L1, tumor

mutational load has been found to contribute to ICB-response but its discriminative value remains insufficient [41]. A more holistic and complete characterization of the tumor and its TME will likely improve the accuracy of current predictive markers [58]. This may include assessing the presence of a CD8+ T-cell infiltrate in combination with the PD-L1 status of a tumor to further delineate whether a tumor might be sensitive to ICB or that other therapies are required to prime the immune system first [122].

Assessing primary immune resistance can be achieved by employing novel tools in immunogenomics including next-generation sequencing on baseline tumor samples [98]. Using genome-wide approaches or eventually specified sets of genes corresponding to specific resistance modules, it will be possible to determine both the tumor antigen- and immunological landscape of tumors [36]. Recently discovered multiplex immunohistochemistry tools will offer localization of certain cell types on often already available paraffin embedded tissue to further aid patient stratification [123]. Elegantly, optimized pipelines designed to predict neo-epitopes using the aforementioned techniques offer the opportunity for personalized immunotherapy using vaccines and TCR-modified/CAR-T-cell approaches [97].

In contrast to primary tumor tissue which is readily available upon disease diagnosis, samples acquired during and after ICB treatment are often difficult to obtain, thereby limiting monitoring of treatment over time. As several groups have demonstrated the predictive value of tumor tissue early during course of treatment [124,125] it will be challenging to find more non-invasive biomarkers that can guide immunotherapy. Attempts have been made to define such markers in peripheral blood of patients yielding promising results by characterizing proliferating PD-1+ CD8+ T cells following  $\alpha$ PD-1 treatment [94,126]. Extending the scope to other circulating immune cells such as myeloid cells could further improve the sensitivity of these analysis.

## CONCLUSION

A recent appreciation of the role our immune system plays in tumors has led to the widespread implementation of immune modulating drugs such as ICBs for the treatment of advanced cancer; with unprecedented clinical success. However, as the majority of patients fails to demonstrate durable responses, rational combinations of conventional and novel anti-cancer therapies will need to be employed on an individualized basis to ensure the best possible responses.

## REFERENCES

- [1] S.H. van der Burg, R. Arens, F. Ossendorp, T. van Hall, C.J. Melief, Vaccines for established cancer: overcoming the challenges posed by immune evasion, *Nat. Rev. Cancer* 16 (2016) 219–233.
- [2] F. Dammeijer, L.A. Lievense, G.D. Veerman, H.C. Hoogsteden, J.P. Hegmans, L. R. Arends, et al., Efficacy of tumor vaccines and cellular immunotherapies in non-small-cell lung cancer: a systematic review and meta-analysis, *J. Clin. Oncol.* 34 (2016) 3204–3212.
- [3] M.A. Postow, M.K. Callahan, J.D. Wolchok, Immune checkpoint blockade in cancer therapy, *J. Clin. Oncol.* 33 (2015) 1974–1982.
- [4] S.L. Topalian, C.G. Drake, D.M. Pardoll, Immune checkpoint blockade: a common denominator approach to cancer therapy, *Cancer Cell* 27 (2015) 450–461.
- [5] E.J. Wherry, M. Kurachi, Molecular and cellular insights into T cell exhaustion, *Nat. Rev. Immunol.* 15 (2015) 486–499.
- [6] T.L. Walunas, D.J. Lenschow, C.Y. Bakker, P.S. Linsley, G.J. Freeman, J.M. Green, et al., CTLA-4 can function as a negative regulator of T cell activation, *Immunity* 1 (1994) 405–413.
- [7] M.F. Krummel, J.P. Allison, CD28 and CTLA-4 have opposing effects on the response of T cells to stimulation, *J. Exp. Med.* 182 (1995) 459–465.
- [8] K. Wing, Y. Onishi, P. Prieto-Martin, T. Yamaguchi, M. Miyara, Z. Fehervari, et al., CTLA-4 control over Foxp3+ regulatory T cell function, *Science* 322 (2008) 271–275.
- [9] T.R. Simpson, F. Li, W. Montalvo-Ortiz, M.A. Sepulveda, K. Bergerhoff, F. Arce, et al., Fc-dependent depletion of tumor-infiltrating regulatory T cells co- defines the efficacy of anti-CTLA-4 therapy against melanoma, *J. Exp. Med.* 210 (2013) 1695–1710.
- [10] C. Twyman-Saint Victor, A.J. Rech, A. Maity, R. Rengan, K.E. Pauken, E. Stelekati, et al., Radiation and dual checkpoint blockade activate non-redundant immune mechanisms in cancer, *Nature* 520 (2015) 373–377.
- [11] D.M. Pardoll, The blockade of immune checkpoints in cancer immunotherapy, *Nat. Rev. Cancer* 12 (2012) 252–264.
- [12] W. Zou, J.D. Wolchok, L. Chen, PD-L1 (B7-H1) and PD-1 pathway blockade for cancer therapy: mechanisms, response biomarkers, and combinations, *Sci. Transl. Med.* 8 (2016) 328rv4.
- [13] J. Lau, J. Cheung, A. Navarro, S. Lianoglou, B. Haley, K. Totpal, et al., Tumour and host cell PD-L1 is required to mediate suppression of anti-tumour immunity in mice, *Nat. Commun.* 8 (2017) 14572.
- [14] E. Hui, J. Cheung, J. Zhu, X. Su, M.J. Taylor, H.A. Wallweber, et al., T cell costimulatory receptor CD28 is a primary target for PD-1-mediated inhibition, *Science* 355 (2017) 1428–1433.
- [15] A.O. Kamphorst, A. Wieland, T. Nasti, S. Yang, R. Zhang, D.L. Barber, et al., Rescue of exhausted CD8 T cells by PD-1-targeted therapies is CD28- dependent, *Science* 355 (2017) 1423–1427.
- [16] F.S. Hodi, S.J. O’Day, D.F. McDermott, R.W. Weber, J.A. Sosman, J.B. Haanen, et al., Improved survival with ipilimumab in patients with metastatic melanoma, *N. Engl. J. Med.* 363 (2010) 711–723.
- [17] J.D. Wolchok, B. Neyns, G. Linette, S. Negrier, J. Lutzky, L. Thomas, et al., Ipilimumab monotherapy in patients with pretreated advanced melanoma: a randomised, double-blind, multicentre, phase 2, dose-ranging study, *Lancet Oncol.* 11 (2010) 155–164.
- [18] C. Robert, J. Schachter, G.V. Long, A. Arance, J.J. Grob, L. Mortier, et al., Pembrolizumab versus ipilimumab in advanced melanoma, *N. Engl. J. Med.* 372 (2015) 2521–2532.
- [19] C. Robert, G.V. Long, B. Brady, C. Dutriaux, M. Maio, L. Mortier, et al., Nivolumab in previously untreated melanoma without BRAF mutation, *N. Engl. J. Med.* 372 (2015) 320–330.
- [20] L.A. Lievense, D.H. Sterman, R. Cornelissen, J.G. Aerts, Checkpoint blockade in lung cancer and mesothelioma, *Am. J. Respir. Crit. Care Med.* (2017) epub ahead of print.
- [21] P. Sharma, S. Hu-Lieskovan, J.A. Wargo, A. Ribas, Primary, adaptive, and acquired resistance to cancer immunotherapy, *Cell* 168 (2017) 707–723.
- [22] J. Larkin, V. Chiarion-Sileni, R. Gonzalez, J.J. Grob, C.L. Cowey, C.D. Lao, et al., Combined nivolumab and ipilimumab or monotherapy in untreated melanoma, *N. Engl. J. Med.* 373 (2015) 23–34.

- [23] J. Larkin, R. Gonzalez, P. Rutkowski, J. Grob, C.L. Cowey, C.D. Lao, et al., Overall survival (OS) results from a phase III trial of nivolumab (NIVO) combined with ipilimumab (IPI) in treatment-naïve patients with advanced melanoma (CheckMate 067), AACR (2017) Abstract nr CT075.
- [24] J. Brahmer, K.L. Reckamp, P. Baas, L. Crino, W.E. Eberhardt, E. Poddubskaya, et al., Nivolumab versus docetaxel in advanced squamous-cell non-small-cell lung cancer, *N. Engl. J. Med.* 373 (2015) 123–135.
- [25] H. Borghaei, L. Paz-Ares, L. Horn, D.R. Spigel, M. Steins, N.E. Ready, et al., Nivolumab versus docetaxel in advanced nonsquamous non-small-cell lung cancer, *N. Engl. J. Med.* 373 (2015) 1627–1639.
- [26] E.B. Garon, N.A. Rizvi, R. Hui, N. Leighl, A.S. Balmanoukian, J.P. Eder, et al., Pembrolizumab for the treatment of non-small-cell lung cancer, *N. Engl. J. Med.* 372 (2015) 2018–2028.
- [27] R.J. Motzer, B. Escudier, D.F. McDermott, S. George, H.J. Hammers, S. Srinivas, et al., Nivolumab versus everolimus in advanced renal-cell carcinoma, *N. Engl. J. Med.* 373 (2015) 1803–1813.
- [28] R.J. Motzer, B.I. Rini, D.F. McDermott, B.G. Redman, T.M. Kuzel, M.R. Harrison, et al., Nivolumab for metastatic renal cell carcinoma: results of a randomized phase II trial, *J. Clin. Oncol.* 33 (2015) 1430–1437.
- [29] J.E. Rosenberg, J. Hoffman-Censits, T. Powles, M.S. van der Heijden, A.V. Balar, A. Necchi, et al., Atezolizumab in patients with locally advanced and metastatic urothelial carcinoma who have progressed following treatment with platinum-based chemotherapy: a single-arm, multicentre, phase 2 trial, *Lancet* 387 (2016) 1909–1920.
- [30] M.M. Gubin, X. Zhang, H. Schuster, E. Caron, J.P. Ward, T. Noguchi, et al., Checkpoint blockade cancer immunotherapy targets tumour-specific mutant antigens, *Nature* 515 (2014) 577–581.
- [31] N.A. Rizvi, M.D. Hellmann, A. Snyder, P. Kvistborg, V. Makarov, J.J. Havel, et al., Cancer immunology: mutational landscape determines sensitivity to PD-1 blockade in non-small cell lung cancer, *Science* 348 (2015) 124–128.
- [32] L.B. Alexandrov, S. Nik-Zainal, D.C. Wedge, S.A. Aparicio, S. Behjati, A.V. Biankin, et al., Signatures of mutational processes in human cancer, *Nature* 500 (2013) 415–421.
- [33] D.T. Le, J.N. Uram, H. Wang, B.R. Bartlett, H. Kemberling, A.D. Eyring, et al., PD-1 blockade in tumors with mismatch-repair deficiency, *N. Engl. J. Med.* 372 (2015) 2509–2520.
- [34] A. Snyder, V. Makarov, T. Merghoub, J. Yuan, J.M. Zaretsky, A. Desrichard, et al., Genetic basis for clinical response to CTLA-4 blockade in melanoma, *N. Engl. J. Med.* 371 (2014) 2189–2199.
- [35] E.M. Van Allen, D. Miao, B. Schilling, S.A. Shukla, C. Blank, L. Zimmer, et al., Genomic correlates of response to CTLA-4 blockade in metastatic melanoma, *Science* 350 (2015) 207–211.
- [36] M.S. Rooney, S.A. Shukla, C.J. Wu, G. Getz, N. Hacohen, Molecular and genetic properties of tumors associated with local immune cytolytic activity, *Cell* 160 (2015) 48–61.
- [37] P.C. Tumeh, C.L. Harview, J.H. Yearley, I.P. Shintaku, E.J. Taylor, L. Robert, et al., PD-1 blockade induces responses by inhibiting adaptive immune resistance, *Nature* 515 (2014) 568–571.
- [38] P.G. Coulie, B.J. Van den Eynde, P. van der Bruggen, T. Boon, Tumour antigens recognized by T lymphocytes: at the core of cancer immunotherapy, *Nat. Rev. Cancer* 14 (2014) 135–146.
- [39] K. Hildner, B.T. Edelson, W.E. Purtha, M. Diamond, H. Matsushita, M. Kohyama, et al., Batf3 deficiency reveals a critical role for CD8 $\alpha$ <sup>+</sup> dendritic cells in cytotoxic T cell immunity, *Science* 322 (2008) 1097–1100.
- [40] M.L. Broz, M. Binnewies, B. Boldajipour, A.E. Nelson, J.L. Pollack, D.J. Erle, et al., Dissecting the tumor myeloid compartment reveals rare activating antigen-presenting cells critical for T cell immunity, *Cancer Cell* 26 (2014) 638–652.
- [41] S. Spranger, J.J. Luke, R. Bao, Y. Zha, K.M. Hernandez, Y. Li, et al., Density of immunogenic antigens does not explain the presence or absence of the T-cell-inflamed tumor microenvironment in melanoma, *Proc. Natl. Acad. Sci. U. S. A.* 113 (2016) E7759–E7768.
- [42] A. Gardner, B. Ruffell, Dendritic cells and cancer immunity, *Trends Immunol.* 37 (2016) 855–865.
- [43] S. Spranger, R. Bao, T.F. Gajewski, Melanoma-intrinsic beta-catenin signalling prevents anti-tumour immunity, *Nature* 523 (2015) 231–235.
- [44] W. Peng, J.Q. Chen, C. Liu, S. Malu, C. Creasy, M.T. Tetzlaff, et al., Loss of PTEN promotes resistance to T cell-mediated immunotherapy, *Cancer Discov.* 6 (2016) 202–216.

- [45] S.C. Casey, L. Tong, Y. Li, R. Do, S. Walz, K.N. Fitzgerald, et al., MYC regulates the antitumor immune response through CD47 and PD-L1, *Science* 352 (2016) 227–231.
- [46] H. Salmon, K. Franciszkiewicz, D. Damotte, M.C. Dieu-Nosjean, P. Validire, A. Trautmann, et al., Matrix architecture defines the preferential localization and migration of T cells into the stroma of human lung tumors, *J. Clin. Invest.* 122 (2012) 899–910.
- [47] C. Feig, J.O. Jones, M. Kraman, R.J. Wells, A. Deonaraine, D.S. Chan, et al., Targeting CXCL12 from FAP-expressing carcinoma-associated fibroblasts synergizes with anti-PD-L1 immunotherapy in pancreatic cancer, *Proc. Natl. Acad. Sci. U. S. A.* 110 (2013) 20212–20217.
- [48] G.T. Motz, S.P. Santoro, L.P. Wang, T. Garrabrant, R.R. Lastra, I.S. Hagemann, et al., Tumor endothelium FasL establishes a selective immune barrier promoting tolerance in tumors, *Nat. Med.* 20 (2014) 607–615.
- [49] YY. Sun, S. Peng, L. Han, J. Qiu, L. Song, Y. Tsai, et al., Local HPV recombinant vaccinia boost following priming with an HPV DNA vaccine enhances local HPV-specific CD8<sup>+</sup> T-cell-mediated tumor control in the genital tract, *Clin. Cancer Res.* 22 (2016) 657–669.
- [50] J.A. Joyce, D.T. Fearon, T cell exclusion, immune privilege, and the tumor microenvironment, *Science* 348 (2015) 74–80. [51] S.F. Ngiew, A. Young, N. Jacquelot, T. Yamazaki, D. Enot, L. Zitvogel, et al., A threshold level of intratumor CD8<sup>+</sup> T-cell PD1 expression dictates therapeutic response to anti-PD1, *Cancer Res.* 75 (2015) 3800–3811.
- [52] R. Noy, J.W. Pollard, Tumor-associated macrophages: from mechanisms to therapy, *Immunity* 41 (2014) 49–61.
- [53] A. Mantovani, F. Marchesi, A. Malesci, L. Laghi, P. Allavena, Tumour-associated macrophages as treatment targets in oncology, *Nat. Rev. Clin. Oncol.* 14 (2017) 399–416.
- [54] W. Hugo, J.M. Zaretsky, L. Sun, C. Song, B.H. Moreno, S. Hu-Lieskovan, et al., Genomic and transcriptomic features of response to anti-PD-1 therapy in metastatic melanoma, *Cell* 165 (2016) 35–44.
- [55] S.P. Arlauckas, C.S. Garris, R.H. Kohler, M. Kitaoka, M.F. Cuccarese, K.S. Yang, et al., In vivo imaging reveals a tumor-associated macrophage-mediated resistance pathway in anti-PD-1 therapy, *Sci. Transl. Med.* (2017) 9.
- [56] S. Ugel, F. De Sanctis, S. Mandruzzato, V. Bronte, Tumor-induced myeloid deviation: when myeloid-derived suppressor cells meet tumor-associated macrophages, *J. Clin. Invest.* 125 (2015) 3365–3376.
- [57] A.K. Palucka, L.M. Coussens, The basis of oncoimmunology, *Cell* 164 (2016) 1233–1247.
- [58] P. Charoentong, F. Finotello, M. Angelova, C. Mayer, M. Efremova, D. Rieder, et al., Pan-cancer immunogenomic analyses reveal genotype-immunophenotype relationships and predictors of response to checkpoint blockade, *Cell Rep.* 18 (2017) 248–262.
- [59] N.P. Restifo, F.M. Marincola, Y. Kawakami, J. Taubenberger, J.R. Yannelli, S.A. Rosenberg, Loss of functional beta 2-microglobulin in metastatic melanomas from five patients receiving immunotherapy, *J. Natl. Cancer Inst.* 88 (1996) 100–108.
- [60] J.M. Zaretsky, A. Garcia-Diaz, D.S. Shin, H. Escuin-Ordinas, W. Hugo, S. Hu-Lieskovan, et al., Mutations associated with acquired resistance to PD-1 blockade in melanoma, *N. Engl. J. Med.* 375 (2016) 819–829.
- [61] H. Ikeda, L.J. Old, R.D. Schreiber, The roles of IFN gamma in protection against tumor development and cancer immunoediting, *Cytokine Growth Factor Rev.* 13 (2002) 95–109.
- [62] B.S. Parker, J. Rautela, P.J. Hertzog, Antitumour actions of interferons: implications for cancer therapy, *Nat. Rev. Cancer* 16 (2016) 131–144. [63] J. Gao, L.Z. Shi, H. Zhao, J. Chen, L. Xiong, Q. He, et al., Loss of IFN-gamma pathway genes in tumor cells as a mechanism of resistance to anti-CTLA-4 therapy, *Cell* 167 (2016) 397–404 (e9).
- [64] J.L. Benci, B. Xu, Y. Qiu, T.J. Wu, H. Dada, C. Twyman-Saint Victor, et al., Tumor interferon signaling regulates a multigenic resistance program to immune checkpoint blockade, *Cell* 167 (2016) 1540–1554 (e12).
- [65] S.D. Blackburn, H. Shin, W.N. Haining, T. Zou, C.J. Workman, A. Polley, et al., Coregulation of CD8<sup>+</sup> T cell exhaustion by multiple inhibitory receptors during chronic viral infection, *Nat. Immunol.* 10 (2009) 29–37.

- [66] S.R. Woo, M.E. Turnis, M.V. Goldberg, J. Bankoti, M. Selby, C.J. Nirschl, et al., Immune inhibitory molecules LAG-3 and PD-1 synergistically regulate T-cell function to promote tumoral immune escape, *Cancer Res.* 72 (2012) 917–927.
- [67] S. Koyama, E.A. Akbay, Y.Y. Li, G.S. Herter-Sprie, K.A. Buczkowski, W.G. Richards, et al., Adaptive resistance to therapeutic PD-1 blockade is associated with upregulation of alternative immune checkpoints, *Nat. Commun.* 7 (2016) 10501.
- [68] E.M. Verdegaal, N.F. de Miranda, M. Visser, T. Harryvan, M.M. van Buuren, R.S. Andersen, et al., Neoantigen landscape dynamics during human melanoma-T cell interactions, *Nature* 536 (2016) 91–95.
- [69] V. Anagnostou, K.N. Smith, P.M. Forde, N. Niknafs, R. Bhattacharya, J. White, et al., Evolution of neoantigen landscape during immune checkpoint blockade in non-small cell lung cancer, *Cancer Discov.* 7 (2017) 264–276.
- [70] K.M. Mahoney, P.D. Rennert, G.J. Freeman, Combination cancer immunotherapy and new immunomodulatory targets, *Nat. Rev. Drug Discov.* 14 (2015) 561–584.
- [71] D.S. Chen, I. Mellman, Elements of cancer immunity and the cancer-immune set point, *Nature* 541 (2017) 321–330.
- [72] J. Gao, J.F. Ward, C.A. Pettaway, L.Z. Shi, S.K. Subudhi, L.M. Vence, et al., VISTA is an inhibitory immune checkpoint that is increased after ipilimumab therapy in patients with prostate cancer, *Nat. Med.* 23 (2017) 551–555.
- [73] J.B. Williams, B.L. Horton, Y. Zheng, Y. Duan, J.D. Powell, T.F. Gajewski, The EGR2 targets LAG-3 and 4-1BB describe and regulate dysfunctional antigen-specific CD8<sup>+</sup> T cells in the tumor microenvironment, *J. Exp. Med.* 214 (2017) 381–400.
- [74] A. Makkouk, C. Chester, H.E. Kohrt, Rationale for anti-CD137 cancer immunotherapy, *Eur. J. Cancer* 54 (2016) 112–119.
- [75] R.R. Weichselbaum, H. Liang, L. Deng, Y.X. Fu, Radiotherapy and immunotherapy: a beneficial liaison? *Nat. Rev. Clin. Oncol.* 14 (2017) 365–379.
- [76] L. Galluzzi, A. Buque, O. Kepp, L. Zitvogel, G. Kroemer, Immunological effects of conventional chemotherapy and targeted anticancer agents, *Cancer Cell* 28 (2015) 690–714.
- [77] E. Beyranvand Nejad, T.C. van der Sluis, S. van Duikeren, H. Yagita, G.M. Janssen, P.A. van Veelen, et al., Tumor eradication by cisplatin is sustained by CD80/86-mediated costimulation of CD8<sup>+</sup> T cells, *Cancer Res.* 76 (2016) 6017–6029.
- [78] C. Pfirschke, C. Engblom, S. Rickelt, V. Cortez-Retamozo, C. Garris, F. Pucci, et al., Immunogenic chemotherapy sensitizes tumors to checkpoint blockade therapy, *Immunity* 44 (2016) 343–354.
- [79] A. Tesniere, F. Schlemmer, V. Boige, O. Kepp, I. Martins, F. Ghiringhelli, et al., Immunogenic death of colon cancer cells treated with oxaliplatin, *Oncogene* 29 (2010) 482–491.
- [80] A. Sistigu, T. Yamazaki, E. Vacchelli, K. Chaba, D.P. Enot, J. Adam, et al., Cancer cell-autonomous contribution of type I interferon signaling to the efficacy of chemotherapy, *Nat. Med.* 20 (2014) 1301–1309.
- [81] L. Deng, H. Liang, M. Xu, X. Yang, B. Burnette, A. Arina, et al., STING-dependent cytosolic DNA sensing promotes radiation-induced type I interferon-dependent antitumor immunity in immunogenic tumors, *Immunity* 41 (2014) 843–852.
- [82] X. Wang, J.E. Schoenhals, A. Li, D.R. Valdecanas, H. Ye, F. Zang, et al., Suppression of type I IFN signaling in tumors mediates resistance to anti-PD-1 treatment that can be overcome by radiotherapy, *Cancer Res.* 77 (2017) 839–850.
- [83] L. Deng, H. Liang, B. Burnette, M. Beckett, T. Darga, R.R. Weichselbaum, et al., Irradiation and anti-PD-L1 treatment synergistically promote antitumor immunity in mice, *J. Clin. Invest.* 124 (2014) 687–695.
- [84] J. Peng, J. Hamanishi, N. Matsumura, K. Abiko, K. Murat, T. Baba, et al., Chemotherapy induces programmed cell death-ligand 1 overexpression via the nuclear factor-kappaB to Foster an immunosuppressive tumor microenvironment in ovarian cancer, *Cancer Res.* 75 (2015) 5034–5045.
- [85] D. Zamarin, R.B. Holmgard, S.K. Subudhi, J.S. Park, M. Mansour, P. Palese, et al., Localized oncolytic virotherapy overcomes systemic tumor resistance to immune checkpoint blockade immunotherapy, *Sci. Transl. Med.* 6 (2014) 226ra32.



- [86] Z. Liu, R. Ravindranathan, P. Kalinski, Z.S. Guo, D.L. Bartlett, Rational combination of oncolytic vaccinia virus and PD-L1 blockade works synergistically to enhance therapeutic efficacy, *Nat. Commun.* 8 (2017) 14754.
- [87] H. van Meir, R.A. Nout, M.J. Welters, N.M. Loof, M.L. de Kam, J.J. van Ham, et al., Impact of (chemo)radiotherapy on immune cell composition and function in cervical cancer patients, *Oncoimmunology* 6 (2017) e1267095.
- [88] M. Talebian Yazdi, M.S. Schinkelshoek, N.M. Loof, C. Taube, P.S. Hiemstra, M.J. Welters, et al., Standard radiotherapy but not chemotherapy impairs systemic immunity in non-small cell lung cancer, *Oncoimmunology* 5 (2016) e1255393.
- [89] C. Vanpouille-Box, A. Alard, M.J. Aryankalayil, Y. Sarfraz, J.M. Diamond, R.J. Schneider, DNA exonuclease Trex1 regulates radiotherapy-induced tumour immunogenicity, *Nat. Commun.* 8 (2017) 15618.
- [90] A. Schietinger, M. Philip, V.E. Krisnawan, E.Y. Chiu, J.J. Delrow, R.S. Basom, et al., Tumor-specific T cell dysfunction is a dynamic antigen-driven differentiation program initiated early during tumorigenesis, *Immunity* 45 (2016) 389–401.
- [91] D.F. Quail, J.A. Joyce, Microenvironmental regulation of tumor progression and metastasis, *Nat. Med.* 19 (2013) 1423–1437.
- [92] J. Liu, S.J. Blake, M.C. Yong, H. Harjunpaa, S.F. Ngiow, K. Takeda, et al., Improved efficacy of neoadjuvant compared to adjuvant immunotherapy to eradicate metastatic disease, *Cancer Discov.* 6 (2016) 1382–1399.
- [93] J.T. Harty, V.P. Badovinac, Shaping and reshaping CD8+ T-cell memory, *Nat. Rev. Immunol.* 8 (2008) 107–119.
- [94] A.C. Huang, M.A. Postow, R.J. Orlowski, R. Mick, B. Bengsch, S. Manne, et al., T-cell invigoration to tumour burden ratio associated with anti-PD-1 response, *Nature* 545 (2017) 60–65.
- [95] L. Yuan, B. Xu, H. Fan, P. Yuan, P. Zhao, Z. Suo, Pre- and post-operative evaluation: percentages of circulating myeloid-derived suppressor cells in rectal cancer patients, *Neoplasma* 62 (2015) 239–249.
- [96] N. McGranahan, A.J. Furness, R. Rosenthal, S. Ramskov, R. Lyngaa, S.K. Saini, et al., Clonal neoantigens elicit T cell immunoreactivity and sensitivity to immune checkpoint blockade, *Science* 351 (2016) 1463–1469.
- [97] M. Yarchoan, B.A. Johnson 3rd, E.R. Lutz, D.A. Laheru, E.M. Jaffee, Targeting neoantigens to augment antitumour immunity, *Nat. Rev. Cancer* 17 (2017) 209–222.
- [98] X.S. Liu, E.R. Mardis, Applications of immunogenomics to cancer, *Cell* 168 (2017) 600–612.
- [99] S. Anguille, E.L. Smits, E. Lion, V.F. van Tendeloo, Z.N. Berneman, Clinical use of dendritic cells for cancer therapy, *Lancet Oncol.* 15 (2014) e257–67.
- [100] R. Cornelissen, J.P. Hegmans, A.P. Maat, M.E. Kaijen-Lambers, K. Bezemer, R.W. Hendriks, et al., Extended tumor control after dendritic cell vaccination with low-dose cyclophosphamide as adjuvant treatment in patients with malignant pleural mesothelioma, *Am. J. Respir. Crit. Care Med.* 193 (2016) 1023–1031.
- [101] B.M. Carreno, V. Magrini, M. Becker-Hapak, S. Kaabinejadian, J. Hundal, A.A. Petti, et al., Cancer immunotherapy. A dendritic cell vaccine increases the breadth and diversity of melanoma neoantigen-specific T cells, *Science* 348 (2015) 803–808.
- [102] J. Fu, D.B. Kanne, M. Leong, L.H. Glickman, S.M. McWhirter, E. Lemmens, et al., STING agonist formulated cancer vaccines can cure established tumors resistant to PD-1 blockade, *Sci. Transl. Med.* 7 (2015) 283ra52.
- [103] J.P. Antonios, H. Soto, R.G. Everson, D. Moughon, J.R. Orpilla, N.P. Shin, et al., Immunosuppressive tumor-infiltrating myeloid cells mediate adaptive immune resistance via a PD-1/PD-L1 mechanism in glioblastoma, *Neuro Oncol.* 19 (2017) 796–807.
- [104] E.M. Doorduijn, M. Sluijter, B.J. Querido, C.C. Oliveira, A. Achour, F. Ossendorp, et al., TAP-independent self-peptides enhance T cell recognition of immune-escaped tumors, *J. Clin. Invest.* 126 (2016) 784–794.

- [105] S.A. Rosenberg, N.P. Restifo, Adoptive cell transfer as personalized immunotherapy for human cancer, *Science* 348 (2015) 62–68.
- [106] C.A. Klebanoff, S.A. Rosenberg, N.P. Restifo, Prospects for gene-engineered T cell immunotherapy for solid cancers, *Nat. Med.* 22 (2016) 26–36.
- [107] Y. Zhu, B.L. Knolhoff, M.A. Meyer, T.M. Nywening, B.L. West, J. Luo, et al., CSF1/CSF1R blockade reprograms tumor-infiltrating macrophages and improves response to T-cell checkpoint immunotherapy in pancreatic cancer models, *Cancer Res.* 74 (2014) 5057–5069.
- [108] G.L. Beatty, E.G. Chiorean, M.P. Fishman, B. Saboury, U.R. Teitelbaum, W. Sun, et al., CD40 agonists alter tumor stroma and show efficacy against pancreatic carcinoma in mice and humans, *Science* 331 (2011) 1612–1616.
- [109] K.B. Long, W.L. Gladney, G.M. Tooker, K. Graham, J.A. Fraietta, G.L. Beatty, IFN $\gamma$  and CCL2 cooperate to redirect tumor-infiltrating monocytes to degrade fibrosis and enhance chemotherapy efficacy in pancreatic carcinoma, *Cancer Discov.* 6 (2016) 400–413.
- [110] M.M. Kaneda, P. Cappello, A.V. Nguyen, N. Ralainirina, C.R. Hardamon, P. Foubert, et al., Macrophage PI3K $\gamma$  drives pancreatic ductal adenocarcinoma progression, *Cancer Discov.* 6 (2016) 870–885.
- [111] M.M. Kaneda, K.S. Messer, N. Ralainirina, H. Li, C.J. Leem, S. Gorjestani, et al., PI3K $\gamma$  is a molecular switch that controls immune suppression, *Nature* 539 (2016) 437–442.
- [112] E. Pure, A. Lo, Can targeting stroma pave the way to enhanced antitumor immunity and immunotherapy of solid tumors? *Cancer Immunol. Res.* 4 (2016) 269–278.
- [113] G.L. Beatty, R. Winograd, R.A. Evans, K.B. Long, S.L. Luque, J.W. Lee, et al., Exclusion of T cells from pancreatic carcinomas in mice is regulated by Ly6C (low) F4/80(+) extratumoral macrophages, *Gastroenterology* 149 (2015) 201–210.
- [114] O. De Henau, M. Rausch, D. Winkler, L.F. Campesato, C. Liu, D.H. Cymerman, et al., Overcoming resistance to checkpoint blockade therapy by targeting PI3K $\gamma$  in myeloid cells, *Nature* 539 (2016) 443–447.
- [115] R. Winograd, K.T. Byrne, R.A. Evans, P.M. Odorizzi, A.R. Meyer, D.L. Bajor, et al., Induction of T-cell immunity overcomes complete resistance to PD-1 and CTLA-4 blockade and improves survival in pancreatic carcinoma, *Cancer Immunol. Res.* 3 (2015) 399–411.
- [116] L.M. Coussens, L. Zitvogel, A.K. Palucka, Neutralizing tumor-promoting chronic inflammation: a magic bullet, *Science* 339 (2013) 286–291.
- [117] G. Wang, X. Lu, P. Dey, P. Deng, C.C. Wu, S. Jiang, et al., Targeting YAP-dependent MDSC infiltration impairs tumor progression, *Cancer Discov.* 6 (2016) 80–95.
- [118] X. Lu, J.W. Horner, E. Paul, X. Shang, P. Troncoso, P. Deng, et al., Effective combinatorial immunotherapy for castration-resistant prostate cancer, *Nature* 543 (2017) 728–732.
- [119] D.E. Sanford, B.A. Belt, R.Z. Panni, A. Mayer, A.D. Deshpande, D. Carpenter, et al., Inflammatory monocyte mobilization decreases patient survival in pancreatic cancer: a role for targeting the CCL2/CCR2 axis, *Clin. Cancer Res.* 19 (2013) 3404–3415.
- [120] F. Arce Vargas, A.J.S. Furness, I. Solomon, K. Joshi, L. Mekkaoui, M.H. Lesko, et al., Fc-optimized anti-CD25 depletes tumor-infiltrating regulatory T cells and synergizes with PD-1 blockade to eradicate established tumors, *Immunity* 46 (2017) 577–586.
- [121] A. Ribas, S. Hu-Lieskovan, What does PD-L1 positive or negative mean? *J. Exp. Med.* 213 (2016) 2835–2840.
- [122] M.W. Teng, S.F. Ngiow, A. Ribas, M.J. Smyth, Classifying cancers based on T-cell infiltration and PD-L1, *Cancer Res.* 75 (2015) 2139–2145.
- [123] T. Tsujikawa, S. Kumar, R.N. Borkar, V. Azimi, G. Thibault, Y.H. Chang, et al., Quantitative multiplex immunohistochemistry reveals myeloid-inflamed tumor-immune complexity associated with poor prognosis, *Cell Rep.* 19 (2017) 203–217.
- [124] W. Roh, P.L. Chen, A. Reuben, C.N. Spencer, P.A. Prieto, J.P. Miller, et al., Integrated molecular analysis of tumor biopsies on sequential CTLA-4 and PD-1 blockade reveals markers of response and resistance, *Sci. Transl. Med.* 9 (2017).

- [125] P.L. Chen, W. Roh, A. Reuben, Z.A. Cooper, C.N. Spencer, P.A. Prieto, et al., Analysis of immune signatures in longitudinal tumor samples yields insight into biomarkers of response and mechanisms of resistance to immune checkpoint blockade, *Cancer Discov.* 6 (2016) 827–837.
- [126] A.O. Kamphorst, R.N. Pillai, S. Yang, T.H. Nasti, R.S. Akondy, A. Wieland, et al., Proliferation of PD-1+ CD8 T cells in peripheral blood after PD-1-targeted therapy in lung cancer patients, *Proc. Natl. Acad. Sci. U. S. A.* 2 (1) (2017).
- [127] F. Dammeijer, L.A. Lievense, M.E.H. Kaijen-Lambers, M. van Nimwegen, K. Bezemer, J.P. Hegmans, et al., Depletion of tumor-associated macrophages with a CSF-1R kinase inhibitor enhances antitumor immunity and survival induced by DC immunotherapy, *Cancer Immunol. Res.* (2017).





# CHAPTER 7

---

Safety and tumor-specific immunological responses of combined dendritic cell vaccination and anti-CD40 agonistic antibody treatment for patients with metastatic pancreatic cancer: a phase I, open-label, single-arm, dose-escalation study (REACTiVe-2 trial)

Sai Ping Lau\*

Freek R. van 't Land\*

Sjoerd H. van der Burg

Marjolein Y.V. Homs

Martijn P. Lolkema

Joachim G.J.V. Aerts

Casper H.J. van Eijck

*\* These authors contributed equally to this work.*

## ABSTRACT

**Introduction:** The prognosis of patients with advanced pancreatic ductal adenocarcinoma (PDAC) is dismal and conventional chemotherapy treatment delivers limited survival improvement. Immunotherapy may complement our current treatment strategies. We previously demonstrated that the combination of an allogeneic tumor-lysate dendritic cell (DC) vaccine with an anti-CD40 agonistic antibody resulted in robust anti-tumor responses with survival benefit in a murine PDAC model. In the REACTiVe-2 trial we aim to translate our findings into patients. This study will determine the safety of dendritic cell/anti-CD40 agonistic antibody combination treatment, and treatment-induced tumor-specific immunological responses.

**Methods and analysis:** In this open-label, single-center (Erasmus University Medical Center, Rotterdam, The Netherlands), single-arm, phase I dose finding study, adult patients with metastatic pancreatic cancer with progressive disease after FOLFIRINOX chemotherapy will receive monocyte-derived DCs loaded with an allogeneic tumor lysate in conjunction with a CD40 agonistic antibody. This combination-immunotherapy regimen will be administered three times every two weeks, and booster treatments will be given after 3 and 6 months following the third injection. A minimum of 12 and a maximum of 18 patients will be included. The primary endpoint is safety and tolerability of the combination immunotherapy. To determine the maximum tolerated dose, DCs will be given at a fixed dosage and anti-CD40 agonist in a traditional 3+3 dose-escalation design. Secondary endpoints include radiographic response according to the RECIST (v1.1) and iRECIST criteria, and the detection of anti-tumor specific immune responses. **Ethics and dissemination:** The Central Committee on Research Involving Human Subjects (CCMO; NL76592.000.21) and the Medical Ethics Committee (METC; MEC-2021-0566) of the Erasmus M.C. University Medical Center Rotterdam approved the conduct of the trial. Written informed consent will be required for all participants. The results of the trial will be submitted for publication in a peer-reviewed scientific journal. **Trial registration:** Netherlands Trial Register, NL9723, <https://www.trialregister.nl/trial/9723>.

## INTRODUCTION

Pancreatic ductal adenocarcinoma (PDAC) is one of the leading causes of cancer-related deaths and carries a grim prognosis with a 5-year survival rate of less than 5%.<sup>(1)</sup> The majority of PDAC patients present with advanced disease not eligible for surgery.<sup>(2)</sup> The current standard-of-care treatment for locally advanced and metastasized pancreatic cancer is FOLFIRINOX chemotherapy, including fluorouracil, leucovorin, irinotecan and oxaliplatin. However, even with this intensive chemotherapy regimen median overall survival is 24.2 months and 11.1 months for locally advanced and metastatic PDAC respectively, with no superior alternatives available.<sup>(3, 4)</sup> In addition, more than half of the patients experience FOLFIRINOX-related toxicity which could lead to early termination of treatment.<sup>(5)</sup> Therefore, we are in need of new treatment modalities to tackle unresectable pancreatic disease.

Immunotherapy, like immune checkpoints inhibitors, delivered impressive results in various malignancies, and changed the treatment strategy for solid tumors like non-small cell lung cancer and melanoma.<sup>(6-9)</sup> Cellular immunotherapies, including chimeric antigen receptor (CAR) T cells, for hematological malignancies also demonstrated promising results leading to US Food and Drug Administration (FDA) approval of multiple CAR T treatments.<sup>(10-13)</sup> Unfortunately, outcomes with immune checkpoint blockers and CAR T cells in PDAC have been disappointing.<sup>(14-17)</sup> PDAC is considered an immunological “cold” tumor with a highly immunosuppressive micro environment lacking the presence of effector T cells.<sup>(18)</sup> Nonetheless, recent studies showed promising results with rational immune-combination strategies demonstrating that comprehensive understanding of the immune composition and tumor biology of PDAC is imperative for successful treatment.<sup>(19, 20)</sup>

Dendritic cells (DCs) play a fundamental role in the anti-tumor response. They capture, process and present tumor antigens and can subsequently induce tumor-specific effector T cells. It has been demonstrated that DC paucity in PDAC impairs immune surveillance, and resurrection of DCs in early PDAC lesions reinvigorates anti-tumor T-cell immunity.<sup>(21)</sup> We have investigated the use of allogeneic-mesothelioma lysate DC vaccination (MesoPher) for resected pancreatic cancer patients (REACTiVe trial; NL7432). Ideally, a personalized lysate of the autologous tumor would be able to redirect the lymphocyte response to the specific disease of the patients. However, in most PDAC patients, it is not possible to collect sufficient tumor material for the production of a tumor lysate. Also sampling differences between patients will result in different quality of lysates. As a reliable alternative, the use of an allogeneic tumor lysate avoids the need for autologous tumor material and standardizes treatment across patients. MesoPher demonstrated clinical activity in mesothelioma patients, and mesothelioma and PDAC share various tumor antigens (*e.g.* mesothelin, WT-1, MUC-1, Survivin).<sup>(22)</sup> In the REACTiVe trial, we have demonstrated the induction of PDAC-specific T cells following MesoPher treatment (Lau *et al.*, 2022, Eur J Cancer, Manuscript accepted). However, the tumor microenvironment of established PDAC encompass dense desmoplastic stroma able to exclude effector T cells.<sup>(23)</sup>



CD40 is a surface molecule on various immune cells, including B cells, monocytes/macrophages and DCs.(24, 25) Its ligand, CD154, is expressed primarily on activated T cells.(25) Because of their expression, CD40-CD154 interaction plays an important role in both humoral and cellular immunity. It has been demonstrated that CD40-agonists are able to induce stromalysis in PDAC by matrix metallo-proteases produced by tumor associated macrophages.(26, 27) Tumor regression was found when CD40 agonist combined with the chemotherapeutic gemcitabine was given, and anti-tumor effect was annihilated when macrophages were depleted.(26) In addition, we have previously demonstrated in a PDAC murine model that although CD40-agonists improved intratumoral T-cell infiltration, T cells displayed hallmarks of exhaustion.(28) The addition of DC vaccination improved T-cell phenotype, and DC/anti-CD40 combination therapy led to survival benefit compared to monotherapy (DC vaccination or anti-CD40) treated animals. Finally, CD40 targeting also licenses endogenous (and administered) DCs to cross-present tumor antigens to T cells, boosting the spontaneously activated tumor immunity.(29, 30) By rationally combining DC vaccination and an anti-CD40 agonist antibody we could convert the classically immunological “cold” PDAC to a “hot” and immunotherapy-sensitive tumor. These pre-clinical results lay the foundation for this clinical trial.

We hypothesize that this bimodal-treatment regime, utilizing DCs to induce tumor-specific T cells and an anti-CD40 agonist to promote introduction of T cells into the tumor, may lead to effective anti-tumor responses in PDAC patients. In the REACTiVe-2 trial, we will investigate the maximum tolerable dose of anti-CD40 agonist antibody in combination with allogeneic-tumor lysate-DC vaccination in patients with metastasized pancreatic cancer after failure of first-line FOLFIRINOX treatment.

## METHODS AND ANALYSIS

### *Study design and treatment*

The Rotterdam Pancreatic Cancer Vaccination-2 (REACTiVe-2) trial is an open-label, dose-finding, single-center (Erasmus University Medical Center, Rotterdam, the Netherlands), single-arm, phase I study consisting of three parts; screening, bridging and treatment phase. A traditional 3+3 design is implemented to investigate Dose-Limiting Toxicity (DLT) of an anti CD40-agonist (mitazalimab) within the MesoPher/mitazalimab combination-immunotherapy regime for pancreatic cancer patients. A minimum of 12 and a maximum of 18 patients will be included.

The study was approved by the Central Committee on Research involving Human Subjects (NL76592.000.21) as defined by the Medical Research Involving Human Subjects Act. Procedures followed were in accordance with the ethical standards of these committees on human experimentation and with the Helsinki Declaration of 1975, as revised in 2008. The trial is registered with the Dutch Trial Register, NL9723. Trial registration details are described in supplementary table 1.

*Screening phase:* Patients with metastatic pancreatic cancer with progression on first-line (modified) FOLFIRINOX are screened for eligibility for the study. Screening will start after 2 weeks after the last cycle of chemotherapy (Figure 1).

*Bridging Phase:* Included patients will start off with a leukapheresis during the bridging phase. A leukapheresis is performed in order to generate monocyte-derived DCs (mo-DC) for MesoPher production. The production of MesoPher is performed according to DC immunotherapy protocols that are approved by the ethics committee (NL24050.000.08, NL44330.000.14, NL62105.000.17, NL67169.000.18, NL76592.000.21). Every vaccination consists of around  $25 \times 10^6$  autologous mo-DCs pulsed with the allogeneic mesothelioma tumor cell line lysate, all produced under Good Manufacturing Practice (GMP)-certified conditions, as described earlier.(22, 31) Quality control testing will be performed before MesoPher release. The manufacturing process of MesoPher takes approximately six weeks. During this bridging phase, patients who experience symptoms from their disease or are considered to be rapidly progressive can receive two bridging chemotherapy cycles with gemcitabine and Nab-Paclitaxel or monotherapy gemcitabine, by decision of the treating oncologist. After the optional and patient-dependent bridging therapy, a baseline CT-scan and a biopsy of an accessible tumor lesion will be performed.

*Treatment Phase:* Within two weeks after the bridging-chemotherapy and regardless of response, all fit-for-treatment patients will start with immunotherapy. MesoPher and mitazalimab will be administered consecutively in one day, three times, biweekly. After the third treatment, booster vaccines will be given after three and six months. MesoPher is administered at a fixed dosage of  $25 \times 10^6$  DCs, and 2/3th will be injected intravenously and 1/3th intradermally. Mitazalimab will be infused at a cohort-dependent dosage. A follow-up CT-scan and tumor biopsy will be performed after three study treatments. Subsequent CT-scans to monitor clinical activity will be performed every 6-8 weeks. Response will be evaluated according to the Response Evaluation Criteria in Solid Tumors (RECIST) (v1.1) and iRECIST criteria.(32) Study treatment will be halted prematurely when patients have radiological and clinical progressive disease during treatment or if unacceptable toxicity occurs. Some radiological progression without clinical deterioration can allow for continuation of the study treatment, in the absence of other treatment options. Peripheral blood collection will be done at baseline and several time points following treatment for immunomonitoring.

A traditional 3+3 design will be used to determine the maximum tolerated dose (MTD) of mitazalimab within the MesoPher/mitazalimab combination treatment (Figure 2). In short, DLTs will be evaluated in three dose-level cohorts. This rule-based design allows dose escalation if no DLT is found in three patients, or if one DLT is found in six patients. In all other cases, dose escalation is stopped and the MTD is found in the previous cohort. Furthermore, the MTD cohort will include at least six evaluable patients. When two DLTs are found in the first three patients in the starting cohort (Dose level 1), de-escalation is required. The first cohort starts at

a dose of 300µg/kg mitazalimab, and depending of found toxicity dose is halved or doubled (Table 1). In this study, a minimum of 12 and a maximum of 18 subjects will be included.

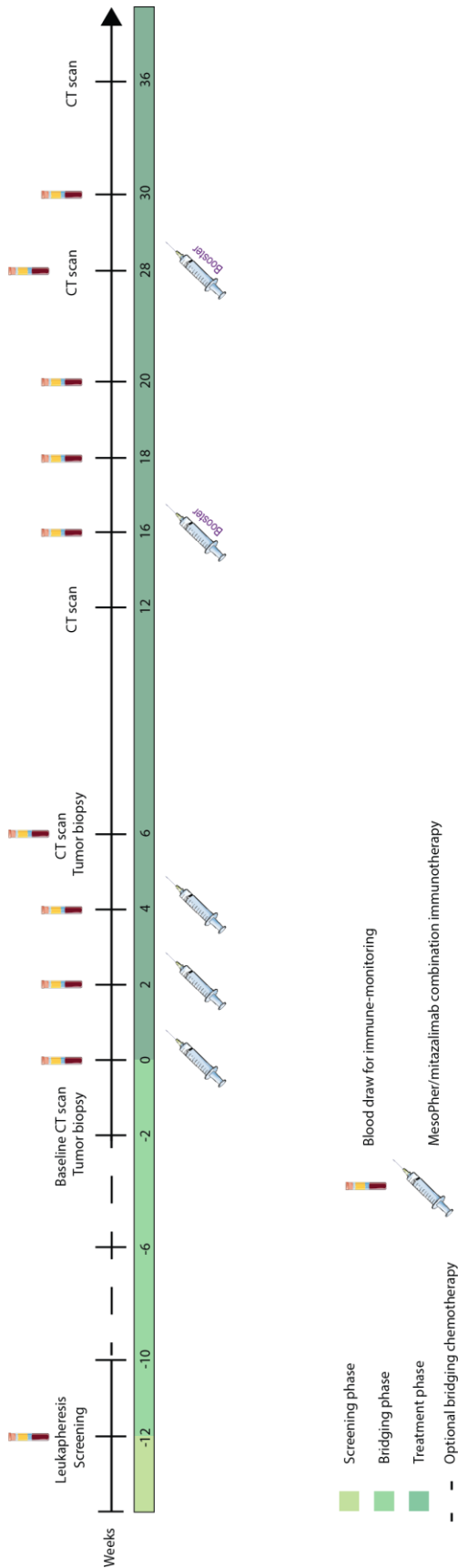


**Figure 1.** Treatment scheme. After screening, a leukapheresis is performed for the production of allogeneic-tumor lysate loaded dendritic cells. The length of the bridging phase can vary between patients, depending whether patients receive chemotherapy or not. Study patients receive combination immunotherapy on week 0, 2, 4 and booster vaccinations are given at week 16 and 28. A tumor biopsy is taken before and after study treatment. Blood for immune-monitoring is drawn at various time points.

### Eligibility criteria

Written informed consent according to ICH-GCP, together with a trained physician, must be given before study treatment is started. The informed consent form, written in Dutch, is attached (Appendix A). Adult pancreatic cancer patients with radiologically suspect metastatic lesions and progressive disease on first-line (modified) FOLFIRINOX are eligible for inclusion. Also, an accessible metastatic lesion for histological tissue analysis and immunomonitoring is required and patients must have a WHO performance status of 0-1. Exclusion criteria include abdominal ascites, (previous) use of anti-CD40 agonistic antibodies and/or anti-tumor vaccinations, use of immunosuppressive drugs, autoimmune disease, organ allograft or active infection. All inclusion and exclusion criteria are listed in supplementary table 2.

Dose level	MesoPher (DCs)	Mitazalimab ( $\mu\text{g}/\text{kg}$ )
-2	$25 * 10^6$	75
-1	$25 * 10^6$	150
1	$25 * 10^6$	300
2	$25 * 10^6$	600
3	$25 * 10^6$	1200

**Table 1.** MesoPher and mitazalimab treatment doses. The first cohort will start at dose level 1. When more than one dose limiting toxicity is found at the first level, we will go to level-1. When 0/3 or 1/6 patients experience a dose limiting toxicity, we will proceed to the next level.

### Study end points

The primary objective of this study is determining the toxicity and tolerability of MesoPher/mitazalimab combination immunotherapy for progressive metastatic pancreatic cancer patients. This will be determined by the frequency of DLTs. Toxicity will be scored according to the Common Terminology Criteria for Adverse Events (CTCAE) version 5.0.(33) Toxicities occurring within 6 weeks after the first vaccination will be considered a DLT (*i.e.* the DLT observation period). All grade 3 or higher adverse events are considered a DLT, except for the toxicities listed in Box 1. Secondary endpoints include radiological responses as defined by RECIST v1.1 and iRECIST criteria, and the assessment of immune responses. The detection of immune responses will be assessed on multiple levels; vaccine-induced delayed type hypersensitivity testing, immune-monitoring of various peripheral immune cell subsets on transcriptomic and protein-level, and the detection of anti-tumor responses.

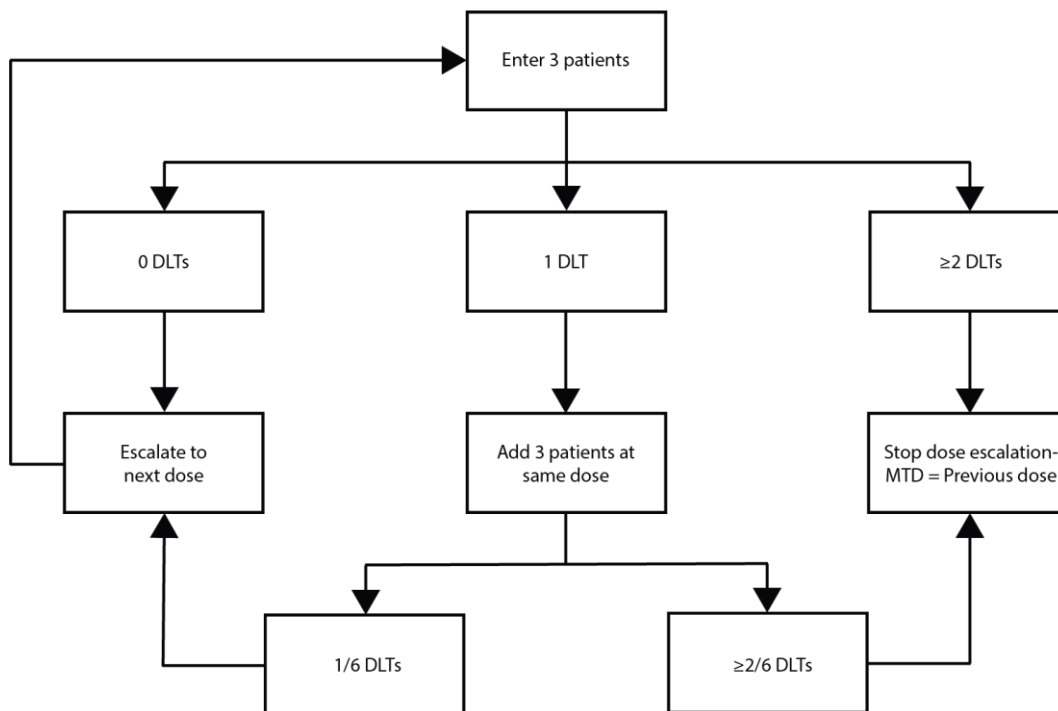


**Figure 2.** 3+3 dose-escalation study design. DLTs, dose-limiting toxicities; MDT, maximum tolerated dose.

**Box 1.** Grade 3 toxicities not considered as DLT.

Any grade 3 or higher toxicity will be considered a DLT with the exception of the following toxicities

*Hematological toxicity*

- Thrombocytopenia grade 3 lasting less than 7 days
- Neutropenia grade 3 lasting less than 7 days without neutropenic fever
- Alanine aminotransferase (ALAT) increased grade 3 resolved within 7 days to grade 1
- Alkaline phosphatase (AF) increased grade 3 resolved within 7 days to grade 1
- Aspartate aminotransferase (ASAT) increased grade 3 resolved within 7 days to grade 1
- Blood bilirubin (Bili) increased grade 3 resolved within 7 days to grade 1

*Non-hematological toxicity*

- Grade 3/4 diarrhea, nausea, vomiting, hypertension if not adequately treated

*Immune-related toxicity*

- Cytokine Release Syndrome (CRS) / infusion related reactions (IRR) will be scored according to the ASTCT guidelines \*. Any grade 3 or higher CRS/IRR will be considered a DLT. Except for grade 3 CRS/IRR if resolved to a lower grade within 24 hours after the onset of symptoms.
- For immune related toxicities we will exclude hypo/hyperthyroidism as a DLT.
- Immune related skin toxicity that is adequately treated with topical therapy will not be considered a DLT

*Laboratory assessments*

- Any grade 3 laboratory abnormalities that are asymptomatic and clinically not significant are not considered DLT

\*Grade 1 = Fever, with or without constitutional symptoms. Grade 2 = Hypotension responding to fluids. Hypoxia responding to <40% FiO<sub>2</sub>. Grade 3 = Hypotension managed with one pressor. Hypoxia requiring ≥40% FiO<sub>2</sub>. Grade 4 = Life-threatening consequences; urgent intervention needed

### *Vaccine-specific response*

Keyhole Limpet Hemocyanin (KLH) is part of the DC vaccine and is known to induce a specific adaptive immune response readily detectable in serum and peripheral blood mononuclear cells (PBMCs) of vaccinated individuals. Humoral responses after vaccination will be detected using a ELISA. Cellular responses to KLH will be measured *in vitro*. KLH pulsed DCs will be co-cultured with PBMCs taken before- and after treatment. After a 24h co-culture, T cells will be stained for activation-, cytotoxic- and degranulation markers and measured by flow cytometry.

### *Immune-monitoring of peripheral immune cell subsets*

Phenotypical analysis of PBMCs will be conducted with Aurora spectral flow cytometry. Liquid nitrogen-stored PBMCs will be stained with antibodies and measured by flow cytometry. These experiments allow to investigate treatment-induced changes in the frequencies of immune cell subsets that represent distinct lineages and/or express different levels of activation, differentiation and co-signaling markers. In addition, 1ml of whole-blood will be freshly measured by flow cytometry to characterize different immune cell populations before and after treatment.

### *Modulation of gene expression levels*

Gene expression of 770 immune related genes will be investigated. RNA pellets of PBMCs will be measured by Nanostring Technologies using the PanCancer Immune Profiling Panel to investigate treatment induced changes in the RNA levels.

### *Anti-tumor responses*

We will perform paired biopsies of all patients at baseline and after three treatments, preferably from the same tumor location, to detect anti-tumor responses. Two biopsies will be taken at one timepoint. One will be formalin-fixed and paraffin-embedded (FFPE) by our pathology department. The pathologist will determine if there are cancerous cells, and post-treatment signs of treatment effect will be evaluated. FFPE tissues will be used to measure RNA expression levels using Nanostring Technologies (PanCancer Immune Profiling Panel) to investigate treatment related effects at tumor site on RNA level. Also, we will use the Digital Spatial Profiler (DSP) by Nanostring Technologies to investigate immune-infiltration in the tumor on protein level. Another biopsy will be freshly processed to single cell suspensions and will be freshly measured using flow cytometry. In addition, in patients where we are not able to perform a post-study treatment biopsy, a delayed-type hypersensitivity (DTH) reaction to MesoPher will be assessed. When this DTH skin test is positive ( $\geq 2$  mm induration), a skin biopsy will be taken. Biopsies will be used for in situ immunostainings of *i.e.*, DCs, myeloid derived suppressor cells (MDSCs) and CD8+ T cells.

*Patient and public involvement*

It was not appropriate or possible to involve patients or the public in the design, or conduct, or reporting, or dissemination plans of our research

*Ethics and dissemination*

The study will be performed in accordance with ethical principles that have their origin in the Declaration of Helsinki (64th version, October 2013) and are consistent with the International Conference on Harmonisation/Good Clinical Practice guidelines, applicable regulatory requirements. The Investigator must also comply with all applicable privacy directives and regulations (*e.g.*, EU Data Protection Directive 95/46/EC). Both the Central Committee on Research Involving Human Subjects (CCMO; NL76592.000.21) and the Medical Ethics Committee (METC; MEC-2021-0566) of the Erasmus MC University Medical Center Rotterdam approved the conduct of the trial. Protocol version 3, date 27-05-2021 was approved. Substantial changes in trial conduct will be proposed to the ethical committee with a substantial protocol amendment. The ethical committee needs to approve this amendment before changes in trial conduct will be implemented. The results of this clinical trial will be submitted for publication in a peer-reviewed scientific journal. All data will be collected, captured and analyzed according to the rules of the Erasmus MC University Medical Center Rotterdam. A Trial Master File and an Investigator Site File is kept. Data will be captured in the cloud-based clinical data management platform Castor. The database is accessible for the researchers, the trial monitor and data managers. All serious adverse events will be reported to the Ethical Committee and to Alligator Bioscience, producer of the mitazalimab. Serious adverse events that are considered to be related to MesoPher treatment will be reported to Amphera. The investigators will provide a monthly update to Alligator Bioscience and Amphera about the trial conduct. Written informed consent will be required for all participants.

*Trial Timeline and Status*

Dutch law (WMO) states that it is mandatory to obtain ethical approval for clinical trials before start of study. Since a special Advanced Therapy Medicinal Product (ATMP) is investigated in the REACTiVe-2 trial, approval first from the central CCMO followed by the local METC is required. Date of approval from the central and local committee is 13th July 2021 and 20th July 2021, respectively. The REACTiVe-2 trial is prospectively registered at the WHO-acknowledged Netherlands Trial Register (NTR). The NTR is currently transitioning to the CCMO register. Our official date of approval/registration as determined by Dutch law is July 20th 2021. We are currently recruiting the first patients. We aim to include all patients by the end of 2022. The first safety data will be available the same year.

## DISCUSSION

Although DC-based platforms may introduce tumor-specific T cells able to mount effective immune responses against occult disease lacking desmoplastic stroma, established PDAC requires a rational multimodal treatment regime. The REACTiVe-2 trial was initiated on the promises of preclinical immune and survival results. In this study, we will determine the MTD of mitazalimab in the MesoPher/mitazalimab combination treatment in metastasized pancreatic cancer patients who are progressive on first-line (modified) FOLFIRINOX treatment. In addition, clinical responses through radiological assessment and the detection of treatment-induced immune responses will be evaluated. This is the first clinical trial investigating anti-CD40 agonistic antibodies combined with DC vaccination in PDAC patients. In a previous dose-escalation trial, we have demonstrated that MesoPher should be administered at an amount of  $25 \times 10^6$  DCs.(22) At this dose, clinical activity was found in mesothelioma patients. This number of DCs has also been implemented in the REACTiVe trial treating resected PDAC patients. Although it has not been demonstrated that this dosage is optimal for PDAC patients, we do find promising results in the REACTiVe trial. At this dosage, we found vaccine-induced tumor-specific T-cell response. Moreover, we did not observe any serious toxicity. It is common practice in dendritic cell immunotherapy to inject the cells both intravenously and intradermally. In our previous DC-vaccination trial, vaccinations were also given both intradermally and intravenously. This strategy induced robust immune responses.(22) (Lau *et al.*, 2022, Eur J Cancer, manuscript accepted) Two different routes of administration are used in an attempt to maximize the interaction between T cells and DCs in different lymphoid compartments and to maximize the subsequent homing patterns of the activated T cells to increase the quality and quantity of the antitumor-immune response. Therefore, this dosage and route of administration will be adopted in the REACTiVe-2 trial. In the phase 1 dose-escalation study for mitazalimab, intravenous doses up to  $1200 \mu\text{g}/\text{kg}$  were considered well tolerated with manageable side effects in patients with advanced solid tumors.(34) Since this trial did not include PDAC patients and prior combination with anti-tumor vaccinations has not been done, we will titrate mitazalimab in this immunotherapy combination regime for PDAC patients.

It should be noted that cancer patients treated with immunotherapy may demonstrate initial transient tumor growth as a result of intra-tumoral immune cell influx and inflammation.(35) This process called pseudoprogression does not reflect true disease progression and may lead to premature discontinuation of effective treatment. Therefore, we will also incorporate the iRECIST criteria and initial radiographical progression can allow for continuation of study treatment in the absence of clinical deterioration.

A limitation of this study is the relatively small number of patients we will include and the single-armed nature of the trial which complicates analyzing clinical efficacy. However, this design and sample size should be sufficient for dose finding. We are aware that finding a MTD for this



combination therapy may differ from the minimal effective dose given the pleiotropic nature of CD40 stimulation. When the combination treatment is safe, we will progress to a larger phase II clinical trial to further investigate the immunological responses and clinical efficacy.

## REFERENCES

1. Siegel RL, Miller KD, Jemal A. Cancer statistics, 2020. *CA Cancer J Clin*. 2020;70(1):7-30.
2. Lau SC, Cheung WY. Evolving treatment landscape for early and advanced pancreatic cancer. *World J Gastrointest Oncol*. 2017;9(7):281-92.
3. Suker M, Beumer BR, Sadot E, Marthey L, Faris JE, Mellon EA, et al. FOLFIRINOX for locally advanced pancreatic cancer: a systematic review and patient-level meta-analysis. *Lancet Oncol*. 2016;17(6):801-10.
4. Conroy T, Desseigne F, Ychou M, Bouché O, Guimbaud R, Bécouarn Y, et al. FOLFIRINOX versus Gemcitabine for Metastatic Pancreatic Cancer. *New England Journal of Medicine*. 2011;364(19):1817-25.
5. Thibodeau S, Voutsadakis IA. FOLFIRINOX Chemotherapy in Metastatic Pancreatic Cancer: A Systematic Review and Meta-Analysis of Retrospective and Phase II Studies. *J Clin Med*. 2018;7(1).
6. Weber JS, D'Angelo SP, Minor D, Hodi FS, Gutzmer R, Neyns B, et al. Nivolumab versus chemotherapy in patients with advanced melanoma who progressed after anti-CTLA-4 treatment (CheckMate 037): a randomised, controlled, open-label, phase 3 trial. *Lancet Oncol*. 2015;16(4):375-84.
7. Robert C, Long GV, Brady B, Dutriaux C, Maio M, Mortier L, et al. Nivolumab in previously untreated melanoma without BRAF mutation. *N Engl J Med*. 2015;372(4):320-30.
8. Larkin J, Chiarion-Sileni V, Gonzalez R, Grob JJ, Cowey CL, Lao CD, et al. Combined Nivolumab and Ipilimumab or Monotherapy in Untreated Melanoma. *N Engl J Med*. 2015;373(1):23-34.
9. Brahmer J, Reckamp KL, Baas P, Crinò L, Eberhardt WEE, Poddubskaya E, et al. Nivolumab versus Docetaxel in Advanced Squamous-Cell Non–Small-Cell Lung Cancer. *New England Journal of Medicine*. 2015;373(2):123-35.
10. Maude SL, Laetsch TW, Buechner J, Rives S, Boyer M, Bittencourt H, et al. Tisagenlecleucel in Children and Young Adults with B-Cell Lymphoblastic Leukemia. *N Engl J Med*. 2018;378(5):439-48.
11. Neelapu SS, Locke FL, Bartlett NL, Lekakis LJ, Miklos DB, Jacobson CA, et al. Axicabtagene Ciloleucel CAR T-Cell Therapy in Refractory Large B-Cell Lymphoma. *N Engl J Med*. 2017;377(26):2531-44.
12. Schuster SJ, Svoboda J, Chong EA, Nasta SD, Mato AR, Anak O, et al. Chimeric Antigen Receptor T Cells in Refractory B-Cell Lymphomas. *N Engl J Med*. 2017;377(26):2545-54.
13. Wang M, Munoz J, Goy A, Locke FL, Jacobson CA, Hill BT, et al. KTE-X19 CAR T-Cell Therapy in Relapsed or Refractory Mantle-Cell Lymphoma. *N Engl J Med*. 2020;382(14):1331-42.
14. Jan N, Dagmar M, Hans L, Goncalo R, Nicole C, Raymond YC, et al. Systemic treatment with anti-PD-1 antibody nivolumab in combination with vaccine therapy in advanced pancreatic cancer. *Journal of Clinical Oncology*. 2016;34(15\_suppl):3092-.
15. Brahmer JR, Tykodi SS, Chow LQ, Hwu WJ, Topalian SL, Hwu P, et al. Safety and activity of anti-PD-L1 antibody in patients with advanced cancer. *N Engl J Med*. 2012;366(26):2455-65.
16. Cutmore LC, Brown NF, Raj D, Chaudhuri S, Wang P, Maher J, et al. Pancreatic Cancer UK Grand Challenge: Developments and challenges for effective CAR T cell therapy for pancreatic ductal adenocarcinoma. *Pancreatol*. 2020;20(3):394-408.
17. Wainberg ZA, Hochster HS, Kim EJ, George B, Kaylan A, Chiorean EG, et al. Open-label, Phase I Study of Nivolumab Combined with nab-Paclitaxel Plus Gemcitabine in Advanced Pancreatic Cancer. *Clin Cancer Res*. 2020;26(18):4814-22.
18. Steele NG, Carpenter ES, Kemp SB, Sirihorachai VR, The S, Delrosario L, et al. Multimodal mapping of the tumor and peripheral blood immune landscape in human pancreatic cancer. *Nature Cancer*. 2020;1(11):1097-112.
19. Brandon George S, Benjamin Leon M, Spyridoula V, Manik K, Ayumi W, Catherine R, et al. A phase I trial targeting advanced or metastatic pancreatic cancer using a combination of standard chemotherapy and adoptively transferred nonengineered, multiantigen specific T cells in the first-line setting (TACTOPS). *Journal of Clinical Oncology*. 2020;38(15\_suppl):4622-.

20. O'Hara MH, O'Reilly EM, Varadhachary G, Wolff RA, Wainberg ZA, Ko AH, et al. CD40 agonistic monoclonal antibody APX005M (sotigalimab) and chemotherapy, with or without nivolumab, for the treatment of metastatic pancreatic adenocarcinoma: an open-label, multicentre, phase 1b study. *Lancet Oncol.* 2021;22(1):118-31.
21. Hegde S, Krishawan VE, Herzog BH, Zuo C, Breden MA, Knolhoff BL, et al. Dendritic Cell Paucity Leads to Dysfunctional Immune Surveillance in Pancreatic Cancer. *Cancer Cell.* 2020;37(3):289-307 e9.
22. Aerts J, de Goeje PL, Cornelissen R, Kaijen-Lambers MEH, Bezemer K, van der Leest CH, et al. Autologous Dendritic Cells Pulsed with Allogeneic Tumor Cell Lysate in Mesothelioma: From Mouse to Human. *Clin Cancer Res.* 2018;24(4):766-76.
23. Whatcott CJ PR, Von Hoff DD, et al. Desmoplasia and chemoresistance in pancreatic cancer. 2012.
24. Grewal IS, Flavell RA. CD40 and CD154 in cell-mediated immunity. *Annu Rev Immunol.* 1998;16:111-35.
25. van Kooten C, Banchereau J. CD40-CD40 ligand. *J Leukoc Biol.* 2000;67(1):2-17.
26. Beatty GL, Chiorean EG, Fishman MP, Saboury B, Teitelbaum UR, Sun W, et al. CD40 agonists alter tumor stroma and show efficacy against pancreatic carcinoma in mice and humans. *Science.* 2011;331(6024):1612-6.
27. Long KB, Gladney WL, Tooker GM, Graham K, Fraietta JA, Beatty GL. IFN $\gamma$  and CCL2 Cooperate to Redirect Tumor-Infiltrating Monocytes to Degrade Fibrosis and Enhance Chemotherapy Efficacy in Pancreatic Carcinoma. *Cancer Discovery.* 2016.
28. Lau SP, van Montfoort N, Kinderman P, Lukkes M, Klaase L, van Nimwegen M, et al. Dendritic cell vaccination and CD40-agonist combination therapy licenses T cell-dependent antitumor immunity in a pancreatic carcinoma murine model. *J Immunother Cancer.* 2020;8(2).
29. Cella M, Scheidegger D, Palmer-Lehmann K, Lane P, Lanzavecchia A, Alber G. Ligation of CD40 on dendritic cells triggers production of high levels of interleukin-12 and enhances T cell stimulatory capacity: T-T help via APC activation. *J Exp Med.* 1996;184(2):747-52.
30. Schuurhuis DH, Laban S, Toes RE, Ricciardi-Castagnoli P, Kleijmeer MJ, van der Voort EI, et al. Immature dendritic cells acquire CD8(+) cytotoxic T lymphocyte priming capacity upon activation by T helper cell-independent or-dependent stimuli. *J Exp Med.* 2000;192(1):145-50.
31. Cornelissen R, Hegmans JP, Maat AP, Kaijen-Lambers ME, Bezemer K, Hendriks RW, et al. Extended Tumor Control after Dendritic Cell Vaccination with Low-Dose Cyclophosphamide as Adjuvant Treatment in Patients with Malignant Pleural Mesothelioma. *Am J Respir Crit Care Med.* 2016;193(9):1023-31.
32. Chai LF, Prince E, Pillarisetty VG, Katz SC. Challenges in assessing solid tumor responses to immunotherapy. *Cancer Gene Therapy.* 2020;27(7):528-38.
33. Common Terminology Criteria for Adverse Events. Version 5.0. Published November 27, 2017. US Department of Health and Human Services. 2020.
34. Calvo E, Moreno V, Perets R, Yablonski-Peretz T, Fournneau N, Girgis S, et al. A phase I study to assess safety, pharmacokinetics (PK), and pharmacodynamics (PD) of JNJ-64457107, a CD40 agonistic monoclonal antibody, in patients (pts) with advanced solid tumors. *Journal of Clinical Oncology.* 2019;37(15\_suppl):2527-.
35. Jia W, Gao Q, Han A, Zhu H, Yu J. The potential mechanism, recognition and clinical significance of tumor pseudoprogression after immunotherapy. *Cancer Biol Med.* 2019;16(4):655-70.





SPIRIT 2013 Checklist: Recommended items to address in a clinical trial protocol and related documents\*

Section/item	ItemNo	Description
<b>Administrative information</b>		
Title	1	Descriptive title identifying the study design, population, interventions, and, if applicable, trial acronym <i>This can be found on the title page of the manuscript.</i>
Trial registration	2a	Trial identifier and registry name. If not yet registered, name of intended registry <i>This can be found in supplementary table 1: WHO Trial Registration Data Set.</i>
	2b	All items from the World Health Organization Trial Registration Data Set <i>This can be found in supplementary table 1: WHO Trial Registration Data Set.</i>
Protocol version	3	Date and version identifier <i>This can be found in supplementary table 1: WHO Trial Registration Data Set.</i>
Funding	4	Sources and types of financial, material, and other support <i>This can be found in supplementary table 1: WHO Trial Registration Data Set.</i>
Roles and responsibilities	5a	Names, affiliations, and roles of protocol contributors <i>This can be found in the title page and on page 17 (Authors' contributions).</i>
	5b	Name and contact information for the trial sponsor <i>This can be found in supplementary table 1: WHO Trial Registration Data Set.</i>
	5c	Role of study sponsor and funders, if any, in study design; collection, management, analysis, and interpretation of data; writing of the report; and the decision to submit the report for publication, including whether they will have ultimate authority over any of these activities <i>Prof. Dr. Joachim Aerts is part of the study steering committee.</i>
	5d	Composition, roles, and responsibilities of the coordinating centre, steering committee, endpoint adjudication committee, data management team, and other individuals or groups overseeing the trial, if applicable (see Item 21a for data monitoring committee) <i>The Study Steering Committee, comprised of the coordinating investigator, sponsor and principal investigator decides to escalate dosages and evaluates toxicities. The study coordinator is responsible for clinical conduct of the trial. The whole team of investigators will evaluate the trial results.</i>

## Introduction

Background and rationale	6a	Description of research question and justification for undertaking the trial, including summary of relevant studies (published and unpublished) examining benefits and harms for each intervention <i>This can be found in the introduction of the manuscript.</i>
	6b	Explanation for choice of comparators <i>Not Applicable</i>
Objectives	7	Specific objectives or hypotheses <i>This can be found in the manuscript on page 12, header study end points.</i>
Trial design	8	Description of trial design including type of trial (eg, parallel group, crossover, factorial, single group), allocation ratio, and framework (eg, superiority, equivalence, noninferiority, exploratory) <i>This can be found in the manuscript, starting at page 7, methods and analysis, study design and treatment.</i>

**Methods: Participants, interventions, and outcomes**

Study setting	9	Description of study settings (eg, community clinic, academic hospital) and list of countries where data will be collected. Reference to where list of study sites can be obtained <i>This information can be found in the manuscript.</i>
Eligibility criteria	10	Inclusion and exclusion criteria for participants. If applicable, eligibility criteria for study centres and individuals who will perform the interventions (eg, surgeons, psychotherapists) <i>There is a table included listing all in and exclusion criteria.</i>
Interventions	11a	Interventions for each group with sufficient detail to allow replication, including how and when they will be administered <i>This is described in the manuscript in the methods and analysis section starting at page 7, also the schematic figure of the treatments schedule gives a visual overview of the trial design.</i>
	11b	Criteria for discontinuing or modifying allocated interventions for a given trial participant (eg, drug dose change in response to harms, participant request, or improving/worsening disease) <i>This is described in the manuscript in the methods and analysis section. Here is described how we will find the maximum tolerated dose. Also, definitions of dose limiting toxicities can be found in the manuscript and in table 3.</i>
	11c	Strategies to improve adherence to intervention protocols, and any procedures for monitoring adherence (eg, drug tablet return, laboratory tests) <i>Not applicable</i>
	11d	Relevant concomitant care and interventions that are permitted or prohibited during the trial <i>Use of steroids is prohibited during the trial, as stated in the in- and exclusion criteria.</i>

Outcomes	12	Primary, secondary, and other outcomes, including the specific measurement variable (eg, systolic blood pressure), analysis metric (eg, change from baseline, final value, time to event), method of aggregation (eg, median, proportion), and time point for each outcome. Explanation of the clinical relevance of chosen efficacy and harm outcomes is strongly recommended <i>This is described in the manuscript on page 12, study end points.</i>
Participant timeline	13	Time schedule of enrolment, interventions (including any run-ins and washouts), assessments, and visits for participants. A schematic diagram is highly recommended (see Figure) <i>This is described in the methods section of the manuscript and also a schematic diagram is added. See figure 1.</i>
Sample size	14	Estimated number of participants needed to achieve study objectives and how it was determined, including clinical and statistical assumptions supporting any sample size calculations <i>Because of the 3+3 dose escalation design we will use a minimum of 12 patients. A maximum of 18 patients will be included and this is stated in the manuscript on page 10.</i>
Recruitment	15	Strategies for achieving adequate participant enrolment to reach target sample size <i>Not applicable</i>

#### **Methods: Assignment of interventions (for controlled trials)**

##### Allocation:

Sequence generation	16a	Method of generating the allocation sequence (eg, computer-generated random numbers), and list of any factors for stratification. To reduce predictability of a random sequence, details of any planned restriction (eg, blocking) should be provided in a separate document that is unavailable to those who enrol participants or assign interventions <i>Not applicable</i>
Allocation concealment mechanism	16b	Mechanism of implementing the allocation sequence (eg, central telephone; sequentially numbered, opaque, sealed envelopes), describing any steps to conceal the sequence until interventions are assigned <i>Not applicable</i>
Implementation	16c	Who will generate the allocation sequence, who will enrol participants, and who will assign participants to interventions <i>Not applicable</i>
Blinding (masking)	17a	Who will be blinded after assignment to interventions (eg, trial participants, care providers, outcome assessors, data analysts), and how <i>Not applicable</i>
	17b	If blinded, circumstances under which unblinding is permissible, and procedure for revealing a participant's allocated intervention during the trial <i>Not applicable</i>

#### **Methods: Data collection, management, and analysis**

- Data collection methods 18a Plans for assessment and collection of outcome, baseline, and other trial data, including any related processes to promote data quality (eg, duplicate measurements, training of assessors) and a description of study instruments (eg, questionnaires, laboratory tests) along with their reliability and validity, if known. Reference to where data collection forms can be found, if not in the protocol.  
*Description how we will evaluate the study end points can be found in the protocol on page 12, study end points.*
- 18b Plans to promote participant retention and complete follow-up, including list of any outcome data to be collected for participants who discontinue or deviate from intervention protocols  
*We will keep patient in follow up for life. We will follow these patients life-long, also in regular care. This will allow us also to collect every relevant data for the trial.*

- Data management 19 Plans for data entry, coding, security, and storage, including any related processes to promote data quality (eg, double data entry; range checks for data values). Reference to where details of data management procedures can be found, if not in the protocol  
*This is stated in the protocol, chapter ethics and dissemination on page 15.*

- Statistical methods 20a Statistical methods for analysing primary and secondary outcomes. Reference to where other details of the statistical analysis plan can be found, if not in the protocol  
*Since the primary endpoints will be dose limiting toxicities, no statistical analysis needs to be done on this. For secondary endpoints we apply paired Wilcoxon signed-ranks tests to flow cytometry data. Also, large gene-expression data will be corrected for multiple testing using Benjamini-Hochberg procedure. Survival data will be plotted as Kaplan–Meier survival curves. In all cases, a p-value of 0.05 and below was considered significant (\*),  $p < 0.01$  (\*\*) and  $p < 0.001$  (\*\*\*) as highly significant.*
- 20b Methods for any additional analyses (eg, subgroup and adjusted analyses)  
*Not applicable*
- 20c Definition of analysis population relating to protocol non-adherence (eg, as randomised analysis), and any statistical methods to handle missing data (eg, multiple imputation)  
*Not applicable*

### **Methods: Monitoring**

- Data monitoring 21a Composition of data monitoring committee (DMC); summary of its role and reporting structure; statement of whether it is independent from the sponsor and competing interests; and reference to where further details about its charter can be found, if not in the protocol. Alternatively, an explanation of why a DMC is not needed  
*This study is monitored by the clinical trial center of the Erasmus Medical Center. They are independent from the sponsor. <https://www.ctc-erasmusmc.nl/>*



	21b	Description of any interim analyses and stopping guidelines, including who will have access to these interim results and make the final decision to terminate the trial <i>Not applicable</i>
Harms	22	Plans for collecting, assessing, reporting, and managing solicited and spontaneously reported adverse events and other unintended effects of trial interventions or trial conduct <i>Toxicity will be scored according to the Common Terminology Criteria for Adverse events (CTCAE) version 5.0, as stated in the manuscript.</i>
Auditing	23	Frequency and procedures for auditing trial conduct, if any, and whether the process will be independent from investigators and the sponsor <i>Not applicable</i>
<b>Ethics and dissemination</b>		
Research ethics approval	24	Plans for seeking research ethics committee/institutional review board (REC/IRB) approval <i>Approval of the trial was given by the research ethics committee, as is stated in the manuscript on page 15, ethics and dissemination.</i>
Protocol amendments	25	Plans for communicating important protocol modifications (eg, changes to eligibility criteria, outcomes, analyses) to relevant parties (eg, investigators, REC/IRBs, trial participants, trial registries, journals, regulators) <i>All substantial changes in trial conduct will be changed in the protocol with a protocol amendment, as stated on page 15 in the manuscript, ethics and dissemination.</i>
Consent or assent	26a	Who will obtain informed consent or assent from potential trial participants or authorised surrogates, and how (see Item 32) <i>This is stated in the manuscript on page 10, eligibility criteria.</i>
	26b	Additional consent provisions for collection and use of participant data and biological specimens in ancillary studies, if applicable <i>This is stated in the patient information folder which the patients sign together with a trained physician. This patient information folder is approved by the Central Committee on Research Involving Human Subjects (CCMO in Dutch) and the Research Ethics Committee (METC in Dutch) of the Erasmus MC. This informed consent form is in Dutch and is attached to the manuscript.</i>
Confidentiality	27	How personal information about potential and enrolled participants will be collected, shared, and maintained in order to protect confidentiality before, during, and after the trial <i>This is stated in the patient information folder which the patients sign together with a trained physician. This patient information folder is approved by the Central Committee on Research Involving Human Subjects (CCMO in Dutch) and the Research Ethics Committee (METC in Dutch) of the Erasmus MC. This informed consent form is in Dutch and is attached to the manuscript.</i>

Declaration of interests	28	Financial and other competing interests for principal investigators for the overall trial and each study site <i>Not applicable</i>
Access to data	29	Statement of who will have access to the final trial dataset, and disclosure of contractual agreements that limit such access for investigators <i>This is stated in the manuscript on page 15, ethics and dissemination.</i>
Ancillary and post-trial care	30	Provisions, if any, for ancillary and post-trial care, and for compensation to those who suffer harm from trial participation. <i>This is stated in the patient information folder which the patients sign together with a trained physician. This patient information folder is approved by the Central Committee on Research Involving Human Subjects (CCMO in Dutch) and the Research Ethics Committee (METC in Dutch) of the Erasmus MC. This informed consent form is in Dutch and is attached to the manuscript</i>
Dissemination policy	31a	Plans for investigators and sponsor to communicate trial results to participants, healthcare professionals, the public, and other relevant groups (eg, via publication, reporting in results databases, or other data sharing arrangements), including any publication restrictions. <i>This is stated in the manuscript on page 15, ethics and dissemination.</i>
	31b	Authorship eligibility guidelines and any intended use of professional writers <i>Not applicable</i>
	31c	Plans, if any, for granting public access to the full protocol, participant-level dataset, and statistical code <i>Not applicable</i>
<b>Appendices</b>		
Informed consent materials	32	Model consent form and other related documentation given to participants and authorised surrogates <i>The consent forms are in the patient information folder which the patients sign together with a trained physician. This patient information folder is approved by the Central Committee on Research Involving Human Subjects (CCMO in Dutch) and the Research Ethics Committee (METC in Dutch) of the Erasmus MC. This informed consent form is in Dutch and is attached to the manuscript.</i>
Biological specimens	33	Plans for collection, laboratory evaluation, and storage of biological specimens for genetic or molecular analysis in the current trial and for future use in ancillary studies, if applicable <i>This is stated in the manuscript, beginning at subheading “vaccine-specific response” until “antitumor responses”.</i>

---

\*It is strongly recommended that this checklist be read in conjunction with the SPIRIT 2013 Explanation & Elaboration for important clarification on the items. Amendments to the protocol should be tracked and dated. The SPIRIT checklist is copyrighted by the SPIRIT Group under the Creative Commons “Attribution-NonCommercial-NoDerivs 3.0 Unported” license.

WHO Trial Registration Data Set	
Primary registry and trial identifying number	EudraCT number: 2021-000289-13 Netherlands trial register: NL9723
Date of registration in primary register	20 <sup>th</sup> July 2021
Protocol version	Version 3, date 27-05-2021
SPIRIT guidelines data set for clinical trials	Attached as a supplementary file
Source of monetary or material support	F.R. van 't Land, Study Coordinator Department of Surgery Erasmus MC University Medical Center, Rotterdam, The Netherlands. E: f.vantland@erasmusmc.nl
Primary Sponsor	Erasmus MC University Medical Center, Department of Pulmonary Medicine, Represented by Prof. Dr. J.G.J.V. Aerts, Rotterdam, The Netherlands
Contact for Public Queries	F.R. van 't Land, Study Coordinator Department of Surgery Erasmus MC University Medical Center, Rotterdam, The Netherlands. E: f.vantland@erasmusmc.nl
Contact for Scientific Queries	C.H.J. van Eijck, Coordinating investigator Department of Surgery Erasmus MC University Medical Center, Rotterdam, The Netherlands. E: c.vaneijck@erasmusmc.nl
Public Title	Combining dendritic cell vaccination and anti-CD40 agonist for metastatic pancreatic cancer patients
Scientific Title	Safety and tumor-specific immunological responses of combined dendritic cell vaccination and anti-CD40 agonistic antibody treatment for patients with metastatic pancreatic cancer: a phase I, open-label, single-arm, dose-escalation study (REACTiVe-2 Trial)
Countries of Recruitment	The Netherlands
Health Condition(s) or Problem(s) Studied	Metastatic pancreatic cancer
Intervention(s)	Vaccinations with autologous dendritic cells pulsed with an allogeneic mesothelioma tumor cell lysate (MesoPher) Anti-CD40 agonist (mitazalimab)
Key Inclusion and Exclusion Criteria	See supplementary table 2
Study Type	Open-label, single-center, phase I dose finding study
Date of First Enrollment	30 <sup>th</sup> August 2021
Sample Size	Minimum of 12, maximum of 18 patients
Recruitment Status	Recruiting
Primary Outcome(s)	Safety and tolerability of MesoPher/mitazalimab combination therapy
Key Secondary Outcomes	Assessment of immune-responses upon therapy Radiographical response rate as defined by RECIST version 1.1 and iRECIST
Ethics Review	Permission for the trial conduct was given by the Central Committee on Research Involving Human Subjects and the Medical Ethics Committee of the Erasmus MC University Medical Center Rotterdam

Supplementary Table 1. WHO trial registration data set.

Inclusion criteria	Exclusion criteria
Metastatic pancreatic cancer as defined by the presence of radiologically suspect metastatic lesions	Medical or psychological impediment to probable compliance with the protocol
Progressive disease on first-line FOLFIRINOX or modified FOLFIRINOX for metastatic pancreatic cancer. No more than 1 line of chemotherapy for metastatic disease is allowed. Prior FOLFIRINOX for locally advanced disease if given within 1 year before screening can be counted as first-line treatment. Any FOLFIRINOX given in the curative intent setting if more than a year before screening will not be considered first line therapy	Current use of steroids (or other immunosuppressive agents). Patients must have had 6 weeks of discontinuation and must stop any such treatment during the time of the study. Prophylactic usage of dexamethasone during chemotherapy is excluded from this 6-week interval
An accessible metastatic lesion for histological tissue collection	Abdominal ascites
Patients must be at least 18 years old and must be able to give written informed consent	Current or previous use of a CD40 antibody and/or anti-tumor vaccinations
WHO performance status 0-1	Serious concomitant disease, or active infections
Patients must have normal organ function and adequate bone marrow reserve: absolute neutrophil count > 1.0 x 10 <sup>9</sup> /l, platelet count > 100 x 10 <sup>9</sup> /l, and Hb > 6.0 mmol/l (as determined during screening). Transfusion in the 2 weeks preceding screening is not allowed	Prior malignancy except adequately treated basal cell or squamous cell skin cancer, superficial or <i>in-situ</i> cancer of the bladder or other cancer for which the patient has undergone curative intent treatment and has been disease-free for two years
Laboratory tests: ASAT/ALAT <5xULN (upper limit of normal), bilirubin <1.5xULN, Creatinine value <1.5xULN, Lactate dehydrogenase value < ULN and albumin value > LLN (lower limit of normal)	Known allergy to shell fish (may contain keyhole limpet hemocyanin (KLH))
Women of childbearing potential must have a negative serum pregnancy test at screening and a negative urine pregnancy test just prior to the first study drug administration on Day 1, and must be willing to use an effective contraceptive method (intrauterine devices, hormonal contraceptives, contraceptive pill, implants, transdermal patches, hormonal vaginal devices, infusions with prolonged release) or true abstinence (when this is in line with the preferred and usual lifestyle)* during the study and for at least 12 months after the last study drug administration	Serious intercurrent chronic or acute illness such as pulmonary disease (asthma or COPD), cardiac disease (NYHA class III or IV), hepatic disease or other illness considered by the study coordinator to constitute an unwarranted high risk for the investigational treatment
Men must be willing to use an effective contraceptive method (e.g. condom, vasectomy) during the study and for at least 12 months after the last study drug administration	Concomitant participation in another clinical intervention trial (except participation in a biobank study)
Ability to return to the hospital for adequate follow-up as required by this protocol	Pregnant or lactating women
Written informed consent according to ICH-GCP	Inadequate vein access to perform leukapheresis
	An organic brain syndrome or other significant psychiatric abnormality which would compromise the ability to give informed consent, and preclude participation in the full protocol and follow-up

**Supplementary Table 2.** All inclusion and exclusion criteria of the REACTiVe-2 trial.



# CHAPTER 8

---

Immunomodulatory effects of stereotactic body radiotherapy and vaccination with heat-killed mycobacterium bbuense (IMM-101) in patients with locally advanced pancreatic cancer

Sai Ping Lau\*

Freek van 't Land\*

Willem de Koning

Larissa Klaase

Madelief Vink

Anneloes van Krimpen

Jasper Dumas

Disha Vadgama

Joost Nuyttens

Dana A.M. Mustafa

Ralph Stadhouders

Marcella Willemsen

Andrew P. Subbs

Joachim G. Aerts

Casper H.J. van Eijck

*\* These authors contributed equally to this work.*

## ABSTRACT

**Background:** Patients with locally advanced pancreatic cancer (LAPC) are treated with chemotherapy. In selected cases, stereotactic body radiotherapy (SBRT) can be added to the regimen. We hypothesized that adding an adjuvant containing a heat-killed mycobacterium (IMM-101) to SBRT may lead to beneficial immuno-modulatory effects, thereby improving survival. This study aims to investigate the safety of adding IMM-101 to SBRT and to investigate the immuno-modulatory effects of the combination treatment in the peripheral blood of LAPC patients. **Methods:** LAPC patients were treated with SBRT (40 Gy) and six intradermal vaccinations of one milligram IMM-101. The primary endpoint was an observed toxicity rate of grade 4 or higher. Targeted gene-expression profiling and multicolor flow cytometry were performed for longitudinal immune-monitoring of the peripheral blood. **Results:** Twenty patients received study treatment. No treatment-related adverse events of grade 4 or higher occurred. SBRT/IMM-101 treatment induced a transient decrease in different lymphocyte subsets and an increase in CD14+CD16-CD11b+HLA-DR<sup>low</sup> myeloid-derived suppressor cells. Importantly, treatment significantly increased activated ICOS+, HLA-DR+ and Ki67+PD1+ T and NK cell frequencies. This was not accompanied by increased levels of most inhibitory markers, such as TIM-3 and LAG-3. **Conclusions:** Combination therapy with SBRT and a heat-killed mycobacterium vaccine was safe and had an immune-stimulatory effect.

## INTRODUCTION

Pancreatic ductal adenocarcinoma (PDAC) is a notoriously lethal malignancy with a five-year survival rate of less than 5% [1]. About thirty-five percent of patients present with locally advanced pancreatic cancer (LAPC) [2]. LAPC is treated with induction chemotherapy, preferably with the multi-agent FOLFIRINOX regimen in young and fit patients [3]. Next to FOLFIRINOX, gemcitabine combined with nab-paclitaxel is another adequate first-line treatment option, which is often better tolerated than FOLFIRINOX [3]. Stereotactic body radiotherapy (SBRT) can be added to the treatment regimen if there are no signs of disease progression after the chemotherapy [4–6].

Radiation therapy is the cornerstone of treatment for many cancer types, with fifty percent of cancer patients being treated with some form of radiotherapy throughout their illness [7]. Traditionally, radiation therapy has been utilized for its direct cytotoxic properties, inducing tumor cell apoptosis [8]. However, besides the direct cytotoxic effect, there is emerging evidence that radiation, particularly SBRT, has potential immuno-modulatory effects. Upregulation of immunogenic cell surface markers such as ICAM-1, MHC-1 and Fas on tumor cells has been described following radiotherapy [9–13]. Cancer cells may escape immune surveillance through the downregulation of MHC-1 molecules [14]. The upregulation of MHC-1 molecules by radiation therapy may revert this escape mechanism. Additionally, irradiation can induce an upregulation of FAS molecules on tumor cells, thereby improving the cytotoxic efficacy of T cells [12]. Moreover, radiotherapy has been demonstrated to be able to induce immunogenic cell death [15], thereby reinforcing the cancer-immunity cycle [16,17]. In our previous LAPC-1 trial, LAPC patients were treated with FOLFIRINOX followed by SBRT [5]. The SBRT treatment was found to be safe, and the median overall survival (OS) in patients who received SBRT after FOLFIRINOX was 17 months (95% CI 14–21). As PDAC is considered an immunological cold tumor, the anti-tumor immune response in LAPC patients treated with SBRT monotherapy after systemic chemotherapy is probably not optimal. Adding an adjuvant to SBRT could improve the immunological conditions for an effective immune response. In this first-in-human trial, the addition of a vaccine containing a heat-killed mycobacterium obuense (IMM-101), to SBRT was investigated. IMM-101 has been demonstrated to induce the activation and maturation of dendritic cells *in vitro* [18]. Moreover, in a pancreatic cancer murine model, IMM-101 demonstrated to be able to produce protective CD8+ T cell responses [19]. A previous randomized controlled trial in patients with advanced pancreatic cancer investigated the value of adding IMM-101 to gemcitabine treatment [20]. The addition of IMM-101 to gemcitabine was associated with an improvement in OS from 4.4 to 7.0 months (95% CI 0.33–0.87,  $p = 0.01$ ) in a pre-defined metastatic subgroup [20]. Next to this, an interesting case report presented a case of a patient with metastasized pancreatic cancer who underwent a synchronous resection of the primary tumor and liver metastases, after multimodality treatment with chemotherapy, IMM-101 and chemoradiation. This patient was free of disease four years after diagnosis [21].



Additionally, promising outcomes have been reported in melanoma patients treated with IMM-101 as well [22,23]. We hypothesize that IMM-101 vaccinations can enhance a host's innate immune response, improving the immuno-modulatory effects and in situ vaccination efficacy of SBRT.

In this study, we present the results of the immuno-monitoring of the peripheral blood in patients with locally advanced pancreatic cancer treated with SBRT and IMM-101, as well as their clinical outcome.

## TREATMENT SCHEME AND METHODS

### *Study Design and Participants*

The LAPC-2 trial was a single-center, single-arm, non-randomized, open-label, phase I/II trial treating biopsy proven LAPC patients with SBRT and IMM-101, after prior treatment with at least 4 cycles of FOLFIRINOX. LAPC was defined according to the guidelines of the Dutch Pancreatic Cancer Group as >90 contact with the superior mesenteric artery, the celiac axis and/or any hepatic artery and/or >270 contact with the superior mesenteric vein or the portal vein and/or occlusion of these veins [24]. Main inclusion criteria were (1) age > 18 years and < 75 years, (2) WHO performance status of 0 or 1, (3) normal renal and liver function, (4) largest tumor size <7 cm x 7 cm x 7 cm, and (5) no evidence of metastatic disease. Main exclusion criteria were (1) prior radiotherapy, chemotherapy other than FOLFIRINOX or pancreatic resection, (2) current or previous treatment with immunotherapeutic drugs, and (3) use of corticosteroids. The study was approved by the Central Committee on Research involving Human Subjects (NL68762.078.19) as defined by the Medical Research Involving Human Subjects Act. Procedures followed were in accordance with the ethical standards of these committees on human experimentation and with the Helsinki Declaration of 1975, as revised in 2008. The trial is registered with the Netherlands Trial Register, NL7578. Written informed consent was obtained from each subject. All detailed inclusion and exclusion criteria are listed in Supplementary Table S1.

### *SBRT and IMM-101 Vaccination*

The tumors were irradiated with the Cyberknife (Accuray Incorporated, Sunnyvale, CA, USA). To accurately guide the radiation, the gastroenterologist placed three radiopaque markers in or near the tumor (within 3cm of the tumor). Patients received a total of 40 Gray (Gy) of SBRT in five fractions on consecutive days. Radiation started at week 2, just after patients received the second vaccination of IMM-101. Immodulon Therapeutics Ltd. (Uxbridge, UK) produced and shipped pre-labelled IMM-101 vials to the pharmacy of the Erasmus MC University Medical Center. IMM-101 was injected intradermally over the deltoid muscle by the standard Mantoux intradermal injection technique. One mL was injected, which contained one milligram of IMM-101. IMM-101 was administered six times: *i.e.*, on week 0, week 2, week 4, week 8, week 10

and week 12. Figure 1 illustrates the treatment schedule. At week 0, week 2, week 4, week 8 and week 14 blood draws were performed for immunomonitoring; *i.e.*, before planned study drug administration or SBRT treatment. One red 10 mL clot activator tube from BD Vacutainer®, one 3 mL Tempus™ RNA stabilisator tube and two 10 mL EDTA tubes from BD Vacutainer® were collected. The blood was processed within six hours after collection. Plasma, serum and peripheral blood mono-nuclear cells (PBMCs) were isolated and cryopreserved.

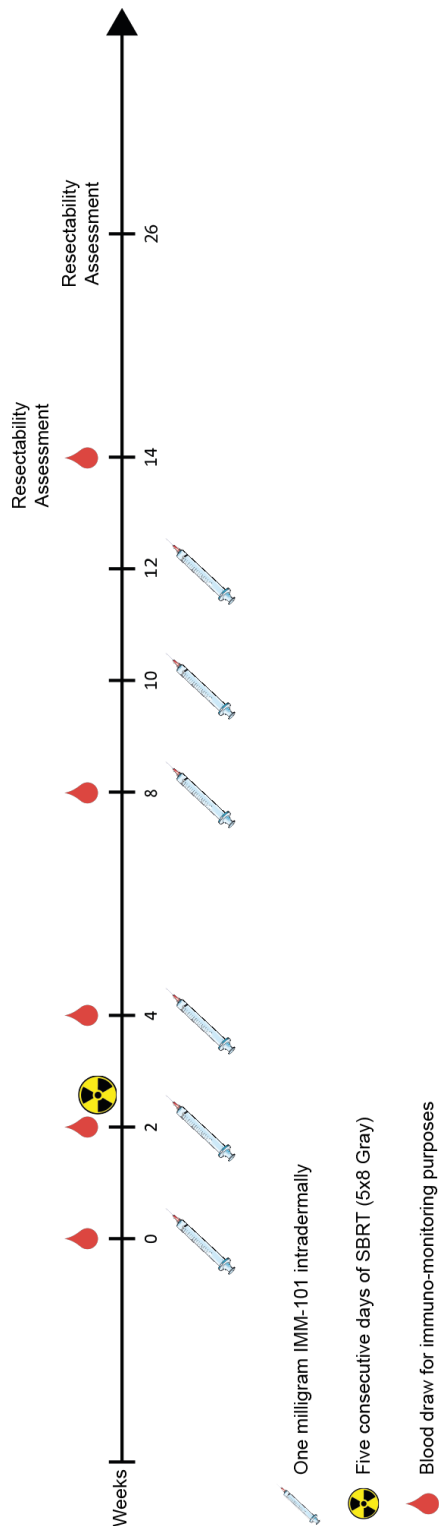


**Figure 1.** Schematic treatment schedule. After discontinuation of FOLFIRINOX treatment, patients were included in the trial. Patients received three bi-weekly intradermal vaccinations of IMM-101 at weeks 0, 2 and 4. At week 2, after the second vaccination, stereotactic body radio-therapy (SBRT) treatment started. Patients received 5 x 8 Gy of SBRT. They received three more vaccinations at weeks 8, 10 and 12. At week 14, the first resectability assessments was per-formed. Some patients were offered an explorative laparotomy with possible resection.

### *Follow up and Resectability Assessments*

At week 14, resectability was assessed based on CT scans, biochemical response and the patients' clinical situation. An explorative laparotomy was performed in fit patients with a possibly resectable tumor and a >50% decrease in CA 19.9. In case of local and distant tumor progression, the patient was referred to the medical oncologist. The decision for an explorative laparotomy was made by a multidisciplinary tumor board consisting of at least a radiologist specialized in abdominal radiology, an experienced pancreas surgeon and a medical oncologist. After completion of IMM-101 treatment, routine follow-up was started until the time of death or 5 years after completion of SBRT. Follow-up visits included regular CT scans and tumor-marker assessments.

### *Objectives and Endpoints*

The primary objective of the phase I study was to determine the safety of adding IMM-101 to SBRT. The endpoint for this objective was an observed toxicity rate of grade 4 or higher related to the study treatment. Toxicities were scored according to CTCAE criteria version 5.0 [25]. The secondary objective was to investigate the immuno-modulatory effects of the combination treatment in the peripheral blood. Endpoints for this were the changes in the circulating immune cell compartment on RNA and protein level.

### *Targeted Gene-Expression Profiling*

RNA was isolated from Tempus blood tubes using Tempus TM Spin RNA Isolation Reagent Kit (Thermo Fisher Scientific, Breda, The Netherlands). Isolated RNA was purified using RNeasy® MinElute® Cleanup Kit (Qiagen, Leiden, The Netherlands). The RNA quantity and quality were measured using the Agilent 2100 BioAnalyzer (Santa Clara, CA, USA). The RNA concentration was corrected to include the fragments  $\geq 300$  bp. For each sample, 200 ng of RNA was hybridized with probes of the PanCancer Immune profiling panel (730 innate and adaptive immune related genes and 40 housekeeping genes) for 17 h at 65 °C, following the manufacturing procedure (NanoString Technologies Inc., Seattle, WA, USA). The nCounter® FLEX platform was used to wash the extra probes, and genes were counted by scanning 490 Fields-of-view (FOV). The raw data of gene counts were uploaded to the nSolver™ Data Analysis software (version 4.0, NanoString, Seattle, WA, USA). The gene counts were normalized using the Advanced Analysis module (version 2.0) of nSolver™.

### *Flow Cytometry Immuno-Monitoring*

For the enumeration of immune subsets, whole blood was freshly stained for flow cytometry. In addition, longitudinal immuno-monitoring was performed on liquid nitrogen stored PBMCs. Cell surface staining was carried out after blocking Fc receptors by incubating cells with fluorescently conjugated mAbs directed against CD4 (SK3), CD11b (ICRF44), CD14 (M5E2), CD19 (HIB19), CD20 (2H7) CD56 (NCAM16.2), CD86 (FUN-1), HLA-DR (G46-6), ICOS (DX29) and ICOS-

L (2D3/B7-H2) (all BD Biosciences, Erebodegem, Belgium); CD8 (SK1), CD11c (BV605), CD15 (HI98), CCR7 (G043H7), LAG-3 (11C3C65), PD-1 (EH12.2H7), TIM-3 (F38-2E2) (all BioLegend, Amsterdam, The Netherlands); and CD3 (UCHT1), CD33 (WM-53), CD45RA (MEM-56), CTLA-4 (14D3), FOXP3 (236A/E7), Ki-67 (20Raj1) (all Thermo Fisher Scientific). Intracellular transcription factor staining was performed using the FoxP3 Staining Buffer Set (Thermo Fisher Scientific). Cells were in addition stained for viability using fixable LIVE/DEAD aqua cell stain (Thermo Fisher Scientific). Data were acquired using the Symphony flow cytometer (BD Biosciences) and analyzed with FlowJo v10.7. Cell subsets are gated as previously described [26,27].

#### *Statistical Analysis—Sample Size Calculation*

The primary objective of the phase I trial was to determine the safety of adding IMM-101 to SBRT. In our previous LAPC-1 trial, the grade 4 toxicity rate of SBRT was 10% [5]. With a sample size of 20 for the phase I trial, we were able to estimate a toxicity rate of 10% within a 95% confidence interval of [1.2–31.7%] using the binomial exact method. This means that a maximum of 6/20 (30%) patients were allowed to have grade 4 toxicity or higher for the treatment to be regarded as safe and before proceeding to the phase II trial.

#### *Statistical Analysis—Data Analysis and Visualisation*

Baseline patient characteristics are summarized using the median and interquartile range for continuous variables and using counts and percentages for categorical variables. PFS and OS were calculated from start date of FOLFIRINOX chemotherapy to the first documented event. Survival estimates were calculated using Kaplan–Meier method. Flow cytometry data were normalized for baseline. Paired Wilcoxon signed-ranks tests were used to test for significance between baseline measurements and other time points. Figures were made using GraphPad Prism software v8.0. Gene-expression data were corrected for multiple testing using the Benjamini–Hochberg procedure. In all cases, a p-value of 0.05 and below was considered significant (\*),  $p < 0.01$ (\*\*) and  $p < 0.001$  (\*\*\*) as highly significant. The heat map was generated using the average log<sub>2</sub> normalized gene expression of the significant differentially expressed genes per week. The heat map was visualized using the web-based tool Morpheus [28]. The Spearman correlations were calculated using the PFS or OS and the absolute difference between baseline and week 4 (after IMM101/SBRT) of activated cell frequencies. The volcano plots and correlations were visualized in R (version 4.1.1).

## RESULTS

#### *Patient and Treatment Characteristics*

A total of 21 patients were included in the phase I, LAPC-2 trial, between October 2019 and June 2020. The first included patient (IMM001) had a liver metastasis, which was found during endoscopic ultrasound that was performed to place the radio-opaque markers for the SBRT.

This patient was, therefore, excluded. Eventually, 20 patients received study treatment. Patients were treated with a median of 8 (8–9) cycles of FOLFI-RINOX before inclusion in the trial. The median time between FOLFIRINOX and the first IMM-101 vaccination was 6.4 (5.2–7.8) weeks. The median age was 63 (60–68) years and 11 (55%) were male. Their median body mass index was 24 (21–28) kg/m<sup>2</sup>. All patients received the total dose of 40 Gy of SBRT. Nineteen patients received the six planned vaccinations with IMM-101 and one patient received only three vaccinations due to disease progression.

Immune analyses of the PBMCs were performed in 19/20 patients due to the absence of sufficient PBMCs in patient IMM016. Gene expression analyses were performed in 19/20 patients because we were not able to isolate RNA from IMM017. Detailed patient and treatment characteristics are shown in Table 1.

Patient Characteristics	N = 20 (IQR) or [%]
Age, years	63 (60–68)
Male sex	11 [55]
BMI, kg/m <sup>2</sup>	24 (21–28)
ECOG performance status *	
0	4 [20]
1	16 [80]
CA 19.9 at inclusion, kU/L	101 (43–137)
CEA at inclusion, µg/L	4.4 (3.5–5.8)
Leukocyte count at inclusion, ×10 <sup>9</sup> /L	6.7 (4.7–9.9)
Platelet count at inclusion, ×10 <sup>9</sup> /L	195 (133–232)
Neutrophil count at inclusion, ×10 <sup>9</sup> /L	3.6 (2.7–7.2)
Lymphocyte count at inclusion, ×10 <sup>9</sup> /L	1.4 (1.2–1.8)
SII, (N x P) / L	624 (311–889)
NLR	3.1 (2.3–5.0)
PLR	147 (87 – 171)
<b>Treatment characteristics</b>	
Biliary stenting at diagnosis	9 [45]
Diagnostic laparoscopy at diagnosis	6 [30]
FOLFIRINOX treatment	20 [100]
FOLFIRINOX, cycles	8 (8–9)
Interval stop FOLFIRINOX and start IMM-101, weeks	6.4 (5.2–7.8)
40 Gray of SBRT	20 [100]
IMM-101	20 [100]
Six vaccinations	19 [95]
Three vaccinations	1 [5]
Resection	4 [20]

**Table 1.** Patient and treatment characteristics. Statistics: Continuous variables are shown as medians with interquartile range and categorical variables are shown as counts with percentages. Abbreviations: BMI = body mass index, ECOG = Eastern Cooperative Oncology Group, CA 19.9 = carbohydrate antigen 19.9, CEA = carcinoembryonic antigen, SII = Systemic-Immune-Inflammation index, NLR = neutrophil to lymphocyte ratio, PLR = platelet to lymphocyte ratio, SBRT = stereotactic body radiotherapy, N = neutrophils, P = platelets, L = lymphocytes. \* ECOG performance status 0 = Fully active, able to carry on all pre-disease performance without restriction. ECOG performance status 1 = Restricted in physically

strenuous activity but ambulatory and able to carry out work of a light or sedentary nature, *e.g.* light housework, office work.

### *Safety and Clinical Outcome*

In 6/20 patients, we observed eleven grade 3 adverse events, of which three were considered to be possibly related to SBRT. None were related to IMM-101. Toxicity of grade 4 or higher was not observed. All patients experienced mild injection-site reactions, ranging from erythema to skin abscesses, with none resulting in systemic symptoms. Table 2 shows all grade 3 or higher toxicities. At present, (*i.e.* May 2022), 18/20 (90%) patients have experienced progression (local or distant) of disease and 17/20 (85%) patients have died. In all patients, the median PFS was 11.7 months (95% CI: 10.2–13.3) and the median OS was 17.8 months (95% CI: 11.3–24.4). The median PFS and median OS of the unresected patients (n = 16) was 11.2 (95% CI: 8.0–14.4) and 17.8 (95% CI: 12.0–23.6) months, respectively. Four (20%) patients underwent a resection of the tumor. In one patient, a small, solitary liver metastasis was found during explorative laparotomy and the primary tumor and the metastasis were both resected. This patient was free of disease 15 months after the operation. Another patient experienced local recurrence of disease four months after the resection. This was treated with systemic chemotherapy. In the absence of disease progression, a re-resection was performed 12 months after the initial resections. This patient was free of disease 8 months after the re-resection. Two patients died from complications from the operation.

Subject	Adverse Event Term	Grade	Relation to SBRT	Relation to IMM-101
IMM003	Gastro-intestinal haemorrhage	3	Possibly	Unrelated
IMM006	Gastro-intestinal haemorrhage	3	Possibly	Unrelated
IMM007	Gastro-intestinal haemorrhage	3	Unrelated	Unrelated
IMM007	Gastro-intestinal haemorrhage	3	Possibly	Unrelated
IMM007	Stent dysfunction	3	Unrelated	Unrelated
IMM007	Cholangitis	3	Unrelated	Unrelated
IMM007	Stent dysfunction	3	Unrelated	Unrelated
IMM008	Cholestasis	3	Unrelated	Unrelated
IMM008	Cholangiosepsis	3	Unrelated	Unrelated
IMM009	Vertigo	3	Unrelated	Unrelated
IMM014	Duodenal obstruction	3	Unrelated	Unrelated

**Table 2.** Grade 3 or higher adverse events. Toxicities were scored according to Common Terminology Criteria for Adverse Events (CTCAE) version 5.0 [25]. The treating physicians judged the possibility of a relation to the study treatment. Adverse events not related to SBRT or IMM-101 were considered to be related to pancreatic ductal adenocarcinoma. Abbreviations: SBRT = stereotactic body radiotherapy.

### *Downregulation of Genes Related to Lymphocyte Subsets and Immune inhibition after IMM-101/SBRT*

Targeted gene expression profiling was performed to investigate the effect of IMM-101 and SBRT on the immune cells. Apart from increased expression of three genes (*i.e.* LTF, CAMP and LCN2) at baseline, no significant differences were observed between baseline (week 0) and after

one vaccination IMM-101 (week 2) (Supplementary Figure S1). However, in week 4, after SBRT combined with IMM-101, profound changes were observed in immune-related gene expression (Figure 2A, B). Various genes related to lymphocyte subsets were downregulated (*i.e.* CD8a, MS4A1, CD22, CD79A, KLR family genes). Furthermore, genes related to lymphocyte inhibition/exhaustion (*i.e.* BTLA, TBX21, KLRC1) were also downregulated after IMM101/SBRT treatment. These results indicate changes in the circulating lymphoid compartment of LAPC patients specifically after combined IMM-101/SBRT treatment.

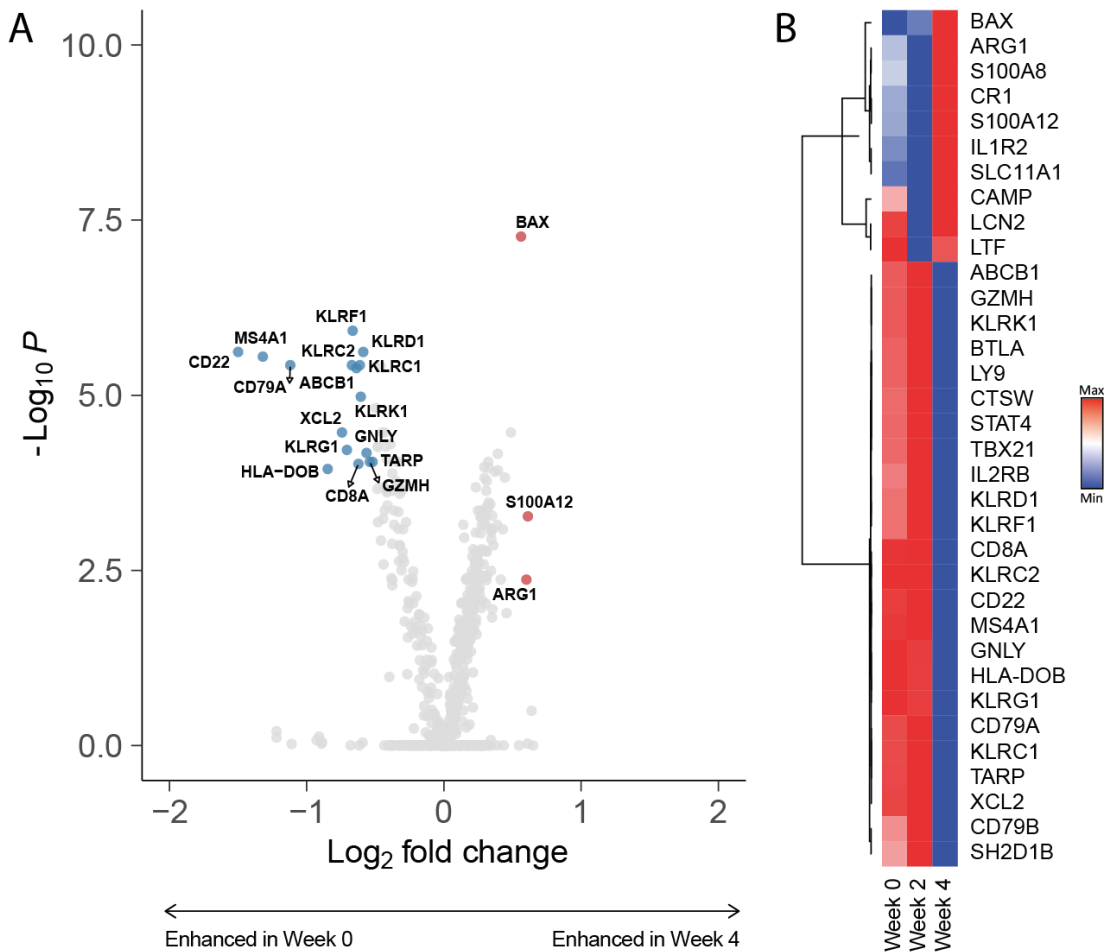


**Figure 2.** SBRT/IMM-101 induced gene expression. (a) Volcano plot demonstrating genes upregulated at baseline versus week 4. Highlighted genes underwent a  $\log_2$  fold change  $< -0.5$  or  $> 0.5$  and  $p$ -value  $< 0.05$ . (b) Heat map of significantly differentially expressed genes between week 0, week 2 and week 4.

#### *Reduced Peripheral Lymphocyte Numbers following IMM-101/SBRT*

We additionally assessed various immune subsets in the peripheral blood using flow cytometry. No significant changes in immune subsets were observed two weeks after the first vaccination with IMM101. The addition of SBRT transiently reduced CD4<sup>+</sup> and CD8<sup>+</sup> T cells, CD19<sup>+</sup> B-lymphocytes and CD56<sup>+</sup> NK cells (Figure 3). SBRT did not curtail the myeloid compartment (*i.e.* CD15<sup>+</sup>CD16<sup>-</sup> eosinophils, CD15<sup>+</sup>CD16<sup>+</sup> neutrophils, CD14<sup>+</sup>CD16<sup>-</sup> monocytes, CD14<sup>-</sup>CD16<sup>-</sup>CD11c<sup>+</sup> dendritic cells). Additionally, the number of CD14<sup>+</sup>CD16<sup>-</sup>CD11b<sup>+</sup>HLA-DR<sup>low</sup> MDSCs

increased after combining SBRT and IMM-101 (Supplementary Figure S2). Lymphocyte cell numbers recovered at week 8, within 6 weeks after SBRT.

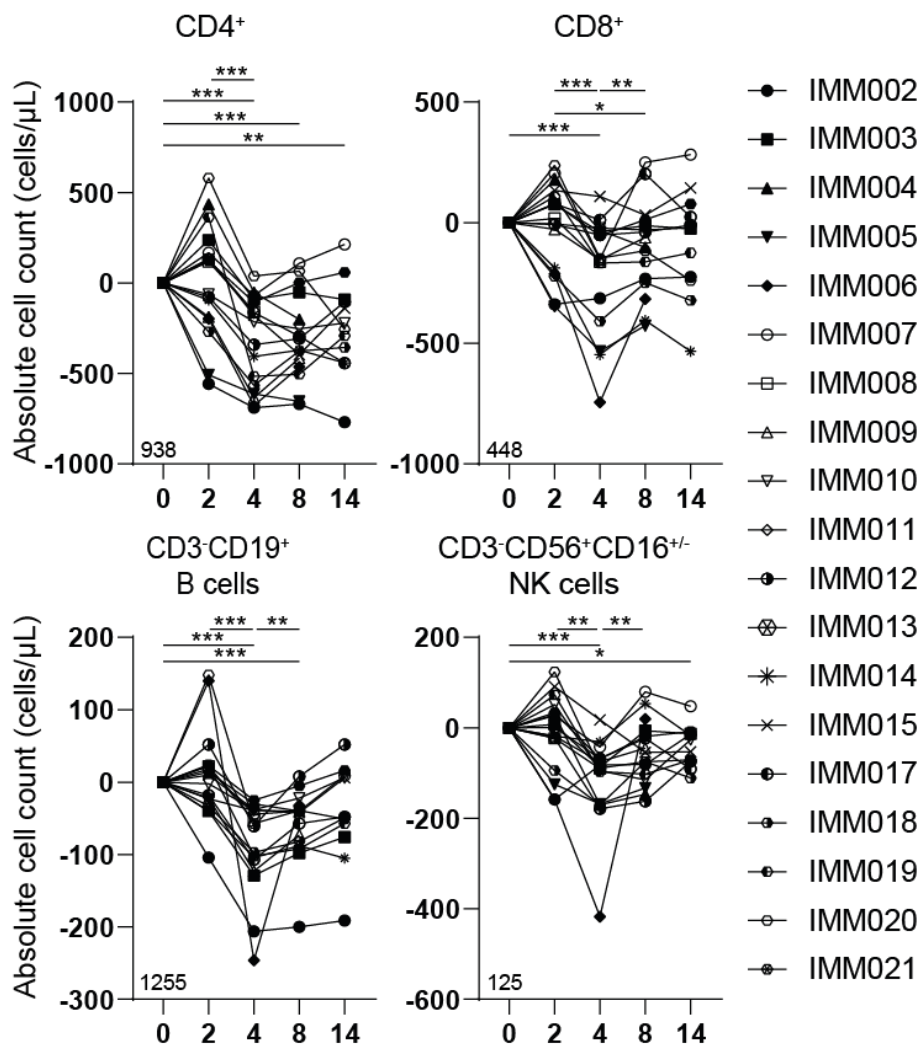


**Figure 3.** SBRT/IMM-101 induced transient lymphodepletion. Number of CD4+, CD8+, CD3-CD19+ and CD3-CD56+CD16+/- peripheral blood lymphocytes per  $\mu\text{L}$  blood.  $N = 19$ . Data were normalized for baseline (week 0) and paired per patient. Percentage in the bottom left corner is the average frequency at baseline. Significance was determined using the paired Wilcoxon signed-rank test. \*  $p < 0.05$ , \*\*  $p < 0.01$ , \*\*\*  $p < 0.0001$ .

#### *IMM-101/SBRT Increased Proportions of Activated Lymphocytes*

In-depth longitudinal immune monitoring was performed to further describe the phenotypic characteristics of immune cells following study therapy. We did not find changes in activation or inhibitory marker expression on CD4+ regulatory T cells or CD4+ T helper cells or cytotoxic CD8+ T cells after one vaccination with IMM-101 in week 2. In contrast, the addition of SBRT significantly increased the frequencies of activated CD4+ and CD8+ T cells and CD56+ NK cells in week 4 as indicated by the markers ICOS, HLA-DR as well as the combined increase in Ki67 and PD-1 levels. Notably, this increase was not observed for the inhibitory markers PD-1, TIM-3 and LAG-3, although we did observe significantly upregulated CTLA-4 levels on the CD4+ Non-



Tregs after combination therapy. Furthermore, the increase in activated CD4+ and CD8+ T cell frequencies was mainly driven by the memory compartment (*i.e.* CCR7+CD45RA- central memory and CCR7-CD45RA- effector memory) [Not shown]. One vaccination of IMM-101 did significantly increase activated CD86+CD19+ B cell frequencies in week 2. The addition of SBRT further activated these CD19+ B cells demonstrated by increased Ki67+PD-1+ and CD86+ frequencies. Lastly, IMM-101/SBRT transiently induced higher frequencies of CD11c+ dendritic cells, HLA-DR+ CD14+ macrophages and HLA-DR-CD14-CD15- DN-MDSCs. Data are shown in detail in Figures 4 and S3.

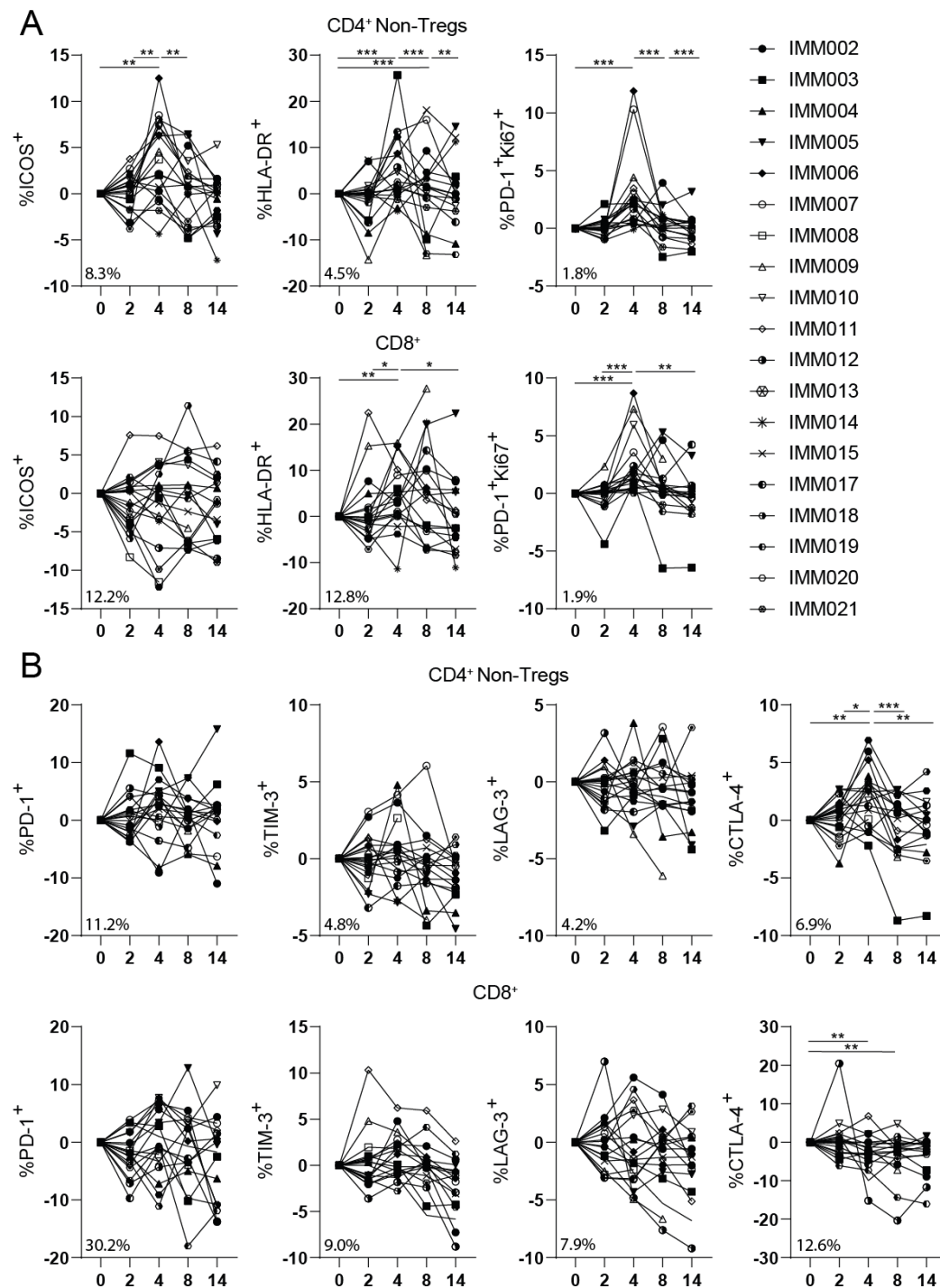


**Figure 4.** SBRT/IMM-101 induced T-cell activation. (a) Percentage of ICOS+, HLA-DR+, PD-1+/Ki67+ subsets of CD4+ Non-Tregs and CD8+ cells. (b) Percentage of PD-1+, TIM-3+, LAG-3, CTLA-4+ subsets of CD4+ Non-Tregs and CD8+ cells. N = 19. Data were normalized for baseline (week 0) and paired per patient. Percentage in the bottom left corner is the average frequency at baseline. Significance was determined using the paired Wilcoxon signed-rank test. \* p < 0.05, \*\* p < 0.01, \*\*\* p < 0.0001.

*Treatment-Induced Increase in Activated Lymphocytes Is Correlated with Survival*

To explore if treatment-induced effects could be translated to clinical outcome, we analyzed if absolute differences in immune cell status between treatment-naïve (week 0) and study treatment samples (week 4) were correlated with survival. Patients who underwent a resection (n = 4) were excluded from this analysis, since a resection possibly influences PFS and OS outcomes. Another patient (IMM016) was excluded from the analysis due to an absence of sufficient PBMCs. Therefore, eventually 15 patients were included in the analysis. We found that increased levels of CD28+ effector memory (CCR7-CD45RA+) cytotoxic T cells correlated with improved PFS and OS (Figure 5).

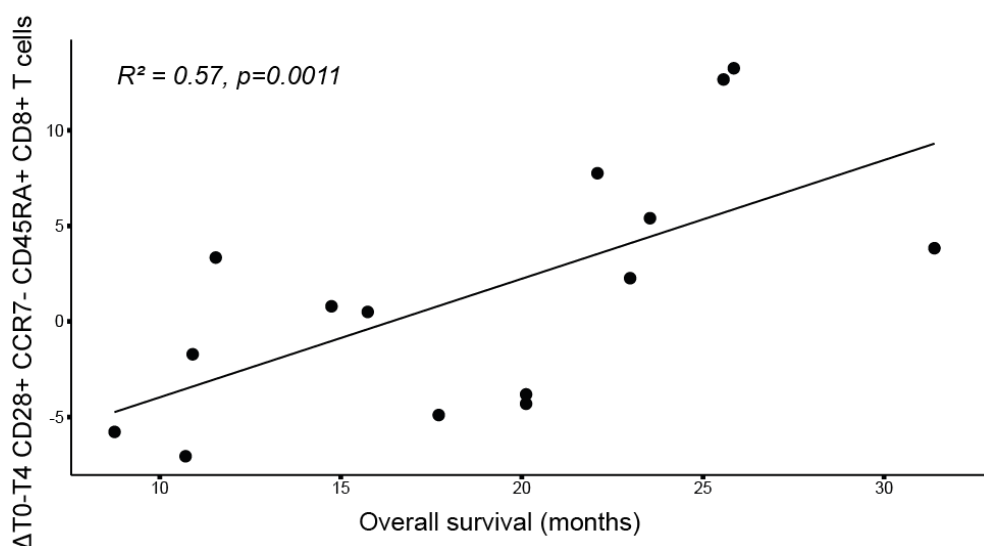
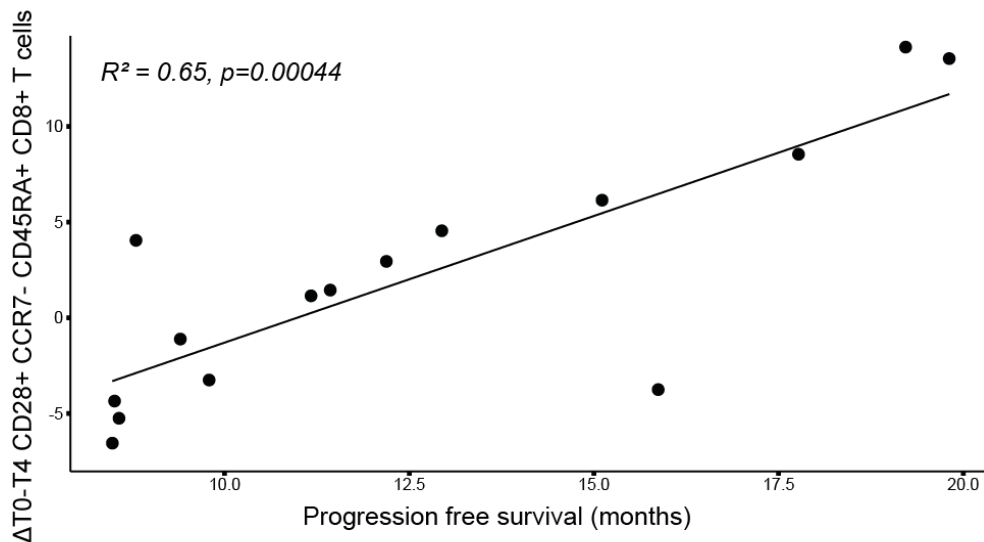


**Figure 5.** Treatment-induced T-cell activation correlated with improved progression-free survival. Spearman correlation plots demonstrating a positive correlation between IMM101/SBRT-induced absolute difference of CD28+ CCR7- CD54RA+ cytotoxic T cells and progression-free survival and overall survival. N = 15.

## DISCUSSION

In this first-in-human trial, we firstly assessed the safety of IMM101/SBRT treatment, in patients with LAPC after prior treatment with FOLFIRINOX chemotherapy.

All patients experienced injection site reactions, which were uncomfortable for some patients. Eleven grade 3 toxicities were observed, of which three were possibly related to SBRT treatment. No grade 4 or higher toxicities were reported and none of the observed toxicities were considered to be related to IMM-101. This treatment approach demonstrated to be safe, and the trial proceeded to the phase II trial.

Secondly, we investigated the immunomodulatory effects of IMM-101/SBRT treatment in the peripheral blood. Two weeks after the first vaccination with IMM-101, no explicit changes on gene expression and protein level in the immune system of LAPC patients could be demonstrated. After treatment with IMM-101 with SBRT, we observed a downregulation of genes related to lymphocyte subsets, and this lymphodepletion was confirmed by flow cytometry. Interestingly, IMM-101/SBRT treatment did induce a rise in the number of MDSCs. Radiotherapy-induced MDSC expansion in patients with PDAC has previously been described [29]. It is also likely that SBRT and not IMM-101 induced the lymphodepletion, seeing that, in a previous study, external beam radiotherapy caused systemic immune-cell depletion [30]. Except MDSCs, cell numbers of other cell subsets within the myeloid compartment did not significantly increase. The latter may be explained by the fact that the radio-resistance of suppressive myeloid cells is stronger than that of lymphocytes [31].

Our combined gene expression and flow cytometry analyses demonstrated therapy-induced activation of T cell and NK cell subsets, with no increase in most inhibitory markers (*i.e.* PD-1, TIM-3 and LAG-3). Interestingly, therapy-induced activation of T cells occurred mainly in the memory compartment, which may be beneficial for seeding the tumor with antigen-specific T cells to mount successful anti-tumor responses. In agreement with this notion, improved PFS and OS were correlated with increased levels of activated effector memory cytotoxic T cells. In pre-clinical models, ablative doses of radio-therapy have been associated with improved intratumoral CD8+ T cell infiltration due to increased antigenicity of malignant cells, or by promoting immuno-stimulatory signals to recruit and activate antigen-presenting cells [32,33]. We found limited significant changes 2 weeks after the first vaccination with IMM-101. Still, the CD86+ expression on B cells increased. Adding SBRT further augmented the B cell activation, as demonstrated by the increase in Ki67+PD-1+ and CD86+ frequencies. A higher B cell activation may be beneficial, as B cell activation has been associated with positive responses to cancer-immunotherapy [34,35].

SBRT may hypothetically improve the anti-tumor efficacy of IMM-101 through anti-gen release upon tumor destruction, inducing in situ vaccination. IMM-101 could concurrently provide enhanced innate immunity to engage robust T cell responses. Unfortunately, the current study design did not allow for us to investigate this mechanism. Next to this, the common limitations of phase I/II trials, such as a small sample size and the lack of a control group, also applied to this study. However, the sample size was adequate to prove the safety of the combination treatment. Moreover, despite the low number of patients, a clear trend in immunological changes could be observed in most patients, which strengthens the hypothesis that treatment-induced immune modulation existed. Due to the lack of a control group, the observed changes could theoretically be better explained by time than by a cause-effect phenomenon caused by the treatment. However, certain factors argue against this. Firstly, between week 0 and 2, no significant changes occurred. In contrast, between week 2 and week 4, drastic changes were observed in the peripheral immunity. This occurred after the second vaccination and the SBRT treatment. The lack of changes in the first two weeks, compared to the extensive changes that occurred between week two and four, combined with the timing of treatment, argue against the hypothesis that the immunological changes were mostly impacted by time. Secondly, the observed immunological changes after SBRT/IMM-101 treatment tended to restore mostly to base-line after time progressed. If time and, thus, disease progression was the main factor explaining the changes in the immune system, one would expect these changes to persist as time progressed. Another limitation of this study is that our analysis was only focused on peripheral immunity. A local assessment of the immune composition would have improved understanding of the study-treatment effect, as SBRT acts directly on the tumor. Nonetheless, the upregulation of immune checkpoints on circulating T cells, including CTLA-4, endorse the addition of immune-checkpoint blocking antibodies in future studies. Moreover, combining checkpoint-blocking antibodies with radiotherapy alone, or possibly with IMM-101, has shown promising results in pre-clinical models [36,37]. In addition to combination with immune-checkpoint-blocking antibodies, intratumoral administration of IMM-101 could improve its clinical efficacy. The most-used mycobacterium vaccine is the live-attenuated Mycobacterium Bovis Bacillus Calmette-Guérin (BCG) vaccine [38]. This tuberculosis vaccine was demonstrated to be able to induce potent anti-tumor immunity and adjuvant intravesical BCG instillations after a transurethral resection of bladder cancer, and was proved to be effective in preventing bladder cancer recurrence [39–43]. The administration of the vaccine at the disease site might be important to its efficacy.

## CONCLUSION

In this open-label, single-center, phase I study, the safety and immunomodulatory effects of intradermal IMM-101 with SBRT were investigated in patients with LAPC. We observed transient lymphodepletion and enhanced T cell activation in the peripheral blood. Increased levels of activated T cells after treatment correlated with improved PFS and OS. Future studies are needed to provide mechanistic insights into how these observations are linked to clinical efficacy. The intratumoral administration of IMM-101 and combinations with other immunotherapeutic agents focusing on adaptive responses (*e.g.* immune checkpoint blockade, adoptive cell transfer therapy) may lead to improved efficacy for this group of patients with limited treatment options.

## REFERENCES

1. Latenstijn, A.E.J.; van der Geest, L.G.M.; Bonsing, B.A.; Groot Koerkamp, B.; Haj Mohammad, N.; de Hingh, I.; de Meijer, V.E.; Molenaar, I.Q.; van Santvoort, H.C.; van Tienhoven, G.; et al. Nationwide trends in incidence, treatment and survival of pancreatic ductal adenocarcinoma. *Eur. J. Cancer* 2020, 125, 83–93.
2. Mizrahi, J.D.; Surana, R.; Valle, J.W.; Shroff, R.T. Pancreatic cancer. *Lancet* 2020, 395, 2008–2020.
3. Tempero, M.A.; Malafa, M.P.; Al-Hawary, M.; Behrman, S.W.; Benson, A.B.; Cardin, D.B.; Chiorean, E.G.; Chung, V.; Czito, B.; Del Chiaro, M.; et al. Pancreatic Adenocarcinoma, Version 2.2021, NCCN Clinical Practice Guidelines in Oncology. *J. Natl. Compr. Cancer Netw.* 2021, 19, 439–457. <https://doi.org/10.6004/jnccn.2021.0017>.
4. Herman, J.M.; Chang, D.T.; Goodman, K.A.; Dholakia, A.S.; Raman, S.P.; Hacker-Prietz, A.; Iacobuzio-Donahue, C.A.; Griffith, M.E.; Pawlik, T.M.; Pai, J.S.; et al. Phase 2 multi-institutional trial evaluating gemcitabine and stereotactic body radiotherapy for patients with locally advanced unresectable pancreatic adenocarcinoma. *Cancer* 2015, 121, 1128–1137. <https://doi.org/10.1002/cncr.29161>.
5. Suker, M.; Nuyttens, J.J.; Eskens, F.; Haberkorn, B.C.M.; Coene, P.L.O.; van der Harst, E.; Bonsing, B.A.; Vahrmeijer, A.L.; Mieog, J.S.D.; Jan Swijnenburg, R.; et al. Efficacy and feasibility of stereotactic radiotherapy after folfinox in patients with locally advanced pancreatic cancer (LAPC-1 trial). *EClinicalMedicine* 2019, 17, 100200. <https://doi.org/10.1016/j.eclinm.2019.10.013>.
6. Quan, K.; Suter, P.; Xu, K.; Bernard, M.E.; Burton, S.A.; Wegner, R.E.; Zeh, H.; Bahary, N.; Stoller, R.; Heron, D.E. Results of a prospective phase 2 clinical trial of induction gemcitabine/capecitabine followed by stereotactic ablative radiation therapy in borderline resectable or locally advanced pancreatic adenocarcinoma. *Pract. Radiat. Oncol.* 2018, 8, 95–106.
7. Delaney, G.; Jacob, S.; Featherstone, C.; Barton, M. The role of radiotherapy in cancer treatment: Estimating optimal utilization from a review of evidence-based clinical guidelines. *Cancer* 2005, 104, 1129–1137. <https://doi.org/10.1002/cncr.21324>.
8. Sia, J.; Szmyd, R.; Hau, E.; Gee, H.E. Molecular Mechanisms of Radiation-Induced Cancer Cell Death: A Primer. *Front. Cell Dev. Biol.* 2020, 8, 41. <https://doi.org/10.3389/fcell.2020.00041>.
9. Chen, Y.; Gao, M.; Huang, Z.; Yu, J.; Meng, X. SBRT combined with PD-1/PD-L1 inhibitors in NSCLC treatment: A focus on the mechanisms, advances, and future challenges. *J. Hematol. Oncol.* 2020, 13, 105. <https://doi.org/10.1186/s13045-020-00940-z>.
10. Sharabi, A.B.; Lim, M.; DeWeese, T.L.; Drake, C.G. Radiation and checkpoint blockade immunotherapy: Radiosensitisation and potential mechanisms of synergy. *Lancet Oncol.* 2015, 16, e498–e509.
11. Reits, E.A.; Hodge, J.W.; Herberts, C.A.; Groothuis, T.A.; Chakraborty, M.; Wansley, E.K.; Camphausen, K.; Luiten, R.M.; de Ru, A.H.; Neijssen, J.; et al. Radiation modulates the peptide repertoire, enhances MHC class I expression, and induces successful antitumor immunotherapy. *J. Exp. Med.* 2006, 203, 1259–1271.
12. Chakraborty, M.; Abrams, S.I.; Camphausen, K.; Liu, K.; Scott, T.; Coleman, C.N.; Hodge, J.W. Irradiation of tumor cells up-regulates Fas and enhances CTL lytic activity and CTL adoptive immunotherapy. *J. Immunol.* 2003, 170, 6338–6347. <https://doi.org/10.4049/jimmunol.170.12.6338>.
13. Sharabi, A.B.; Nirschl, C.J.; Kochel, C.M.; Nirschl, T.R.; Francica, B.J.; Velarde, E.; Deweese, T.L.; Drake, C.G. Stereotactic Radiation Therapy Augments Antigen-Specific PD-1-Mediated Antitumor Immune Responses via Cross-Presentation of Tumor Antigen. *Cancer Immunol. Res.* 2015, 3, 345–355.
14. Cornel, A.M.; Mimpfen, I.L.; Nierkens, S. MHC Class I Downregulation in Cancer: Underlying Mechanisms and Potential Targets for Cancer Immunotherapy. *Cancers* 2020, 12, 1760.
15. Golden, E.B.; Apetoh, L. Radiotherapy and immunogenic cell death. *Semin. Radiat. Oncol.* 2015, 25, 11–17.
16. Kroemer, G.; Galluzzi, L.; Kepp, O.; Zitvogel, L. Immunogenic cell death in cancer therapy. *Annu. Rev. Immunol.* 2013, 31, 51–72. <https://doi.org/10.1146/annurev-immunol-032712-100008>.

17. Ahmed, A.; Tait, S.W.G. Targeting immunogenic cell death in cancer. *Mol. Oncol.* 2020, 14, 2994–3006. <https://doi.org/10.1002/1878-0261.12851>.
18. Bazzi, S.; Modjtahedi, H.; Mudan, S.; Achkar, M.; Akle, C.; Bahr, G.M. Immunomodulatory effects of heat-killed *Mycobacterium obuense* on human blood dendritic cells. *Innate Immun.* 2017, 23, 592–605. <https://doi.org/10.1177/1753425917727838>.
19. Elia, A.; Lincoln, L.; Brunet, L.R.; Hagemann, T. Treatment with IMM-101 induces protective CD8+ T cell responses in clinically relevant models of pancreatic cancer. *J. Immunother. Cancer* 2013, 1, P215.
20. Dalgleish, A.G.; Stebbing, J.; Adamson, D.J.; Arif, S.S.; Bidoli, P.; Chang, D.; Cheeseman, S.; Diaz-Beveridge, R.; Fernandez-Martos, C.; Glynne-Jones, R.; et al. Randomised, open-label, phase II study of gemcitabine with and without IMM-101 for advanced pancreatic cancer. *Br J. Cancer* 2016, 115, e16.
21. Costa Neves, M.; Giakoustidis, A.; Stamp, G.; Gaya, A.; Mudan, S. Extended Survival after Complete Pathological Response in Metastatic Pancreatic Ductal Adenocarcinoma Following Induction Chemotherapy, Chemoradiotherapy, and a Novel Immunotherapy Agent, IMM-101. *Cureus* 2015, 7, e435. <https://doi.org/10.7759/cureus.435>.
22. Stebbing, J.; Dalgleish, A.; Gifford-Moore, A.; Martin, A.; Gleeson, C.; Wilson, G.; Brunet, L.R.; Grange, J.; Mudan, S. An intra-patient placebo-controlled phase I trial to evaluate the safety and tolerability of intradermal IMM-101 in melanoma. *Ann. Oncol.* 2012, 23, 1314–1319.
23. Dalgleish, A.G.; Mudan, S.; Fusi, A. Enhanced effect of checkpoint inhibitors when given after or together with IMM-101: Significant responses in four advanced melanoma patients with no additional major toxicity. *J. Transl. Med.* 2018, 16, 227.
24. Dutch Pancreatic Cancer, G. CT Staging for Adenocarcinoma of the Pancreatic Head and Uncinate Process, Criteria for Resectability. 2012. Available online: [https://dpcg.nl/wp-content/uploads/2020/04/Criteria\\_resectabiliteit.pdf](https://dpcg.nl/wp-content/uploads/2020/04/Criteria_resectabiliteit.pdf) (accessed on 1 May 2019).
25. CTEP. Common Terminology Criteria for Adverse Events (CTCAE); version 5.0; U.S. Department of Health and Human Services: Washington, DC, USA, 2017.
26. Lau, S.P.; Klaase, L.; Vink, M.; Dumas, J.; Bezemer, K.; van Krimpen, A.; van der Breggen, R.; Wismans, L.V.; Doukas, M.; de Koning, W.; et al. Autologous dendritic cells pulsed with allogeneic tumour cell lysate induce tumour-reactive T-cell responses in patients with pancreatic cancer: A phase I study. *Eur. J. Cancer* 2022, 169, 20–31.
27. Kunert, A.; Basak, E.A.; Hurkmans, D.P.; Balcioglu, H.E.; Klaver, Y.; van Brakel, M.; Oostvogels, A.A.M.; Lamers, C.H.J.; Bins, S.; Koolen, S.L.W.; et al. CD45RA(+)CCR7(-) CD8 T cells lacking co-stimulatory receptors demonstrate enhanced frequency in peripheral blood of NSCLC patients responding to nivolumab. *J. Immunother. Cancer* 2019, 7, 149.
28. Morpheus, Versatile Matrix Visualisation and Analysis Software. Available online: <https://software.broadinstitute.org/morpheus> (accessed on: 3 January 2022).
29. Oweida, A.J.; Mueller, A.C.; Piper, M.; Milner, D.; Van Court, B.; Bhatia, S.; Phan, A.; Bickett, T.; Jordan, K.; Proia, T.; et al. Response to radiotherapy in pancreatic ductal adenocarcinoma is enhanced by inhibition of myeloid-derived suppressor cells using STAT3 anti-sense oligonucleotide. *Cancer Immunol. Immunother.* 2021, 70, 989–1000.
30. van Meir, H.; Nout, R.A.; Welters, M.J.; Loof, N.M.; de Kam, M.L.; van Ham, J.J.; Samuels, S.; Kenter, G.G.; Cohen, A.F.; Melief, C.J.; et al. Impact of (chemo)radiotherapy on immune cell composition and function in cervical cancer patients. *Oncoimmunology* 2017, 6, e1267095.
31. Barker, H.E.; Paget, J.T.E.; Khan, A.A.; Harrington, K.J. The tumour microenvironment after radiotherapy: Mechanisms of resistance and recurrence. *Nat. Rev. Cancer* 2015, 15, 409–425. <https://doi.org/10.1038/nrc3958>.
32. Lee, Y.; Auh, S.L.; Wang, Y.; Burnette, B.; Wang, Y.; Meng, Y.; Beckett, M.; Sharma, R.; Chin, R.; Tu, T.; et al. Therapeutic effects of ablative radiation on local tumor require CD8+ T cells: Changing strategies for cancer treatment. *Blood* 2009, 114, 589–595. <https://doi.org/10.1182/blood-2009-02-206870>.
33. Verbrugge, I.; Hagekyriakou, J.; Sharp, L.L.; Galli, M.; West, A.; McLaughlin, N.M.; Duret, H.; Yagita, H.; Johnstone, R.W.; Smyth, M.J.; et al. Radiotherapy increases the permissiveness of established mammary tumors to rejection by immunomodulatory antibodies. *Cancer Res.* 2012, 72, 3163–3174.

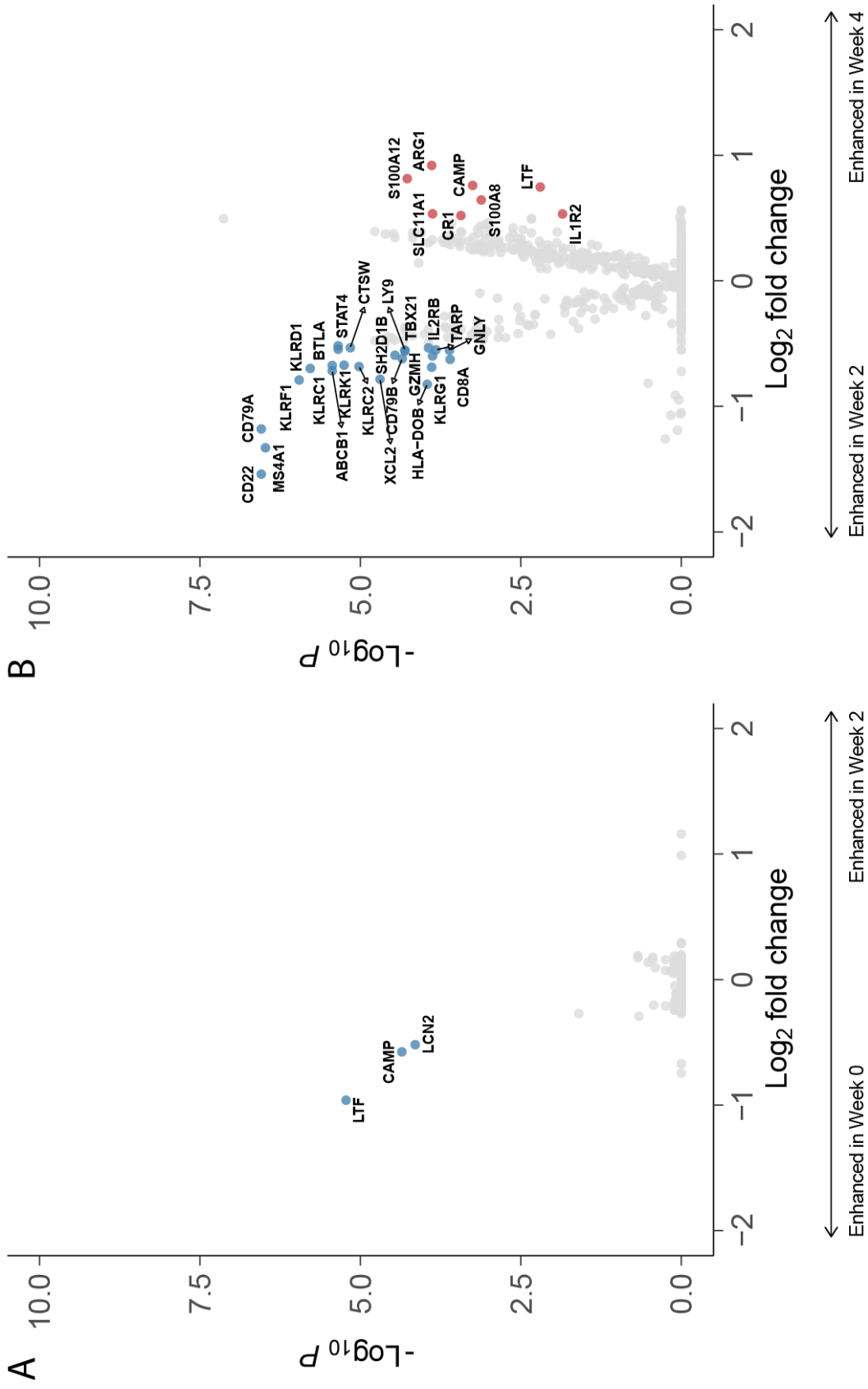
34. Helmink, B.A.; Reddy, S.M.; Gao, J.; Zhang, S.; Basar, R.; Thakur, R.; Yizhak, K.; Sade-Feldman, M.; Blando, J.; Han, G.; et al. B cells and tertiary lymphoid structures promote immunotherapy response. *Nature* 2020, 577, 549–555. <https://doi.org/10.1038/s41586-019-1922-8>.
35. Petitprez, F.; de Reyniès, A.; Keung, E.Z.; Chen, T.W.-W.; Sun, C.-M.; Calderaro, J.; Jeng, Y.-M.; Hsiao, L.-P.; Lacroix, L.; Bougouïn, A.; et al. B cells are associated with survival and immunotherapy response in sarcoma. *Nature* 2020, 577, 556–560. <https://doi.org/10.1038/s41586-019-1906-8>.
36. Wei, J.; Montalvo-Ortiz, W.; Yu, L.; Krasco, A.; Ebstein, S.; Cortez, C.; Lowy, I.; Murphy, A.J.; Sleeman, M.A.; Skokos, D. Sequence of alphaPD-1 relative to local tumor irradiation determines the induction of abscopal antitumor immune responses. *Sci. Immunol.* 2021, 6, DOI: 10.1126/schiimmunol.abg0117.
37. Crooks, J.; Brown, S.; Gauthier, A.; de Boisferon, M.H.; MacDonald, A.; Brunet, L.R. The effects of combination treatment of IMM-101, a heat-killed whole cell preparation of *Mycobacterium obuense* (NCTC 13365) with checkpoint inhibitors in pre-clinical models. *Poster* 2016, 10, 20
38. Mukherjee, N.; Julián, E.; Torrelles, J.B.; Svatek, R.S. Effects of *Mycobacterium bovis* Calmette et Guérin (BCG) in oncotherapy: Bladder cancer and beyond. *Vaccine* 2021, 39, 7332–7340.
39. Malmstrom, P.U.; Sylvester, R.J.; Crawford, D.E.; Friedrich, M.; Krege, S.; Rintala, E.; Solsona, E.; Di Stasi, S.M.; Witjes, J.A. An individual patient data meta-analysis of the long-term outcome of randomised studies comparing intravesical mitomycin C versus bacillus Calmette-Guerin for non-muscle-invasive bladder cancer. *Eur. Urol.* 2009, 56, 247–256.
40. Shelley, M.D.; Kynaston, H.; Court, J.; Wilt, T.J.; Coles, B.; Burgon, K.; Mason, M.D. A systematic review of intravesical bacillus Calmette-Guerin plus transurethral resection vs transurethral resection alone in Ta and T1 bladder cancer. *BJU Int.* 2001, 88, 209–216.
41. Han, R.F.; Pan, J.G. Can intravesical bacillus Calmette-Guerin reduce recurrence in patients with superficial bladder cancer? A meta-analysis of randomized trials. *Urology* 2006, 67, 1216–1223.
42. Shelley, M.D.; Wilt, T.J.; Court, J.; Coles, B.; Kynaston, H.; Mason, M.D. Intravesical bacillus Calmette-Guerin is superior to mitomycin C in reducing tumour recurrence in high-risk superficial bladder cancer: A meta-analysis of randomized trials. *BJU Int.* 2004, 93, 485–490.
43. Bohle, A.; Jocham, D.; Bock, P.R. Intravesical bacillus Calmette-Guerin versus mitomycin C for superficial bladder cancer: A formal meta-analysis of comparative studies on recurrence and toxicity. *J. Urol.* 2003, 169, 90–95. <https://doi.org/10.1097/01.ju.0000039680.90768.b3>.



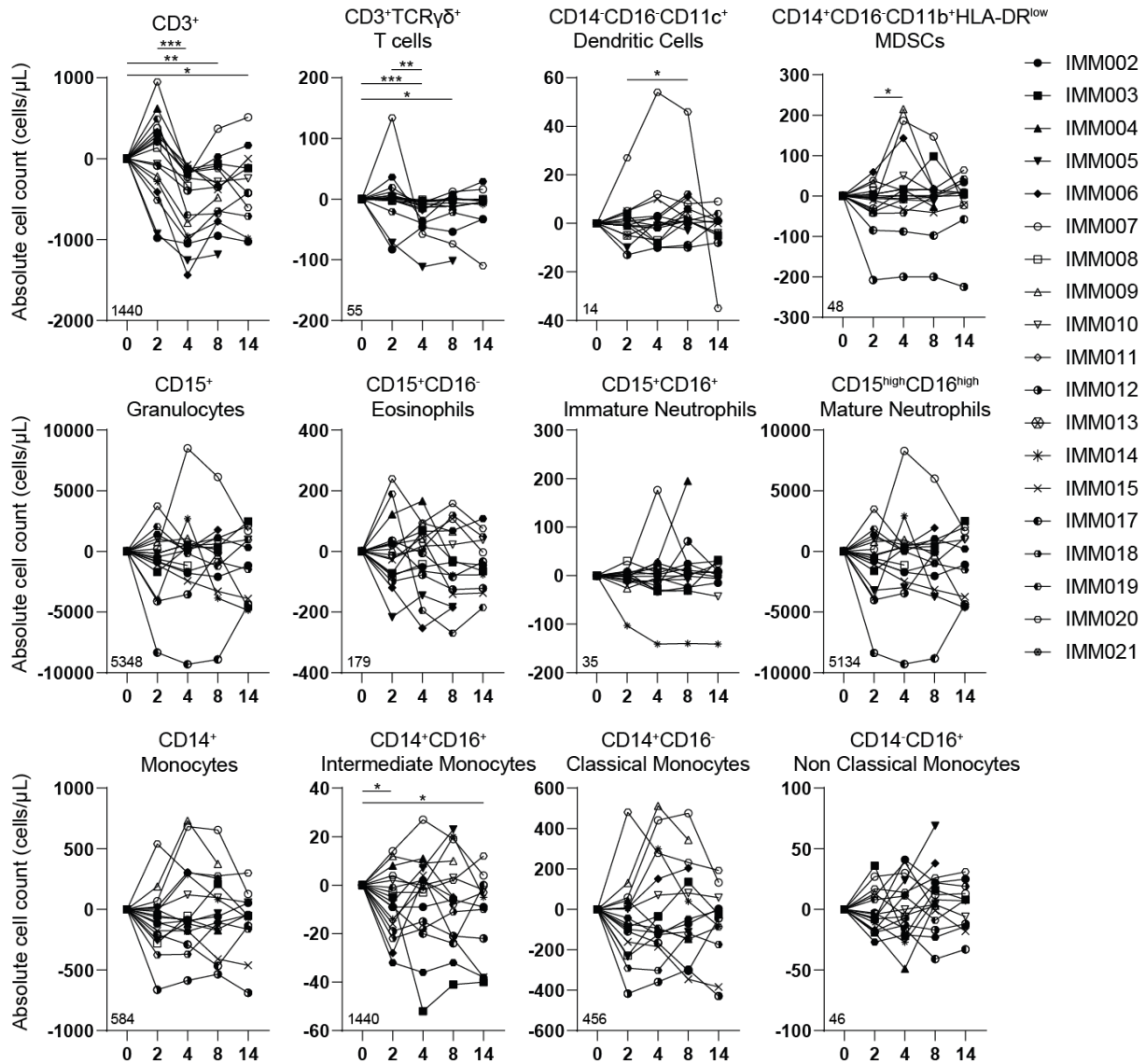
Inclusion criteria	Exclusion criteria
Histologically confirmed pancreatic cancer, as indicated by a definite cytology report	Prior radiotherapy, chemotherapy other than FOLFIRINOX or pancreatic resection
Tumor considered locally advanced after diagnostic work-up including CT-imaging, using the DPCG criteria for locally advanced disease and diagnostic laparoscopy *	Second primary malignancy except in situ carcinoma of the cervix, adequately treated non-melanoma skin cancer, or other malignancy treated at least 5 years previously to diagnosis of pancreatic cancer and without evidence of recurrence
Age > 18 years and < 75 years	Current or previous treatment with immunotherapeutic drugs
European Cooperative Oncology Group (ECOG) performance status of 0 or 1	Previous allergic reaction to any mycobacterial product
American Society of Anesthesiologists (ASA) classification 1 or 2	Prolonged systemic corticosteroid or immunosuppressant medication use ( <i>i.e.</i> >2 weeks)
No evidence of metastatic disease	Lymph node metastases from primary tumor outside the field of radiation
Largest tumor size < 7 cm x 7 cm x 7 cm No direct tumor involvement of the stomach, colon or small bowel	Pregnancy, breast feeding Serious concomitant systemic disorders that would compromise the safety of the patient or his/her ability to complete the study, at the discretion of the investigator
Normal renal function (Creatinine $\leq$ 30 ml/min)	Known history of Human Immunodeficiency Virus (HIV) (HIV-1/2 antibodies)
Normal liver tests (bilirubin < 1.5 times normal**; Alanine transaminase or aspartate transaminase < 5 times normal)	An active autoimmune disease that has required systemic treatment in past 2 years ( <i>i.e.</i> with use of disease modifying agents, corticosteroids or immunosuppressive drugs). Replacement therapy ( <i>e.g.</i> thyroxine, insulin, or physiologic corticosteroid replacement therapy for adrenal or pituitary insufficiency, etc.) is not considered a form of systemic treatment
Normal bone marrow function (White blood cell count > 3.0 x 10e9/L, platelet count > 100 x 10e9/L and hemoglobin > 5.6 mmol/l)	Diagnosis of immunodeficiency or receiving systemic steroid therapy or any other form of immunosuppressive therapy within 7 days prior to the planned first dose of the study. The use of physiologic doses of corticosteroids may be approved after consultation with the Sponsor
Ability to wear an Actiwatch device on non-dominant arm	Known active Hepatitis B ( <i>e.g.</i> HBsAg reactive) or Hepatitis C ( <i>e.g.</i> HCV RNA [qualitative] is detected)
Effective contraceptive methods	Live virus vaccine within 30 days of planned start of trial treatment
Written informed consent	Use of herbal remedies, including traditional Chinese herbal products ( <i>e.g.</i> mistletoe)

\* If patients are referred from an external hospital after completion of FOLFIRINOX chemotherapy, no diagnostic laparoscopy has to be performed. \*\* If bilirubin is higher than 35  $\mu$ mol/L, the placement of a metal biliary stent is mandatory.

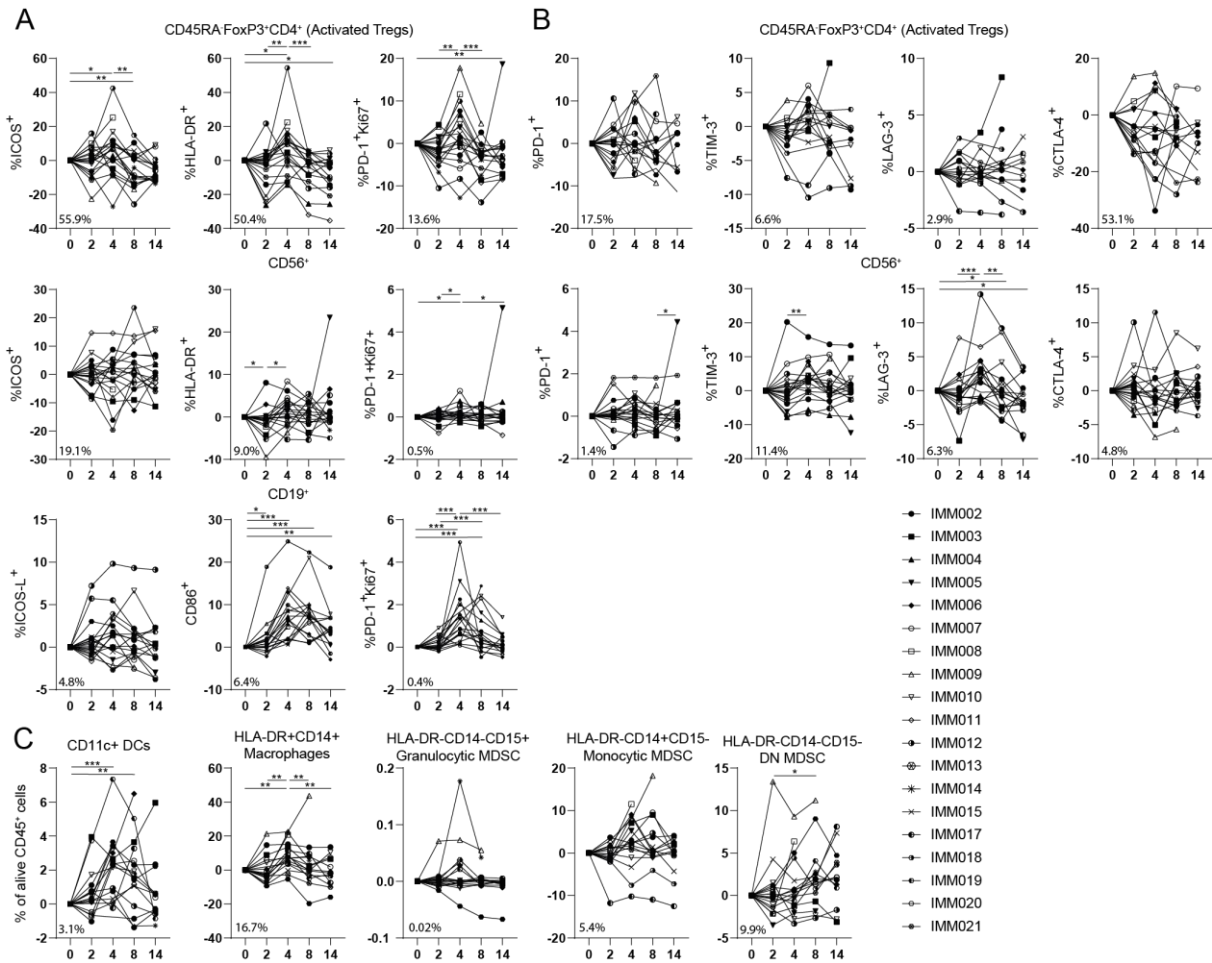
**Supplementary Table 1.** All inclusion and exclusion criteria



**Supplementary Figure 1.** One vaccination of IMM-101 has limited effect on immune-related gene expression. (a) Volcano plot demonstrating genes upregulated in week 2 compared to baseline (week 0). Highlighted genes have a  $\log_2$  fold change  $< 0.5$  and  $p$ -value  $< 0.5$ . (b) Volcano plot demonstrating genes upregulated in week 4 compared to week 2. Highlighted genes have a  $\log_2$  fold change  $< 0.5$  and  $p$ -value  $< 0.5$ .



**Supplementary Figure 2.** SBRT/IMM-101 induced transient lymphodepletion. Number of CD3+, CD3+TCRγδ+, CD14-CD16-CD11c+, CD14+CD16-CD11b+HLA-DR<sup>low</sup>, CD15+, CD15+CD16-, CD15+CD16+, CD15<sup>high</sup>CD16<sup>high</sup>, CD14+, CD14+CD16+, CD14+CD16- and CD14-CD16+ peripheral blood lymphocytes per μL blood. N = 19. Data were normalized for baseline (week 0) and paired per patient. Percentage in the bottom left corner is the average frequency at baseline. Significance was determined using the paired Wilcoxon signed-rank test. \*p < 0.05, \*\*p < 0.01, \*\*\*p < 0.0001.



**Supplementary Figure 3.** SBRT/IMM-101 induced T-cell activation. (a) Percentage of ICOS<sup>+</sup>, HLA-DR<sup>+</sup>, PD-1<sup>+</sup>/Ki67<sup>+</sup> subsets of CD45RA-FOXP3<sup>+</sup>CD4<sup>+</sup> Tregs, CD56<sup>+</sup> and CD19<sup>+</sup> cells. (b) Percentage of PD-1<sup>+</sup>, TIM-3<sup>+</sup>, LAG-3<sup>+</sup>, CTLA-4<sup>+</sup> subsets of CD45RA-FOXP3<sup>+</sup>CD4<sup>+</sup> Tregs and CD56<sup>+</sup> cells. (c) Percentage of CD11<sup>+</sup> dendritic cells, HLA-DR<sup>+</sup>CD14<sup>+</sup> macrophages, HLA-DR<sup>-</sup>CD14<sup>-</sup>CD15<sup>+</sup> granulocytic myeloid derived suppressor cells, HLA-DR<sup>-</sup>CD14<sup>+</sup>CD15<sup>-</sup> monocytic myeloid derived suppressor cells and HLA-DR<sup>-</sup>CD14<sup>-</sup>CD15<sup>-</sup> double negative myeloid derived suppressor cells compared to the total percentage of alive CD45<sup>+</sup> cells. N = 19. Data were normalized for baseline (week 0) and paired per patient. Percentage in the bottom left corner is the average frequency at baseline. Significance was determined using the paired Wilcoxon signed-rank test. \*p < 0.05, \*\*p < 0.01, \*\*\*p < 0.0001.



# CHAPTER 9

---

Discussion and future perspectives

## DISCUSSION AND FUTURE PERSPECTIVES

As current conventional treatment options don't provide durable responses in PDAC, and immunotherapy revolutionized both cancer treatment and clinical prospects for other types of tumors, we aim to explore new effective immunotherapeutic options for pancreatic cancer in this thesis. It has been demonstrated that DCs are limited and DC-mediated T-cell priming is impaired during pancreatic carcinogenesis.(1) Overcoming DC deficiency and restoration of DC function induced tumor-restraining immunity in PDAC.(1) Therefore, the use of DC vaccination was explored. We first investigated the efficacy of allogeneic-lysate DC vaccination in a poorly immunogenic murine model of PDAC to acquire preclinical support of our rationale. As the off-the-shelf product MesoPher (allogeneic-mesothelioma lysate-DC vaccination) was capable of inducing immunological and clinical effects in patients with mesothelioma(2), and shared antigens can be found between mesothelioma and PDAC, the use of an allogeneic-mesothelioma lysate was also introduced in our murine model. The finding of T-cell driven cross-reactive tumor-specific responses in our murine model substantiated the application of MesoPher in the REACTiVe trials. Although our pilot experiment demonstrated robust systemic immune activation following therapy, clinical efficacy was only observed when DCs were administered in prophylactic setting. We ascribe this to the dense and highly immunosuppressive tumor microenvironment of established PDAC impeding T-cell immunity. Consequently, we targeted patients with resected disease without radiographic signs of recurrence in the REACTiVe-1 trial. This is desired as 80% of all patients with resected PDAC develop tumor recurrence within 5-years after surgery(3), and thus occult pancreatic cancer must be present in the majority of these patients. We demonstrated that MesoPher was safe and treatment-induced tumor-specific T-cell responses could be found in the REACTiVe-1 trial. As the majority of patients present with unresectable pancreatic disease, we also investigated if modulation of the tumor microenvironment may improve T-cell immunity. Clinically effective antitumor responses in established tumors could be found when DC therapy was combined with an anti-CD40 agonist in our murine model. CD40-agonistic antibody treatment was able to remodel the tumor microenvironment and improve intratumoral T-cell infiltration of mice. We therefore initiated the REACTiVe-2 trial; here we explore the safety and efficacy of DC/anti-CD40 combination therapy for patients with metastatic pancreatic disease.

At last, we build upon the results of the LAPC-1 trial(4), [in which patients with locally advanced pancreatic cancer (LAPC) were treated with sequential FOLFIRINOX chemotherapy and SBRT], and treated patients with LAPC with a heat-inactivated mycobacterium (IMM-101) next to SBRT in the LAPC-2 trial. It has been demonstrated that the adjuvant IMM-101 improves the activation and maturation of DCs(5) and this in relation with radiation-induced immunogenic cell death may lead to synergistic immune responses. We mainly focused on the safety and treatment-induced immunomodulatory effects in the LAPC-2 study. In short, SBRT/IMM-10

combination therapy was safe and induced transient lymphodepletion and signs of immune activation.

Several remarks can be made about the design and readout of the studies. For the REACTiVe-1 study, we argue that in general an autologous lysate is preferred when an optimal antitumor response is pursued as trivial patient-specific tumor antigens may be absent in the MesoPher lysate. However, acquiring autologous tumor for DC loading provides considerable logistical challenges which cannot (yet) be tackled. Also, recurrence of disease may occur during the time-consuming processing of autologous tumor material as pancreatic cancer is known to rapid progression to metastatic disease. More importantly, the amount of pancreatic tumor retrieved from patients for generating lysate is commonly not sufficient for DC loading considering the relatively modest size of the primary tumor. At last, our murine data advocates for both approaches as comparable efficacy of mesothelioma and pancreatic cancer-lysate loaded DCs was observed in the prophylactic setting.

The use of a lysate-based approach like MesoPher may be favorable compared to a single or selection of peptides as a broad selection of tumor antigens is addressed. This has previously been demonstrated in a meta-analysis of 173 clinical trials; studies exploiting DCs loaded with whole tumor (cell) lysate induced better objective clinical responses than studies using DCs loaded with defined antigens.(6) The administration of multitude-TAA might improve antigenic strength. Implementing a cancer cell lysate-based approach may also increase feasibility as the determination of individual antigens is not required and as it is applicable to tumors in which specific TAAs are unknown.

Also, the induction of cross-reactive T-cell responses with allogeneic lysates derived from other malignancies apart from mesothelioma was not investigated. This may be plausible as multiple tumors share several analogous tumor antigens. We did find considerable overlap of tumor antigens between the murine KPC-3 pancreatic, AE17 mesothelioma cell line and the unrelated B16F10 melanoma and MC38 colon tumor cell line. Also, splenocytes of mice treated with KPC-3 lysate loaded-DCs were able to cross-react against B16F10-loaded DCs but not unloaded DCs, indicating the involvement of shared antigens. However, the magnitude of response will presumably be dictated by the abundance and affinity of epitopes from shared tumor antigens. Regarding the transcriptome analysis of tumor cell lines, we had trouble to discriminate tumor antigens from other self-proteins as a clear definition of tumor antigens is lacking. Tumor antigens can be overexpressed, differentiated or mutated and a comprehensive list of such antigens is currently missing. To tackle this problem, we have therefore chosen to utilize a published list prioritizing established tumor antigens based on several criteria such as selective tumor expression, oncogenicity and immunogenicity.(7) We generated an unbiased Venn-diagram to illustrate the overlap of tumor cell line transcriptomes demonstrating more selective shared expression in mesothelioma and pancreatic tumor, compared to melanoma and colon adenocarcinoma. The same list of tumor antigens was used for our proteomics analysis between the drug product and tumor of study patients. This selection may have led to a biased view of



presented tumor antigens; however, our sole objective was to detect the presence of shared antigens.

We designed, validated and utilized an *in vitro* assay in which we could detect generated T-cell responses against autologous tumor. This assay includes a considerable number of controls (pre and post-vaccination samples, unloaded-DCs, reactivated controls) in order to present bona fide reactions. Although we were able to accurately demonstrate the presence of tumors-specific immune responses, this assay did not provide information about tumor cell killing. One may also wonder if detection of confined peptides may contribute to and improve the feasibility of the assay. However, as a whole tumor lysate was applied in the drug product, the *in vitro* detection of immune responses against one or several peptides may not accurately reflect the *in-situ* induced cross-reactive T-cell responses.

Due to the relative short follow up of the REACTiVe-1 trial, improvement of clinical efficacy as a result of MesoPher administration could not yet be determined. There was also no intention to collect tumor material if local recurrence after immunotherapy would occur. Although these specimens are yet of high importance to investigate treatment-induced efficacy, the collection of such material does not outweigh the potential complications associated with tumor retrieval. In one patient, we did sample a solitary pulmonary metastasis after DC therapy. Subsequent experiments will determine if immunological treatment-related responses can also be found in distant metastasis. Nonetheless, vaccine-specific activation, as demonstrated by post-vaccination enrichment of peripheral activated T-cell clones found in MesoPher-challenged skin, and vaccine-induced responses against autologous tumor of study patients were observed.

Although our study mainly focused on lymphocytes, we did find increases of MDSCs and TAMs after DC vaccination. Also, increase of PD-L1 expression on various myeloid cells was observed. This may encourage the use of anti-PD-L1 antibodies in combination with DC vaccination. Synergy was indeed established in a preclinical and clinical study in mesothelioma.(8) Furthermore, ligation of CD40 in the REACTiVe-2 trial can induce activation of various myeloid cells (*e.g.* DCs, macrophages).(9) Further in-depth studies are needed to formally dissect the spatiotemporal roles of DC vaccination and anti-CD40 agonist on myeloid cells for promoting antitumor immune responses.

Interestingly, DC vaccination demonstrated pronounced activation of the CD4+ T-cell compartment in peripheral blood in both our murine experiments as in patients in the REACTiVe-1 trial. Enrichment and activation of CD8+ T cells was found when mice were treated with an anti-CD40 agonist. The invigoration of CD8+ T cells in peripheral blood may therefore also be indicative for anti-CD40-induced immune responses in human subjects. Unfortunately, the REACTiVe-2 trial doesn't allow us to investigate this hypothesis as this is a dose-escalation feasibility study lacking mono-therapy arms. However, if in human both T-cell compartments demonstrate improved activation after DC vaccination/anti-CD40 combination therapy, this may suggest CD40-mediated CD8+ T cell activation.

The immuno-modulatory effects of SBRT and IMM-101 have been explored in the LAPC-2 trial. Previously, the introduction of SBRT to patients with LAPC did generate promising survival.(4)

We found robust immune-activation after combination therapy, however the contribution of individual treatments remains enigmatic in the current study setup. Looking at the results, it is nonetheless provocative that the transient immune responses were propelled by radiotherapy. In addition, the interpretation of the correlation analysis, in which patients with improved survival demonstrate more increased activated T cells after treatment, remains challenging as no *in vitro* functional assays have been performed. This observation may be driven by bystander effects and be biased, and validation in a larger cohort is needed.

## OVERALL CONCLUSION AND FUTURE PERSPECTIVES

To unlock the potential of immunotherapy in pancreatic cancer, understanding the immunobiological keystones of PDAC is required. Knowledge of interplay between immune cells and the tumor microenvironment will lead to the design of rational orthogonal combination treatment regimes. Only then major breakthroughs, imperative to revolutionize therapy for PDAC, can be achieved.

Multiple immunotherapeutic options for pancreatic cancer have been studied in this thesis. These results form the foundation for future immunological studies in order to understand and tackle this disease effectively. Due to the promising results and survival of the REACTiVe-1 trial, an expansion cohort has been initiated. These results will provide us better understanding of the clinical efficacy of MesoPher-DC immunotherapy for patients with resected PDAC following standard-of-care treatment.

Although at the time of writing the REACTiVe-2 trial is actively recruiting and running, we may already anticipate and contemplate on the next frontier for the REACTiVe line-up. While the DC/anti-CD40 combination therapy yields promising clinical activity in murine experiments, results in patients are not guaranteed. A few factors contributing to this ambiguity includes tumor-intrinsic differences in which murine tumors doesn't faithfully mimic human carcinogenesis, difference in physiology with variation in pharmacokinetics between mice and human, discrepancy in study drug, and the diversity in a human study population versus the uniform nature of a laboratory mice strain.

We demonstrated that DC vaccination induced a PD-L1 rich TME arguing future combination strategies with immune checkpoint blockers. A recent study with anti-CD40 agonist/chemotherapy in combination with an immune checkpoint blocker for patients with metastatic PDAC showed no significant clinical differences with or without nivolumab.(10, 11) Based on their multi-omic results, the authors hypothesized that the addition of nivolumab led to a hyperactivation of the immune system and a terminally exhausted state of T cells which is unfavorable for antitumor response. We found that anti-CD40 monotherapy also promotes profound intratumoral T-cell exhaustion dampening its tumor-restraining capabilities. With this in mind, the addition of an immune-activating immune checkpoint blocker to DC/aCD40 therapy

may not provide the most effective combination strategy; refinement of T-cell priming against the tumor may be of more importance.

A current topic of high interest is mutation-induced novel epitopes of self-antigens also called neoantigens. Neoantigens are able to induce strong antitumor immune responses as these antigens are only expressed by tumor cells and are not affected by central tolerance.(12) Therapeutic vaccines directed to personalized neoantigens might therefore provide the answer to effective tumor clearance. However, challenges related to identifying immunogenic neoantigens are the requirement of laborious computational prediction algorithms and the current high costs associated with these deep learning techniques. In addition, validation of the numerous available MHC epitope prediction tools is still lacking. The presence of neoantigens was not explored in this thesis but might be of strong interest in future research. Neoantigen peptides may be implemented as a vaccine-based therapy or used to load autologous DCs. A clinical trial for patients with resectable PDAC would consist of tumor resection followed by neoantigen prediction and peptide production. These peptides will subsequently be presented to endogenous DCs or used to load autologous DCs *ex vivo* for DC therapy during adjuvant chemotherapy, followed by peptide vaccine or DC therapy after standard-of-care treatment.

We have not investigated the role of sequential versus concurrent administration of DC vaccination in relation to anti-CD40 treatment. Timing may be crucial as newly formed tumor-specific T cells needs to be present at the tumor site when inflammation and stromalysis have been initiated. It has previously also been demonstrated that the sequence of treatment with anti-CD40 and chemotherapy is important to mitigate toxicity. When anti-CD40 was administered within 3 days of chemotherapy, significant macrophage-induced hepatotoxicity was observed. This was abrogated when anti-CD40 was administered directly after chemotherapy or when chemotherapy was given more than 5 days after anti-CD40.(13) This underlines the importance of timing of combination strategies, and needs to be addressed in our future studies.

For the LAPC-2 trail, a multi-arm design may be implemented to examine the immunomodulatory effects of SBRT and IMM-101-monotherapy, as well as determining synergistic effects. This may be desired considering the rationale behind combining SBRT and IMM-101. Also, the assessment of changes within tumor immune composition following therapy may be worthwhile as SBRT is given “locally”. In the near future, we plan to deliver IMM-101 directly into the tumor which may circumvent systemic immunosuppression and promote local antitumor response.(14)

These next steps will provide us more knowledge about our study therapies and will lead to new insights and additional follow-up questions for future research.

In conclusion, to implement immunotherapy to PDAC successfully, combination therapy targeting at different stages of the cancer-immunity cycle is needed. Some future rational combinations with our investigated immunotherapeutic options for PDAC may include agents which skew myeloid/T-cell ratio(15, 16), modulate the tumor micro-environment(17, 18), immunotherapy which sensitize PDAC for conventional chemo or radiotherapy(19), or

chemotherapy itself to promote antigen presentation and myeloid-cell ablation.(20, 21) The incorporation of virotherapy might be compelling as preliminary results demonstrate that virotherapy is able to induce an immune-inflamed signature in PDAC.(22) In the future, we may even take in account the intratumoral microbiome as host-microbe interactions can attenuates antitumor response in PDAC.(23, 24) This demonstrates the vast amount of questions yet to be investigated and presents the enticing field of onco-immunology for PDAC. With the current enthusiasm for immunotherapy and promising results of preclinical/early-phase studies, clinical effective (combination) therapy will emerge in the upcoming decade for PDAC.

## REFERENCES

1. Hegde S, Krisnawan VE, Herzog BH, Zuo C, Breden MA, Knolhoff BL, et al. Dendritic Cell Paucity Leads to Dysfunctional Immune Surveillance in Pancreatic Cancer. *Cancer Cell*. 2020;37(3):289-307 e9.
2. Aerts J, de Goeje PL, Cornelissen R, Kaijen-Lambers MEH, Bezemer K, van der Leest CH, et al. Autologous Dendritic Cells Pulsed with Allogeneic Tumor Cell Lysate in Mesothelioma: From Mouse to Human. *Clin Cancer Res*. 2018;24(4):766-76.
3. Groot VP, Rezaee N, Wu W, Cameron JL, Fishman EK, Hruban RH, et al. Patterns, Timing, and Predictors of Recurrence Following Pancreatectomy for Pancreatic Ductal Adenocarcinoma. *Ann Surg*. 2018;267(5):936-45.
4. Suker M, Nuyttens JJ, Eskens F, Haberkorn BCM, Coene PLO, van der Harst E, et al. Efficacy and feasibility of stereotactic radiotherapy after folfirinix in patients with locally advanced pancreatic cancer (LAPC-1 trial). *EClinicalMedicine*. 2019;17:100200.
5. Bazzi S, Modjtahedi H, Mudan S, Achkar M, Akle C, Bahr GM. Immunomodulatory effects of heat-killed Mycobacterium obuense on human blood dendritic cells. *Innate Immun*. 2017;23(7):592-605.
6. Neller MA, López JA, Schmidt CW. Antigen for cancer immunotherapy. *Semin Immunol*. 2008;20(5):286-95.
7. Cheever MA, Allison JP, Ferris AS, Finn OJ, Hastings BM, Hecht TT, et al. The prioritization of cancer antigens: a national cancer institute pilot project for the acceleration of translational research. *Clin Cancer Res*. 2009;15(17):5323-37.
8. van Gulijk M, Belderbos B, Dumoulin D, Cornelissen R, Bezemer K, Klaase L, et al. Combination of PD-1/PD-L1 checkpoint inhibition and dendritic cell therapy in mice models and in patients with mesothelioma. *Int J Cancer*. 2022.
9. van Kooten C, Banchereau J. CD40-CD40 ligand. *J Leukoc Biol*. 2000;67(1):2-17.
10. O'Hara MH, O'Reilly EM, Varadhachary G, Wolff RA, Wainberg ZA, Ko AH, et al. CD40 agonistic monoclonal antibody APX005M (sotigalimab) and chemotherapy, with or without nivolumab, for the treatment of metastatic pancreatic adenocarcinoma: an open-label, multicentre, phase 1b study. *Lancet Oncol*. 2021;22(1):118-31.
11. Padrón LJ, Maurer DM, O'Hara MH, O'Reilly EM, Wolff RA, Wainberg ZA, et al. Sotigalimab and/or nivolumab with chemotherapy in first-line metastatic pancreatic cancer: clinical and immunologic analyses from the randomized phase 2 PRINCE trial. *Nature Medicine*. 2022;28(6):1167-77.
12. Peng M, Mo Y, Wang Y, Wu P, Zhang Y, Xiong F, et al. Neoantigen vaccine: an emerging tumor immunotherapy. *Molecular Cancer*. 2019;18(1):128.
13. Byrne KT, Leisenring NH, Bajor DL, Vonderheide RH. CSF-1R-Dependent Lethal Hepatotoxicity When Agonistic CD40 Antibody Is Given before but Not after Chemotherapy. *J Immunol*. 2016;197(1):179-87.
14. Melero I, Castanon E, Alvarez M, Champiat S, Marabelle A. Intratumoural administration and tumour tissue targeting of cancer immunotherapies. *Nature Reviews Clinical Oncology*. 2021;18(9):558-76.
15. Nywening TM, Belt BA, Cullinan DR, Panni RZ, Han BJ, Sanford DE, et al. Targeting both tumour-associated CXCR2(+) neutrophils and CCR2(+) macrophages disrupts myeloid recruitment and improves chemotherapeutic responses in pancreatic ductal adenocarcinoma. *Gut*. 2018;67(6):1112-23.
16. Ho WJ, Jaffee EM. Macrophage-Targeting by CSF1/1R Blockade in Pancreatic Cancers. *Cancer Res*. 2021;81(24):6071-3.
17. Biffi G, Oni TE, Spielman B, Hao Y, Elyada E, Park Y, et al. IL1-Induced JAK/STAT Signaling Is Antagonized by TGFβ to Shape CAF Heterogeneity in Pancreatic Ductal Adenocarcinoma. *Cancer Discov*. 2019;9(2):282-301.

18. Kanteti R, Batra SK, Lennon FE, Salgia R. FAK and paxillin, two potential targets in pancreatic cancer. *Oncotarget*. 2016;7(21):31586-601.
19. Nywening TM, Wang-Gillam A, Sanford DE, Belt BA, Panni RZ, Cusworth BM, et al. Targeting tumour-associated macrophages with CCR2 inhibition in combination with FOLFIRINOX in patients with borderline resectable and locally advanced pancreatic cancer: a single-centre, open-label, dose-finding, non-randomised, phase 1b trial. *Lancet Oncol*. 2016;17(5):651-62.
20. Wang Z, Till B, Gao Q. Chemotherapeutic agent-mediated elimination of myeloid-derived suppressor cells. *Oncoimmunology*. 2017;6(7):e1331807.
21. Wan S, Pestka S, Jubin RG, Lyu YL, Tsai YC, Liu LF. Chemotherapeutics and radiation stimulate MHC class I expression through elevated interferon-beta signaling in breast cancer cells. *PLoS One*. 2012;7(3):e32542.
22. Groeneveldt C, Kinderman P, van Stigt Thans JJC, Labrie C, Griffioen L, Sluijter M, et al. Preinduced reovirus-specific T-cell immunity enhances the anticancer efficacy of reovirus therapy. *Journal for ImmunoTherapy of Cancer*. 2022;10(7):e004464.
23. Pushalkar S, Hundeyin M, Daley D, Zambirinis CP, Kurz E, Mishra A, et al. The Pancreatic Cancer Microbiome Promotes Oncogenesis by Induction of Innate and Adaptive Immune Suppression. *Cancer Discov*. 2018;8(4):403-16.
24. McAllister F, Khan MAW, Helmink B, Wargo JA. The Tumor Microbiome in Pancreatic Cancer: Bacteria and Beyond. *Cancer Cell*. 2019;36(6):577-9.



# CHAPTER 10

---

General summary



## GENERAL SUMMARY

In 2017 pancreatic ductal adenocarcinoma (PDAC) surpassed breast cancer and became the third-leading cause of cancer-related death, and if current trends hold up, it is expected to become the second leading cause of cancer-related death by 2030.(1, 2) Surgery is the only treatment with curative intent for PDAC but relapse rates are high. Other conventional treatment options, like chemotherapy, only improve survival with months and is accompanied by severe toxicities leading to early termination of cancer treatment.(3) Despite that cancer immunotherapy revolutionized cancer treatment and clinical prospects, we are still waiting for phase 3 trials with positive clinical results in PDAC. Even dual checkpoint blockade using anti-PD-L1 and anti-CTLA-4 antibodies to target non-redundant pathways of T-cell suppression did not demonstrate favorable results.(4) With exception of a small portion of individuals with genomic instability, the majority of PDAC patients are refractory to current immunotherapy strategies contributing to its immunologic “cold” signature.(5) Multilateral challenges characteristic for pancreatic cancer drive and sustain immune-resistant. The current understanding of pivotal contributors to this immune-resistance consist of [1] tumor-intrinsic mechanisms like the unique genomic landscape directed by oncogenic drivers. The potency of tumor antigens, also called “antigenic strength”, dictates immune response.(6) Especially tumor specific neo-epitopes generated through non-synonymous mutations during carcinogenesis can induce robust anti-tumor T-cell responses. In PDAC, the tumor mutational burden is low.(7) Although survival-correlating neo-antigens are present, PDAC generally exhibits low neoantigenicity.(8) [2] Furthermore, PDAC is recognized as an immune-privileged tumor where the priming, trafficking and function of effector T cells is impaired contributing to a tumor devoid of robust T-cell immunity.(9) [3] The immunosuppressive tumor microenvironment consists of various cells promoting tumor formation. Next to regulatory lymphoid cells, a central role is reserved for myeloid influx and inflammation.(10) The presence of abundant tumor-associated neutrophils, macrophages and myeloid-derived suppressor cells lead to immune evasion by constraining T-cell function.(11, 12) [4] Characteristic for pancreatic cancer is the bulk presence of dense multi-faceted desmoplastic stroma consisting of an immunosuppressive extracellular matrix such as collagen, hyaluron acid and fibronectin, and a complex intertwining of cells, like cancer associated fibroblast and myofibroblast-like pancreatic stellate cells.(13) The stroma can hamper appropriate vascularization, impeding the delivery of drugs and acting as a physical wall for immune cells.(13, 14)

These hurdles possess a major challenge for effective cancer treatment in PDAC. Effective treatment requires comprehensive understanding of the PDAC biology and its relation to the immune system. This justifies the need for a two or three-pronged immunotherapy strategy targeting the aforementioned contributors of immune-resistance transforming PDAC into an immune-inflamed “hot” tumor.

In this thesis, we aim to find new meaningful immunotherapies and therapy-induced immune responses for PDAC. We start with elaborating on the immunobiological foundation of PDAC which contributes to the therapy resistance and its dismal prognosis (**Chapter 2**). We also discuss how immunotherapy can successfully be implemented in this type of cancer based on immunological studies with compelling results. In **chapter 3**, we investigate if DC vaccination loaded with a mesothelioma lysate can generate a cross-reactive immune response against pancreatic cancer in a murine model. We first demonstrate that shared tumor antigens between mesothelioma (AE17) and pancreatic cancer (KPC3) are present. Prophylactic vaccination with DCs loaded with mesothelioma or pancreatic cancer lysate was able to delay KPC3 growth compared to untreated mice. Also, increased frequencies of activated circulating and tumor infiltrating T cells could be found following DC therapy without concomitant Treg-induction. We demonstrated that delay in KPC3 growth after mesothelioma lysate DC vaccination was motivated by tumor antigen-specific responses. To generate clinically effective immune responses in established tumors, we combined DC vaccination, to prime robust T-cell responses, with an anti-CD40 agonist, to reorganize the tumor-micro environment. Anti-CD40/DC combination therapy was able to constrain tumor outgrowth in the majority of mice and significantly prolong survival. This was not observed when mice with established tumors were treated with anti-CD40 or DC monotherapy. Extensive analysis on immune parameters was performed to further dissect the prerequisites and immunological mechanisms of anti-CD40/DC combination therapy. We found that therapeutic response of anti-CD40/DC combination therapy was CD8+ T-cell dependent. Monotherapy DC vaccination induced higher frequencies of activated CD4+ T cells, while monotherapy anti-CD40 induced higher frequencies of activated CD8+ T cells in peripheral blood and tumor compared to untreated mice. Mice treated with anti-CD40/DC combination therapy had higher frequencies of both activated CD4+ and CD8+ T cells in peripheral blood and tumor, and yielded the highest frequencies of effector memory T cells over time. Gene-expression analysis of tumors revealed unique remodeling of the tumor micro-environment of treated mice. Lower transcript amounts of inhibitory receptors (*i.e. Pdc1, Ctla4, Entpd1, Vsr, Cd244, Havcr2, Tigit*) were found in tumors of mice treated with anti-CD40/DC combination therapy, while tumors of mice treated with monotherapy anti-CD40 or DC vaccination demonstrated higher transcript amounts of inhibitory receptors and effector molecules (*i.e. Prf1, Gzma, Gzmb, Ifng*) compared to untreated mice. We ascribed this finding to a terminally exhausted T-cell phenotype in monotherapy-treated mice, and gene-set enrichment analysis confirmed this in tumors of anti-CD40 treated mice. In addition, in both transcriptome analysis as histochemical stainings, we observed decreased collagen, and signs of angiogenesis in tumors of anti-CD40 treated mice indicating tumor microenvironment remodeling. Altogether, these findings offer an explanation of clinical efficacy in mice with established tumors treated with anti-CD40/DC therapy. Anti-CD40 therapy is able to induce stromalysis and promote the influx of T cells, while the addition of DC vaccination precludes the formation of T cells exhibiting an exhaustion phenotype, and combination therapy led to restricted tumor growth.

Based on the preclinical results, a single-center, non-randomized, open-label phase I clinical trial was initiated with DC vaccination for patients with resected PDAC after standard-of-care treatment without radiological signs of recurrence [Rotterdam Pancreatic Cancer Vaccination; REACTiVe trial] (**Chapter 4**).  $25 \times 10^6$  allogeneic tumor lysate-loaded autologous monocyte-derived DCs (MesoPher) were administered three times every two weeks. After the third injection, a delayed-type hypersensitivity (DTH) skin test was performed, and booster vaccinations were given after 3 and 6 months. The primary objective was feasibility, and the secondary objectives were safety, clinical outcome and the presence of immune reactivity after MesoPher in patients with resected pancreatic cancer. Ten patients were included in the study. The production and administration of MesoPher vaccinations were feasible for all included patients. No vaccine-related serious adverse events were observed. Seven out of ten patients have not experienced disease recurrence or progression at a median follow-up of 25 months (15- 32 months). The presence of shared tumor antigens between the drug product and tumors of study patients could be found. All patients developed a positive DTH skin reaction subsequent to MesoPher vaccination. A transient increase in absolute numbers of CD3+ and CD4+ T cells, and an increased frequency of activated CD4+ non-regulatory T cells could be found in peripheral blood after DC vaccination. In addition, an increase in the fraction of shared  $v\beta$ TCR repertoires between MesoPher-challenged skin and peripheral blood post-vaccination could be found, indicating vaccine-specific activation. This enrichment of shared TCRs was found in PD-1+CD4+ T-cell compartment. At last, we demonstrated MesoPher-induced cross-reactive tumors-specific T-cell responses *in vitro*. This was found in both CD4+ and CD8+ T-cell compartment. In **chapter 5**, we elaborate on the technique and findings of our proteomic analysis on the allogeneic-tumor cell lysate (PheraLys) and tumors of study patients of the REACTiVe trail. Next to transcriptome analysis, mass spectrometry was performed in order to find and confirm the presence of shared tumor antigens. For mass spectrometry, samples were first enzymatically digested and labeled with tandem mass tags (TMT). The samples were fractionated and analyzed using a data-dependent MS2 shotgun/survey method. In this analysis, 61 tumor antigens were identified. In the second phase of the proteomic analysis, this set of 61 tumor antigens was targeted using a serial precursor selection MS3 method to acquire MS3 reporter ion spectra with enhanced accuracy and selectivity. Peptide identification and relative quantification was possible using the data from the MS2 and MS3 method respectively. This led to the final identification and quantification of 51 proteins.

In this thesis, we also discussed the efficacy of immune-checkpoint blockers (ICB) in cancer immunotherapy (**Chapter 6**). We describe the mechanisms underlying primary and secondary ICB-resistance leading to the lack of durable clinical response. Features contributing to the primary resistance of ICB are a tumor with a low mutational load, lack of immune recognition, and/or profound immune suppression within the tumor microenvironment. The loss of tumor antigen expression, refractory to immune effector cytokines, and/or upregulation of co-inhibitory molecules/hyperexhaustion can be distinctive for secondary ICB resistance. Moreover, we propose rational combination strategies targeting ICB-resistance mechanisms in

order to maximize therapeutic effect. Finally, we touch upon personalized medicine to stratify and optimize ICB treatment.

Based on previously acquired preclinical support, we initiated a clinical study implementing DC vaccination and an anti-CD40 agonistic antibody for patients with metastatic PDAC [REACTiVE-2 trail]. In **chapter 7**, we clarify the rationale for this combination strategy and disclose the study protocol. This is an open-label, single-center, single-arm, phase I dose finding study in which MesoPher is combined with mitazalimab (anti-CD40 agonist) for patients with progressive metastatic pancreatic disease after first-line FOLFIRINOX chemotherapy. The primary endpoint is safety and tolerability of the combination immunotherapy. To determine the maximum tolerated dose, MesoPher will be given at a fixed dosage of  $25 \times 10^6$  cells and mitazalimab in a traditional 3+3 dose-escalation design. Secondary objectives are radiological response according to the (i)RECIST criteria, and the detection of treatment-induced anti-tumor immune responses. This combination immunotherapy is administered three times every two weeks, and a booster treatment is given 3 and 6 months after the third treatment. Furthermore, a leukapheresis is performed to generate monocyte-derived DCs for MesoPher production, peripheral blood is collected at several time points for immunomonitoring, and a biopsy of an accessible tumor lesion will be obtained before and after combination treatment to determine treatment-induced immune responses. With the 3+3 design, a minimum of 12 and maximum of 18 patients will be included.

At last, we investigated the safety and immunomodulatory effects of stereotactic body radiotherapy (SBRT) and vaccination with heat-killed mycobacterium obuense (IMM-101) in patients with locally advanced pancreatic cancer (LAPC-2 trail) (**Chapter 8**). Nineteen of 20 LAPC-2 study patients were analyzed. This single-arm, open-label, phase I trial includes FOLFIRINOX-treated patients with LAPC, and study patients received six times 1 mg IMM-101 every 2-4 weeks, and 5x8 gray SBRT after the second IMM-101 vaccination. The primary objective was safety of adding IMM-101 to SBRT. Secondary objective was the detection of the immunomodulatory effects of IMM-101/SBRT combination therapy in the peripheral blood. No treatment-related grade 4 or higher adverse events were observed. Gene-expression profiling demonstrated reduced transcript amounts of genes related to lymphocyte subsets and immune inhibition following IMM-101/SBRT combination therapy in the peripheral blood. Various immune subsets were assessed with flow cytometry and no significant changes were observed two weeks after the first IMM-101 vaccination. However, the addition of SBRT transiently reduced CD4+ and CD8+ T cells, CD19+ B cells, and CD56+ NK cells numbers. Also, concurrent increase of ICOS+, HLA-DR+ and PD-1+Ki67+ frequencies of T and NK lymphocytes, and CD86+ and PD-1+Ki67+ frequencies of B lymphocytes without upregulation of inhibitory markers could be observed indicating lymphocyte activation after IMM-101/SBRT combination therapy.

## SAMENVATTING (DUTCH SUMMARY)

In 2017 haalde het pancreas ductaal adenocarcinoom (PDAC) borstkanker in en werd het de op twee na grootste oorzaak van kanker-gerelateerde dood. Als de huidige trends aanhouden is de verwachting dat PDAC tegen 2030 de tweede belangrijkste kanker-gerelateerde doodsoorzaak zal worden.(1, 2) Chirurgie is de enige behandeling met curatieve intentie maar de recidiefpercentages zijn hoog. Andere conventionele behandelingsopties, zoals chemotherapie, verbeteren de overleving met enkele maanden en gaan gepaard met ernstige bijwerkingen die leiden tot het vroegtijdig stoppen van de behandeling.(3) Ondanks dat immunotherapie een kentering teweegbracht in de behandeling van kanker en klinische vooruitzichten, wachten we nog steeds op positieve fase 3-studies in PDAC. Zelfs het tegelijkertijd gebruik van meerdere immunecheckpointblockers (anti-PD-L1- en anti-CTLA-4-antilichamen), welke richten op belangrijke routes van T-celonderdrukking, leverde geen gunstige resultaten op.(4) Met uitzondering van een klein deel van de patiënten met genomische instabiliteit is de meerderheid van de PDAC-patiënten ongevoelig voor de huidige immunotherapiestrategieën, wat de immunologische "koude" karakter van PDAC ondersteunt.(5) Multilaterale uitdagingen kenmerkend voor pancreaskanker stimuleren en onderhouden immuunresistentie. Cruciale bijdragers aan deze immuunresistentie bestaat uit [1] tumor-intrinsieke mechanismen zoals het unieke genomische landschap. De potentie van tumorantigenen, ook wel "antigenic strenght", dicteert de immuunrespons.(6) Vooral tumorspecifieke neo-epitopen die worden gegenereerd door niet-synonieme mutaties tijdens carcinogenese kunnen krachtige antitumor-T-celresponsen induceren. Bij PDAC is de tumormutatiegraad laag.(7) Hoewel overlevingscorrelerende neo-antigenen aanwezig zijn, vertoont PDAC over het algemeen een lage neo-antigeniciteit.(8) [2] Bovendien wordt PDAC erkend als een immuungeïsoleerde tumor waar de priming, circulatie en functie van effector-T-cellen is aangetast, wat bijdraagt aan een tumor zonder robuuste T-celimmunitet.(9) [3] De immunosuppressieve tumormicro-omgeving bestaat uit verschillende cellen die tumorvorming stimuleren. Naast regulerende lymfoïde cellen is een centrale rol weggelegd voor verschillende myeloïde cellen.(10) De aanwezigheid van tumor-geassocieerde neutrofielen, macrofagen en van myeloïd-afgeleide suppressorcellen leidt tot immunosuppressie door de T-celfunctie te inhiberen.(11, 12) [4] Kenmerkend voor pancreaskanker is de overvloedige aanwezigheid van dets desmoplastisch stroma dat bestaat uit een immunosuppressieve extracellulaire matrix zoals collageen, hyaluronzuur en fibronectine, en een complexe verstrengeling van cellen, zoals kankergeassocieerde fibroblasten en myofibroblastachtige stellaatcellen van het pancreas.(13) Dit stroma kan adequate vascularisatie en toegediende therapieën belemmeren, en fungeren als een fysieke barrière voor immuuncellen.(13, 14)

Deze obstakels vormen een grote uitdaging voor effectieve behandeling van PDAC. Adequate behandeling vereist uitgebreide kennis van de tumorbiologie en de relatie ervan tot het

immuunsysteem. Dit rechtvaardigt een combinatiestrategie die gericht is op meerdere wegen van immuunresistentie die PDAC transformeert tot een immunologische "hete" tumor.

In dit proefschrift streven we naar het vinden van nieuwe zinvolle immunotherapieën en therapie-geïnduceerde immuunresponsen voor PDAC. We beginnen met het uiteenzetten van de immunobiologische fundering van PDAC die bijdraagt aan de therapieresistentie en de sombere prognose ervan (**Hoofdstuk 2**). We bespreken ook hoe immunotherapie met succes kan worden geïmplementeerd bij dit type kanker op basis van immunologische studies met hoopgevende resultaten. In **hoofdstuk 3** onderzoeken we in een muismodel of mesothelioomlysaat-beladen dendritische cellen (DC's) een kruisreactieve immuunrespons kan genereren tegen pancreaskanker. We tonen aan dat gedeelde tumorantigenen tussen mesothelioom (AE17) en pancreaskanker (KPC3) aanwezig zijn. Profylactische vaccinatie met DC's beladen met AE17- of KPC3-lysaat was in staat de groei van KPC3 te vertragen in vergelijking met onbehandelde muizen. Ook konden verhoogde percentages van geactiveerde circulerende en tumor-infiltrerende T-cellen worden gevonden na DC-therapie zonder gelijktijdige inductie van Treg's. We hebben aangetoond dat inhibitie in KPC3 tumorgroei door mesothelioomlysaat DC-vaccinatie werd veroorzaakt door tumorantigeen-specifieke immuunreacties. Om klinisch effectieve responsen te genereren in gevestigde tumoren combineerden we DC-vaccinatie, voor robuuste T-celresponsen, met een anti-CD40-agonist, om de tumormicro-omgeving te reorganiseren. Anti-CD40/DC-combinatietherapie was in staat om de uitgroei van tumoren bij de meerderheid van de muizen te remmen en de overleving significant te verlengen. Dit werd niet waargenomen wanneer muizen met gevestigde tumoren werden behandeld met anti-CD40- of DC-monotherapie. Uitgebreide analyse van immuunparameters werd uitgevoerd om de immunologische mechanismen achter anti-CD40/DC-combinatietherapie verder te ontleden. We vonden dat de therapeutische respons van combinatietherapie afhankelijk was van CD8+ T-cellen. Monotherapie DC-vaccinatie zorgde voor hogere frequenties van geactiveerde CD4+ T-cellen, terwijl monotherapie anti-CD40 hogere frequenties van geactiveerde CD8+ T-cellen in perifeer bloed en tumor induceerde in vergelijking met onbehandelde muizen. Muizen die werden behandeld met combinatietherapie hadden hogere frequenties van zowel geactiveerde CD4+ als CD8+ T-cellen in perifeer bloed en tumor, en hadden over tijd de hoogste frequenties van effectorgeheugen-T-cellen. Genexpressie-analyse van tumoren onthulde een unieke remodelering van de tumormicro-omgeving van behandelde muizen. Lagere transcripthoeveelheden van inhiberende receptoren (*Pdcd1, Ctla4, Entpd1, Vsir, Cd244, Havcr2, Tigit*) werden gevonden in tumoren van muizen die werden behandeld met anti-CD40/DC-combinatietherapie, terwijl tumoren van muizen die werden behandeld met monotherapie anti-CD40 of DC vaccinatie hogere transcripthoeveelheden vertoonde van inhiberende receptoren en effectormoleculen (*Prf1, Gzma, Gzmb, Ifng*) in vergelijking met onbehandelde muizen. We schreven deze bevinding toe aan een terminaal uitgeput T-celfenotype bij met monotherapie behandelde muizen, en gen-set verrijkinganalyse bevestigde dit in tumoren van met anti-CD40 behandelde muizen.

Bovendien zagen we in zowel transcriptoomanalyse als histochemische kleuringen aanwijzingen voor verminderd collageen en angiogenese in tumoren van met anti-CD40 behandelde muizen, wat duidt op remodelering van de tumormicro-omgeving. Al met al bieden deze bevindingen een verklaring voor de klinische effectiviteit bij muizen met gevestigde tumoren die zijn behandeld met anti-CD40/DC-therapie. Anti-CD40-therapie kan stromalyse induceren en de instroom van T-cellen in de tumor bevorderen terwijl de toevoeging van DC-vaccinatie de vorming van T-cellen met een uitputtingsfenotype beperkt, en combinatietherapie leidde tot inhibitie van tumorgroei.

Op basis van de preklinische resultaten is een single-center, niet-gerandomiseerde, open-label klinische fase I-studie geïnitieerd met DC-vaccinatie voor patiënten met geresecteerd PDAC na standaardbehandeling zonder radiologische tekenen van recidief [Rotterdam Pancreatic Cancer Vaccination; REACTiVe trial] (**Hoofdstuk 4**).  $25 \times 10^6$  allogene tumorlysaat-beladen autologe monocyt-afstammende DC's (MesoPher) werden drie keer per twee weken toegediend. Na de derde vaccinatie werd een delayed-type-hypersensitivity (DTH) huidtest uitgevoerd, en na 3 en 6 maanden werden boostervaccinaties gegeven. De primaire eindpunt was haalbaarheid en de secundaire eindpunten waren veiligheid, klinische uitkomst en de aanwezigheid van immuunreactiviteit na MesoPher bij patiënten met geresecteerd pancreaskanker. Er werden tien patiënten geïnccludeerd. De productie en toediening van MesoPher-vaccinaties was haalbaar voor alle geïnccludeerde patiënten. Er werden geen ernstige vaccingelerelateerde bijwerkingen waargenomen. Bij een mediane follow-up van 25 maanden (15- 32 maanden) hadden zeven van de tien patiënten geen recidief of progressie van de ziekte. We vonden gedeelde tumorantigenen tussen MesoPher en tumoren van studiepatiënten. Alle patiënten ontwikkelden een positieve DTH-huidreactie na MesoPher-vaccinatie. Een tijdelijke toename van het absolute aantal CD3+ en CD4+ T-cellen, en een verhoogd percentage van geactiveerde CD4+ niet-regulerende T-cellen kon worden gevonden in perifere bloed na DC-vaccinatie. Bovendien kon een toename worden gevonden in de fractie van gedeelde  $v\beta$ TCR-repertoires tussen door MesoPher-gestimuleerde huid en postvaccinatie perifere bloed, wat wijst op vaccinspecifieke activering. Deze verrijking van gedeelde TCR's werd gevonden in het PD-1+CD4+ T-celcompartiment. Ook hebben we *in vitro* MesoPher-geïnduceerde kruisreactieve tumorspecifieke T-celresponsen aangetoond. Dit werd gevonden in zowel het CD4+ als CD8+ T-celcompartiment. In **hoofdstuk 5** gaan we dieper in op de techniek en bevindingen van onze proteomische analyse van het allogene tumorcellysaat (PheraLys) en tumoren van studiepatiënten van de REACTiVe studie. Naast transcriptoomanalyse werd massaspectrometrie uitgevoerd om de aanwezigheid van gedeelde tumorantigenen te vinden en te bevestigen. Voor massaspectrometrie werden monsters eerst enzymatisch afgebroken en gelabeld met tandem mass tags (TMT). Deze monsters werden vervolgens gefractioneerd en geanalyseerd met behulp van een data-afhankelijke MS2 shotgun/survey-methode. In deze analyse werden 61 tumorantigenen geïdentificeerd. In de tweede fase van de proef werd deze set van 61 tumorantigenen onderzocht met behulp van een seriële precursorselectie MS3-methode om MS3-reporterionenspectra te verkrijgen met verbeterde nauwkeurigheid en selectiviteit.

Peptide-identificatie en relatieve kwantificering was mogelijk met behulp van de gegevens van respectievelijk de MS2- en MS3-methode. Dit leidde tot de definitieve identificatie en kwantificering van 51 eiwitten.

In dit proefschrift hebben we ook de effectiviteit van immuun-checkpoint-blokkers (ICB) besproken (**Hoofdstuk 6**). We beschrijven de mechanismen die ten grondslag liggen aan primaire en secundaire ICB-resistentie die leiden tot de afwezigheid van duurzame klinische respons. Factoren die bijdragen aan de primaire resistentie van ICB zijn een tumor met een lage mutatiebelasting, gebrek aan immuunherkenning en/of immuunsuppressie in de tumormicro-omgeving. Het verlies van tumorantigeenexpressie, weerstand voor effector cytokines en/of opregulatie van co-inhiberende moleculen/uitputting kan kenmerkend zijn voor secundaire ICB-resistentie. Daarnaast stellen we rationele combinatiestrategieën voor die gericht zijn op ICB-resistentiemechanismen om het therapeutische effect te maximaliseren. Ten slotte bespreken we gepersonaliseerde benaderingen om ICB-behandeling te stratificeren en te optimaliseren. Op basis van eerder verworven preklinische resultaten zijn we een klinische studie gestart met DC-vaccinatie en een anti-CD40 agonist voor patiënten met gemetastaseerd PDAC [REACTiVE-2-trail]. In **hoofdstuk 7** zetten we de rationale uiteen en bespreken we het onderzoeksprotocol. Dit is een open-label, single-center, single-arm, fase I dosisbepalingsstudie waarin MesoPher wordt gecombineerd met mitazalimab (anti-CD40 agonist) voor patiënten met progressief gemetastaseerde PDAC na eerstelijns FOLFIRINOX-chemotherapie. Het primaire eindpunt is de veiligheid en haalbaarheid van de combinatie-immunotherapie. Om de maximaal getolereerde dosis te bepalen wordt MesoPher gegeven in een vaste dosering van  $25 \times 10^6$  DC's en mitazalimab in een traditioneel 3+3 dosisescalatie design. Secundaire eindpunten zijn radiologische respons volgens de (i)RECIST-criteria en de detectie van therapie-geïnduceerde antitumor immuunresponsen. Deze combinatie-immunotherapie wordt drie keer per twee weken toegediend, en 3 en 6 maanden na de derde behandeling wordt een boostervaccinatie gegeven. Verder wordt een leukaferese uitgevoerd voor MesoPher-productie, wordt op verschillende tijdstippen perifeer bloed afgenomen voor immunomonitoring en wordt voor en na de behandeling een biopsie van een toegankelijke tumorlaesie verkregen om therapie-geïnduceerde immuunresponsen te objectiveren. Gezien het 3+3 design worden er minimaal 12 en maximaal 18 patiënten geïncludeerd.

Ten slotte onderzochten we de veiligheid en immunomodulerende effecten van stereotactische bestraling (SBRT) en vaccinatie met hitte-geïnactiveerde mycobacterium obuense (IMM-101) bij patiënten met lokaal gevorderde pancreaskanker (LAPC-2 studie) (**Hoofdstuk 8**). Negentien van de 20 LAPC-2 studiepatiënten werden geanalyseerd. Deze mono-arm, open-label fase I-studie includeerde FOLFIRINOX-behandelde patiënten met LAPC, en studiepatiënten kregen zes keer 1 mg IMM-101 elke 2-4 weken, en 5x8 gray SBRT na de tweede IMM-101-vaccinatie. Het primaire eindpunt was veiligheid van het toevoegen van IMM-101 aan SBRT. Secundaire eindpunt was het vinden van de immunomodulerende effecten van IMM-101/SBRT-combinatietherapie in het perifere bloed. Er werden geen graad 4 of hoger behandelingsgerelateerde bijwerkingen gevonden. Genexpressie-analyse toonde verminderde



transcripthoeveelheden aan van genen gerelateerd aan lymfocyten en immuuninhibitie na IMM-101/SBRT-combinatietherapie in het perifere bloed. Met flowcytometrie werden verschillende celsubsets beoordeeld en twee weken na de eerste IMM-101-vaccinatie werden geen significante veranderingen waargenomen. De toevoeging van SBRT zorgde echter voor tijdelijk vermindering van het totaal aantal CD4+ en CD8+ T-cellen, CD19+ B-cellen en CD56+ NK-cellen. Tegelijkertijd kon er ook een toename in het percentage van ICOS+, HLA-DR+ en PD-1+Ki67+ T- en NK-lymfocyten, en CD86+ en PD-1+Ki67+ B-lymfocyten worden gevonden, wat wijst op activering van lymfocyten na IMM-101/SBRT combinatietherapie.

## REFERENCES

1. Siegel RL, Miller KD, Fuchs HE, Jemal A. Cancer statistics, 2022. *CA Cancer J Clin.* 2022;72(1):7-33.
2. Rahib L, Smith BD, Aizenberg R, Rosenzweig AB, Fleshman JM, Matrisian LM. Projecting cancer incidence and deaths to 2030: the unexpected burden of thyroid, liver, and pancreas cancers in the United States. *Cancer Res.* 2014;74(11):2913-21.
3. Thibodeau S, Voutsadakis IA. FOLFIRINOX Chemotherapy in Metastatic Pancreatic Cancer: A Systematic Review and Meta-Analysis of Retrospective and Phase II Studies. *J Clin Med.* 2018;7(1).
4. O'Reilly EM, Oh D-Y, Dhani N, Renouf DJ, Lee MA, Sun W, et al. Durvalumab With or Without Tremelimumab for Patients With Metastatic Pancreatic Ductal Adenocarcinoma: A Phase 2 Randomized Clinical Trial. *JAMA Oncology.* 2019;5(10):1431-8.
5. Le DT, Durham JN, Smith KN, Wang H, Bartlett BR, Aulakh LK, et al. Mismatch repair deficiency predicts response of solid tumors to PD-1 blockade. *Science.* 2017;357(6349):409-13.
6. Evans RA, Diamond MS, Rech AJ, Chao T, Richardson MW, Lin JH, et al. Lack of immunoediting in murine pancreatic cancer reversed with neoantigen. *JCI Insight.* 2016;1(14).
7. Alexandrov LB, Nik-Zainal S, Wedge DC, Aparicio SAJR, Behjati S, Biankin AV, et al. Signatures of mutational processes in human cancer. *Nature.* 2013;500(7463):415-21.
8. Balachandran VP, Łuksza M, Zhao JN, Makarov V, Moral JA, Remark R, et al. Identification of unique neoantigen qualities in long-term survivors of pancreatic cancer. *Nature.* 2017;551(7681):512-6.
9. Hegde S, Krisnawan VE, Herzog BH, Zuo C, Breden MA, Knolhoff BL, et al. Dendritic Cell Paucity Leads to Dysfunctional Immune Surveillance in Pancreatic Cancer. *Cancer Cell.* 2020;37(3):289-307 e9.
10. Clark CE, Hingorani SR, Mick R, Combs C, Tuveson DA, Vonderheide RH. Dynamics of the immune reaction to pancreatic cancer from inception to invasion. *Cancer Res.* 2007;67(19):9518-27.
11. Candido JB, Morton JP, Bailey P, Campbell AD, Karim SA, Jamieson T, et al. CSF1R(+) Macrophages Sustain Pancreatic Tumor Growth through T Cell Suppression and Maintenance of Key Gene Programs that Define the Squamous Subtype. *Cell Rep.* 2018;23(5):1448-60.
12. Reid MD, Basturk O, Thirabanjasak D, Hruban RH, Klimstra DS, Bagci P, et al. Tumor-infiltrating neutrophils in pancreatic neoplasia. *Mod Pathol.* 2011;24(12):1612-9.
13. Provenzano PP, Cuevas C, Chang AE, Goel VK, Von Hoff DD, Hingorani SR. Enzymatic targeting of the stroma ablates physical barriers to treatment of pancreatic ductal adenocarcinoma. *Cancer Cell.* 2012;21(3):418-29.
14. Jacobetz MA, Chan DS, Neesse A, Bapiro TE, Cook N, Frese KK, et al. Hyaluronan impairs vascular function and drug delivery in a mouse model of pancreatic cancer. *Gut.* 2013;62(1):112-20.



# APPENDICES

---

List of publications

List of contributing authors

PhD portfolio

Acknowledgements

Curriculum vitae auctoris

## LIST OF PUBLICATIONS

### THIS THESIS

Immunomodulatory effects of stereotactic body radiotherapy and vaccination with heat-killed mycobacterium obuense (IMM-101) in patients with locally advanced pancreatic cancer

**Lau SP**, Van 't Land FR, De Koning W, Klaase L, Vink M, Van Krimpen A, Dumas J, Vadgama D, Nuyttens JJ, Mustafa DAM, Stadhouders R, Willemsen M, Stubbs AP, Aerts JG, Van Eijck CHJ  
*Cancers*, 2022 Oct 27;14(21), 5299. doi.org/10.3390/cancers14215299

Autologous dendritic cells pulsed with allogeneic tumour cell lysate induce tumour-reactive T-cell responses in patients with pancreatic cancer: A phase I study

**Lau SP**, Klaase L, Vink M, Dumas J, Bezemer K, Van Krimpen A, Van der Breggen R, Wismans LV, Doukas M, De Koning W, Stubbs AP, Mustafa DAM, Vroman H, Stadhouders R, Nunes JB, Stingl C, De Miranda NFCC, Luider TM, Van der Burg SH, Aerts JG, Van Eijck CHJ  
*Eur J Cancer*. 2022 Apr 28;169:20-31. doi: 10.1016/j.ejca.2022.03.015.

Dataset from a proteomics analysis of tumor antigens shared between an allogenic tumor cell lysate vaccine and pancreatic tumor tissue

**Lau SP**, Stingl C, Van der Burg SH, Aerts JG, Van Eijck CHJ, Luider TM  
*Data in Brief*, 2022 Jul 25;44:108490. doi: 10.1016/j.dib.2022.108490. eCollection 2022 Oct.

Safety and tumour-specific immunological responses of combined dendritic cell vaccination and anti-CD40 agonistic antibody treatment for patients with metastatic pancreatic cancer: protocol for a phase I, open-label, single-arm, dose-escalation study (REACTiVe-2 trial)

**Lau SP**, Van 't Land FR, Van der Burg SH, Homs MYV, Lolkema MP, Aerts JGJV, Van Eijck CHJ  
*BMJ Open*. 2022 Jun 16;12(6):e060431. doi: 10.1136/bmjopen-2021-060431.

Dendritic cell vaccination and CD40-agonist combination therapy licenses T cell-dependent antitumor immunity in a pancreatic carcinoma murine model

**Lau SP**, Van Montfoort N, Kinderman P, Lukkes M, Klaase L, Van Nimwegen M, Van Gulijk M, Dumas J, Mustafa DAM, Lievense LA, Groeneveldt C, Stadhouders R, Li Y, Stubbs A, Marijt KA, Vroman H, Van der Burg SH, Aerts JG, Van Hall T, Dammeijer F, Van Eijck CHJ  
*J Immunother Cancer*. 2020 Jul;8(2):e000772. doi: 10.1136/jitc-2020-000772.

Pancreatic cancer: not immune for therapy? Developments in immunotherapy for ductal adenocarcinoma of the pancreas

**Lau SP**, Dammeijer F, Van Eijck CHJ  
*Ned Tijdschr Oncol*. 2019;16:309–16.

Rationally combining immunotherapies to improve efficacy of immune checkpoint blockade in solid tumors

**Lau SP**, Dammeijer F, Van Eijck CHJ, Van der Burg SH, Aerts JGJV.

*Cytokine Growth Factor Rev.* 2017 Aug;36:5-15. doi: 10.1016/j.cytogfr.2017.06.011.

## OTHER PUBLICATIONS

Lymphohematopoietic graft-versus-host responses promote mixed chimerism in patients receiving intestinal transplantation

Fu J, Zuber J, Shonts B, Obradovic A, Wang Z, Frangaj K, Meng W, Rosenfeld AM, Waffarn EE, Liou P, **Lau SP**, Savage TM, Yang S, Rogers K, Danzl NM, Ravella S, Satwani P, Luga A, Ho SH, Griesmeyer A, Shen Y, Luning Prak ET, Martinez M, Kato T, Sykes M

*J Clin Invest.* 2021 Apr 15;131(8):e141698. doi: 10.1172/JCI141698.

The PD-1/PD-L1-checkpoint restrains T cell immunity in tumor-draining lymph nodes

Dammeijer F, Van Gulijk M, Mulder E, Lukkes M, Klaase L, Van den Bosch T, Van Nimwegen M, **Lau SP**, Latupeirissa K, Schetters S, Van Kooyk Y, Boon L, Moyaart A, Mueller YM, Katsikis PD, Eggermont AM, Vroman H, Stadhouders R, Hendriks RW, Von der Thüsen J, Grünhagen DJ, Verhoef C, Van Hall T, Aerts JG

*Cancer Cell.* 2020 Nov 9;38(5):685-700.e8. doi: 10.1016/j.ccell.2020.09.001. Epub 2020 Oct 1.

Deletion of donor-reactive T cell clones following human liver transplantation

Savage TM, Shonts BA, **Lau SP**, Obradovic A, Robins H, Shaked A, Shen Y, Sykes M.

*Am J Transplant.* 2020 Feb;20(2):538-545. doi: 10.1111/ajt.15592. Epub 2019 Oct 3.

Human intestinal allografts contain functional hematopoietic stem and progenitor cells that are maintained by a circulating pool

Fu J, Zuber J, Martinez M, Shonts B, Obradovic A, Wang H, **Lau SP**, Xia A, Waffarn EE, Frangaj K, Savage TM, Simpson MT, Yang S, Guo XV, Miron M, Senda T, Rogers K, Rahman A, Ho SH, Shen Y, Griesemer A, Farber DL, Kato T, Sykes M.

*Cell Stem Cell.* 2019 Feb 7;24(2):227-239.e8. doi: 10.1016/j.stem.2018.11.007. Epub 2018 Nov 29.

Early expansion of donor-specific Tregs in tolerant kidney transplant recipients

Savage TM, Shonts BA, Obradovic A, Dewolf S, **Lau SP**, Zuber J, Simpson MT, Berglund E, Fu J, Yang S, Ho SH, Tang Q, Turka LA, Shen Y, Sykes M.

*JCI Insight.* 2018 Nov 15;3(22):e124086. doi: 10.1172/jci.insight.124086.

Quantifying size and diversity of the human T cell alloresponse

DeWolf S, Grinshpun B, Savage T, **Lau SP**, Obradovic A, Shonts B, Yang S, Morris H, Zuber J, Winchester R, Sykes M, Shen Y.

*JCI Insight*. 2018 Aug 9;3(15):e121256. doi: 10.1172/jci.insight.121256.

Origin of enriched regulatory T cells in patients receiving combined kidney/bone marrow transplantation to induce transplantation tolerance

Sprangers B, DeWolf S, Savage TM, Morokata T, Obradovic A, LoCascio SA, Shonts B, Zuber J, **Lau SP**, Shah R, Morris H, Steshenko V, Zorn E, Preffer FI, Olek S, Dombkowski DM, Turka LA, Colvin R, Winchester R, Kawai T, Sykes M.

*Am J Transplant*. 2017 Aug;17(8):2020-2032. doi: 10.1111/ajt.14251. Epub 2017 Apr 10.

Bidirectional intragraft alloreactivity drives the repopulation of human intestinal allografts and correlates with clinical outcome

Zuber J, **Lau SP**, Shonts B, Obradovic A, Fu J, Yang S, Lambert M, Coley S, Weiner J, Thome J, DeWolf S, Farber DL, Shen Y, Caillat-Zucman S, Bhagat G, Griesemer A, Martinez M, Kato T, Sykes M.

*Sci Immunol*. 2016 Oct;1(4):eaah3732. doi: 10.1126/sciimmunol.aah3732. Epub 2016 Oct 7.

Macrochimerism in intestinal transplantation: association with lower rejection rates and multivisceral transplants, without GVHD

Zuber J, Rosen S, Shonts B, Sprangers B, Savage TM, Richman S, Yang S, **Lau SP**, DeWolf S, Farber D, Vlad G, Zorn E, Wong W, Emond J, Levin B, Martinez M, Kato T, Sykes M.

*Am J Transplant*. 2015 Oct;15(10):2691-703. doi: 10.1111/ajt.13325. Epub 2015 May 18.

Anatomical study of the dorsal cutaneous branch of the ulnar nerve (DCBUN) and its clinical relevance in TFCC Repair

Poublon AR, Kraan G, **Lau SP**, Kerver AL, Kleinrensink GJ.

*J Plast Reconstr Aesthet Surg*. 2016 Jul;69(7):983-7. doi: 10.1016/j.bjps.2016.02.002.





## LIST OF CONTRIBUTING AUTHORS

**J.G. Aerts**

Department of Pulmonary Medicine, Erasmus University Medical Center  
Rotterdam, The Netherlands

**K. Bezemer**

Department of Pulmonary Medicine, Erasmus University Medical Center  
Rotterdam, The Netherlands

**R. van der Breggen**

Department of Pathology, Leiden University Medical Center  
Leiden, The Netherlands

**S.H. van der Burg**

Department of Medical Oncology, Oncode Institute, Leiden University Medical Center  
Leiden, The Netherlands

**M. Doukas**

Department of Pathology, Erasmus University Medical Center  
Rotterdam, The Netherlands

**J. Dumas**

Department of Pathology, The Tumor Immuno-Pathology Laboratory, Erasmus University  
Medical Center  
Rotterdam, The Netherlands

**C.H.J. van Eijck**

Department of Surgery, Erasmus University Medical Center  
Rotterdam, The Netherlands

**C. Groeneveldt**

Department of Medical Oncology, Oncode Institute, Leiden University Medical Center  
Leiden, The Netherlands

**M. van Gulijk**

Department of Pulmonary Medicine, Erasmus University Medical Center  
Rotterdam, The Netherlands

**T. van Hall**

Department of Medical Oncology, Oncode Institute, Leiden University Medical Center  
Leiden, The Netherlands

**M.Y.V. Homs**

Department of Medical Oncology, Erasmus MC, Rotterdam  
Rotterdam, The Netherlands

**P. Kinderman**

Department of Medical Oncology, Oncode Institute, Leiden University Medical Center  
Leiden, The Netherlands

**L. Klaase**

Department of Pulmonary Medicine, Erasmus University Medical Center  
Rotterdam, The Netherlands

**W. de Koning**

Department of Pathology, Clinical Bioinformatics Unit, Erasmus University Medical Center  
Rotterdam, The Netherlands

**A. van Krimpen**

Department of Pulmonary Medicine, Amphia Hospital  
Breda, The Netherlands

**F.R. van 't Land**

Department of Surgery, Erasmus University Medical Center  
Rotterdam, The Netherlands

**Y. Li**

Department of Pathology, Clinical Bioinformatics Unit, Erasmus University Medical Center  
Rotterdam, The Netherlands

**L.A. Lieveense**

Department of Pulmonary Medicine, Amphia Hospital  
Breda, The Netherlands

**M.P. Lolkema**

Department of Medical Oncology, Erasmus MC, Rotterdam  
Rotterdam, The Netherlands

**T.M. Luider**

Department of Neurology, Clinical and Cancer Proteomics, Erasmus University Medical Center  
Rotterdam, The Netherlands

**M. Lukkes**

Department of Pulmonary Medicine, Erasmus University Medical Center  
Rotterdam, The Netherlands

**N.F.C.C. de Miranda**

Department of Pathology, Leiden University Medical Center  
Leiden, The Netherlands

**N. van Montfoort**

Department of Medical Oncology, Oncode Institute, Leiden University Medical Center  
Leiden, The Netherlands

**K.A. Marijt**

Department of Medical Oncology, Oncode Institute, Leiden University Medical Center  
Leiden, The Netherlands

**D.A.M. Mustafa**

Department of Pathology, The Tumor Immuno-Pathology Laboratory, Erasmus University  
Medical Center  
Rotterdam, The Netherlands

**M. van Nimwegen**

Department of Pulmonary Medicine, Erasmus University Medical Center  
Rotterdam, The Netherlands

**J.B. Nunes**

Department of Pathology, Leiden University Medical Center  
Leiden, The Netherlands

**J.J. Nuyttens**

Department of Radiation Oncology, Erasmus University Medical Center  
Rotterdam, The Netherlands

**R. Stadhouders**

Department of Cell Biology, Erasmus University Medical Center  
Rotterdam, The Netherlands

**C. Stingl**

Department of Neurology, Clinical and Cancer Proteomics, Erasmus University Medical Center  
Rotterdam, The Netherlands

**A.P. Stubbs**

Department of Pathology, Clinical Bioinformatics Unit, Erasmus University Medical Center  
Rotterdam, The Netherlands

**D. Vadgama**

Department of Pathology, The Tumor Immuno-Pathology Laboratory, Erasmus University  
Medical Center  
Rotterdam, The Netherlands

**H. Vroman**

Department of Pulmonary Medicine, Erasmus University Medical Center  
Rotterdam, The Netherlands

**M. Willemsen**

Department of Pulmonary Medicine, Erasmus University Medical Center  
Rotterdam, The Netherlands

**M. Vink**

Department of Pulmonary Medicine, Erasmus University Medical Center  
Rotterdam, The Netherlands

**L.V. Wismans**

Department of Surgery, Erasmus University Medical Center  
Rotterdam, The Netherlands



## PHD PORTFOLIO

PhD Candidate	Sai Ping Lau
Erasmus MC	Department of Surgery
Promotor	Prof.dr. C.H.J. van Eijck, Prof.dr. J.G.J.V. Aerts
PhD Period	2017 – 2023

PhD Training	Year	Workload (ECTS)
<b>Courses</b>		
Course on Laboratory Animal Science (Article 9)	2017	3.0
NFU eBROK course (Good Clinical Practice)	2019	1.5
Scientific integrity course	2019	0.3
Biostatistical Methods I: Basic Principles	2020	5.7
<b>Presentations &amp; Conferences</b>		
Wetenschapsdag Heelkunde, Rotterdam, The Netherlands	2018	0.3
MolMed Day, Rotterdam, The Netherlands	2018	0.3
Dutch Tumor Immunology Meeting, Breukelen, The Netherlands	2018	0.6
International Cancer Immunotherapy Conference, New York, USA (Poster)	2018	1.2
Dutch Tumor Immunology Meeting, Breukelen, The Netherlands	2019	0.6
International Cancer Immunotherapy Conference, Paris, France (Poster)	2019	1.2
Symposium Experimenteel Onderzoek Heelkundige Specialismen (SEOHS), Amsterdam, The Netherlands (Oral)	2019	1.0
Wetenschapsdag Heelkunde, Rotterdam, The Netherlands (Oral)	2020	1.0
MolMed Day, Rotterdam, The Netherlands (Oral)	2020	1.0
2nd Symposium ACE TI-IT, Rotterdam, The Netherlands (Oral)	2021	1.0
European Pancreatic Club, virtual conference	2021	1.0
<b>Teaching</b>		
Supervisor I&I Research Master Student: 9-month internship K. Latupeirissa, project entitled: Identifying exhausted-T-cell precursor cells in tumor-draining lymph nodes	2019 - 2020	5.0
Teacher Junior Med School	2018 - 2020	0.9
Teacher on Immuno-Oncology for Capita Selecta	2017	2.0
<b>Miscellaneous</b>		
Peer reviewing for medical journals	2018 - 2020	3.0

Appendices

## DANKWOORD

- REDACTED-

- REDACTED-



Appendices

- REDACTED-

- REDACTED-

Appendices

- REDACTED-





## CURRICULUM VITAE

Sai Ping Lau was born on January 28<sup>th</sup> 1991 in The Hague, the Netherlands. In 2009, he graduated from the Oranje Nassau College in Zoetermeer with an economic pre-university education profile. In the following year, he obtained his degree in biology and natural sciences in order to enter medical school.



In 2011, he started his medical training at the Erasmus University in Rotterdam. During medical school, he obtained interest in surgery and became an employee of the student dissection team at the Department of Neuroscience/Anatomy at the Erasmus MC. In 2012, he also started the research master Infection and Immunity (I&I) at the same institute. As part of the Master of Science program I&I, he did a 2-year research internship at the Columbia Center for Translational Immunology at the Department of Surgery at Columbia University Medical Center (CUMC) in New York City, United States. As a visiting researcher in the Sykes Lab, he focused on graft-cell repopulation of the human intestinal graft under the supervision of prof. M. Sykes (CUMC), dr. J. Zuber (CUMC) and dr. F.J.M.F. Dor (Erasmus MC).

He obtained his medical and research master's degree in 2017 after which he started his PhD at the Department of Surgery in the Erasmus MC under supervision of prof.dr. C.H.J. van Eijck and prof.dr. J.G.J.V. Aerts focusing on immunotherapy for pancreatic cancer which led to this thesis. In 2021, He became a surgical resident (ANIOS) at the IJsselland hospital followed by the Erasmus MC. He is currently working as a surgical resident (ANIOS) at the Haaglanden Medisch Centrum, The Hague, the Netherlands.

